

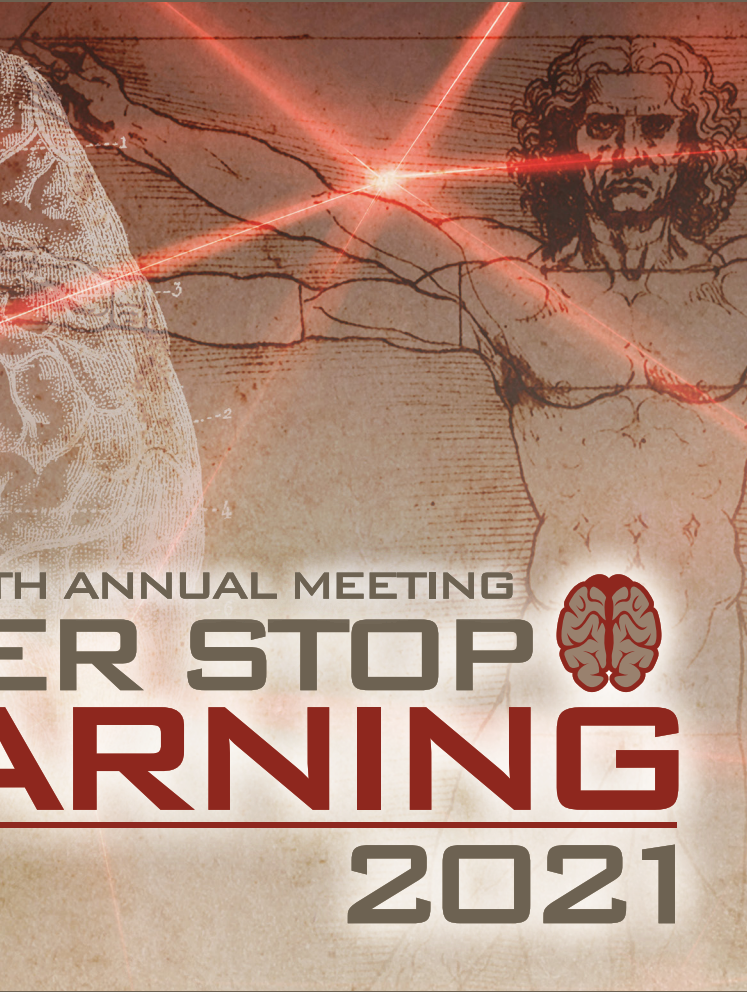
LI

LABORATORY INVESTIGATION

THE BASIC AND TRANSLATIONAL PATHOLOGY RESEARCH JOURNAL

ABSTRACTS

HEMATOPATHOLOGY (664-756)



USCAP 110TH ANNUAL MEETING
**NEVER STOP
LEARNING**
2021

MARCH 13-18, 2021

VIRTUAL AND INTERACTIVE

Published by
SPRINGER NATURE
www.ModernPathology.org

 **USCAP** AN OFFICIAL JOURNAL OF THE
UNITED STATES AND CANADIAN
ACADEMY OF PATHOLOGY
Creating a Better Pathologist

EDUCATION COMMITTEE

Jason L. Hornick
Chair

Rhonda K. Yantiss, Chair
Abstract Review Board and Assignment Committee

Kristin C. Jensen
Chair, CME Subcommittee

Laura C. Collins
Interactive Microscopy Subcommittee

Raja R. Seethala
Short Course Coordinator

Ilan Weinreb
Subcommittee for Unique Live Course Offerings

David B. Kaminsky
(Ex-Officio)
Zubair W. Baloch
Daniel J. Brat
Sarah M. Dry
William C. Faquin
Yuri Fedoriw
Karen Fritchie
Jennifer B. Gordetsky
Melinda Lerwill
Anna Marie Mulligan

Liron Pantanowitz
David Papke,
Pathologist-in-Training
Carlos Parra-Herran
Rajiv M. Patel
Deepa T. Patil
Charles Matthew Quick
Lynette M. Sholl
Olga K. Weinberg
Maria Westerhoff
Nicholas A. Zoumberos,
Pathologist-in-Training

ABSTRACT REVIEW BOARD

Benjamin Adam
Rouba Ali-Fehmi
Daniela Allende
Ghassan Allo
Isabel Alvarado-Cabrero
Catalina Amador
Tatjana Antic
Roberto Barrios
Rohit Bhargava
Luiz Blanco
Jennifer Boland
Alain Borczuk
Elena Brachtel
Marilyn Bui
Eric Burks
Shelley Caltharp
Wenqing (Wendy) Cao
Barbara Centeno
Joanna Chan
Jennifer Chapman
Yunn-Yi Chen
Hui Chen
Wei Chen
Sarah Chiang
Nicole Cipriani
Beth Clark
Alejandro Contreras
Claudiu Cotta
Jennifer Cotter
Sonika Dahiya
Farbod Darvishian
Jessica Davis
Heather Dawson
Elizabeth Demicco
Katie Dennis
Anand Dighe
Suzanne Dintzis
Michelle Downes

Charles Eberhart
Andrew Evans
Julie Fanburg-Smith
Michael Feely
Dennis Firchau
Gregory Fishbein
Andrew Folpe
Larissa Furtado
Billie Fyfe-Kirschner
Giovanna Giannico
Christopher Giffith
Anthony Gill
Paula Ginter
Tamar Giorgadze
Purva Gopal
Abha Goyal
Rondell Graham
Alejandro Gru
Nilesh Gupta
Mamta Gupta
Gillian Hale
Suntrea Hammer
Malini Harigopal
Douglas Hartman
Kammi Henriksen
John Higgins
Mai Hoang
Aaron Huber
Doina Ivan
Wei Jiang
Vickie Jo
Dan Jones
Kirk Jones
Neerja Kambham
Dipti Karamchandani
Nora Katabi
Darcy Kerr
Francesca Khani

Joseph Khoury
Rebecca King
Veronica Klepeis
Christian Kunder
Steven Lagana
Keith Lai
Michael Lee
Cheng-Han Lee
Madelyn Lew
Faqian Li
Ying Li
Haiyan Liu
Xiuli Liu
Lesley Lomo
Tamara Lotan
Sebastian Lucas
Anthony Magliocco
Kruti Maniar
Brock Martin
Emily Mason
David McClintock
Anne Mills
Richard Mitchell
Neda Moatamed
Sara Monaco
Atis Muehlenbachs
Bitu Naini
Dianna Ng
Tony Ng
Michiya Nishino
Scott Owens
Jacqueline Parai
Avani Pendse
Peter Pytel
Stephen Raab
Stanley Radio
Emad Rakha
Robyn Reed

Michelle Reid
Natasha Rekhman
Jordan Reynolds
Andres Roma
Lisa Rooper
Avi Rosenberg
Esther (Diana) Rossi
Souzan Sanati
Gabriel Sica
Alexa Siddon
Deepika Sirohi
Kalliopi Siziopikou
Maxwell Smith
Adrian Suarez
Sara Szabo
Julie Teruya-Feldstein
Khin Thway
Rashmi Tondon
Jose Torrealba
Gary Tozbikian
Andrew Turk
Evi Vakiani
Christopher VandenBussche
Paul VanderLaan
Hannah Wen
Sara Wobker
Kristy Wolniak
Shaofeng Yan
Huihui Ye
Yunshin Yeh
Anjana Yeldandi
Gloria Young
Lei Zhao
Minghao Zhong
Yaolin Zhou
Hongfa Zhu

To cite abstracts in this publication, please use the following format: **Author A, Author B, Author C, et al. Abstract title (abs#). In "File Title." *Laboratory Investigation* 2021; 101 (suppl 1): page#**

664 Role of Immunohistochemistry in Minimal Residual Disease Detection in NPM1-Mutated AML

Nidhi Aggarwal¹, Erin Alston², Geraldine Pinkus², Olga Weinberg³

¹University of Pittsburgh, School of Medicine, Pittsburgh, PA, ²Brigham and Women's Hospital, Boston, MA, ³UTSouthwestern Medical Center, Dallas, TX

Disclosures: Nidhi Aggarwal: None; Erin Alston: None; Geraldine Pinkus: None; Olga Weinberg: None

Background: Minimal residual disease (MRD) testing in nucleophosmin (*NPM1*)- mutated acute myelogenous leukemia (AML) is predictive of outcome. While flow cytometry (FCM) and molecular methods are well established to detect MRD, they may not be accessible, or applicable (depend on type of *NPM1* mutation) or lack fresh sample to perform the test. In this study, we examine the utility of *NPM1* immunohistochemistry (IHC) with respect to MRD testing, and compared it to molecular and FCM methods.

Design: We identified 144 samples from 63 (29 UPMC+ 34 BWH) *NPM1*-mutated AML patients with available high resolution FCM for MRD testing. Of these 72 (50%) had additional quantitative *NPM1* molecular testing performed (PCR or NGS). *NPM1* IHC staining was done on corresponding bone marrow biopsy using *NPM1* mutant protein-specific antibody (ThermoFisher Scientific, Rockford, IL; Catalog #: PA1-46356) and quantified (positive: total cells, 500 total). We evaluated test characteristics (sensitivity, specificity, positive predictive value (PPV), negative predictive value (NPV), and accuracy) of *NPM1* IHC staining using MRD positive results based on FCM and/ or molecular testing as the gold standard (cut off 0.1 and 0.01%).

Results: 13.8% (20/144) and 17.3% (25/144) of the samples were positive for MRD by FCM and 29/72 (40.2%) and 34/72 (47.2%) by molecular methods at cut off of 0.1% and 0.01% respectively. *NPM1* IHC was positive in 23.6% (34/144) of samples. *NPM1* IHC positivity ranged from (<0.2 to 100%, median 2.6%). When compared to MRD positive cases (at cut off of 0.1% FCM and/or molecular), *NPM1* IHC had excellent specificity and NPV and reasonable sensitivity and PPV. Using 0.01% as the cut off for MRD positivity, *NPM1* IHC continued to have excellent specificity and PPV and good NPV, however, sensitivity drops to 62.5% (see table). The false negatives by IHC (at cut off of 0.1%) (9/144, 6.25%) included 2 cases that were positive by FCM (molecular studies not performed) at 0.1% and 0.3% and 7 that were positive by quantitative PCR (negative on FCM) at <0.4% (range 0.1%-0.39%) . The false positive cases (6/144, 4.1%) included 3 cases that were positive by FCM at <0.1% (molecular not done) and 3 in which the IHC was positive at <0.2% (<1/500 cells, molecular done in 1/3 cases and was negative).

Test characteristics for NPM1 IHC when compared to flow cytometry and quantitative molecular methods in detection of MRD		
Test characteristics for IHC in % (confidence interval)	MRD+ (FCM and/or molecular + @ 0.1% cut off)	MRD+ (FCM and/or molecular+ @ 0.01% cut off)
Sensitivity	76.32 (59.76-88.56%)	63.27 (48.29-76.58%)
Specificity	94.34 (88.09-97.89%)	96.84 (91.05-99.34%)
PPV	82.86 (68.53-91.47%)	91.18 (76.88-96.98%)
NPV	91.74 (86.24-95.17%)	83.64 (77.94-88.09%)
Accuracy	89.58 (83.40-94.05%)	85.42 (78.58-90.74%)

Figure 1 - 664

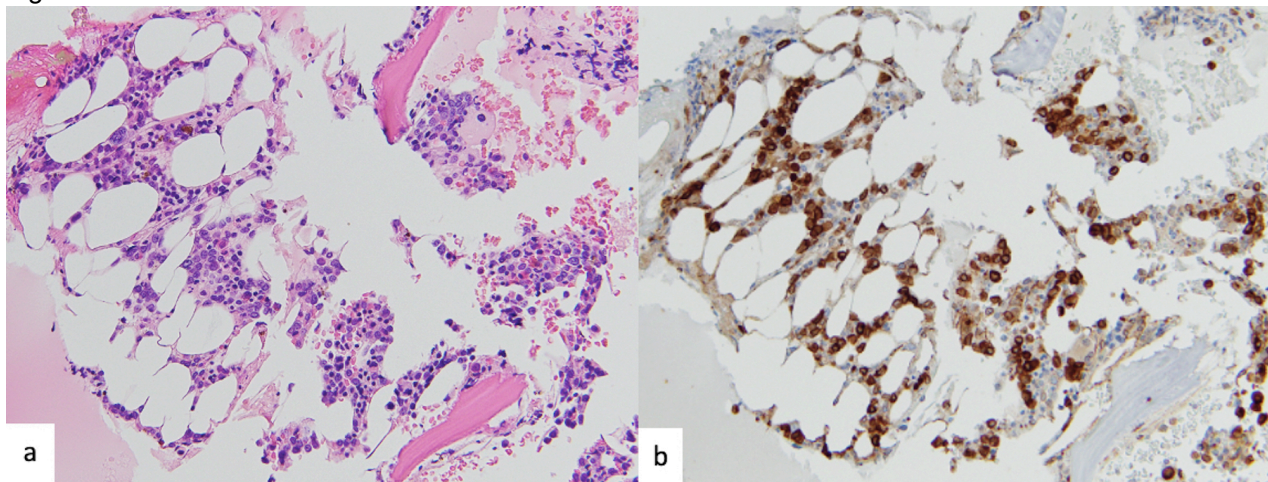


Figure 1: Bone marrow involved by residual *NPM1*-mutated acute myeloid leukemia: H&E (a) and *NPM1* immunohistochemical stain (b), 40x

Conclusions: Our findings indicate that *NPM1* IHC analysis for MRD detection is highly concordant with flow cytometry and molecular methods. While IHC cannot currently replace the existing methods of detection of MRD by flow cytometry and molecular studies, it represents a sensitive, fast, inexpensive, and accessible method for detecting MRD. It can help select cases for further evaluation, and would be extremely useful if fresh sample is not available for other modalities of testing and in cases where the commonly used molecular testing cannot detect and quantify the *NPM1* mutation (non A, B or D type).

665 Immune Checkpoint Molecule (PD-1, PD-L1, PD-L2) Expression, 9p24.1 Gene Locus Alterations and Tumor Microenvironment Status of Primary Central Nervous System Lymphoma and Their Clinical Relevance: A Quantitative Analysis

Dilara Akbulut¹, Seher Yuksel², Ekin Kircali², Burak Yasin Aktas³, Gulsah Kaygusuz², Arzu Saglam⁴, Figen Soylemezoglu⁵, Aysegul Uner⁴, Muhit Ozcan², Alev Turker³, Isinsu Kuzu²

¹Memorial Sloan Kettering Cancer Center, New York, NY, ²Ankara University School of Medicine, Ankara, Turkey, ³Hacettepe University Cancer Institute, Ankara, Turkey, ⁴Hacettepe University, Ankara, Turkey, ⁵Hacettepe University Faculty of Medicine, Ankara, Turkey

Disclosures: Dilara Akbulut: None; Seher Yuksel: None; Ekin Kircali: None; Burak Yasin Aktas: None; Gulsah Kaygusuz: None; Arzu Saglam: None; Figen Soylemezoglu: None; Aysegul Uner: None; Muhit Ozcan: Grant or Research Support, Janssen; Grant or Research Support, Celgene; Grant or Research Support, Takeda; Grant or Research Support, Archigen; Grant or Research Support, Roche; Alev Turker: None; Isinsu Kuzu: None

Background: Primary central nervous system lymphoma (PCNSL) is a rare aggressive immune privileged site lymphoma, usually with a diffuse large B cell morphology. Immune checkpoint molecules PD-1/PD-L1 are candidates for explaining the biology of the disease. Promising results with immune checkpoint inhibitor therapy on few relapsed/refractory cases were achieved and ongoing clinical trials are being conducted with PCNSL patients. Our aim in this study was to examine the relation of PD-1, PD-L1, PD-L2 expression and molecular alterations in 9p24.1 gene locus, as well as composition of the tumor microenvironment (TME) and its relation with clinical prognostic parameters in a PCNSL cohort.

Design: 57 PCNSL and as a control group 45 systemic DLBCL cases of activated B cell phenotype were included. Cases were represented in 3 tissue microarray (TMA) blocks. CD3, CD8, CD68, CD163, PD-1, PD-L1, PD-L2 immunostaining, EBER ISH, PD-L1/PD-L2 FISH were performed on TMA sections. The quantitative evaluations were done on digital images. Results were compared with the clinical and pathological parameters. Statistically $p < 0.05$ was accepted significant.

Results: T cells and histiocytes were lower in PCNSL TME($p=0.000$) than the control group, independent from preoperative steroid therapy. Cytotoxic T cell ratio was higher in PCNSL($p=0.000$). PD-1 and PD-L1 expression in PCNSL TME were 89% and 96%, positively correlated with T cell and histiocyte count ($p<0.05$). PD-L1 and PD-L2 expression in PCNSL tumor cells were 31% and 34%, respectively. Chromosomal alterations detected with amplification and break-apart FISH probes in either PCNSL and DLBCL were not correlated with PDL-1, PDL-2 expression. TME cell count, PD-1, PD-L1, PD-L2 expression and genetic alterations were not associated with overall survival. PD-L1 expression was higher in EBV positive cases ($p<0.05$).

Clinicopathological and immunohistochemical details of PCNSL cases	
Sex (F/M)	25/32
Mean age (range)	56.26 (17-80)
Deep brain involvement	16/52 (30.8%)
Multifocality	19/45 (42.2%)
High serum LDH levels	24/38 (63.2%)
Growth pattern <ul style="list-style-type: none"> • Diffuse • Perivascular • Scattered 	<ul style="list-style-type: none"> • 32 (57%) • 21 (38%) • 3 (5%)
ECOG Score (46/57) <ul style="list-style-type: none"> • 0 • 1 • 2 • 3 	<ul style="list-style-type: none"> • 7 (15%) • 19 (42%) • 12 (26%) • 8 (17%)
Preoperative steroid treatment	32/43 (74%)
EBER+ cases	4/56 (7.1%)
PD-1+ cases	50/56 (89%)
PD-L1+ cases (tumor)	17/56 (31%)
PD-L1+ cases (TME)	54/56 (96%)
PD-L2+ cases (tumor)	13/53 (34%)
PD-L2+ cases (TME)	41/54 (77%)
9p24.1 gene locus alterations (45/57) <ul style="list-style-type: none"> • Normal • Polysomy • CNA • Amplification • Translocation 	<ul style="list-style-type: none"> • 37 (81.5%) • 5 (11%) • 1 (2.5%) • 1 (2.5%) • 1 (2.5%)
CD3+ T lymphocytes (/mm ²)	1104 (70-7000)
CD8+ T lymphocytes (/mm ²)	852 (55-6540)
CD68+ histiocytes (/mm ²)	835 (94-1825)
CD163+ histiocytes (/mm ²)	1051 (200-2091)
CD8/CD3 ratio	0.76
CD163/CD68 ratio	1.41

Conclusions: In PCNSL, lower TME cell count compared to DLBCL and high expression of checkpoint molecules could be the reason of worse prognosis. In the light of current literature, our results and ongoing clinical trials, PCNSL is a potential candidate for immunotherapy with checkpoint inhibitors. On the other hand, 9p24.1 gene alterations in tumor cells are correlated with PDL-1 and PDL-2 expression only in 40-50% of the PCNSL and nodal DLBCL cases and have no prognostic relevance.

666 IgA Myeloma; Why So Aggressive?

Yamac Akgun¹, Andrea Espejo-freire¹, Nicolas Millan¹, Melissa Duarte², Jennifer Chapman³, Julio Poveda³
¹University of Miami/Jackson Memorial Hospital, Miami, FL, ²University of Miami/Jackson Health System, Miami, FL, ³University of Miami, Miller School of Medicine, Miami, FL

Disclosures: Yamac Akgun: None; Andrea Espejo-freire: None; Nicolas Millan: None; Melissa Duarte: None; Jennifer Chapman: None; Julio Poveda: None

Background: Multiple myeloma (MM) is a malignant disorder in which plasma cells of a single clone proliferate and accumulate in the bone marrow. The disease is treatable however not curable. The exact cause of this disease is still unknown. IgA type myeloma accounts for 20% of all myeloma subtypes and it is the second most common subtype after IgG myeloma. IgA myeloma has an aggressive clinical course as well as a poor prognosis. In this study we highlight cytogenetic abnormalities as well as flow cytometry analysis in order to explain the aggressiveness of IgA myeloma compared to other types.

Design: Sixty-one IgA type MM patients from University of Miami Hospitals were studied. Demographic, laboratory, bone marrow biopsy, flow cytometry and cytogenetics data were extracted from the medical charts. By fluorescence in situ hybridization the high-risk group is classified as t(4;14)(p16;q32)FGFR3-IGH, t(14;16;)(q32;q23)IGH-MAF, 17p13 (TP53) deletion, and 1q21 gain; intermediate-risk group is classified as (13q deletion), and low-risk group is classified as t(11;14)(q13;q32)CCND1-IGH and all others

Results: Demographics showed that there were 34 men (56%) and 27 women (44%). The mean age was 66.0 years +/- 10 (range: 40.0–90.0 years). The most common clinical presentations were related to bone involvement (64%), anemia (33%), and renal disease (30%). Extra-medullary plasmacytosis occurred in 20% and the amyloid deposition was seen in 8% of the patients. In addition, the flow cytometry and FISH studies using multiple myeloma associated probes can be found in Table 1.

Table 1: Flow Cytometry(n=53) and FISH studies(n=47) using multiple myeloma associated probes

Flow cytometry for multiple myeloma	28(52.8%)
Aberrant expression of CD56	13(24.5%)
Aberrant expression of CD117	9(17.0%)
Expression of CD56 +CD117	7(13.2%).
Co-expression of CD20	1(1.9%)
Co-expression of CD56+CD117+CD20	18(34.0%)
No aberrant expression of CD56, CD117 and CD20	
FISH for multiple myeloma	5(10.6%)
1q21 gain	4(8.5%)
del17p	5(10.5%)
t(4;14)	18(38.3%)
del 13	5(10.6%)
t(11;14)	6(12.8%)
Normal	4(8.5%)
Other(Low-risk)	

Conclusions: Using the cytogenetic risk stratification schema, 68.1% were of either intermediate or high risk. The aggressive clinical behavior described in the literature may be related to high frequency of intermediate/high risk genetic lesions such as 1q21 gain, del 17, and del13, however our results were not significantly different compared to other types of myelomas, thus cytogenetics alone cannot explain the aggressiveness of IgA myeloma. Flow cytometry analysis revealed that CD56 expression was less frequent when compared to the other types of multiple myeloma based on the literature(52.8% vs 70-80%). CD56 is an homophilic binding glycoprotein with role in cell to cell adhesion. In plasma cells it is normally not expressed however in multiple myeloma is aberrantly expressed in up to 80% of cases. Our study demonstrated lower frequency of CD56 expression (52.8%) which we hypothesize may play a significant role in the aggressive clinical behavior due to the loss of cell to cell adhesion which may explain why may explain the frequent bone metastases within this cohort. Expression of CD117 and/or CD20 with or without CD56 expression did not significantly correlate with any other parameters.

667 Triple-Negative Primary Myelofibrosis: A Bone Marrow Pathology Group (BMPG) Study

Yahya Al-Ghamdi¹, Jonathan Lake², Adam Bagg³, Beenu Thakral⁴, Sa Wang⁴, Carlos Bueso-Ramos⁴, Heesun Rogers⁵, Eric Hsi⁶, Jonathon Gralewski⁷, Kathryn Foucar⁷, Tracy George⁸, Anton Rets⁹, Robert Hasserjian¹⁰, Olga Weinberg¹¹, Daniel Arber¹², Osvaldo Padilla¹³, Attilio Orazi¹³, Wayne Tam¹⁴
¹New York-Presbyterian/Weill Cornell Medicine, New York, NY, ²Hospital of the University of Pennsylvania, Philadelphia, PA, ³University of Pennsylvania, Philadelphia, PA, ⁴The University of Texas MD Anderson Cancer Center, Houston, TX, ⁵Cleveland Clinic, Cleveland, OH, ⁶Wake Forest Baptist Health, Winston-Salem, NC, ⁷University of New Mexico, Albuquerque, NM, ⁸The University of Utah, Salt Lake City, UT, ⁹ARUP Laboratories, University of Utah, Salt Lake City, UT, ¹⁰Massachusetts General Hospital, Harvard Medical School, Boston, MA, ¹¹UTSouthwestern Medical Center, Dallas, TX, ¹²University of Chicago, Chicago, IL, ¹³Texas Tech University Health Science Center, El Paso, TX, ¹⁴Weill Cornell Medicine, New York, NY

Disclosures: Yahya Al-Ghamdi: None; Jonathan Lake: None; Adam Bagg: None; Beenu Thakral: None; Sa Wang: None; Carlos Bueso-Ramos: None; Heesun Rogers: None; Eric Hsi: None; Jonathon Gralewski: None; Kathryn Foucar: None; Tracy George: None; Anton Rets: None; Robert Hasserjian: None; Olga Weinberg: None; Daniel Arber: None; Osvaldo Padilla: None; Attilio Orazi: None; Wayne Tam: None

Background: Primary myelofibrosis (PMF) is a clonal, *BCR-ABL1*-negative myeloproliferative neoplasm characterized by a proliferation of abnormal megakaryocytes and increased granulopoiesis in the bone marrow (BM), associated with fibrosis in its overt form. The majority of the cases harbor *JAK2* V617F, *CALR* exon 9, or *MPL* exon 10 mutations which are collectively known as PMF with driver mutations (DM-PMF); cases negative for DMs are termed triple-negative PMF (TN-PMF). We aimed to identify the clinicopathologic and molecular genetic differences between TN-PMF and DM-PMF.

Design: 61 TN-PMF cases and 89 DMs positive PMF control cases were collected from the above listed BMPG member institutions. All cases fulfilled the 2016 WHO diagnostic criteria for PMF. The clinical, hematologic, pathologic, cytogenetic, and molecular data were reviewed. Targeted next-generation sequencing (NGS) was performed on DNA extracted from the BM when available. Statistical analyses were performed using SAS Version 9.4. Log-rank test was used to compare the overall survival between the two groups.

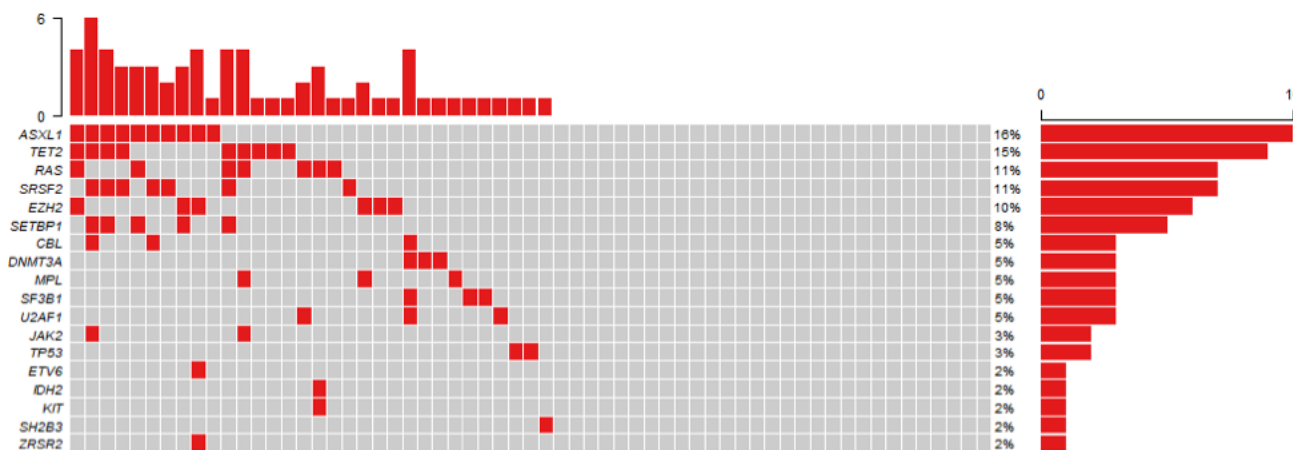
Results: Data comparisons between the two groups are listed in Table 1. The median age of TN-PMF was 62 years (52-68) and the male to female ratio was ~1:1, similar to DM-PMF. Compared to the control group, TN-PMF patients were less likely to have an organomegaly, and had a lower percentage of basophils and a higher percentage of lymphocytes. There was no statistical difference in LDH level, total white blood cell count, monocyte %, eosinophil %, hemoglobin level, platelet count, BM cellularity, myeloid to erythroid ratio, fibrosis grade, or megakaryocytic morphology. TN-PMF cases, however, showed fewer BM granulocytic elements and more frequent dyserythropoiesis. Cytogenetic analysis showed a higher incidence of trisomy 8 and a lower incidence of del 20q in TN-PMF. Targeted NGS showed a lower frequency of *ASXL1* mutations but an enrichment of *ASXL1/SRSF2* co-mutations in TN-PMF, a combination often associated with chronic myelomonocytic leukemia. However, both groups showed similar frequencies of *TET2*, *DNMT3A*, *IDH1/2*, *EZH2*, *TP53*, *ETV6*, *RUNX1*, *SRSF2*, *SF3B1*, *U2AF1*, *ZRSR2*, *SETBP1*, *CBL*, *RAS*, *KIT*, and *SH2B3* mutations (Figure 1). The median follow-up time was 26.4 months for TN-PMF and 81 months for DM-PMF. There was no statistically significant difference in overall survival.

Table 1. Demographic and clinicopathologic variables for both TN-PMF and control groups. Note: PB= Peripheral blood; BM= Bone marrow; M:E = Myeloid: Erythroid.

	TN-PMF	DM-PMF	P value
Age (median)	62	64	0.35
Male (%)	50.8	67.4	0.06
Organomegaly (%)	58.1	73.5	0.02
Treated with chemotherapy (%)	69	83.1	0.06
Underwent SCT	14	18.5	0.64
LDH (mean)	897	666	0.10
WBC (x 10 ⁹ /L, mean)	15.44	15.68	0.95
PB Granulocytes (% , mean)	61.11	64.33	0.16
PB Monocytes (% , mean)	5.64	6.39	0.42

PB Basophils (% , mean)	0.70	1.31	0.01
PB Basophils (x 10 ⁹ /L, mean)	0.08	0.23	0.05
PB Eosinophils (% , mean)	2.06	2.12	0.93
PB Lymphocytes (% , mean)	23.77	18.45	0.03
PB Lymphocytes (x 10 ⁹ /L, mean)	2.20	1.95	0.43
PB Blasts (% , mean)	1.01	0.71	0.34
Hemoglobin (g/dL, mean)	10.16	10.63	0.22
Platelets (x 10 ⁹ /L, mean)	366	427	0.37
BM Blasts (% , mean)	1.68	2.18	0.29
BM Eosinophils (% , mean)	1.96	2.64	0.31
BM Basophils (% , mean)	0.47	0.90	0.18
BM Monocytes (% , mean)	2.47	3.46	0.08
BM Granulocytes (% , mean)	36.46	59.51	<0.01
BM hypercellularity (%)	77	70.1	0.71
Increased M:E (%)	47.5	58.3	0.32
Increased Megakaryocytes (%)	91.5	82.8	0.37
MPN-like Megakaryocytes (%)	93.3	96.5	0.45
MDS-like Megakaryocytes (%)	22	26.1	0.70
MF2-3 reticulin fibrosis (%)	65.6	69.7	0.61
Dysgranulopoiesis (present, %)	5.1	5.6	1.00
Dyserythropoiesis (present, %)	7	0	0.04
Ring sideroblasts (present, %)	8.3	0	0.12
Dysmegakaryopoiesis (present, %)	16.4	11	0.46
Abnormal cytogenetics (%)	37	44	0.48
Trisomy 8 (%)	19	4	0.01
Del 20q (%)	8.5	16	0.048
Del 13q (%)	3	5	0.66
ASXL1 mutation (%)	18.5	38.1	0.025
ASXL1/SRSF2 co-mutation (%)	9.3	3.2	<0.01

Figure 1 – 667



Conclusions: Our findings demonstrated some clinicopathologic and molecular differences between TN-PMF and DM-PMF. TN-PMF cases are more likely to show dyserythropoiesis, less likely to have organomegaly, and more likely to show trisomy 8 and ASXL1/SRSF2 co-mutation. These findings, particularly the observed mutation profile characterized by enrichment of co-mutated ASXL1 and SRSF2, suggest that TN-PMF is biologically different from DM-PMF, with some features more akin to myelodysplastic/myeloproliferative neoplasms.

668 Decrease Granulocyte CD177 Expression in Myeloid Neoplasms is Associated with NPM1, RUNX1, TET2, and U2AF1 S34F Mutations

Khaled Alayed¹, Howard Meyerson²

¹King Saud University, Case Western Reserve University, University Hospitals/Case Medical Center, Aurora, IL, ²University Hospital Case Medical Center, Cleveland, OH

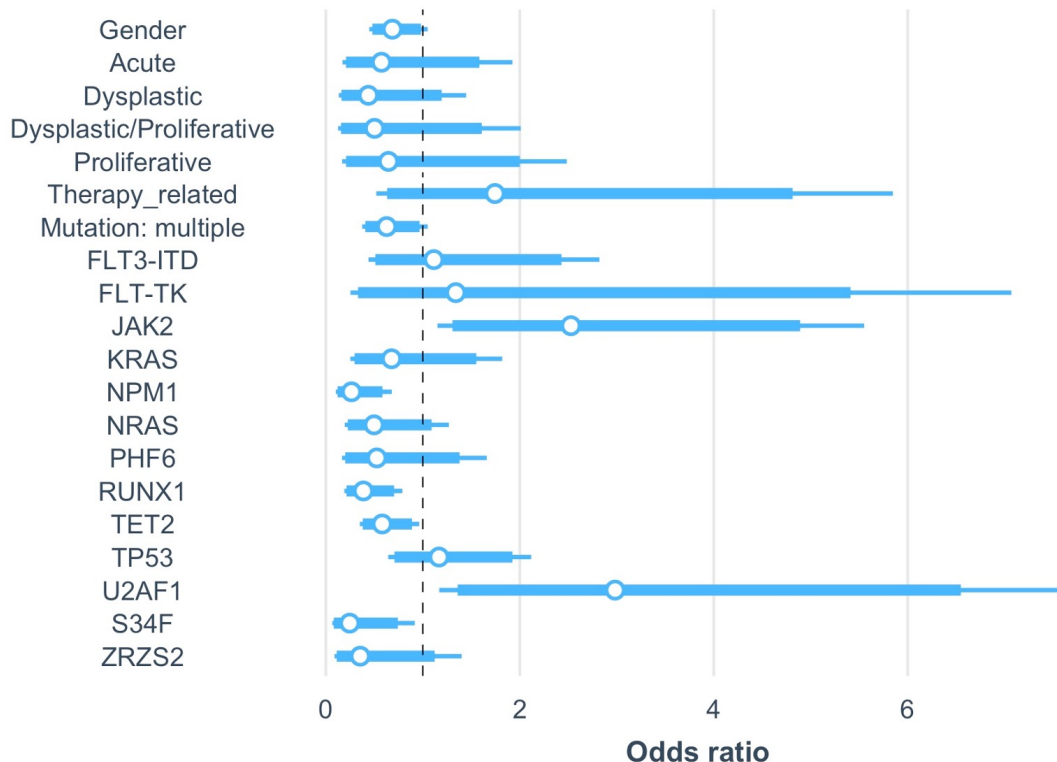
Disclosures: Khaled Alayed: None; Howard Meyerson: None

Background: Recently we published decreased percentage of CD177-positive granulocytes is a useful flow cytometry (FCM) marker correlated with myelodysplastic syndrome (MDS). The underlying molecular mechanisms leading to low percentage of CD177 expression in MDS have not been fully explained. The aim of this study was to investigate molecular mutations in myeloid neoplasms to identify potential molecular events associated with low expression of CD177.

Design: 507 myeloid neoplasms with one or more pathogenic molecular abnormality by NGS in which CD177 expression was assessed were collected. Cases were diagnosed according to the 2017 WHO classification and assigned into four different groups, ACUTE (167 cases) includes AML and MPAL cases, DYSPLASTIC (201) includes MDS, CCUS, CHIP and aplastic anemia with clonal hematopoiesis, PROLIFERATIVE (82) includes all MPN cases in any phase, DYSPLASTIC/PROLIFERATIVE (41) includes all MDS/MPN cases, and THERAPY-RELATED (16) includes all t-MN cases. CD177 expression was determined on CD16+CD11b+ granulocytes in all cases. Hot spot regions in genes evaluated by targeted next-generation sequencing (NGS) were ASXL1, BRAF, CALR, CBL, CSF3R, CEBPa, DNMT3A, ETV6, EZH2, FLT3-ITD, FLT3-TK, GATA-2, GNAS, IDH1, IDH2, JAK2, JAK3, C-KIT, KRAS, MPL, MYD88, NPM1, NRAS, PHF6, PTPN11, RUNX1, SETBP1, SF3B1, SRSF2, TET2, TP53, U2AF1, WT1, and ZRZS2.

Results: 39 variables include age, gender, disease group, presence of single or multiple mutations, and NGS gene mutations were used for analysis to determine any association with CD177 (40% cutoff for low/high percentage). 16 variables that were significant by univariate analysis. These were then tested in multivariate analysis (Fig 1). NPM1 (OD 0.26, 95% CI 0.11,0.63), RUNX1 (OD 0.39, 95% CI 0.19,0.75), TET2 (OD 0.58, 95% CI 0.36,0.94), and U2AF1 S34F (OD 0.25, 95% CI 0.06,0.77) mutations were associated with low CD177%. JAK2 (OD 2.5, 95% CI 1.2,5.6) and U2AF1 mutations other than S34F (OD 2.98, 95% CI 1.3,7.3) were associated with high CD177%.

Figure 1 - 668



Conclusions: There is a significant association between low CD177% and *NPM1*, *RUNX1*, *TET2* and *U2AF1* S34F mutations. The findings support low CD177% is an acquired alteration in granulocytes and points to potential molecular causes for the abnormality. The associated with *TET2* may account for the relatively high prevalence of low CD177% in MDS.

669 Increased Expression of GPR137 is Associated With Adverse Prognosis in AML

Emily Alvey¹, Amanda Kornfield², Deniz Peker¹

¹Emory University, Atlanta, GA, ²Emory University School of Medicine, Atlanta, GA

Disclosures: Emily Alvey: None; Amanda Kornfield: None; Deniz Peker: *Advisory Board Member, Seattle Genetics; Consultant, Georgia Composite Medical Boards*

Background: Acute myeloid leukemia (AML) is the most common acute leukemia in adults with a 5-year survival rate of only 50% in adults and less than 10% in elderly population. AML is an overly complex disease with multiple disease subtypes involving various chromosomal abnormalities and mutations. The abnormal epigenetics play an important role in the pathogenesis of AML. G protein-coupled receptor 137 (GPR137) is a lysosome controlling protein that plays a role in autophagy. It has been shown that downregulation of GPR137 inhibits proliferation of leukemic cells, enhances apoptosis and is a potential therapeutic target. We investigated GPR137 expression levels in adult AML and its impact on survival.

Design: Data used was retrieved from TCGA database downloaded from UALCAN. The analysis included AML cases categorized based on FAB Classification.

Results: Data included 173 cases of AML. FAB classification was available in 173 (figure 1). Age was available for all except one case, and 95 cases were 21 to 60 years of age while 77 cases were over 61 years. Male to female ratio was 1.2 (M=93, F=80). Majority of patients were Caucasian (n=156) with three African American and two Asian cases. Out of 16 AML-M3, PML-RARA status was available in 12; seven cases were negative and five cases were positive. There was no difference in GPR137 expression in PML-RARA positive and negative groups. Fifty

cases had FLT3 mutation while 116 were negative, and GPR137 expression levels were not significantly different in these two groups. GPR137 expression was statistically significant between age groups with higher expression in elderly (61 to 80 years; $p=0.049$). The overall survival was significantly decreased in cases with high expression of GPR137 ($p=0.038$, figure 2). The survival did not correlate with FLT3 status, gender, or race. Additionally, the analysis for correlated genes indicated that there was a positive correlation in expression levels between GPR137 and ATG2A, another autophagy gene (Pearson CC- 0.78).

Figure 1 - 669

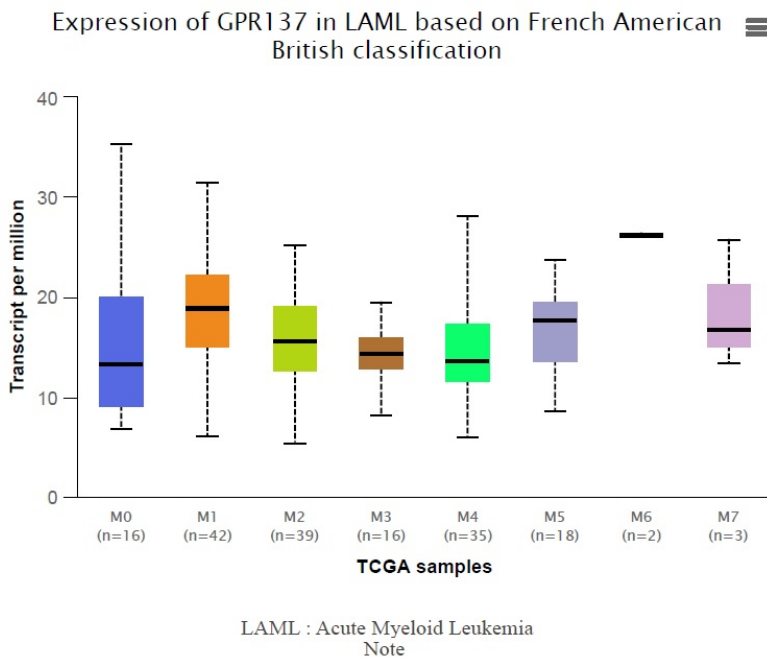
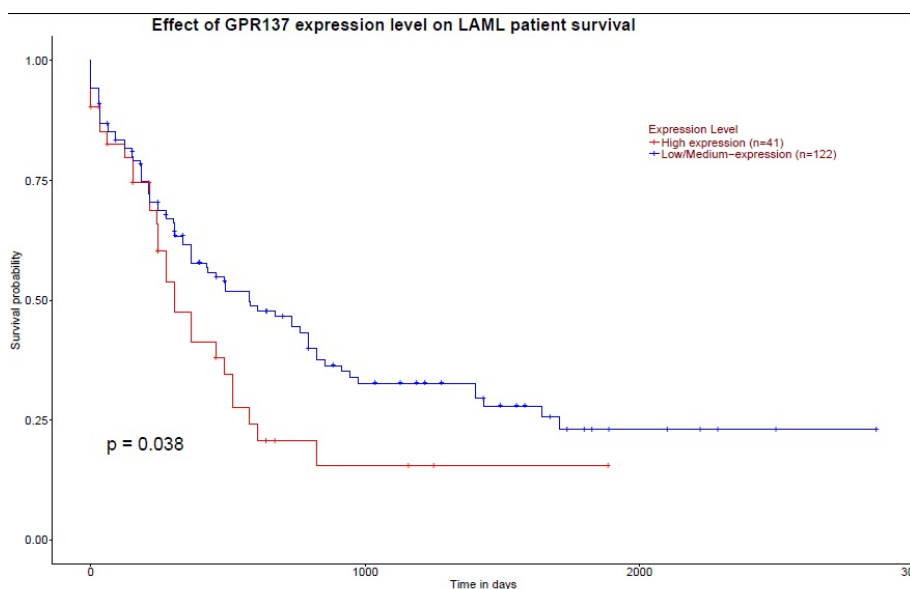


Figure 2 – 669



Conclusions: GPR137 gene plays a role in apoptosis, and increased expression levels result in adverse prognosis in AML independent of FLT3 status. Furthermore, the relationship between GPR137 and ATG2 genes has not been

studied to this date and such analysis may yield important information about autophagy activity in AML. Larger scale studies are warranted to better understand the pathophysiologic role of GPR137 in AML and develop potential targeted treatments.

670 Clinicopathologic Study of Myeloid/Lymphoid Neoplasms with Altered PDGFRA, PGDFRB, FGFR1 and PCM1-JAK2

Barina Aqil¹, Madina Sukhanova¹, Lawrence Jennings¹, Xinyan Lu¹, Yi-Hua Chen², Juehua Gao²

¹Northwestern University Feinberg School of Medicine, Chicago, IL, ²Northwestern Memorial Hospital, Chicago, IL

Disclosures: Barina Aqil: None; Madina Sukhanova: None; Yi-Hua Chen: None; Juehua Gao: None

Background: Myeloid/lymphoid neoplasms with *PDGFRA*, *PGDFRB*, *FGFR1* and *PCM1-JAK2* rearrangement are grouped together as a provisional category in the WHO Classification of Tumors of Hematopoietic and Lymphoid Tissue. Besides the detection of the rearrangements, risk-adapted therapy requires morphological, clinical evaluation, as well as better understanding of the accompanying genetic alterations in these entities, which are not well characterized.

Design: We identified 10 cases of myeloid/lymphoid neoplasms with *PDGFRA*, *PGDFRB*, *FGFR1* and *PCM1-JAK2* chromosomal rearrangements. In addition, we included 9 cases of myeloid/lymphoid neoplasms with mutations in the *PDGFRA*, *PGDFRB*, and *FGFR1* genes. Benign and likely benign variants were excluded. Clinical, pathologic and genetic information was collected (Table 1).

Results: Patients in our study include 14 males and 5 females with a median age of 66. Cases with *PDGFRA*, *PGDFRB*, *FGFR1*, and *PCM1-JAK2* presented as AML (n=4), MPN (n=4), T ALL (n=1), or aggressive B cell lymphoma (n=1). Five of 8 cases with *PDGFRA* or *PGDFRB* chromosomal rearrangements had no additional cytogenetic abnormalities. Two cases revealed gain of chromosome 8. Two cases with *FGFR1* and *PCM1-JAK2* rearrangements had complex karyotype. Next generation sequencing (NGS) detected variants in the genes commonly mutated in myeloid neoplasms (*i.e.* *DNMT3A*, *TET2*, *U2AF1*, *ASXL1*) in 4 of the 10 cases (2 *PDGFRA*, 1 *JAK2-PCM1*, and 1 *FGFR1*), additional mutations in common myeloid genes, including *DNMT3A*, *TET2*, *U2AF1*, *ASXL1* were identified. Three patients (1 AML with *PDGFRA*, 1 T ALL with *PDGFRA* and 1 AML with *PGDFRB*) died despite aggressive chemotherapy and stem cell transplant.

We also identified mutations in *PDGFRA* (2 t-MNs), *PGDFRB* (2 AML-MRC, 1 MDS-EB1 and 1 t-MN) and *FGFR1* (1 AML-MRC, 1 MPN and 1 Plasma cell neoplasm). Complex karyotypes were observed in 3 of 8 cases with available cytogenetic information, including 1 t-MN with *PDGFRA* mutation, 1 AML-MRC, and 1 t-MDS with *PGDFRB* mutations. All three patients died from disease. In 8 out of 9 cases, NGS identified additional mutations commonly present in myeloid neoplasms, such as *DNMT3A*, *TET2*, *NPM1*, *IDH2*, *JAK2*, *CALR*, and *RUNX1*. *TP53* was also identified in 3 cases (2 with *PDGFRA* variant and 1 with *PGDFRB* variant).

Case #	Age	Sex	Diagnosis	CBC	PDGFR/FGFR/PCM1-JAK2 abnormalities	Cytogenetics	Additional Molecular Findings	Treatment	Outcome	
1	71	M	Myeloid neoplasm with eosinophilia and PDGFR rearrangement	Leukocytosis with eosinophilia	PDGFR rearrangement	47,XY,-8[6]/46,XY[14]	TET2 p.S1039*, DNMT3A p.N797K, SH2B3 p.S488Y	Imatinib	Alive	
2	76	M	Acute myeloid leukemia with PDGFR rearrangement	Leukocytosis with 30% blasts, macrocytic anemia and thrombocytopenia	PDGFR rearrangement	46,XY,(4;12)(q12;p13)[20]	No mutations	Az+Vencix, Imatinib	In-Remission	
3	66	F	Acute myeloid leukemia with PDGFRB rearrangement	Pancytopenia	PDGFRB rearrangement	46,XX[20]	UZF1 p.S34F, BCOR p.W1629*, ASK1 p.V1471M, GATA2 p.L359V	azacitidine + venetoclax	Refractory to treatment, Deceased 9 months after diagnosis	
4	51	F	T lymphoblastic lymphoma with PDGFR rearrangement and focal neoplastic myeloid proliferation	Lymphadenopathy	PDGFR rearrangement	46,XX[13]	Not done	CHOP + 6 cycles, Imatinib and later SCT	Disease progression, deceased 6 months after diagnosis	
5	31	M	Myeloid neoplasm with eosinophilia and PDGFR rearrangement	Leukocytosis with eosinophilia	PDGFR rearrangement	46,XY[20]	Not done	Imatinib/dasatinib, nilotinib	Alive	
6	55	M	Acute myeloid leukemia arising in a myeloid neoplasm with eosinophilia with FIP1L1-PDGFR fusion	Leukocytosis with 20% blasts	PDGFR rearrangement	47,XY,+8[1]	46,XY[17]	Not done	Chemo+SCT	Deceased 8 months after diagnosis
7	70	M	Myeloproliferative neoplasm with eosinophilia associated with PDGFR rearrangement	Leukocytosis with eosinophilia	PDGFR rearrangement	46,XY[20]	Not done	On Imatinib	Alive	
8	46	M	Myeloproliferative neoplasm with eosinophilia associated with PDGFR rearrangement	Leukocytosis with eosinophilia	PDGFR rearrangement	Not performed	Not done	On Imatinib	Alive	
9	37	M	Aggressive B-cell neoplasm with PCM1-JAK2 rearrangement	Leukocytosis with lymphoma cells, no lymphadenopathy	PCM1-JAK2 rearrangement	46,XY,+1,del(1;3)(p12;p25),t(8;9)(p22;p24.1),der(9)t(8;9)(p22;p24.1)	IGL-MYC rearrangement, BRCA2 p.E1482*, CDKN2A p16INK4a R80*, p14ARF P94L	CODOX-M + IVAC with Rituxan; Vidaza+Venetoclax; nivolumab; SCT	Alive	
			Myeloid neoplasm consistent with acute myeloid leukemia with PCM1-JAK2 rearrangement	Leukocytosis with blasts		46,XY,(8;9)(p22;p24)[19]	Not done			
10	72	M	Myeloid neoplasm with PCM1-JAK2 rearrangement and AXL with MDS-IC and FGFR1	Leukocytosis with 67% blasts and eosinophilia	FGFR rearrangement	47,XY,-7,t(8;19)(p11.2;q13.3),+11,+15[20]	DNMT3A p.C541fs, ASK1 p.G1397s	Vyxeos	Alive	
11	72	F	Acute myeloid leukemia with myelodysplasia-related changes	Pancytopenia	PDGFRB p.S748L	46,XX,del(5)(q13q33)[5]/6,idem,der(16)t(16)(q21;q22)[5]/46,idem,add(1)(q32),der(16)t(16)(q21;q22)[5]/45,idem,add(1)(q32),der(1;2)(q10;q10),der(16)(t16)(q21;q22)[3]	None	Aza+Vidaza; Refractory	Deceased in 2 yrs after diagnosis	
12	60	M	Therapy-related myeloid neoplasm (8% blasts)	Pancytopenia	PDGFR p.Y574F	46,XY[15]	TP53 splice site 783-1G>T	Vidaza+SCT	Alive	
13	44	F	Acute myeloid leukemia with myelodysplasia-related changes	Leukocytosis with 40% blasts	FGFR1 p.L57M	46,XX,del(9)(q13q22)[5]/46,XX[25]	DNMT3A p.G685R and p.M801, MPL R120Q, TET2 P174H, IDH2 R140Q, NPM1 W2905*fs, PTPN11 G503R	Chemotherapy	Alive	
14	70	M	Acute myeloid leukemia with myelodysplasia-related changes transformed from MDS/MPN	Leukocytosis with 60% blasts	PDGFRB p.R459H	45,XY,-7[20]	DNMT3A p.M880T and p.R596P, RUNX1 D198G, DNMT3A Q356*, GATA2 S201fs*1, GATA2 P274fs*8, ASK1 G646fs*12, EZH2 T25fs*25, NRAS G12S, JAK2 V617F, IDH1 R132S	NA	Deceased; 2 months later	
15	76	M	Myelodysplastic syndrome with excess blasts (9% blasts)	Macrocytic anemia and thrombocytopenia	PDGFRB S408C	45,XY,-18]/46,XY[2]	RUNX1 S314fs*285, SF3B1 K700E	Decitabine + Sorafenib	Deceased 2 years later	
16	69	F	Therapy-related myelodysplastic syndrome with increased blasts (>10-15% blasts)	Anemia and thrombocytopenia	PDGFRB p.M544I	44,XX,del(4)(q28q34),der(5;7)(p10;p10),der(15;18)(q10;p10)[15]/44*45,idem,der(4)-,p,add(1)(p11.2),add(1)(3)(q12)[c4]/46,XX[11]	TP53 p.C141Y, TET2 p.S1591fs	NA	Deceased 2 months later	
17	69	M	Therapy related myeloid neoplasm with ring sideroblasts	Pancytopenia	PDGFR p.G467E	46,XY,der(5;7)(p10;p10),+8[13]/44,XY,der(5;7)(p10;p10),add(9)(p24,-21)[4],ish add(9)(p24)(RUNX1+1)/46,XY[3]	TP53 p.R342* and p.R213P	SCT	Deceased 1 year later diagnosis of MDS	
18	56	M	MPN (ET) with fibrosis	Longstanding history of ET	FGFR1 p.R675W	Not done	IDH1 p.R132H, CALR p.L367fs, SF3B1 K700E	SCT	Alive	
19	62	M	Plasma cell neoplasm	Thrombocytopenia	FGFR1 p.DL524EL	46,XY[19]	ASK1 p.G738*	Revlimid	Alive	

Conclusions: Myeloid/lymphoid neoplasms with *PDGFRA*, *PGDFRB*, *FGFR* and *PCM1-JAK2* rearrangement or mutations can present as a variety of hematologic neoplasms. Additional cytogenetic abnormalities were present in a subset of patients. Accompanying mutations involving other myeloid associated genes were usually present, and may play a role in response to the treatment and clinical outcome. Additional studies are needed to further elucidate the genetic complexity in these cases.

671 Interrogation of Immune-Response Dysregulation in Richter Transformation: Overexpression of LAG3 and Other Immune Checkpoint Molecules in Neoplastic B-Cells
 Amir Behdad¹, Matthew Schipma¹, Yi-Hua Chen², Qing Chen¹
¹Northwestern University Feinberg School of Medicine, Chicago, IL, ²Northwestern Memorial Hospital, Chicago, IL

Disclosures: Amir Behdad: *Speaker*, ThermoFisher; Matthew Schipma: None; Yi-Hua Chen: None; Qing Chen: None

Background: Richter transformation (RT) is aggressive progression of chronic lymphocytic leukemia (CLL), often to diffuse large B cell lymphoma (DLBCL), with poor prognosis and limited response to standard therapy. Our prior studies have shown differences in immune checkpoint molecule expression between RT and CLL; in particular, expression of programmed cell death 1 (PD1) in lymphoma cells and its ligands (PDL1) in background immune cells. Significantly, we have shown high PD1 expression in RT predicts its clonal-relatedness to CLL. Current investigation evaluates immune-response pathway dysregulation in RT utilizing NGS gene expression profiling.

Design: We studied 15 patients diagnosed with RT and 18 with CLL. We performed a 400-gene targeted NGS gene expression profiling on RT and CLL cases using the OncoPrint immune-response assay from ThermoFisher. Data analysis (RNA-seq with STAR and DESeq2) was done by aligning quality-sufficient reads to the human genome. Gene normalization and differential expression were calculated, adjusted p-values <0.05 considered significant. A pathway analysis was performed (Metascape) among the differentially expressed genes. We performed PD1 immunohistochemical (IHC) stain in all cases and LAG3 IHC on 14 RT and 7 CLL cases.

Results: Gene profiling analysis revealed significant difference in expression levels of 86 immune-response genes. The top upregulated genes in RT comparing to CLL included checkpoint pathway genes (PD-1, LAG3, TIM-3), Interferon/ cytokine signaling pathway genes (IL10, CCR1, IL1B, IL18, ICAM1), and innate immune-related genes (S100A9, S100A8). In addition to immune-response genes, MYC, TP63 and several cell proliferation pathway genes were upregulated in RT. The top down-regulated genes in RT compared to CLL included CD79B, checkpoint pathway gene CD160, T-cell regulation genes (KLF2, CD40LG) and CIITA, involved in interferon signaling. Interestingly, overexpression of checkpoint molecules is observed in PD1+ (defined by IHC) but not in PD1- RT cases. The latter are not clonally-related to CLL. To further confirm these findings we performed LAG3 IHC in a subset of cases. LAG3 was highly expressed by large neoplastic B-cell in PD1+ RT and only in scattered large cells in proliferation centers of CLL and largely negative in PD1- RT cases. Average positive neoplastic cells were 66% in PD1+ RT (n=10), 2.8% in PD1- RT (n=4), and 5.8% in CLL (n=7).

Figure 1 – 671

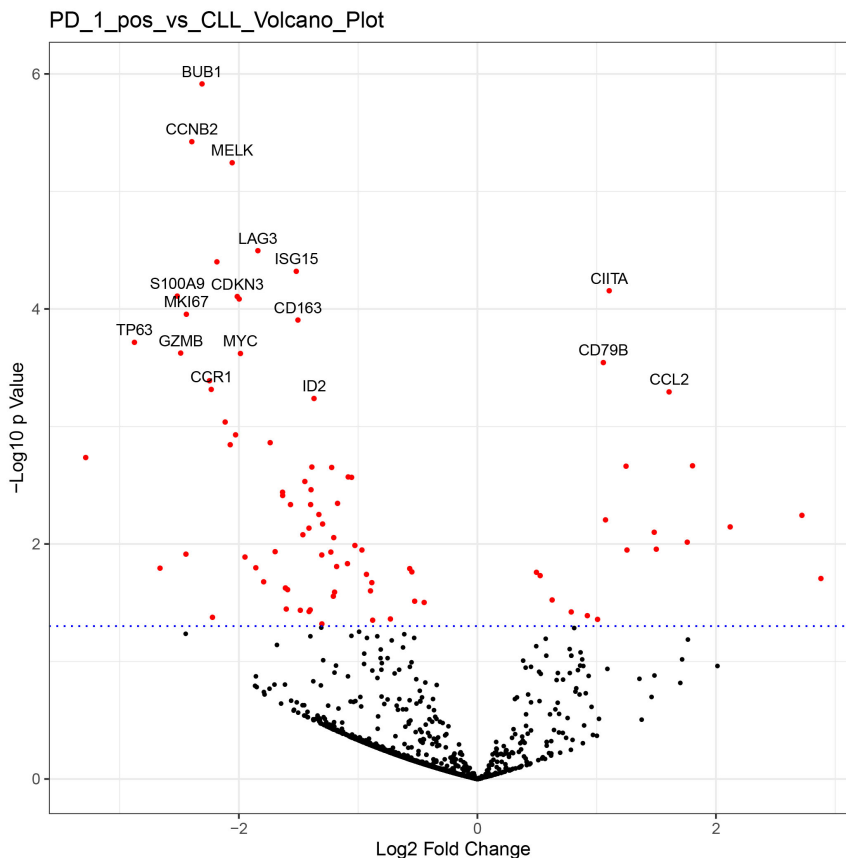
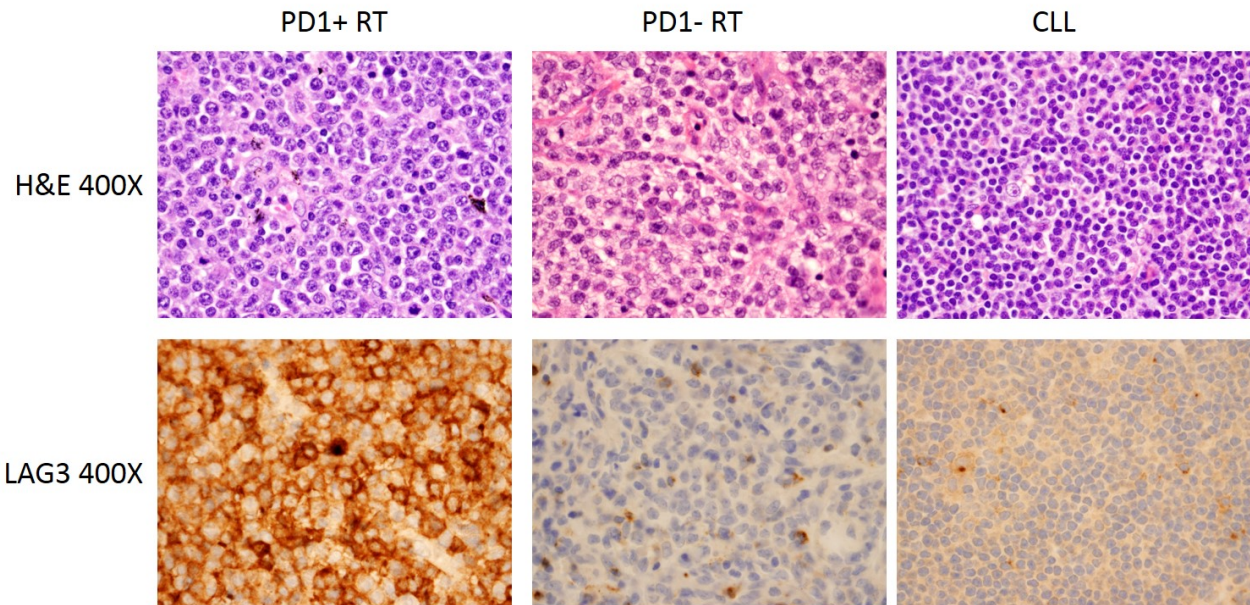


Figure 2 - 671



Conclusions: For the first time, we demonstrate a significant difference in expression of immune-response genes in RT vs CLL. In particular, we found upregulation in checkpoint pathway genes PD1, LAG3 and TIM-3. Overexpression of LAG3 in large neoplastic B-cells of RT, specifically in cases clonally-related to CLL is a novel finding that may serve as a diagnostic and prognostic marker. Furthermore upregulated checkpoint molecules LAG3 and TIM-3 could be new immune-therapy targets for this difficult-to-treat disease.

672 Molecular, Cytogenetic and Phenotypic Studies Highlight a Subset of Adult B-Lymphoblastic Leukemia/Lymphomas That More Closely Resembles Mature High Grade B-Cell Lymphomas

Shweta Bhavsar¹, Yen-Chun Liu², Svetlana Yatsenko¹, Steven Swerdlow²

¹University of Pittsburgh Medical Center, Pittsburgh, PA, ²University of Pittsburgh School of Medicine, Pittsburgh, PA

Disclosures: Shweta Bhavsar: None; Yen-Chun Liu: None; Svetlana Yatsenko: None; Steven Swerdlow: None

Background: The distinction between mature B-cell lymphomas (BCL) with partial TdT expression or which transform to a TdT+ neoplasm and true B-lymphoblastic leukemias/lymphomas (B-LBL) has become blurred with some suggesting that the latter cases should be segregated from the former cases. Our previous study looking at mature B-cell lymphomas (BCL) with partial TdT expression suggested a mutational profile more like mature BCL. In order to further investigate this potential heterogeneity among cases we currently diagnose as B-LBL in adults, a multiparameter investigation of 41 adults with overt B-LBL was undertaken and the CD34- cases (known to be enriched in mature BCL with TdT) studied in greater detail for their mutational landscape.

Design: 41 adult patients with B-LBL were identified after excluding any with *BCR-ABL1*. Morphologic preparations of PB/BM (41), lymph node (1), and pleural fluid (1), PB and BM blast counts, flow cytometric, immunohistologic and cytogenetic studies including array CGH and clinical data including follow-up were reviewed. Based on a prior study, CD34- cases with available material had targeted NGS mutational analysis, array CGH (if not already performed) and IGH mutational studies.

Results: The 41 patients were 28-82 yrs old with M:F 20:21 and median BM blast count of 84% (Table 1). All but one case had either unmutated IGH or was indeterminate. 13/41 B-LBL were CD34- and of those, 4/13 had *MYC* rearranged (R) (3 also *BCL2R*) vs. 0/19 CD34+ cases ($p < 0.05$). 3 CD34- cases were known transformations from definite or probable follicular lymphoma (2) or DLBCL (1). The CD34- cases were more likely

to have CD20 expression by flow cytometry, IRF4/MUM1 expression, Ki-67>75%, a complex karyotype and showed a trend for a worse survival (Table 1). Four CD34+ cases and 1 CD34- case showed t(4;11). Among the CD34- cases studied, all of the *CREBBP*, *BCL2* and *KMT2D* mutations were found among *MYC* R cases and the 4 cases with *NRAS* mutation were all *MYC*R negative (Figure 1).

Table 1. Clinicopathologic and phenotypic findings in B-LBL based on CD34 expression.

Feature	Overall (38-41)	CD34 neg (11-13)	CD34 pos (27-28)
Age, yrs, med (range)	54 (28-82)	61 (31-82)	53 (28-73)
Gender, M:F	20:21	6:07	14:14
WBC x10 ⁹ /L, med (range)	4.5 (0.4 – 435)	6.65 (1.4 – 84.3)	3.5 (0.4 – 435)
BM blasts, %, med (range)	84 (10 – 99)	89.2 (10 – 96.7)	78.3 (31.3 – 99)
PB blasts, %, med (range)	23 (0-92.5)	49.5 (0-82)	14 (0-92.5)
CD20+ by flow*	66%	92%	54%
CD19+ by flow	100%	100%	100%
CD10+ by flow	78%	92%	71%
CD45+ by flow	73%	85%	68%
CD38+ by flow	92%	100%	89%
K+ or L+ by flow	7%	8%	7%
CD13+ by flow	33%	17%	41%
CD33+ by flow	32%	27%	33%
CD 20+ by IHC	64%	75%	59%
CD10+ by IHC	82%	92%	78%
BCL6+ by IHC	10%	17%	7%
IRF4/MUM1+ by IHC***	23%	50%	11%
MYC >40% by IHC	59%	75%	52%
MYC >70% by IHC	21%	33%	15%
BCL2 >70% by IHC	93%	92%	93%
Ki67 > 75% by IHC*	26%	50%	15%
Cytogenetics Complex**	25%	54%	11%
Median survival, months	21	14	38

K-kappa, L-lambda, *p<0.05,** p<0.02; ***p=0.01

Figure 1 - 672

Figure 1. Mutational landscape of *MYC* rearrangement (R) positive and negative CD34 Negative B lymphoblastic leukemia/ lymphoma

Gene	Overall %	<i>MYC</i> R pos (n=3)	<i>MYC</i> R neg (n=9)
<i>TP53</i>	42%	1	4
<i>NRAS</i>	33%	0	4
<i>CREBBP</i> *	17%	2	0
<i>KRAS</i>	17%	1	1
<i>SBDS</i>	17%	1	1
<i>DNMT3A</i>	8%	0	1
<i>PTPN11</i>	8%	0	1
<i>DDX41</i>	8%	0	1
<i>IDH1</i>	8%	0	1
<i>DIS3</i>	8%	0	1
<i>CHEK2</i>	8%	1	0
<i>KMT2D</i>	8%	1	0
<i>SOCS1</i>	8%	1	0
<i>BCL2</i>	8%	1	0
<i>PIM1</i>	8%	1	0
<i>SH2B3</i>	8%	1	0

*p<0.05

Conclusions: As supported by the mutational studies even in these limited number of cases, adult B-LBL includes a subset of cases which appear to be more closely related to transformed mature B-cell lymphomas and the large B-cell lymphomas with partial TdT positivity rather than to classic B-LBL, even if a history of a prior low-grade lymphoma is lacking. The most convincing cases were CD34- with *MYC* R, and had mutations often associated with mature BCL. It is difficult to determine how many of the CD34- cases lacking *MYC* rearrangements might be similar to this most definite subset with the CD34+ cases the most different. Although currently the combination of *MYC* rearrangement and CD34 negativity appear to be the best way to identify these distinctive cases, additional studies are required to determine the best criteria for their recognition.

673 B-cell Enriched Tumor Microenvironment Predicts Favorable Prognosis in Angioimmunoblastic T-cell Lymphoma (AITL)

Jeffrey Cannatella¹, Sunandini Sharma¹, Alyssa Bouska¹, Timothy Greiner¹, Francesco Damore², Martin Pedersen², Choon Kiat Ong³, Andreas Rosenwald⁴, German Ott⁵, Julie Vose¹, Dennis Weisenburger⁶, Wing Chan⁶, Javeed Iqbal¹, Catalina Amador⁷

¹University of Nebraska Medical Center, Omaha, NE, ²Aarhus University Hospital, Aarhus, Denmark, ³National Cancer Centre Singapore, Singapore, Singapore, ⁴Universität Würzburg, ⁵Robert-Bosch-Krankenhaus, Stuttgart, Germany, ⁶City of Hope National Medical Center, Duarte, CA, ⁷University of Nebraska, Omaha, NE

Disclosures: Jeffrey Cannatella: None; Sunandini Sharma: None; Alyssa Bouska: None; Timothy Greiner: None; Francesco Damore: None; Martin Pedersen: None; Choon Kiat Ong: None; Andreas Rosenwald: None; German Ott: None; Julie Vose: None; Dennis Weisenburger: None; Wing Chan: None; Javeed Iqbal: None; Catalina Amador: None

Background: AITL is a neoplasm of T follicular helper (TFH) cells with a prominent inflammatory tumor microenvironment (TME). Using gene expression profiling (GEP), we demonstrated that AITL with high B-cell signatures have superior outcomes, whereas cases with dendritic cell/macrophage-rich TME have inferior survival. We used immunohistochemistry (IHC) to validate the GEP-defined prognostic role of the TME in AITL and developed practical IHC prognostication parameters.

Design: We analyzed 204 AITL cases using CIBERSORT, an *in-silico* computational program to deconvolute the cellular components from the bulk GEP (n=129) or RNA-seq data (n=75). Dividing the cases into high and low B-cell signature groups showed an association with overall survival (OS) (p<0.01). To validate the findings, we evaluated 39 cases with GEP and/or RNAseq data and available FFPE tissues for B-cell (CD20), plasma cell (CD138), TFH (PD-1, ICOS), macrophage (CD68) and follicular dendritic cell (CD21) markers, KI67, PDL-1 and EBER in situ hybridization. The IHC slides were evaluated using *QuPath*, digital image analysis software. The CD20 slides were also manually assessed by two pathologists. A CD20 threshold to categorize the cases as B-cell rich or B-cell depleted was derived using the GEP-defined high and low B-cell subgroups. We subsequently evaluated the CD20 expression and performance of the derived threshold in an independent validation series (n=31) without GEP or RNA-seq data.

Results: A significant difference in CD20 expression by manual scoring (50% vs. 20%, p<0.001) and by image analysis (50% vs. 44%, p=0.01) was observed between the GEP-defined high and low B-cell groups. The CD20 percent positivity correlated with the corresponding mRNA expression (r=0.6), and showed high inter-observer correlation (r=0.82). Similar expression of KI67, PDL1 and other TME components was found between high and low B-cell groups. There was no significant difference in TFH marker expression, suggesting similar tumor burden between high and low B-cell groups.

Using a >30% positive cutoff for CD20 positivity, 31 of 39 (79%) cases were accurately classified as B-cell rich or depleted when compared to the GEP/RNA-seq data. B-cell rich cases by IHC were significantly associated with a superior OS in both the training and validation cohorts (p<0.05).

Conclusions: We have confirmed that clinical outcome is correlated with the TME in AITL and have demonstrated by IHC that abundant B-cells in the TME are associated with a good prognosis.

674 Significance of MYD88 L265P Mutation Status and EBV Latency Programs in Primary Central Nervous System Lymphoproliferative Disorders in Immunocompromised and Immunocompetent Individuals

Miguel Cantu¹, Samuel Yamshon¹, Sarah Rutherford¹, Raphael Mwangi², Thomas Habermann², Rebecca King², Michael Kluk³, Amy Chadburn³

¹New York-Presbyterian/Weill Cornell Medical Center, New York, NY, ²Mayo Clinic, Rochester, MN, ³Weill Cornell Medical College, New York, NY

Disclosures: Miguel Cantu: None; Samuel Yamshon: None; Sarah Rutherford: *Consultant*, Juno/Celgene; *Consultant*, Kite; *Consultant*, Karyopharm; *Primary Investigator*, Karyopharm; *Primary Investigator*, Genentech; Raphael Mwangi: None; Thomas Habermann: None; Rebecca King: None; Michael Kluk: None; Amy Chadburn: None

Background: Myeloid differentiation factor 88 (MYD88) L265P is a “hotspot” somatic mutation that accounts for ~90% of known MYD88 mutations and is associated with lymphomas occurring in immune privilege sites, including primary CNS lymphomas (PCNSL). MYD88 L265P has been shown to have a role in DLBCL subtyping and predicting response to ibrutinib therapy in some lymphomas. The status of MYD88 in PCNSL has been largely studied in immunocompetent (IC) patients, but not in CNS lymphoproliferative lesions (PCNS-LPDs) from immunocompromised individuals, i.e. post-transplant and HIV+ patients. As the PCNS-LPDs from immunocompromised patients are largely Epstein Barr virus (EBV) positive, the relationship of the EBV latency genes and MYD88 mutations in the pathogenesis of these lesions is unknown.

Design: The 78 PCNS-LPDs (all B cell origin), including 32 PTLDs (1998-2020), 10 HIV-LPDs (1997-2018; absolute CD4 count 1-70 cells/uL) and 36 IC- PCNSLs (2007-2020), were classified by 2017 WHO criteria. Genomic DNA was extracted from FFPE tissues to assess MYD88 L265P mutation status by quantitative digital droplet PCR (75 cases; 31 PTLDs, 9 HIV-LPDs, 35 PCNSLs). IHC was performed on FFPE tissues to assess cell of origin by the Hans criteria (78 cases: CD10, BCL6, MUM1). EBV status was determined by EBER ISH (latency 1/2/3) and IHC for LMP1 (latency 2/3), EBNA2 (latency 3). Continuous and nominal variables were compared with Fisher exact test and Kruskal-Wallis test, respectively.

Results: All PTLDs and 9/10 HIV-LPDs were EBV+ (Table 1). 31/32 (97%) of PTLDs were EBV latency 2/3, polymorphic lesions. Only one PTLD was EBV latency 0/1 and monomorphic (DLBCL). 9/10 (90%) of HIV-LPDs were EBV latency 2/3 and 8/10 were DLBCL. 35/36 of IC-PCNSLs were EBV negative DLBCLs. All PTLDs were MYD88 Wild Type. 24/36 (66.7%) of IC-PCNSLs were MYD88 L265P+. Both MYD88 L256P+ HIV-LPDs were EBV+, latency 3. All PTLDs and HIV-LPDs, and 28/36 (78%) of IC-PCNSLs were non-GC. GC lesions (CD10+) were seen only in the IC group (22%). Survival was poor, particularly in the PTLD (5.2 mo, $p=0.0112$) and HIV+ (2.5 mo, $p=0.0296$) patients compared to IC (96.9 mo). MYD88 L265P status did not correlate with poor survival ($p=0.0839$) but EBV status (EBV+, latency 2/3) did ($p=0.0017$).

Table 1. Clinicopathologic Features of Primary CNS Lymphoproliferative Disorders

	Immunocompetent	Immunosuppressed (PTLD; HIV-LPD)	p-Value
	N=36	N=42 (32; 10)	
B Cell Origin, no.	36	42	>0.9999
Polymorphic Morphology, no.	1	33 (31; 2)	<0.0001****
Monomorphic, DLBCL Morphology; no.	35	9 (1; 8)	–
CD10+; no.	8	0	0.001***
BCL6+; no.	34	14 (13; 1)	<0.0001****
MUM1+; no.	36	42	>0.9999
non-GC; no.	28	42	0.0013**
EBER+; no.	1	41 (32; 9)	<0.0001****
EBV Latency 0/1; no.	0	1 (1; 0)	–
EBV Latency 2/3; no.	1	40 (31; 9)	–
MYD88 L265P; no. (N=75)	24	2 (0; 2)	<0.0001****
Sex, Male; no.	17	21 (13; 8)	0.8243
Age, Years; Median	70 (22-90)	45.5 (8-73)	<0.001****
Absolute Lymphocyte Count, 10 ³ /uL; Median (N=62)	1.3 (0.4-13.4)	0.5 (0.08-2.4)	0.0003***
LDH, U/L; Median (N=53)	185 (82-287)	244 (72-612)	0.0008***
PTLD Median Survival (Months)	–	5.2	0.0112*

HIV-LPD Median Survival (Months)	–	2.5	0.0296*
IC-PCNSL Median Survival (Months)	96.9	–	–
MYD88-WT vs L265P Median Survival (Months)	11.4 vs 245		0.0839
EBV- vs EBV+ Median Survival (Months)	96.9 vs 4.01		0.0017**
no.= number; non-GC= non-germinal center (Hans criteria); LDH= lactate dehydrogenase, IC= immunocompetent, WT= wild type			

Conclusions: PCNS-LPDs are aggressive with worse survival in immunosuppressed patients. MYD88 L265P is much more frequent in IC-PCNSLs (most DLBCLs) and rare in immunocompromised PCNS-LPDs (most polymorphic LPDs). These latter lesions are EBV+, latency 2/3, and thus are likely driven by EBV (LMP1-NFκB pathway; LMP2-survival signals). The presence of MYD88 L265P in most IC-PCNSLs suggests a role for targeted therapy, while restoring immune competence may be more effective for immunosuppressed patients.

675 IRTA1 Positivity in Primary Cutaneous Marginal Zone Lymphomas (PCMZL) Is Uncommon and Associated with IgM+ Cases and with Monocytoid B-Cell Morphology

Eric Carlsen¹, James Cook², Steven Swerdlow³

¹University of Pittsburgh Medical Center, Pittsburgh, PA, ²Cleveland Clinic, Cleveland, OH, ³University of Pittsburgh School of Medicine, Pittsburgh, PA

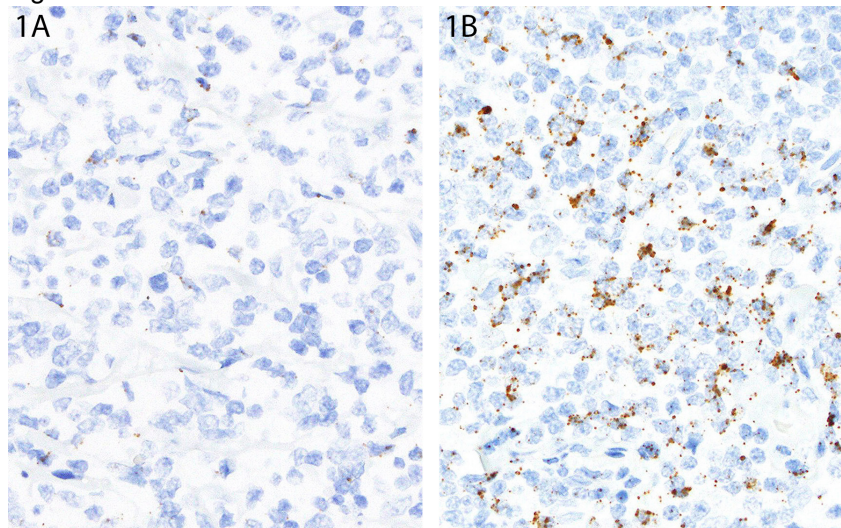
Disclosures: Eric Carlsen: None; James Cook: None; Steven Swerdlow: None

Background: PCMZL include 2 major subsets, a dominant class-switched subset which has several features different from many other MALT lymphomas, and an IgM+ subset which resembles other MALT lymphomas more closely. One of the distinctive features of marginal zone lymphomas (MZL) including MALT lymphomas is their common, although not invariable, expression of IRTA1, an Ig-like protein with B-cell signaling functions that is expressed by benign monocytoid B-cells and some marginal zone B-cells. Although much less specific, many MZL also express MNDA, a myelomonocytic transcriptional regulator. The expression of IRTA1 and MNDA in PCMZL and whether they would further support the distinctive nature of the 2 subsets is unknown.

Design: 24 PCMZL were stained for Ig heavy and light chains (HC/LC) and MNDA by IHC. IRTA1 expression was assessed by in situ hybridization. IRTA and MDNA staining was assessed as absent, positivity <20% and ≥20% positive cells. The findings were correlated with the results of HC/LC staining and histopathologic characteristics. 3 patients had >1 biopsy with different HC/LC expression, which were considered separately for analysis.

Results: All cases showed some MNDA positivity with 14/19 class-switched cases and 4/5 IgM+ cases showing ≥20% positive cells. 3/18 class-switched cases showed at least some IRTA1 positivity versus 4/5 IgM+ cases (p=0.009). Only 4 PCMZL (2 IgM+, IgA+, IgG+) showed ≥20% IRTA1+ cells. These 4 cases demonstrated monocytoid B-cell areas vs. none of the other cases (p<0.00001, Phi coefficient). The two biopsies with the greatest proportion of IRTA1+ cells (1 IgG+ and 1 IgM+) were metachronous lesions from the same patient.

Figure 1 - 675



1A: PCMZL with only rare IRTA1+ cells (<5%). 1B: PCMZL with more numerous IRTA1+ cells.

Conclusions: These findings lend further support to the distinctive nature of the two subsets of PCMZL and the greater similarity of IgM+ cases to other MALT lymphomas. The low proportion of positive cells in some cases may relate to a low proportion of neoplastic cells being present. However, the results are also consistent with our prior suggestion that these 2 PCMZL subsets are probably not defined solely by their heavy chain staining. The association of marked IRTA1 positivity with monocytoid B-cell morphology is consistent with prior observations with IRTA1 and suggests this subjective feature might be of additional significance in the subcategorization of PCMZL. Frequent MND4 expression in both class-switched and IgM+ cases appears to mirror expression patterns in in many MZL and other non-follicular small B-cell lymphomas.

676 Mutational Differences Between EBV-Negative and EBV-Positive HIV-Associated Diffuse Large B-cell Lymphomas

Jennifer Chapman¹, Alyssa Bouska², Weiwei Zhang², Juan Alderuccio³, Izidore Lossos⁴, Shuhua Yi⁵, Wing Chan⁶, Francisco Vega⁷, Joo Song⁶

¹University of Miami, Miller School of Medicine, Miami, FL, ²University of Nebraska Medical Center, Omaha, NE, ³University of Miami/Jackson Memorial Hospital, Miami, FL, ⁴University of Miami/Sylvester Cancer Center, FL, ⁵City of Hope Medical Center, Tianjin, China, ⁶City of Hope National Medical Center, Duarte, CA, ⁷The University of Texas MD Anderson Cancer Center, Houston, TX

Disclosures: Jennifer Chapman: None; Alyssa Bouska: None; Weiwei Zhang: None; Juan Alderuccio: None; Izidore Lossos: None; Shuhua Yi: None; Wing Chan: None; Francisco Vega: *Speaker*, Society of Hematology Oncology; *Grant or Research Support*, CRISP Therapeutics; *Speaker*, i3Health; Joo Song: None

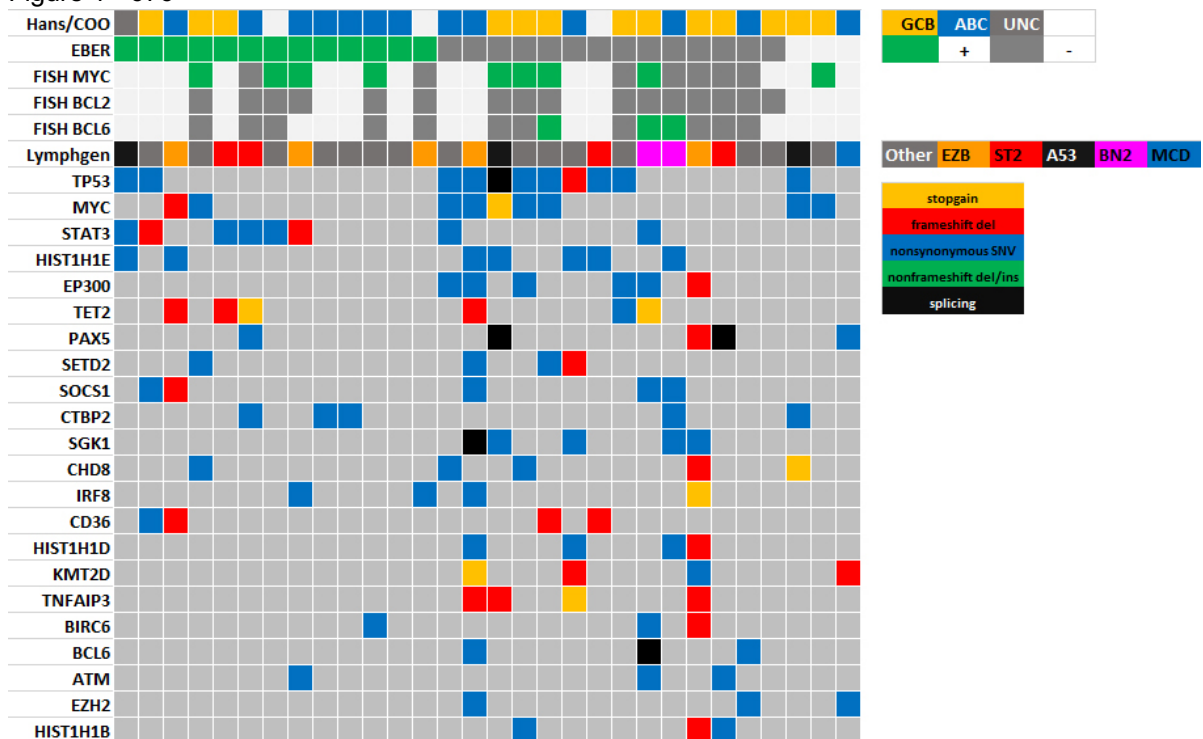
Background: Patients with HIV have a significant risk for developing non-Hodgkin lymphoma, most commonly diffuse large B-cell lymphoma (DLBCL). EBV is more frequently seen in HIV-associated DLBCL (HIV DLBCL) compared to DLBCL occurring in immunocompetent hosts. We sought to understand the genomic profile of HIV DLBCL as well as compare EBV-positive and EBV-negative cases.

Design: We identified cases of HIV DLBCL from two medical centers. Burkitt lymphoma or high grade B-cell lymphoma, NOS were excluded. Cases were characterized by immunophenotype (IHC), EBV status as determined by EBER-ISH, FISH analysis, cell of origin (COO) by gene expression profiling/IHC, and targeted deep sequencing using a custom mutation panel of 334 genes. We also applied the Lymphgen tool (Wright et al. Cancer Cell 2020) to determine the genetic subtype of DLBCL.

Results: We identified 30 cases of HIV DLBCL. The median age was 46 years, male:female ratio 5. 13 cases (48%) were EBV-positive and 14 (52%) were EBV-negative. Fourteen cases (48%) were GCB, 13 (48%) were

ABC, 1 case (4%) was unclassified and three cases had insufficient material. Of 16 cases analyzed by FISH for *BCL2*, *BCL6*, and *MYC* rearrangements, 9 cases (56%) showed a *MYC* rearrangement, of which 4 (44%) were EBV positive. None of the cases had *BCL2* translocations, while 3 cases (19%) had *BCL6* rearrangements, 2 of which were double-hit *MYC/BCL6*. Using the Lymphgen tool, the majority of cases were classified as other (50%) with the rest of the groups representing ST2 (13%), EZB (17%), A53 (10%), BN2 (7%), and MCD (3%). The mutation spectra between EBV-positive and EBV-negative HIV DLBCL showed mutational differences. The EBV-positive cases showed a higher proportion of *STAT3* mutations as compared to EBV-negative DLBCL (46% vs 14%; P=0.10) while the EBV-negative HIV DLBCL showed a higher number of *TP53* mutations (57% vs 15%; P=0.046), *MYC* mutations (36% vs 15%; P=0.38), *SGK1* (36% vs 0%; P=0.04), *EP300* (43% vs 0%; P=0.02) and histone modifying genes (e.g. *HIST1H1E*, *HIST1H1D*) (79% vs 31%; P=0.02) compared to EBV-negative cases. EBV was more frequent in patients with lower CD4 counts at diagnosis (median 46.5 vs 101)(p=0.018). Although not statistically significant, overall survival did show a trend of being worse in EBV positive cases (p=0.11).<

Figure 1 - 676



Conclusions: We find that *MYC* rearrangements are frequent in HIV DLBCL, but occur nearly equally in EBV positive and negative cases. *BCL2* translocations were not seen. We find that *STAT3* mutations are more frequent in EBV-positive HIV DLBCL while EBV-negative cases have a higher proportion of *TP53*, *MYC*, *SGK1*, and histone modifying gene mutations similar to *de novo* DLBCL. EBV positivity in HIV DLBCL correlates with lower CD4 count at diagnosis, and worse OS, indicating that the state of an HIV positive patient’s immune status at the time of lymphoma diagnosis matters. These findings elucidate the heterogeneous biology of HIV DLBCL and show that EBV-positive HIV DLBCL appears to be unique.

677 Clinicopathological Features of Hyper eosinophilic Patients with An Activating STAT5B N642H Mutation

Jinjun Cheng¹, Xiaoping Sun², Amy Klion³, Irina Maric⁴
¹Icahn School of Medicine at Mount Sinai, New York, NY, ²Clinical Center, National Institutes of Health, ³National Institute of Allergy and Infectious Diseases, National Institutes of Health, ⁴National Institutes of Health, Bethesda, MD

Disclosures: Jinjun Cheng: None; Xiaoping Sun: None; Amy Klion: None; Irina Maric: None

Background: Eosinophilia is common in clinical practice. Identifying the cause of eosinophilia is critical for patient management. A recent study identified the presence of a *STAT5B N642H* oncogenic mutation in a subset of patients with hypereosinophilia. Systematic study is needed to better characterize the clinical features, including prognosis and response to therapy, in this patient subset.

Design: We used competitive allele-specific TaqMan PCR (CastPCR) to screen 40 adult patients enrolled on a natural history trial to study eosinophilia (NCT00001406). We identified two cases with *STAT5B N642H* mutations and investigated their clinical, hematological, and histopathological features.

Results: *STAT5B N642H* mutations were detected in only 2/40 patients with hypereosinophilic syndromes. However, both patients demonstrated complex combinations of molecular and histopathological findings that presented diagnostic classification and treatment challenge.

The first patient (75 year-old female) presented with persistent hypereosinophilia, basophilia, thrombocytosis and mild anemia. CastPCR identified a *STAT5B N642H* mutation with 48.3% VAF. Additional molecular studies, including NGS assay using a 141-gene targeted myeloid panel (Qiagen) revealed *SF3B1 K666N* (49% VAF), *TP53 G244D* (14% VAF) and *BCR V1094fs*17* (12%VAF) mutations. Cytogenetic study revealed 46, XX, del(20)(q11.2) in 6/20 metaphases. The marrow biopsy showed hypercellularity, increased dysplastic megakaryocytes and markedly increased dysplastic eosinophils. Mast cells were normal. Iron staining revealed numerous ring sideroblasts and no increase in blasts. She failed multiple therapies and repeat bone marrow biopsies showed no significant improvement. The patient expired of respiratory failure five years after diagnosis.

The second patient (81 year-old male) presented with persistent hypereosinophilia, absolute monocytosis and thrombocytosis. CastPCR detected a *STAT5B N482H* mutation with 64.2% VAF. In addition, *KIT D816V* (1.3% VAF), *U2AF1 S34Y* (45% VAF) and *TET2* (0.5%) mutations were detected. Cytogenetic analysis revealed loss of Y chromosome in 19/20 metaphases. The marrow biopsy showed marked hypercellularity with increased megakaryocytes and increased eosinophils, but no dysplasia. Mast cells were mostly spindle-shaped and positive for CD25, but were not significantly increased. Serum tryptase was not increased. Blasts were not increased. 12-month follow-up revealed disease progression with a marked increase in eosinophils.

Conclusions: *STAT5B N642H* mutations were identified in 2/40 (5%) hypereosinophilic patients studied. Both patients had unusual, complex combinations of histopathological and molecular features and poor clinical outcomes.

678 Deep Optical Blood Analysis: COVID-19 Detection as a Case Study in Next Generation Blood Screening

Colin Cooke¹, Kanghyun Kim¹, Shiqi Xu¹, Xing Yao¹, Xi Yang¹, Carolyn Glass², Jadee Neff², Patricia Pittman³, Chad McCall¹, Xiaoyin “Sara” Jiang¹, Roarke Horstmeyer¹

¹Duke University, Durham, NC, ²Duke University Medical Center, Durham, NC, ³Duke University School of Medicine, Durham, NC

Disclosures: Colin Cooke: None; Kanghyun Kim: None; Shiqi Xu: None; Xing Yao: None; Xi Yang: None; Carolyn Glass: None; Jadee Neff: None; Patricia Pittman: None; Chad McCall: None; Xiaoyin “Sara” Jiang: None; Roarke Horstmeyer: *Stock Ownership*, Ramona Optics Inc.; *Stock Ownership*, SafineAI Inc.

Background: Converging evidence suggests that COVID-19 infections can be detected through analysis of peripheral blood smears. Simultaneously, the use of digital slide scanners within pathology labs and hospitals has been rapidly increasing; nearly 50% of pathologists currently analyze digital slides.

This presents an opportunity to test modern deep-learning-based image analysis methods, which provide a powerful, data-driven approach to automated screening. Not only do deep learning systems offer the opportunity to detect previously undetectable diseases, but recent work has also shown that they can replicate nearly every functionality provided by automated complete blood count (CBC) machines.

Design: We collected two datasets of digitized peripheral blood smears. The first dataset (Group A) included 236 patients admitted to the hospital, 53% of whom tested positive for COVID-19 (using a RT-PCR based test). Other than their test results, no other information about Group A patients was recorded. The second dataset (Group B) included 40 patients who were hospitalized with COVID-19-like symptoms, but tested negative for the virus. We cropped images of white blood cells from the peripheral smears for each patient, yielding an average of 130 images per patient.

We trained a neural network on COVID-19 positive and negative patients to predict the infection status of each patient from white blood cell images alone. The results from individual cells were then combined to provide a per-patient screening metric. We compared our ability to differentiate between positive and negative patients by sweeping the trade-off between true and false positive rates.

Results: Our machine learning based system was able to effectively differentiate between those infected, and uninfected with COVID-19 within both groups. We achieved an *Area Under the Curve (AUC)* of 0.91 for Group A and 0.84 for Group B, or effective average accuracies of 88% and 84% respectively.

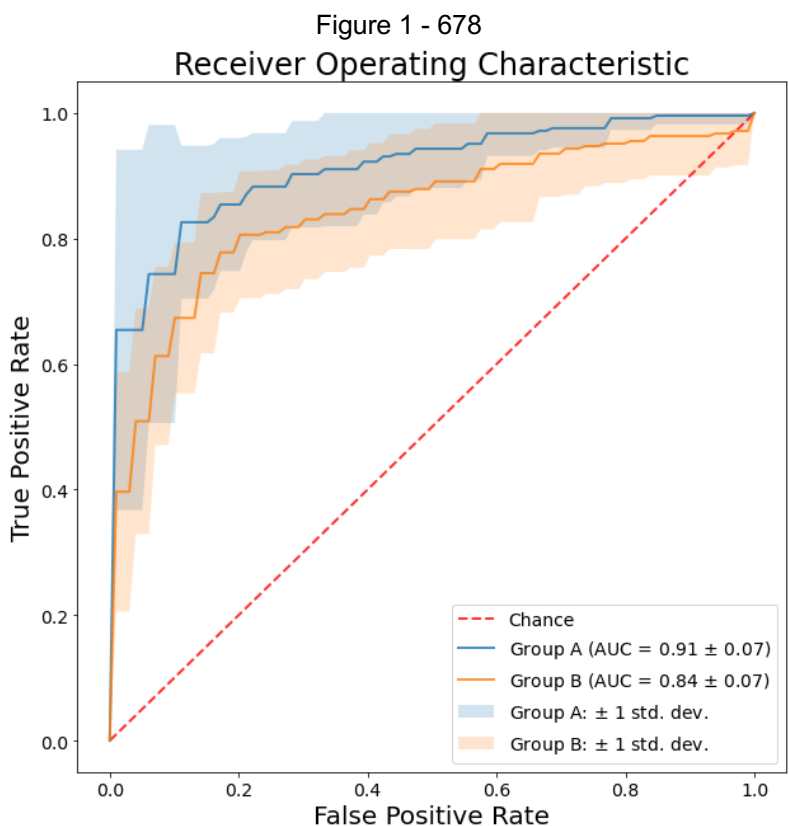
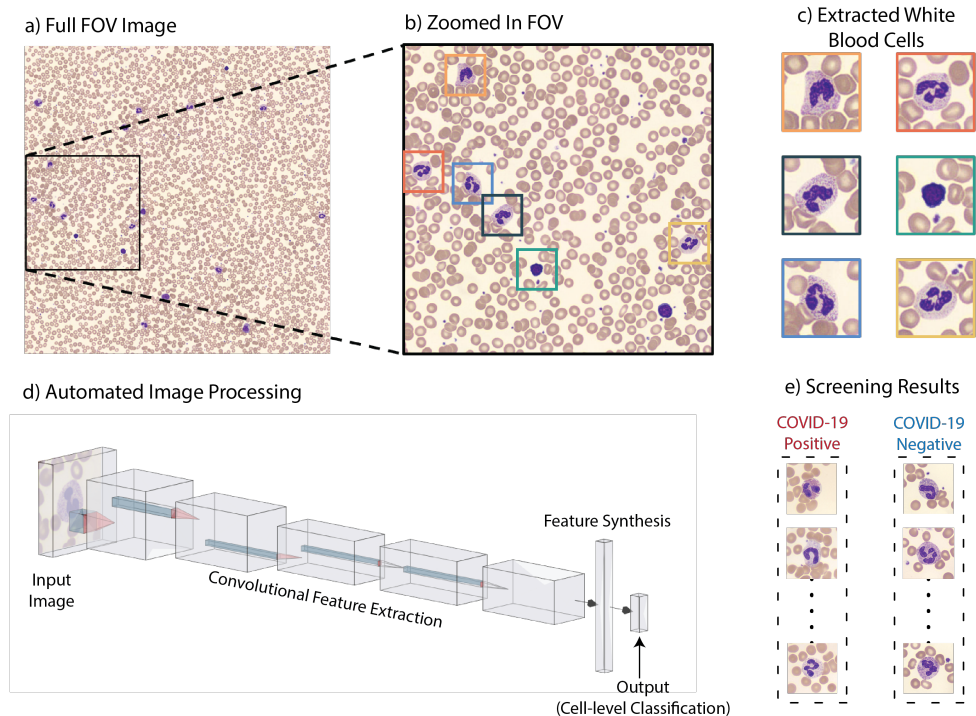


Figure 2 - 678



Conclusions: Deep optical blood analysis is a next generation blood screening technology that is in its early stages of development. Our results demonstrate the significant ability to detect COVID-19 directly from digital images of blood and add to a growing list of capabilities provided by deep optical blood analysis. The digitization of peripheral blood smears is already standard of care at many institutions, and deep learning provides a useful mechanism to help maximize the diagnostic potential of these large existing digital image datasets.

679 Increased CD25+CD4+T-cells Proportion and FOXP3+ cells are Associated with Advanced Stage in Follicular Lymphomas ---- A Single-Institute Study

Yanna Ding¹, Sally Self¹, Kathryn Lindsey¹
¹Medical University of South Carolina, Charleston, SC

Disclosures: Yanna Ding: None; Sally Self: None; Kathryn Lindsey: None

Background: Disease stage of Follicular Lymphoma (FL) is a predictor of prognosis and is critical for clinical management. The imbalance of immune microenvironment bears diagnostic and prognostic significance in diseases. Increased regulatory T (Treg) cells has been associated with improved survival in FL; and FOXP3 cell distribution is associated with transformation risk. Here we report a contrary finding of an association of increased CD25+CD4+ T-cells proportion and FOXP3+ cells with increased clinical stage.

Design: Forty-seven FL cases were identified for study. The percentage of CD25+CD4+ T-cells and the ratio of CD4+ to CD8+ T-cells were determined by flow cytometric analysis. Immunohistochemical (IHC) stains of CD3, BCL2 and FOXP3 were performed on paraffin embedded tissue. FOXP3+ cells were quantified by cell count and ImageJ software analysis. Relationships of these parameters to the clinical stage, pathology grade, and disease progression were analyzed by regression analysis. The differences between groups were analyzed by T test.

Results: Distribution of clinical and pathology variables of the cases are shown in Table 1. There is no significant difference of CD25+CD4+T-cells percentage in cases of different pathology grade (p=0.369). However, the CD25+CD4+T-cells percentages in advanced diseases (stage 3 and stage 4) are significantly higher than that in limited diseases (stage 1-2) (p=0.023, and p=0.01, respectively) (Figure 1B). It is positively correlated with the

disease stage ($p=0.023$), and age ($p=0.033$), but not pathology grade. CD4+ to CD8+ T-cell ratio is not correlated with disease stage. Interestingly, the CD25+CD4+T-cells percentage is positively correlated with disease relapse, transformation or solid organ involvement ($p=0.021$), while the CD4+ to CD8+ T-cell ratio is negatively correlated ($p=0.021$). IHC stains of BCL2, CD3 and FOXP3 show that the FOXP3 stain reflects the CD3 stain (Figure 1C), indicating that the FOXP3+ cells are most likely Treg cells. The number of FOXP3+ cells tends to increase with increased disease stage. The FOXP3+ cell count is significantly higher in groups of stage 3 and 4, compared with stage 1 and 2 (Figure 2 A-E). Quantification of FOXP3+ cells by ImmunoRatio in ImageJ, shows a similar increase in advanced diseases (Figure 2 F). In limited diseases, the FOXP3+ cells distributing pattern is perifollicular only, while in stage 3, intrafollicular and diffuse patterns predominate. In stage 4, the diffuse pattern is most common (Figure 2 G and H).

Table 1. Distribution of clinical and pathology variables in different groups of Follicular Lymphomas

Ann Arbor staging		Stage 1	Stage 2	Stage 3	Stage 4
Clinical Features	Total cases number	4	6	18	19
	age median & (mix-max) (year)	58 (56-73)	65 (45-81)	66 (25-82)	63.5 (41-80)
	Male: Female (number of patients)	1:3	4:2	8:10	9:10
	Survival status	living	living	living	living
Pathology Grade	Grade 1-2	3	5	16	16
	Grade 3a	1	1	2	1
	Grade 3b	0	0	0	2

Figure 1 - 679

Figure 1. Flow cytometry analysis of CD25+CD4 T cells percentage and CD4/CD8 T cells and immunostain of FOXP3 + cells in FL cases

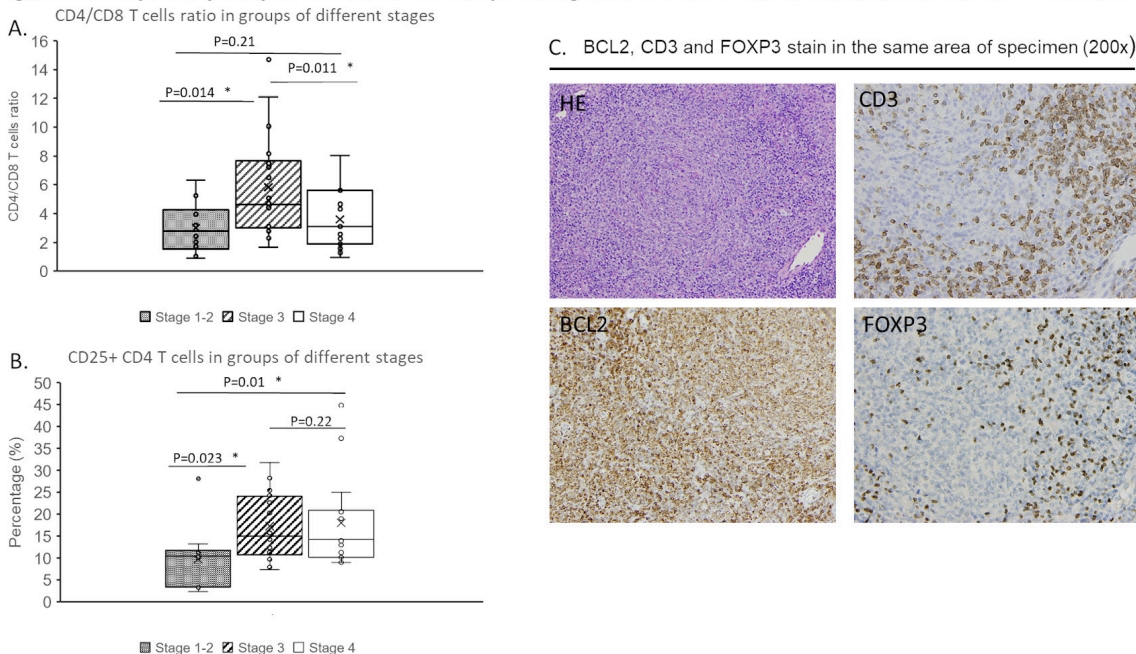
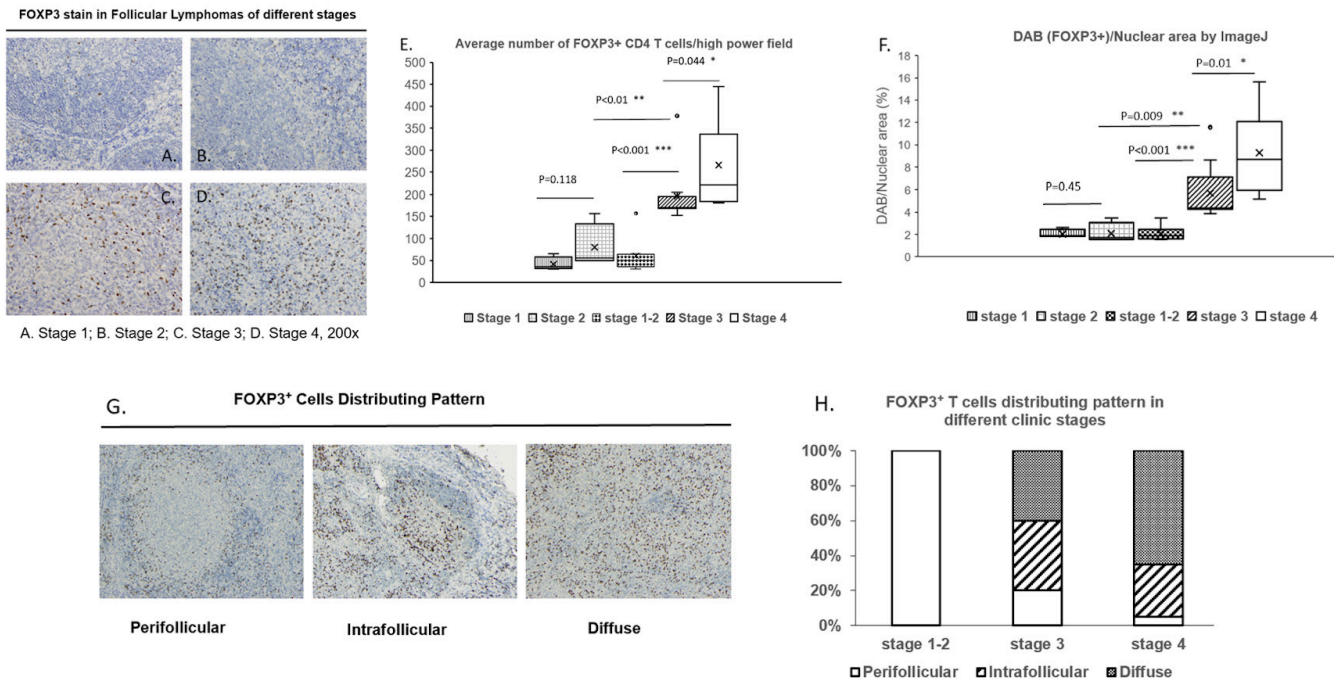


Figure 2 – 679

Figure 2. FOXP3+ cells staining quantification and distributing pattern in FL cases of different clinical stages



Conclusions: The CD25+CD4+T-cells percentage and FOXP3+ cells are significantly increased in advanced disease of FL and are positively correlated with disease stage. The diffuse distributing pattern of FOXP3+ cells is restricted to advanced diseases. Flow cytometric analysis of CD25+CD4+T-cell percentage and IHC stain of FOXP3 may help differentiate disease stages and may be useful as independent prognostic markers in FL.

680 Emerging WT1mut Clones Contribute to Relapse in NPM1mut AML Patients

Siba Hussein¹, Courtney DiNardo¹, Joseph Khoury¹, Hong Fang¹, Kirill Lyapichev¹, Sofia Garces², Rashmi Kanagal-Shamanna¹, Chi Young Ok¹, Keyur Patel¹, Mark Routbort¹, L. Jeffrey Medeiros¹, Sa Wang¹, Sanam Loghavi¹

¹The University of Texas MD Anderson Cancer Center, Houston, TX, ²The Hospital of the University of Pennsylvania, Philadelphia, PA

Disclosures: Siba El Hussein: None; Courtney DiNardo: Grant or Research Support, Abbvie; Grant or Research Support, Agios; Grant or Research Support, Novartis; Grant or Research Support, ImmuneOnc; Grant or Research Support, Daiichi Sankyo; Joseph Khoury: None; Hong Fang: None; Kirill Lyapichev: None; Sofia Garces: None; Rashmi Kanagal-Shamanna: None; Chi Young Ok: None; Keyur Patel: None; Mark Routbort: None; L. Jeffrey Medeiros: None; Sa Wang: None; Sanam Loghavi: None

Background: Mutations in the tumor suppressor gene *WT1* are detected in 10% of acute myeloid leukemia (AML) cases at diagnosis. *WT1* mutations are considered to be an independent poor risk factor in cytogenetically normal AML, and frequently co-occur with *NPM1* mutations. Recent studies have shown successful targeting of *WT1* mutant clones using T-cell receptor gene therapy in the post-transplant setting. Here, we sought to investigate the impact of *WT1* mutations as they pertain to clonal evolution and relapse in *NPM1*^{mut} AML.

Design: 67 consecutive patients (pts) with *de novo* *NPM1*^{mut} AML treated at our institution between 01/2017 and 11/2019 were included. Whole bone marrow (BM) DNA was interrogated with an 81-gene myeloid next-generation

sequencing (NGS) panel using an Illumina MiSeq sequencer (Illumina, Inc., San Diego, CA, USA) with a sensitivity: 1% variant allelic frequency (VAF). Mutations and their VAFs were characterized at baseline, *NPM1*-wild type remission, and relapse. VAF was used to infer clonal dominance.

Results: *WT1* mutations were present in 5 (7%) *NPM1*^{mut} AML cases at baseline, with only one mutation per case; all mutations were truncating frameshift alterations. Four (80%) of these cases had a diploid karyotype and one (20%) had a complex karyotype. The *WT1* mutant clones were presumed to be clonal in 3/5 and subclonal in 2/5 cases when compared with the dominant *NPM1*^{mut} clone, based on VAF. Other co-mutated genes in the *WT1*^{mut} group included *DNMT3A* (n=2), *FLT3*, *TET2*, *NRAS*, *PTPN11*, *BCOR*, *SUZ12*, *IKZF1* and *CREBBP* (n=1 each). *WT1* mutations became undetectable as patients achieved *NPM1*-wild type remission. 15/67 (22%) pts in the entire *NPM1*^{mut} cohort relapsed during the follow up period. Among these 15 pts, 4 (27%) relapsed with *WT1* mutant AML; none of these pts had detectable *WT1* mutation at baseline. *WT1* mutations at relapse included missense (25%), nonsense (25%) and truncating frameshifts (50%) variants. 3/4 cases had one *WT1* mutation whereas one case had 3 concomitant mutations, all with subclonal VAF. *WT1* mutations had clonal (n=2) and subclonal (n=1) VAFs in the other 3 cases.

Conclusions: These data suggest that acquired *WT1* mutations contribute to clonal evolution and relapse in *NPM1*^{mut} AML pts, including pts who present with wild type *WT1* disease at baseline. These findings support sequential analysis to evaluate the stability of *WT1* during disease surveillance, in particular in the setting of relapse, given the presence of novel therapeutic options for targeted treatment of *WT1* mutant AML.

681 Clone Size Evolution Does Not Predict Clinical Response in Patients with Persistent PNH Clones

Siba Hussein¹, Sanam Loghavi¹, L. Jeffrey Medeiros¹, Sofia Garces², Roberto Miranda¹, Sa Wang¹, Wei Wang¹

¹The University of Texas MD Anderson Cancer Center, Houston, TX, ²The Hospital of the University of Pennsylvania, Philadelphia, PA

Disclosures: Siba El Hussein: None; Sanam Loghavi: None; L. Jeffrey Medeiros: None; Sofia Garces: None; Roberto Miranda: None; Sa Wang: None; Wei Wang: None

Background: Paroxysmal nocturnal hemoglobinuria (PNH) clones can be detected in patients with classic (c) PNH, and aplastic anemia (AA). However, little is known about the clinical impact of PNH clonal evolution in patients with underlying AA/cPNH.

Design: 21 patients with positive PNH clones in blood samples detected by flow cytometry immunophenotypic analysis and who had clinical follow-up were analyzed. The antibody panel consisted of CD15, CD24, CD45, CD64, CD157, FLAER for granulocytes and monocytes; and CD235a and CD59 for red blood cells (RBC), divided into type II and type III RBCs. A positive PNH clone was defined as ≥0.01% cells with lack of GPI-link proteins observed in at least 2 lineages. In this cohort, 14 patients had acquired AA, 4 had bone marrow failure likely resulting from cPNH and 3 patients had cPNH. We assessed for the presence of clinical/subclinical hemolysis by review of serum LDH, bilirubin and haptoglobin levels; PNH clone sizes in the granulocytic, monocytic and RBC populations at initial presentation, and at follow-up (median, 9.8 months); and mutation status by next generation sequencing (NGS) when applicable. We also assessed for evidence of clinical response defined by improved blood cell counts.

Results: 18/21 patients presented with clinical/subclinical hemolysis. The median size of PNH clones was 7.19% for granulocytes, 10.07% for monocytes, and 2.0% for RBCs (with 0.13% for type II and 0.54% for type III RBCs). In a given patient, the largest PNH clone was frequently detected in monocytes (14/21 patients) followed by granulocytes (7/21 patients), and was almost always the smallest in RBCs. Treatment consisted of a combination of cyclosporin, eltrombopag, prednisone and anti-thymocyte globulin (ATG). 3/21 patients showed no clinical response, likely associated with therapy discontinuation for various reasons (e.g: noncompliance or intolerable side effects), with 2 patients experiencing increased clone size and 1 showing decreased clone size. The remaining patients were therapy compliant and showed clinical response. The PNH clone decreased in 7/21 patients and increased in 11/21 patients at follow-up. 5 of the latter group harbored mutations in *BCOR*, *WT1*, *PIGA*, *EZH2*, *DNMT3A*, *BRAF*.

Conclusions: Bone marrow failure associated with a PNH clone often shows a good response to immunosuppressive therapy. However, PNH clone size does not correlate with clinical response, as more than half of the clinical responders showed increased PNH clone size at follow-up. It is uncertain if emerging mutations are detected as a result of PNH clonal expansion.

682 Prognostic Implications of NOTCH1 Pathway Activation Through Transforming Growth Factor-B (TGF-Beta) / SETBP1 in Childhood Acute Myeloid Leukemia (AML); Report of a Pilot Study

Ghaleb Elyamany¹, Ariz Akhter², Hamza Kamran², Hassan Rizwan², Meer-Taher Shabani-Rad³, Adnan Mansoor²

¹Prince Sultan Military Medical City, Riyadh, Saudi Arabia, ²University of Calgary, Calgary, Canada, ³Cumming School of Medicine, University of Calgary, Calgary, Canada

Disclosures: Ghaleb Elyamany: None; Ariz Akhter: None; Hamza Kamran: None; Hassan Rizwan: None; Meer-Taher Shabani-Rad: None; Adnan Mansoor: None

Background: Genomic variation drives biological and clinical behavior in AML. Novel investigational platforms are providing effective risk stratification through mutational profile in elderly AML patients. These criteria are less applicable in pediatric AML; hence the response to conventional therapy is variable with frequent relapses. Thus, improved insight into the biology of AML, especially in children is warranted to explore new therapeutic targets. NOTCH1 is now established to play a key role in the prognosis of several hematological malignancies, however, its role in AML remains controversial as NOTCH1 activating mutations are rare in AML. It is now established that NOTCH1 activation ensues through ligands (DII1& DII4) and the Notch1 receptors. Notch proteins are multifaceted and involved in several key cellular functions with extensive crosstalk with other critical pathways. Since signal transduction is fundamental to the understanding of cancer biology; therefore, it is important to investigate NOTCH1 expression and its influence on other oncogenic pathways molecules in childhood AML. In this pilot study, we correlated NOTCH1 and other associated pathway expression patterns among childhood AML patients and compared it with hematological parameters and overall survival (OS) data.

Design: RNA from diagnostic BM biopsies (n=35) were subjected to expression analysis employing nCounter Pan-Cancer pathway panel by Nanostring technologies. Laboratory and clinical data were correlated with the expression of NOTCH1 and several other oncogenic signaling pathways (n=780).

Results: 35 -AML patients (median age 8 yrs., range1-18 yrs.) were dichotomized into low NOTCH1 (17/35; 49%) and high NOTCH1(18/35; 51%) groups based on ROC curve analysis (74% AUC; 82% sensitivity /68% specificity). Age, gender, hematological data, or molecular risk factors (FLT3 mutation/ molecular fusion) exposed no significant differences across these two distinct NOTCH1 expression groups (P > 0 .05). High NOTCH1 expression was linked with a high expression of NOTCH1 ligand (DII1) (P<0.001/fold >2.5). Our data also showed that high NOTCH1 mRNA is interrelated with the heightened expression of positive regulators of the NOTCH signaling pathway (DTX1/DTX3) (Figure1A). High NOTCH1 samples also showed a high expression of *TGFR-β* associated protein SETBP1(P<0.001/fold >2.5) (Figure 1A). NOTCH1 expression did not correlate with mortality {5/17 (29%) vs. 6/17; (35%) P > 0.05}. Low NOTCH1 expressers showed better OS {740 days vs. 579 days; log-rank P=< 0.007; HR 6.3 (1.36-29.26)} (Figure1B)

Figure 1 - 682

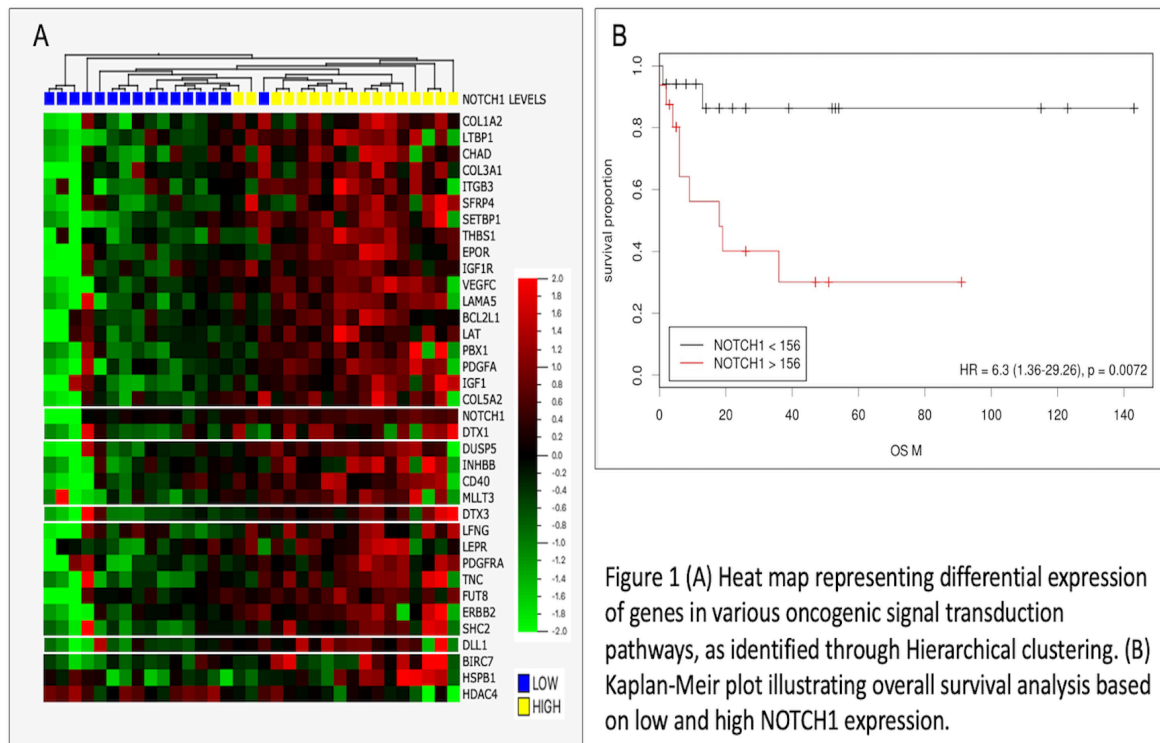


Figure 1 (A) Heat map representing differential expression of genes in various oncogenic signal transduction pathways, as identified through Hierarchical clustering. (B) Kaplan-Meier plot illustrating overall survival analysis based on low and high NOTCH1 expression.

Conclusions: Our pilot study has identified that high expression of the molecules linked with the NOTCH1 pathway is an important poor prognostic marker among childhood AML patients. *NOTCH1* expression also shows cross-talk with several other signal transduction pathways especially *TGFβ* / *SETBP1* which are also linked with poor prognosis.

683 Autopsy Findings from Patients Diagnosed with COVID-19 Demonstrate Unique Morphologic Patterns in Bone Marrow and Lymph Node

Mark Evans¹, Jack Guccione², Robert Edwards², Geraldine Pinkus¹, Robert Padera¹, Annette Kim¹, Olga Pozdnyakova¹

¹Brigham and Women's Hospital, Boston, MA, ²UC Irvine Health, Orange, CA

Disclosures: Mark Evans: None; Jack Guccione: None; Robert Edwards: None; Geraldine Pinkus: None; Robert Padera: None; Annette Kim: *Consultant*, LabCorp, Inc; *Grant or Research Support*, Multiple myeloma research foundation; Olga Pozdnyakova: None

Background: Although the number of deaths from COVID-19 has exceeded 1,000,000 globally, only a limited number of case series have focused on the autopsy findings in lymphoid or hematopoietic tissues.

Design: Bone marrow and lymph node specimens from SARS-CoV2-positive autopsies performed between April 1, 2020 and June 1, 2020 were examined by two board-certified hematopathologists, who recorded morphologic features in a blinded fashion. Clinical and laboratory data at the time of diagnosis and demise, when available, was documented retrospectively for correlation with the microscopic findings. Statistical analysis included Student T-test for continuous data and Chi-squared test for categorical data.

Results: Table 1 summarizes the data for 31 patients; clinical and laboratory data was available for only 25. Bone marrows (BM) demonstrated two distinct morphologic patterns: with (n=9) and without (n=16) hemophagocytic macrophages. Those cases featuring hemophagocytosis occurred more frequently in patients with a longer hospital stay (p=0.035) and were associated with increased interstitial B lymphocytes (67% vs 25%; p=0.042) and plasma

cells (44% vs 6%; p=0.022) in BM, as well as more prominent germinal centers in the lymph node (LN) (44% vs 19%; p=0.058). Interestingly, despite a tendency for lower peripheral blood counts in the group with hemophagocytic macrophages, there was no significant difference at diagnosis or demise. On the other hand, the presence of increased plasmacytoid cells in LN, a distinct morphologic pattern observed in 20 autopsies, both at diagnosis and demise, was associated with decreased absolute monocyte count (p=0.036 and p=0.008, respectively) and decreased serum ferritin (p=0.034 and p=0.029, respectively). In addition, this pattern was associated with a significantly lower white blood cell count (p=0.0061) and absolute neutrophil count (p=0.0036) at the time of death. Increased hemophagocytic LN macrophages were also more prevalent in this group (89% vs 40%; p=0.023).

Clinical Features of SARS-CoV2-positive Patients	All patients (n = 31)	BM hemophagocytic pattern			LN plasmacytoid pattern		
		present (n = 9)	absent (n = 16)	p-value	present (n = 20)	absent (n = 5)	p-value
Age in years, mean (range) (n = 31) ^a	68 (45-96)	65 (45-86)	65.5 (49-96)	0.72	65.5 (45-90)	58 (49-96)	0.92
Gender (Male:Female) (n = 31) ^a	2.1:1	3.5:1	1.3:1	0.28	1.9:1	4:01	0.52
Hospitalization Length in days, mean (range) (n = 25)	11 (1-36)	20 (1-36)	9.5 (1-21)	0.035*	13 (1-36)	3 (2-11)	0.058
Complete Blood Count at Diagnosis (n = 25)							
WBC count (K/μL), mean (range)	6.9 (1.5-39.5)	4.8 (3.1-18.7)	8.1 (1.5-39.5)	0.22	6.0 (1.5-39.5)	10.1 (2.9-12.6)	0.95
Absolute neutrophil count (K/μL), mean (range)	4.6 (0.03-37.1)	3.3 (2.1-7.0)	6.1 (0.03-37.1)	0.26	4.2 (0.03-37.1)	6.0 (2.0-9.6)	0.83
Absolute lymphocyte count (K/μL), mean (range)	0.7 (0.0-2.9)	0.6 (0.2-1.4)	0.8 (0.0-2.9)	0.24	0.6 (0.0-1.6)	1.3 (0.3-2.9)	0.019*
Absolute monocyte count (K/μL), mean (range)	0.3 (0.0-2.0)	0.3 (0.2-0.6)	0.5 (0.0-2.0)	0.12	0.3 (0.0-2.0)	0.8 (0.4-1.4)	0.036*
Hemoglobin (g/dL), mean (range)	12.5 (5.5-19.7)	12.4 (9.3-15.7)	13.4 (5.5-19.7)	0.89	12.1 (5.5-16.9)	13.8 (12.5-19.7)	0.069
Platelets (K/μL), mean (range)	156 (6-450)	128 (46-208)	164.5 (6-450)	0.53	156 (6-450)	156 (38-169)	0.74
Complete Blood Count at Demise (n = 25)							
WBC count (K/μL), mean (range)	11.8 (0.3-64.9)	11.7 (2.2-19.2)	11.9 (0.3-64.9)	0.55	11.1 (0.3-28.8)	18.8 (12.8-64.9)	0.0061*
Absolute neutrophil count (K/μL), mean (range)	8.6 (0.03-42.2)	8.4 (1.5-18.1)	8.9 (0.03-42.2)	0.63	7.6 (0.03-18.1)	16.9 (8.9-42.2)	0.0036*
Absolute lymphocyte count (K/μL), mean (range)	0.8 (0.1-2.9)	1.2 (0.3-2.9)	0.8 (0.1-2.9)	0.68	0.7 (0.1-2.9)	1.7 (0.6-2.6)	0.19
Absolute monocyte count (K/μL), mean (range)	0.8 (0.01-5.2)	0.8 (0.07-1.3)	0.4 (0.01-5.2)	0.86	0.7 (0.01-1.5)	1.1 (0.6-5.2)	0.0084*
Hemoglobin (g/dL), mean (range)	8.9 (5.7-17.9)	8.5 (7.2-11.3)	9.6 (5.7-17.9)	0.2	8.7 (5.7-15.1)	13.4 (8.3-17.9)	0.011*
Platelets (K/μL), mean (range)	166 (10-642)	259 (47-642)	160 (10-569)	0.33	189 (10-642)	162 (114-264)	0.49
SOFA Score (≥ 9), predictive of poor prognosis (n = 25) ^a	22	8	14	0.2	18	4	0.0028*
Satisfying HLH-2004 Criteria for HLH (n = 25)^a							
Ferritin at Diagnosis (mg/L), mean (range) (n = 23)	1347 (46-8369)	439 (80-972)	1931 (46-8369)	0.13	827 (46-6088)	3220 (224-8369)	0.035*
Ferritin at Demise (mg/L), mean (range) (n = 19)	2443 (178-12761)	650 (178-1426)	3489 (410-12761)	0.1	1693 (340-12761)	6445 (1769-9644)	0.030*

Abbreviations: BM - bone marrow, LN - lymph node, WBC - white blood cell, SOFA - Sequential Organ Failure Assessment, HLH - hemophagocytic lymphohistiocytosis. * - indicates statistical significance (also bolded)

^aP-values determined by Chi-squared analysis. All other analyses performed by Student T-test.

Conclusions:

1. Autopsy results demonstrate distinct morphologic patterns in bone marrow, without or without hemophagocytic macrophages, and in lymph node, with or without increased plasmacytoid cells.

2. Circulating lymphopenia and monocytopenia likely represent migration of cells into tissues, as a result of concomitant macrophage activation syndrome with cytokine storm, but without fulfilling criteria for hemophagocytic lymphohistiocytosis in most cases.

684 Expression Pattern and Diagnostic Utility of BCL11B in T and NK-cell Neoplasms

Hong Fang¹, Joseph Khoury¹, Carlos Torres-Cabala¹, Siok-Bian Ng², Siba Hussein¹, Shimin Hu¹, L. Jeffrey Medeiros¹, Wei Wang¹

¹The University of Texas MD Anderson Cancer Center, Houston, TX, ²National University of Singapore, Singapore, Singapore

Disclosures: Hong Fang: None; Joseph Khoury: None; Carlos Torres-Cabala: None; Siok-Bian Ng: None; Siba El Hussein: None; Shimin Hu: None; L. Jeffrey Medeiros: None; Wei Wang: None

Background: BCL11B is an essential transcription factor for T lineage commitment and T-cell maturation. It is activated by NOTCH signaling at the double negative (CD4-/CD8-) stage. BCL11B expression is further upregulated and maintained in all later stages. The dysregulation of BCL11B has been shown to be associated with T-cell lymphomagenesis. In this study, we investigated the pattern of BCL11B expression in different types of T and NK-cell neoplasms, with the aims of determining whether BCL11B expression is disrupted, and/or can be used a marker for diagnosis of these diseases.

Design: We optimized and validated a BCL11B immunohistochemical stain for use in formalin-fixed paraffin-embedded tissue sections. Different types of T and NK-cell neoplasms as well as benign cutaneous reactive conditions were collected and stained with BCL11B antibody (MA5-31434, Thermo Fisher Scientific, MA). An H-score was calculated, defined as the intensity of positive staining (scale 1-4) multiplied by the percentage of positively stained neoplastic cells. Reactive T cells in the background were used as internal controls and their staining intensity was arbitrarily set as 2 using a scale of 1-4. In total, 171 cases were evaluated and stained with BCL11B antibody.

Results: The neoplastic cells in all mycosis fungoides (MF) and T-prolymphocytic leukemia (T-PLL) cases showed strong BCL11B expression with intensity much higher than background reactive T cells (Figure). In contrast, the neoplastic cells of anaplastic large cell lymphomas (ALCL) were negative for BCL11B in 93% (14/15) of the examined cases (Figure). Most cases of peripheral T-cell lymphoma (PTCL) and angioimmunoblastic T-cell lymphoma maintained BCL11B expression with intensity comparable to reactive T cells. All lymphomas derived from NK cells were negative for BCL11B (Figure). BCL11B results are summarized in Table 1. In addition, a total of 34 cases with B-cell lymphomas were evaluated and all were negative for BCL11B, including diffuse large B-cell lymphoma (n=8), low-grade B-cell lymphoma (n=8), high-grade B-cell lymphoma (n=4), classic Hodgkin lymphoma (n=4), and Burkitt lymphoma (n=2).

Table 1. BCL11B expression on T/NK-cell neoplasms and reactive conditions

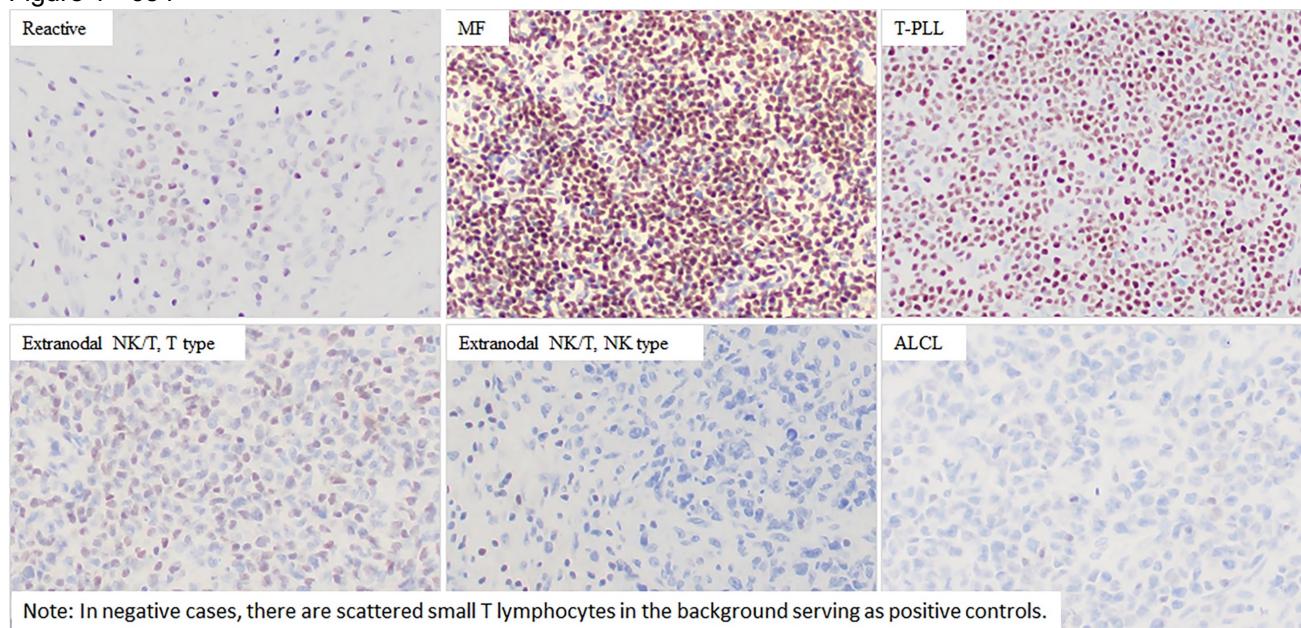
Category	Diagnosis	#	Positive	H-score
			n (%)*	median (range)
T-lineage	Mycosis fungoides	21	21 (100%)	240 (70-400)
	ALCL	19	1 (5%)	0 (0-50)
	PTCL	17	12 (71%)	80 (0-270)
	AITL	15	14 (93%)	120 (10-270)
	T-PLL	6	6 (100%)	270 (30-300)
	SPTCL	4	1 (25%)	5 (0-80)
	CTCL, unclassifiable	4	3 (75%)	85 (10-140)
	HSTL	4	2 (50%)	15 (0-80)
	Intestinal TCL	2	1 (50%)	15 (0-30)
	T-LGLL	2	0 (0%)	0 (0-0)
	Benign cutaneous reactive conditions**	19	19 (100%)	80 (20-210)
NK-lineage	ANKL	4	0 (0%)	0 (0-0)
	Extranodal NK/T			
	T-cell lineage	6	3 (50%)	10 (0-80)
	NK-cell lineage	3	0 (0%)	0 (0-0)
	NK or T, undetermined	11	2 (18%)	0 (0-40)

*Positivity is defined as $\geq 20\%$ of positive cells with any scale of intensity.

**Including dermatitis, anthropod assault reaction, lichenoid changes, scabies, syphilis, etc.

Note: AITL, angioimmunoblastic T-cell lymphoma; ALCL, anaplastic large cell lymphoma; ANKL, aggressive NK-cell leukemia; CTCL, cutaneous T-cell lymphoma; HSTL, hepatosplenic T-cell lymphoma; PTCL, peripheral T-cell lymphoma; SPTCL, subcutaneous panniculitis-like T-cell lymphoma; T-LGLL, T-large granular lymphocytic leukemia; T-PLL, T-cell prolymphocytic leukemia

Figure 1 - 684



Conclusions: BCL11B shows a distinct expression pattern in various T and NK-cell neoplasms, indicating that its potential role in lymphomagenesis is different in various entities. BCL11B is a valuable marker for the differential diagnosis, especially between MF and reactive skin conditions, ALCL and PTCL, as well as NK and T lymphomas.

685 Reactive Intravascular Immunoblastic Proliferations Mimicking Aggressive Lymphomas

Hong Fang¹, Wei Wang¹, Qi Shen², L. Jeffrey Medeiros¹

¹The University of Texas MD Anderson Cancer Center, Houston, TX, ²Central Florida Pathology Associates, Orlando, FL

Disclosures: Hong Fang: None; Wei Wang: None; Qi Shen: None; L. Jeffrey Medeiros: None

Background: Intravascular lymphocytosis composed of small reactive lymphocytes in appendiceal specimens has been described. However, reactive intravascular immunoblastic proliferations (IVIPs) have not been studied and may mimic an aggressive lymphoma, particularly intravascular large B-cell lymphoma. In this study, we characterized the clinicopathologic features of patients with IVIPs.

Design: Cases of IVIP were collected and their clinicopathologic features were reviewed retrospectively.

Results: Eight cases of IVIP were evaluated, including 5 men and 3 women, with a median age of 54 years (range, 4-67 years). All patients had no evidence of lymphadenopathy, organomegaly, or other findings suggestive of lymphoma by either physical examination or radiologic imaging. They were evaluated for suspected appendicitis, bowel obstruction, diverticulitis, or tumor dissection. Seven specimens were gastrointestinal tract specimens and one was lymph node. The IVIP was incidentally identified in these cases. Among these 8 cases, one case was

initially misdiagnosed as CD30-positive diffuse large B-cell lymphoma (intrasinusoidal variant) and suggestive of intravascular large B-cell lymphoma. Another case was diagnosed as diffuse large B-cell lymphoma, and later T/NK lymphoma with prominent intravascular involvement before the final diagnosis of IVIP was made.

In all cases, there was dilation of lymphovascular spaces, expanded by predominantly large-sized lymphoid cells with round to slightly irregular nuclear contours, vesicular chromatin, prominent nucleoli, and moderate amounts of cytoplasm. Seven cases showed immunoblasts of B lineage, and one case showed a mixture of B and T immunoblasts, as assessed by T cell markers (including CD3, CD2, and/or CD5), CD20, CD79a, PAX5, and kappa/lambda immunoglobulin light chains. CD38 (n=4), CD43 (n=7), CD79a (n=5), and MUM1/IRF4 (n=4) were positive in all cases tested. In 4 of 7 (57%) cases, the B immunoblasts were negative for CD20 and/or PAX5. Immunohistochemical analysis for immunoglobulin light chains was performed in 4 cases and showed a polytypic pattern of light chain expression. Five of 6 (83%) cases showed expression of CD30. EBV encoded small RNA (EBER) was assessed by in situ hybridization and was negative in all 4 cases tested. The proliferation index measured by Ki-67 was high in 7 cases tested (median: 80%; range, 60%-100%).

Conclusions: Rarely, reactive intravascular immunoblastic proliferations (IVIPs) can be observed incidentally, especially in gastrointestinal surgical specimens. The immunoblasts are predominantly of B lineage with a post-germinal center immunophenotype and a high proliferation rate. It is critical to distinguish IVIPs from intravascular large B-cell lymphoma as the clinical management and prognosis of these lesions differ greatly.

686 TOX is a Useful Marker in the Differential Diagnosis of Mycosis Fungoides vs. Morphologically Similar Cutaneous T Cell Lymphomas and Benign Reactive Dermatitis

David Gajzer¹, Pukhraz Basra², Ling Zhang³, Lubomir Sokol³, Xiaohui Zhang³

¹University of Miami Miller School of Medicine/Jackson Memorial Hospital, Miami, FL, ²H. Lee Moffitt Cancer Center & Research Institute, University of South Florida, Tampa, FL, ³H. Lee Moffitt Cancer Center & Research Institute, Tampa, FL

Disclosures: David Gajzer: None; Pukhraz Basra: None; Ling Zhang: None; Lubomir Sokol: *Advisory Board Member, Kiowa-Kirin, Inc; Advisory Board Member, Kymera Therapeutics; Consultant, Dren Bio*; Xiaohui Zhang: None

Background: Mycosis fungoides (MF) is a neoplasm of CD4+ helper T lymphocytes showing significant morphologic overlap with other primary cutaneous entities including benign reactive dermatitis (BRD) and other cutaneous T cell lymphomas (CTCL) such as primary cutaneous CD30-positive T-cell lymphoproliferative disorders (CD30+ LPD). We previously demonstrated that GATA-3 is helpful in the differential diagnosis of cutaneous lymphoproliferative disorders. Transcription factor thymocyte selection-associated HMG box protein (TOX) has been demonstrated to be increased in MF/CTCL and proposed as a diagnostic marker for MF. We aimed to characterize TOX expression in our cohort of primary cutaneous conditions including MF, MF with large cell transformation (MF with LCT), BRD, and CD30+ LPD.

Design: TOX protein expression was assessed by immunohistochemical staining on paraffin-embedded tissue sections of skin specimens in a clinically well-characterized cohort of surgical pathology specimens at Moffitt Cancer Center including MF (n = 16), MF with LCT (n = 13), CD30+ LPD (n = 13), and BRD (n = 10). Immunohistochemical stains were performed on 3-4 µm paraffin-embedded sections utilizing a TOX primary antibody (HPA018322, Sigma Aldrich, St. Louis, MO) at 1:200 concentration in Dako antibody diluent (Dako, Carpinteria, CA). Percentages of TOX positivity in the lymphoid populations were assessed by two pathologists. Student's t-test was used to compare TOX protein expression rates between specimen groups. Results were considered statistically significant where p < 0.05.

Results: TOX expression rates were significantly higher in MF with LCT (81±17%) than in MF (44±23%; p < 0.0001), CD30+ LPD (27±23%; p < 0.0001), and BRD (17.2±6%; p < 0.0001). Of note, MF also demonstrated significantly higher TOX expression than BRD (p = 0.002) but not CD30+ LPD (p = 0.06). No significant difference was observed in CD30+ LPD vs. BRD (p = 0.2).

Table 1. TOX and GATA-3 Expression in MF, CD30+ LPD, and Benign Reactive Dermatitis

<u>Disease</u>	<u>N of Cases</u>	<u>TOX Positive Rate (%)</u>	<u>GATA-3 Positive Rate (%)</u>	<u>TOX p-value</u>	<u>GATA-3 p-value</u>
<u>MF</u>	16	44±23	59±14	0.002, when compared with BRD* < 0.0001, when compared with MF with LCT* 0.06, when compared with CD30+ LPD	0.011, when compared with BRD* 0.118, when compared with MF with LCT 0.012, when compared with CD30+ LPD*
<u>MF with LCT</u>	13	81±17	70±24	< 0.0001, when compared with MF, CD30+LPD *	0.003, when compared with CD30+ LPD*
<u>CD30+ LPD</u>	13	27±23	39±25		
<u>BRD</u>	10	17.2±6	38±23	< 0.0001, when compared with MF with LCT* 0.2, when compared with CD30+ LPD	0.005, when compared with MF with LCT* 0.961, when compared with CD30+ LPD

MF: Mycosis fungoides; MF with LCT: Mycosis fungoides with large cell transformation; CD30+ LPDs: CD30 positive lymphoproliferative disorders; BRD: Benign reactive dermatitis.
*. $p < 0.05$, TOX and GATA-3 positive rates were compared using independent samples t test

Conclusions: TOX expression is increased in MF and MF with LCT when compared with benign dermatitis. Interestingly, MF with LCT shows significantly higher TOX expression than CD30+ LPD, supporting the use of TOX as a diagnostic marker in the differential diagnosis of cutaneous lymphoproliferative disorders exhibiting similar morphology. Furthermore, TOX expression trends with GATA-3 expression in our cohort (Table 1), supporting the combined use of both markers in the workup of MF and its mimics.

687 Histiocytic Sarcoma Presenting in Bone Marrow is Associated with Concurrent Myelomonocytic Neoplasm

Catherine Gestrich¹, Priyatharsini Nirmalanantham¹, Navid Sadri², Kwadwo Oduro¹, Howard Meyerson³, Rose Beck⁴

¹University Hospitals Cleveland Medical Center, Case Western Reserve University, Cleveland, OH, ²University Hospitals Cleveland Medical Center, Cleveland, OH, ³University Hospital Case Medical Center, Cleveland, OH, ⁴University Hospitals of Cleveland, Case Western Reserve University, Cleveland, OH

Disclosures: Catherine Gestrich: None; Priyatharsini Nirmalanantham: None; Navid Sadri: None; Kwadwo Oduro: None; Howard Meyerson: None; Rose Beck: None

Background: Histiocytic sarcoma (HS) is a rare, aggressive neoplasm arising from non-Langerhans histiocytes, typically involving extranodal sites (soft tissue, skin, and GI tract). HS has an association with other neoplasms such as follicular lymphoma, lymphoblastic leukemia, and mediastinal germ cell tumor. By definition, HS cells express ≥ 1 histiocytic marker (eg, CD163, CD68, lysozyme) and lack expression of Langerhans cell, dendritic cell (DC), and B/T cell markers. A recent study showed high incidence of RAS/MAPK pathway mutations in extramedullary HS. HS involving bone marrow (BM) is very rare, with few case reports in the literature. We describe the largest series to date of HS with primary BM presentation.

Design: We identified 5 cases of HS involving BM, evaluated between 2010-2020. Histology and immunostains were re-examined for each case. Karyotype, FISH, and next generation sequencing (NGS) data were each available in 4/5 cases. Chart review was performed for clinical details.

Results: Age range at HS diagnosis was 65-81 years. 4/5 patients were male. All patients had concurrent myeloid malignancy. 3 patients had history of chronic myelomonocytic leukemia, with 1 transformed to acute myelomonocytic leukemia (AMML) at time of HS diagnosis; 1 had concurrent AMML and 1 had prior

myelodysplastic syndrome with excess blasts transformed to AMML at time of HS diagnosis. In all cases, there was no radiologic evidence for extramedullary disease or lymphoma. In BM aspirates, HS cells were large with abundant eosinophilic cytoplasm and round to oval nuclei, often admixed with atypical monocytes and hematopoietic cells. 2 cases exhibited hemophagocytosis by HS cells. In core biopsies, HS cells formed focal lesions and interstitial infiltrates. All cases expressed ≥ 1 histiocytic marker (CD68, CD163, lysozyme) but not S100 or DC markers; 3 cases expressed aberrant CD56. Karyotype was complex in 2/4 cases. All FISH was negative for recurring translocations. 3/4 cases had RAS/MAPK pathway alterations (Table 1). All cases had poor outcome, with 3 discharged to hospice soon after diagnosis and 2 expired within 1 month of diagnosis.

Case	Age/gender	Underlying malignancy	Positive IHC markers	Molecular alterations
1	74/M	CMML	Lysozyme, CD56, CD 68 (weak), NSE	SRSF2, TET2, KRAS
2	73/M	CMML	CD163, CD68, lysozyme, CD56 (weak)	Not performed
3	65/M	MDS-EB-1, AMML	CD163, lysozyme, CD68 (weak),	TP53, TET2, ASXL1, RUNX1
4	81/M	CMML, AMML	CD68, CD163, CD56, lysozyme, Factor XIIIa	JAK2, KRAS, NRAS, TET2
5	66/F	AMML	CD163, Factor XIIIa	KRAS

Conclusions: HS involving BM is associated with antecedent or concurrent myeloid neoplasms, typically with monocytic differentiation, suggesting HS cells arise from the same malignant stem cell. HS must be distinguished from other lesions as it carries a dismal prognosis, even worse than the accompanying myeloid neoplasm.

688 Restricted Immunoglobulin Joining Chain (IgJ) Protein Expression in B Lymphoblastic Leukemia (B-ALL) Based on B-ALL Subtype

Catherine Gestrich¹, Kwadwo Oduro¹

¹University Hospitals Cleveland Medical Center, Case Western Reserve University, Cleveland, OH

Disclosures: Catherine Gestrich: None; Kwadwo Oduro: None

Background: IgJ protein concatenates monomers of immunoglobulins IgM or IgA into multimers in mature B lymphocytes but is reportedly overexpressed at the mRNA level in Philadelphia-like (Ph-like) B-ALL lymphoblasts. Ph-like B-ALL is a B-ALL subtype with a gene expression profile similar to Philadelphia positive (Ph+) B-ALL but lacking the BCR-ABL1 fusion. We sought to determine the protein expression of IgJ in B-ALL and to determine whether IgJ immunohistochemistry (IHC) may be employed in identifying particular subtypes of B-ALL.

Design: We selected a total of 46 B-ALL cases at our institution including 5 Ph-like, 7 Ph+ and 34 cases representing the other most commonly recognized WHO subtypes of B-ALL. Our cohort included 23 pediatric cases and 24 adult cases and the patients ranged from 1 to 82 years old at the time of diagnosis. A total of 8 normal bone marrow cases were used as controls. IgJ IHC was performed on B-plus fixed paraffin embedded bone marrow biopsy specimens using an anti-IgJ monoclonal antibody. Cellular staining in the lymphoblasts was scored as diffusely positive, partially positive, or negative in a blinded manner by 2 observers. IgM IHC was performed on a subset of positive cases.

Results: All normal bone marrow controls cases were negative for IgJ cellular staining. A total of 11/46 (23%) B-ALL cases demonstrated partial or diffuse cellular staining for IgJ in the lymphoblasts. This included 4/5 (80%) Ph-like cases, 5/7 (71%) Ph+ cases, 1/3 MLL rearranged cases and 1/6 ETV6-RUNX1. All TCF3-PBX1 (0/4), hyperdiploid B-ALL (0/10), hypodiploid B-ALL (0/2), and B-ALL, NOS cases (0/9) were negative for IgJ. Diffuse IgJ staining was restricted to Ph-like (2/4) or Ph+ (2/5) B-ALL subtypes; the positive MLL rearranged and ETV6-RUNX1 B-ALL cases only showed weak partial staining. IgJ protein was significantly expressed in Ph+/Ph-like B-ALL ($p < 0.0001$) and in our cohort, detected these cases with a 75% sensitivity, 95% specificity, 82% positive predictive value and 92% negative predictive value. There was 98% agreement between both observers (kappa test 0.94). None of the IgJ positive cases tested was positive for IgM (0/8).

Conclusions: IgJ protein expression occurs in a subset of B-ALL in an IgM independent manner and is predominantly restricted to Ph+ and Ph-like cases. Although these findings will need to be validated in larger studies, our results suggest that IgJ IHC may be useful as an adjunctive technique in rapidly and cost-effectively identifying Ph-like B-ALL.

689 Clinicopathologic Characteristics of Polycythemia Vera with JAK2 exon 12 Mutations

Julia Geyer¹, Olga Weinberg², Heesun Rogers³, Jonathan Lake⁴, Luke Lauridsen⁵, Jay Patel⁶, Michael Kluk⁷, Eric Hsi⁸, Adam Bagg⁹, Daniel Arber⁵, Attilio Orazi¹⁰

¹Weill Cornell Medicine, New York, NY, ²UTSouthwestern Medical Center, Dallas, TX, ³Cleveland Clinic, Cleveland, OH, ⁴Hospital of the University of Pennsylvania, Philadelphia, PA, ⁵University of Chicago, Chicago, IL, ⁶The University of Utah/ARUP Laboratories, Salt Lake City, UT, ⁷Weill Cornell Medical College, New York, NY, ⁸Wake Forest Baptist Health, Winston-Salem, NC, ⁹University of Pennsylvania, Philadelphia, PA, ¹⁰Texas Tech University Health Science Center, El Paso, TX

Disclosures: Julia Geyer: None; Olga Weinberg: None; Heesun Rogers: None; Jonathan Lake: None; Michael Kluk: None; Eric Hsi: None; Adam Bagg: None; Daniel Arber: None; Attilio Orazi: None

Background: The presence of *JAK2* exon 12 mutations (~3% of patients with polycythemia vera (PV)) is included by the 2016 WHO Classification as a major criterion for diagnosing PV. Although results are relatively sparse, in most of the published series only a subset of these patients display polycythemic (P) peripheral blood (PB) counts, while most of the cases are characterized by isolated erythrocytosis (IE). In addition, it is unclear whether the latter patients show bone marrow (BM) panmyelosis, another WHO requirement for diagnosing PV. The study aimed to determine whether patients with *JAK2* exon 12 mutations fulfil the WHO Classification criteria for PV and whether there are differences between the P and the IE variants in their respective BM and PB findings, specific types of *JAK2* exon 12 mutations, presence of co-mutations, disease progression and outcome.

Design: All cases of PV with *JAK2* exon 12 mutations were identified from the files of 7 large academic institutions. Available clinical and pathologic information was recorded. All cases were classified according to the 2016 WHO Classification. Cytogenetic and molecular genetic information was recorded.

Results: Thirty three cases of PV with *JAK2* exon 12 mutation were identified. 14 had complete CBC and BM data at disease onset. Patients' median age at diagnosis was 48 (range, 2 weeks to 92) years. All had low erythropoietin levels. At diagnosis, 8/14 patients had normal WBC and platelet counts (IE subset); while 6/14 had elevated WBC and/or platelets (P subset). The BM cellularity was increased in 12/14 cases (mean IE: 75%, vs P: 93%). The myeloid to erythroid ratio (M:E) was 2 (range: 0.4- 5.1); mean IE was 1.8, vs mean P of 2.6. All had absent storage iron. Karyotype was normal in all onset cases. Mean and median *JAK2* variant allele frequency (VAF) was 16% and 8%, respectively (range: 2-83%), with no significant difference between the cohorts. Two *JAK2* deletion types were detected in the P cases (p.N542_E543 and p.E543_D544), while the IE cohort was more heterogeneous. Other frequent co-mutations included *TET2*, *DNMT3A* and *ASXL1* with similar distribution in the 2 cohorts. Overall, 4/14 cases did not fulfill WHO criteria for PV. There was no significant difference in patients' clinical course and outcome depending on the variant present.

Conclusions: Two subsets of PV with *JAK2* exon 12 mutation were identified. Isolated erythrocytosis (IE) cases showed lower BM cellularity and decreased M:E. Polycythemic cases were characterized by panmyelosis and 2 dominant *JAK2* mutation subtypes. Thus, the diagnostic criteria for PV may require modification to account for the variant CBC and BM findings. Comparing this data to published literature on *JAK2* V617F mutated PV, there were no significant differences between *JAK2* exon 12 and *JAK2* V617F mutation associated PV in relation to key clinical data and outcome.

690 Myeloid Proliferations Associated with Down Syndrome: Clinicopathologic Characteristics of Thirty Six Cases

Julia Geyer¹, Yen-Chun Liu², Jennifer Chapman³, Olga Weinberg⁴

¹Weill Cornell Medicine, New York, NY, ²University of Pittsburgh School of Medicine, Pittsburgh, PA, ³University of Miami, Miller School of Medicine, Miami, FL, ⁴UTSouthwestern Medical Center, Dallas, TX

Disclosures: Julia Geyer: None; Yen-Chun Liu: None; Jennifer Chapman: None; Olga Weinberg: None

Background: The incidence of myelodysplastic syndrome (MDS) and acute myeloid leukemia (AML) is significantly increased in young children with Down syndrome (DS). The WHO classification groups these cases as myeloid leukemia associated with DS (ML-DS) due to their similar clinical outcome. In addition, children with DS may present with transient abnormal myelopoiesis (TAM)-- a self-limiting condition that does not require therapy. The differential diagnosis between these myeloid proliferations (MP) may be challenging. We sought to review the clinical, pathologic, immunophenotypic and molecular genetic features of MP-DS, since this data is currently limited.

Design: All cases of MP-DS were identified from the files of 4 large academic institutions. Available clinical and pathologic information was recorded. Cases were classified according to the 2016 WHO Classification. Cytogenetic and molecular genetic information was recorded.

Results: 36 cases of MP-DS (27 ML-DS and 9 TAM) were identified. The median age for TAM was 4 days (range: 1 day - 3 years) versus 17 months (range: 6 -33) for ML-DS. TAM patients had significantly increased WBC (23.6 vs 8 k/uL, p=0.003) and MCV (109.7 vs 89 fL, p<0.001), compared to ML-DS patients who had decreased hemoglobin (9.6 vs 14.3 g/dL, p<0.001) and platelet counts (54.4 vs 183.5 k/uL, p<0.001). There was no significant difference in the mean number of circulating blasts (TAM: 24% vs ML-DS 13%) or bone marrow (BM) blasts (TAM: 14.5% vs ML-DS: 24%). Similar to ML-DS, 50% of TAM cases had megakaryoblastic differentiation. ML-DS with increased blasts comprised 24/27 (89%) cases, while 3 cases had multilineage dysplasia but no increase in blasts. Dyserythropoiesis was present in 67% of ML-DS versus 0% TAM patients (p=0.03). Dysgranulopoiesis was minimal to absent in both subsets. 75% ML-DS patients had BM fibrosis, compared to 33% TAM patients (p=0.2). 80% ML-DS patients had structural cytogenetic abnormalities, compared to 0/7 TAM patients (p<0.001). *GATA1* mutation was detected in 3/8 ML-DS patients vs 0/2 TAM patients. 20/22 ML-DS patients achieved complete remission after induction (CR1), while 2/22 had minimal residual disease.

Conclusions: Patients with TAM have significant differences in clinical presentation compared to ML-DS including younger median age and leukocytosis with preserved hemoglobin and platelet counts. ML-DS patients were likely to present with anemia and thrombocytopenia. Blast counts did not appear to differentiate between TAM and ML-DS. Presence of erythroid dysplasia appeared unique to ML-DS in this small study set. TAM patients had constitutional trisomy 21 but no other cytogenetic abnormalities, while ML-DS showed cytogenetic abnormalities in 80% of cases, supporting that these diseases are genetically distinct despite overlapping histopathologic features.

691 Human Herpesvirus 8 (HHV8)-Negative Effusion-Based Large B-cell Lymphoma: A Multicenter Clinicopathologic Study of 42 Cases and Review of the Literature

Savanah Gisriel¹, Ji Yuan², Xueyan Chen³, Xiaojun Wu⁴, Jenna McCracken⁵, Mingyi Chen⁶, Nathan Paulson⁷, Endi Wang⁸, Mina Xu⁹, Zenggang Pan⁷

¹Yale School of Medicine, Yale New Haven Hospital, New Haven, CT, ²Mayo Clinic, Rochester, MN, ³University of Washington, Seattle, WA, ⁴Johns Hopkins School of Medicine, Baltimore, MD, ⁵Duke Health, Durham, NC, ⁶UTSouthwestern Medical Center, Dallas, TX, ⁷Yale School of Medicine, New Haven, CT, ⁸Duke University Medical Center, Durham, NC, ⁹Yale University, New Haven, CT

Disclosures: Savanah Gisriel: None; Ji Yuan: None; Xueyan Chen: None; Xiaojun Wu: None; Jenna McCracken: None; Mingyi Chen: None; Nathan Paulson: None; Endi Wang: None; Mina Xu: None; Zenggang Pan: None

Background: Rare cases of Human Herpesvirus 8 (HHV8)-negative effusion-based large B-cell lymphomas (EB-LBCL) have been observed in the body cavities without associated tumor masses. However, it is not certain

whether EB-LBCL exists along the clinical spectrum of conventional diffuse large B-cell lymphoma (DLBCL) or is a distinct entity. Moreover, the clinicopathologic features remain to be further investigated.

Design: A total of 42 cases of HHV8-negative EB-LBCL were selected from our institutions from 2000 to 2020. All cases had no tumor masses prior to the diagnosis or during lymphoma staging. An additional 84 cases of EB-LBCL were retrieved from the literature for a comprehensive review. The major demographic, clinicopathologic, immunohistochemical, and molecular features are summarized in Table 1.

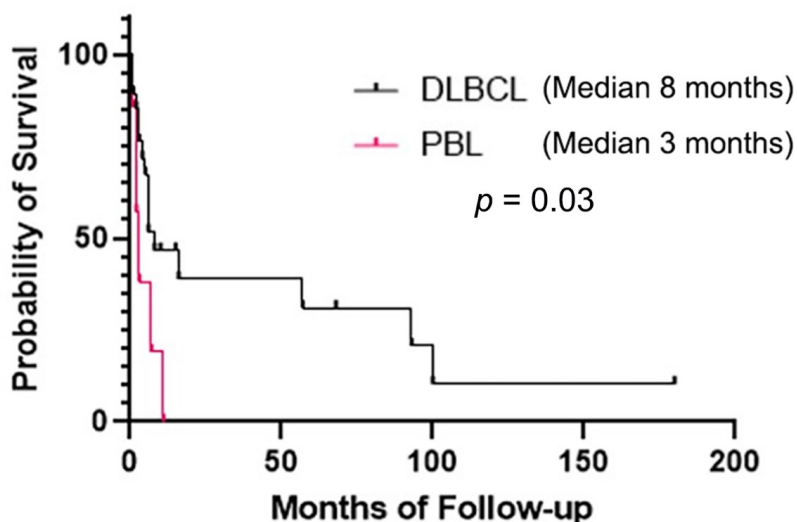
Results: The 42 cases in our study included 33 cases of DLBCL and 9 of plasmablastic lymphoma (PBL) with a male to female ratio of 1.6:1 and a median age of 78 years (range 35-95). The pleural cavity was the most common site (26/42, 62%), followed by the pericardial cavity (8/42, 19%). Most cases (22/26, 85%) were classified as non-germinal center B-cell (GCB) subtype based on Hans' algorithm. Two of 30 (7%) cases were positive for Epstein-Barr virus (EBV), but none had infection of HHV8 (0/30). Only one of 17 cases had double or triple rearrangements of *MYC*, *BCL2* and *BCL6*. Of the 34 cases with follow-up data, 22 were deceased (65%) during a median follow-up of 4 months (range 1-180). Only 5 of 36 patients developed extracavitary solid lymphoma masses during follow-up with a median interval of 52 months (range 5-180). The EB-LBCL in our study had an unfavorable prognosis with a median survival of 6 months; the PBL-type EB-LBCL was associated with a significantly poorer prognosis (median survival 3 months) than the DLBCL-type (median survival 8 months) ($p = 0.03$) (Figure 1).

The 84 cases of HHV8-negative EB-LBCL from the literature demonstrated similar clinicopathologic features to our cases (Table 1), which involved elderly patients (median age 77 years) and were mostly non-GCB subtype (16/21, 76%). However, the median overall survival was longer at 27.5 months.

	Our Study	Literature
Total Case Number	42	84
Median Age (Years)	78 (35-95)	77 (29-95)
Male/Female	26/16	43/41
Risk of Fluid Overload	19/32 (59%)	26/33 (79%)
History of Edema/Effusion	13/24 (54%)	
Effusion Sites		
Pleural	26/42 (62%)	47/82 (57%)
Pericardial	8/42 (19%)	6/82 (7%)
Peritoneal	3/42 (7%)	15/82 (18%)
Mixed	5/42 (12%)	14/82 (17%)
Follow Up (Median, Months)	4 (1-180)	8 (1-144)
Outcome (Deceased)	22/34 (65%)	38/77 (49%)
Overall Survival (Median, Months)	6	27.5
CD45	29/33 (88%)	
CD20	33/42 (79%)	
PAX5	12/20 (60%)	
BCL2	22/24 (92%)	
BCL6	14/26 (58%)	
CD10	4/43 (9%)	
MUM1	21/24 (88%)	
MYC	9/16 (56%)	
CD30	10/24 (42%)	
HHV8	0/30 (0%)	0/84 (0%)
EBER-ISH	2/30 (7%)	15/84 (18%)
GCB Subtype	4/26 (15%)	5/21 (24%)
<i>BCL2</i> Rearrangement	1/15 (7%)	1/17 (6%)
<i>BCL6</i> Rearrangement	4/14 (29%)	6/18 (33%)
<i>MYC</i> Rearrangement	3/18 (17%)	7/35 (20%)
HGBCL, Double- or Triple-Hit	1/17 (6%)	1/30 (3%)

Figure 1 - 691

Figure 1: DLBCL vs. PBL



Conclusions: Compared with conventional DLBCL, HHV8-negative EB-LBCL demonstrates some unique features; it tends to occur in older, immunocompetent individuals with no associated solid lymphomas. There is no HHV8 infection and EBV is mostly negative. It is mostly of non-GCB subtype and associated with a worse prognosis than previously reported.

692 Alpha-6 Integrin and CNS Metastasis of Chemoresistant Diffuse Large B-Cell Lymphoma

Savanah Gisriel¹, Mina Xu²

¹Yale School of Medicine, Yale New Haven Hospital, New Haven, CT, ²Yale University, New Haven, CT

Disclosures: Savanah Gisriel: None; Mina Xu: None

Background: Alpha-6 integrin ($\alpha 6i$) is a transmembrane protein that mediates cell-cell and cell-matrix adhesion. Recent literature has revealed that B-cell acute lymphoblastic leukemia (B-ALL) appears to metastasize to the central nervous system (CNS) via $\alpha 6i$ and that $\alpha 6i$ blockade may restore chemotherapy sensitivity in murine models. We have previously shown preliminary evidence that $\alpha 6i$ is similarly involved in the pathway of CNS infiltration by malignant cells in diffuse large B-cell lymphoma (DLBCL), but its association with chemotherapy resistance in CNS-infiltrative DLBCL has yet to be studied.

Design: From an initial cohort of 1185 DLBCLs from our institution, 182 cases had evaluable CSF. Of these, a total of 26 cases of patients demonstrated CNS metastasis by cytology or tissue diagnosis. Nineteen of these 26 cases were available for morphologic review and immunohistochemistry application. Each case was reviewed by two hematopathologists and the initial tissue biopsy was stained with anti- $\alpha 6i$; cases with at least 20% positivity in the lymphoma cells were considered positive. Each case was additionally reviewed for evidence of chemoresistance, which was defined as disease progression on pathology and/or radiology despite standard chemotherapy.

Results: 16 of the 19 cases had adequate follow-up data for evaluation of chemoresistance. Of the 5 cases that showed positivity for anti- $\alpha 6i$, 5 (100%) were determined to have chemoresistant disease. Of the remaining 11 cases that were negative for anti- $\alpha 6i$, 8 (73%) of them were found to have chemoresistance.

Conclusions: Our data suggest that anti- $\alpha 6i$ positivity on immunohistochemistry may be associated with chemoresistant disease in CNS-infiltrative DLBCL. Further investigation with a larger cohort, including in-vitro and in-vivo studies, is warranted to evaluate whether or not $\alpha 6i$ plays a major role in the development of adhesion-mediated chemotherapy resistance in CNS-infiltrative DLBCL.

693 Concurrent or Subsequent Lymphomatous Effusion in Diffuse Large B-Cell Lymphoma Portends Worse Prognosis

Savanah Gisriel¹, Ji Yuan², Jenna McCracken³, Vesal Yaghoobi¹, Nathan Paulson⁴, Myrto Moutafi⁵, Xiaojun Wu⁶, Endi Wang⁷, Mina Xu⁸, Zenggang Pan⁴

¹Yale School of Medicine, Yale New Haven Hospital, New Haven, CT, ²Mayo Clinic, Rochester, MN, ³Duke Health, Durham, NC, ⁴Yale School of Medicine, New Haven, CT, ⁵Yale University School of Medicine, New Haven, CT, ⁶Johns Hopkins School of Medicine, Baltimore, MD, ⁷Duke University Medical Center, Durham, NC, ⁸Yale University, New Haven, CT

Disclosures: Savanah Gisriel: None; Ji Yuan: None; Jenna McCracken: None; Vesal Yaghoobi: None; Nathan Paulson: None; Myrto Moutafi: None; Xiaojun Wu: None; Endi Wang: None; Mina Xu: None; Zenggang Pan: None

Background: Occasional cases of diffuse large B-cell lymphoma (DLBCL) develop concurrent or subsequent lymphomatous effusions (E-DLBCL) in the body cavities. It remains to be elucidated whether E-DLBCL represents a clinicopathologic entity distinct from its solid lymphoma counterpart. Further investigation is necessary for optimal risk stratification and therapeutic considerations.

Design: A total of 88 cases of E-DLBCL with concurrent or preceding solid lymphoma were selected from 2000 to 2020. Additional 101 cases of stage-IV DLBCL without an effusion component were included as a control cohort. The clinicopathologic characteristics of both cohorts are summarized in Table 1.

Results: The 88 cases of E-DLBCL equally affected males and females with a median age of 65.5 years. Approximately 22% (17/78) of patients were at risk for fluid overload and 32% (27/84) had a history of edema and/or benign effusions. Fifty-four patients presented with concurrent solid and effusion lymphomas, whereas 34 patients developed lymphomatous effusions after solid lymphoma with a median interval of 34 months (range 3-175). The malignant effusions mostly involved the pleural cavity (66/88, 75%).

Based on the Hans' algorithm, the E-DLBCL consisted mostly of germinal center B-cell (GCB) subtype (43/77; 56%). Approximately half (22/43, 51%) of the cases had dual over-expression of BCL2 and MYC. BCL2, BCL6, and MYC gene rearrangements were detected in 18/41 (44%), 8/23 (35%), and 20/52 (38%), respectively, including 22% (11/51) with MYC and BCL2 and/or BCL6 rearrangements. Neither the Hans' classification nor the double/triple-hit status of E-DLBCL were associated with overall survival.

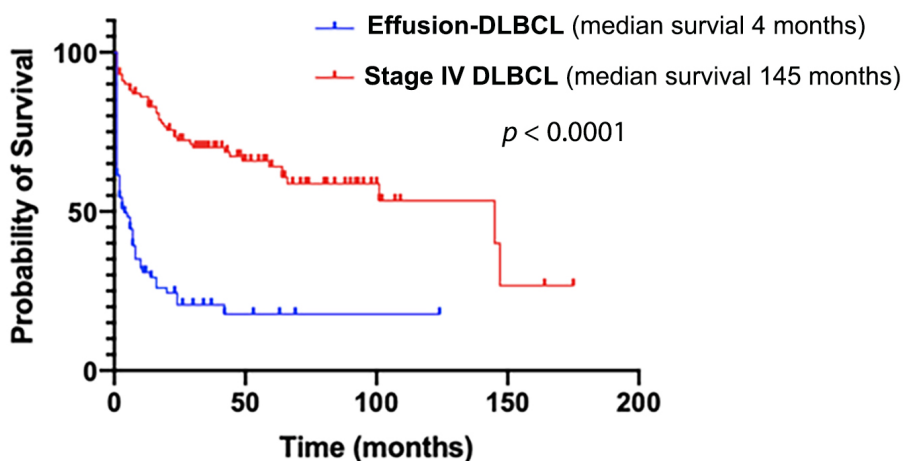
In our study, E-DLBCL revealed similar clinicopathologic characteristics to stage-IV DLBCL (Table 1). However, compared with the control cohort, E-DLBCL had a significantly shorter median survival (4 months vs. 145 months; $p < 0.0001$) (Figure 1) and a higher frequency of MYC rearrangement (38% vs. 18%; $p = 0.02$) and MYC expression (66% vs. 31%; $p = 0.004$). E-DLBCL had a higher proportion of BCL2/MYC dual over-expression (51% vs. 29%; $p = 0.03$).

	Effusion-DLBCL	Stage-IV DLBCL	P-Value
Total Case Number	88	101	
Median Age (Years)	65.5 (9-94)	66 (31-93)	0.64
Male/Female	47/41	48/53	0.47
Risk of Fluid Overload	17/78 (22%)		
History of Edema/Effusion	27/84 (32%)		
Effusion Sites			
Pleural	66/88 (75%)		
Pericardial	2/88 (2%)		
Peritoneal	11/88 (13%)		
Mixed	9/88 (10%)		
BM Involvement	17/48 (35%)	17/34 (50%)	0.26
Follow Up (Median, Months)	3 (1-124)	42 (1-175)	0.0001
Outcome (Deceased)	65/88 (74%)	39/101 (39%)	0.0001
Overall Survival (Median, Months)	4	145	<0.0001
CD45	35/35 (100%)		
CD20	79/85 (93%)		
PAX5	33/33 (100%)		
BCL2	60/71 (85%)	70/83 (84%)	1

BCL6	59/75 (79%)	77/90 (86%)	0.31
CD10	36/83 (43%)	33/94 (35%)	0.28
MUM1	39/61 (64%)	41/82 (50%)	0.13
MYC	27/41 (66%)	21/59 (31%)	0.004
CD30	3/24 (13%)		
HHV8	0/16 (0%)		
EBER-ISH	2/30 (7%)	3/32 (9%)	
<i>BCL2</i> Rearrangement	18/41 (44%)	17/39 (44%)	1
<i>BCL6</i> Rearrangement	8/23 (35%)	3/8 (38%)	1
<i>MYC</i> Rearrangement	20/52 (38%)	12/65 (18%)	0.02
GCB Subtype	43/77 (56%)	50/91 (55%)	1
<i>BCL2</i> / <i>MYC</i> Double Expressor	22/43 (51%)	18/63 (29%)	0.03
Double- or Triple-Hit	11/51 (22%)	6/59 (10%)	0.12

Figure 1 - 693

Effusion-DLBCL vs. Stage IV DLBCL



Conclusions: In contrast to conventional DLBCL, E-DLBCL has significantly higher frequencies of *MYC* rearrangement and *MYC*/*BCL2* dual expression. E-DLBCL is associated with a dismal prognosis, which is not predicted by the status of GCB subtype or double/triple-hit. These findings suggest that E-DLBCL may be a distinct entity that necessitates unique management.

694 Expression of Myeloid/Histiocytic Markers in Subtypes of Anaplastic Large Cell Lymphoma –Tissue Microarray Associated Immunohistochemical Panel Study

Benjamin Graham¹, Sanjay Bridgelall², Lubomir Sokol³, Qianxing Mo³, Poorvi Desai³, Wenyi Fan³, Ling Zhang³

¹H. Lee Moffitt Cancer Center & Research Institute, University of South Florida, Tampa, FL, ²University of South Florida Morsani College of Medicine, Tampa, FL, ³H. Lee Moffitt Cancer Center & Research Institute, Tampa, FL

Disclosures: Benjamin Graham: None; Sanjay Bridgelall: None; Ling Zhang: None

Background: Anaplastic large cell lymphoma (ALCL) is a mature T-cell lymphoma which is divided into systemic (sALCL, ALK(+)) or ALK(-)) and primary cutaneous (cALCL) forms. ALK(-) ALCL is associated with a poor prognosis compared to ALK+ ALCL. cALCL differs from systemic type wherein it is a more indolent disease with an excellent prognosis.

Diagnosis of ALCL is based on morphology and by immunohistochemistry (IHC) which show diffuse expression of CD30, ALK1, and T-cell markers. The diagnosis can still be challenging in ALK(-) cases or aberrant loss of T-cell markers (i.e. null type). Previous studies have shown expression of myeloid ((CD13, CD33) by flow cytometry), and histiocytic ((CD68-KP1) by IHC), markers by ALCL can be misdiagnosed as myeloid sarcoma. However, the expression of myelomonocytic markers (CD33, CD123, CD63, lysozyme, CD117) in different ALCL types is not well studied. This study aims to test the expression of myeloid and histiocytic markers and BCL-2, a marker reported to be negative in ALK+ ALCL, in the three subtypes of ALCL and determine if they can aid in the diagnosis of ALCL and pr

Design: Of 59 patients with ALCL from 2001-2016, 65 tissue samples (18 ALK+, 13 ALK-, 23 pCALCL, and 6 controls) met eligibility criteria. Tissue microarrays (TMAs) were constructed from formalin-fixed, paraffin-embedded skin and lymph node biopsies. Immunohistochemistry was performed with antibodies to the selected proteins (CD33, CD123, CD63, Lysozyme, BCL2, and CD117). Stained TMA slides were manually reviewed by two separate observers to determine staining intensity of each biomarker stain with staining intensity levels scored as follows: No staining=0, weak staining=+1, moderate staining=+2, and strong staining=+3. A positive result was a score of 2 or greater. Statistical analysis via Fisher's exact test and log-rank test were performed.

Results: IHC showed positive expression for CD30 and CD163 in all ALCL types, and with only few cases showing positivity for other myeloid markers (CD33, CD117, and CD123). Aberrant lysozyme stain was only found in 20% of ALCL-ALK+. BCL-2 stain was identified in the majority of cALCL when compared with sALCL ALK (-). Unexpectedly, 35.3% of sALCL-ALK+ also expressed BCL-2 (Table 1).

Table 1. Immunohistochemical (IHC) expression of myeloid/histiocytic/lymphoid markers in different subtypes of anaplastic large cell lymphoma (ALCL).

	Systemic ALCL ALK(-)	Systemic ALCL ALK(+)	Cutaneous ALCL ALK(-)	P-value
CD163	6/8 (75%)	17/17 (100%)	22/23 (95.65%)	0.5378
Lysozyme	0/9 (0%)	3/15 (20%)	0/23 (0%)	0.0332*
CD33	3/13 (23.10%)	4/18 (22.30%)	6/23 (26.10%)	0.1979
CD123	1/10, (0%)	0/17 (0%)	2/19 (9.52%)	0.6835
BCL-2	2/9 (22.20%)	6/17 (35.3%)	16/22 (71.75%)	0.0042*
CD117	1/9 (11.10%)	0/16 (0%)	3/23 (13%)	0.3835
Average age (years)	69	57	60	
Gender (male/female)	2.75	2	1.56	
# of cases	15	18	23	

*Indicates statistically significant p-values (p<0.05) as determined via Fisher's exact test.

Conclusions: Aberrant expression of CD163, but no other myeloid/monocytic markers (CD117, CD33, lysozyme and CD123), are identified in >75% of ALCL cases, regardless of the subtype. These findings must be carefully used for discrimination between ALCL and myeloid/monocytic neoplasms. Additional analyses showed aberrant expression of CD163 and BCL-2 were not associated with a poor clinical outcome (p>0.05).The clinical significance of CD163 is currently undetermined due to the low number of cases in the study. The expression of BCL-2 was found in cALCL-ALK(-) and a subset of sALCL-ALK(+), which might be targetable by using an anti-BCL-2 inhibitor, Venetoclax, for therapy in these patients.

695 Impact of Immunodeficiency on the Tumor Microenvironment in EBV-Positive Diffuse Large B-cell Lymphoma. Exploratory Study Using Gene Expression Analysis

Jose Guerrero Pineda¹, Luis Veloza², Christos Masaoutis³, Marco Buehler⁴, Inmaculada Ribera⁵, Sandra Sanchez¹, Olga Balagué¹, Manel Juan¹, Antonio Martinez⁵

¹Hospital Clinic, University of Barcelona, Barcelona, Spain, ²University of Barcelona, Barcelona, Spain, ³National and Kapodistrian University of Athens, Athens, Greece, ⁴Hospital Clinic-IDIBAPS, University of Barcelona, ⁵Hospital Clinic, Barcelona, Spain

Disclosures: Jose Guerrero Pineda: None; Luis Veloza: None; Christos Masaoutis: None; Marco Buehler: None; Inmaculada Ribera: None; Sandra Sanchez: None; Olga Balagué: None; Manel Juan: None; Antonio Martinez: None

Background: DLBCL arising in the context of immunosuppression, such as HIV infection, post-transplant immunosuppression or immune senescence, represents a major cause of mortality in these populations, which at least in part seems to be due to poor antitumoral and antiviral immune responses. However, the role of the tumor microenvironment (TME) in the clinical behaviour of EBV+ immunodeficiency-associated DLBCL is largely unknown and immune-related therapeutic targets are lacking in this setting.

Design: We performed gene expression profiling (GEP) using the HTG EdgeSeq Precision Immuno-Oncology Panel of 1392 immune-related genes (HTG Molecular Diagnostics, Inc. Tucson, AZ) in 16 FFPE tissue specimens of adult nodal EBV+ B-cell LPD: 8 EBV+ PTLD (4 DLBCL and 4 polymorphic PTLD), 4 EBV+ HIV+ DLBCL and 4 EBV+ DLBCL, NOS (Figure 1). Analysis of differentially expressed genes (DEG) between subgroups were performed using the R package DESeq2 (adj. p<0.10). The DAVID bioinformatics database was used for functional gene annotation according to Gene Ontology terms. GEP results were validated by selected IHC studies (Figure 2).

Results: We identified 33 DEG in EBV+ HIV+ DLBCL compared to EBV+ DLBCL, NOS. Genes with higher expression in EBV+ HIV-associated DLBCL showed an enrichment in biological processes related to extracellular matrix, cell chemotaxis and adhesion (p-value<0.016). *CXCL12* and *MMP2* were upregulated in EBV+ HIV+ DLBCL, while *MMP12*, *CCL17* and *ICOS* showed a higher expression in EBV+ DLBCL, NOS. No significant DEG between monomorphic (DLBCL) and polymorphic PTLD were observed, these subtypes were grouped together in further analyses. Comparing EBV+ PTLD to EBV+ DLBCL, NOS revealed 49 DEG: EBV+ PTLD showed higher expression of *IL6*, *IL17A* and genes with enrichment in cellular response to interleukin 1 (adj. p-value 0.01), while EBV+ DLBCL, NOS had higher expression levels of Treg related genes (*FOXP3*, *TIGIT*), *MMP9* and *FASL*. Several known genes involved in cancer immune-evasion pathways, such as *PDCD1*, *CD274*, *PDCD1LG2*, *LAG3*, *CTLA4*, *CD163*, *IDO*, *TGFB1* and *CD70* were not differentially expressed.

Figure 1 - 695

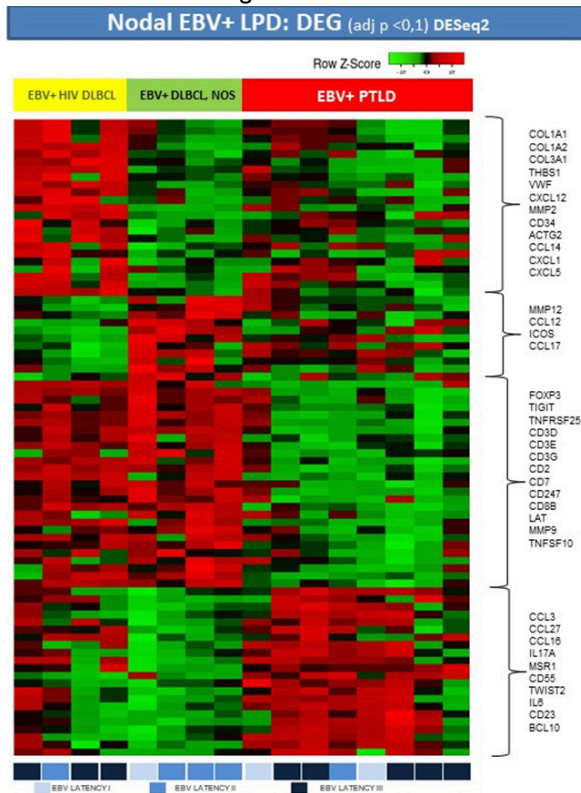
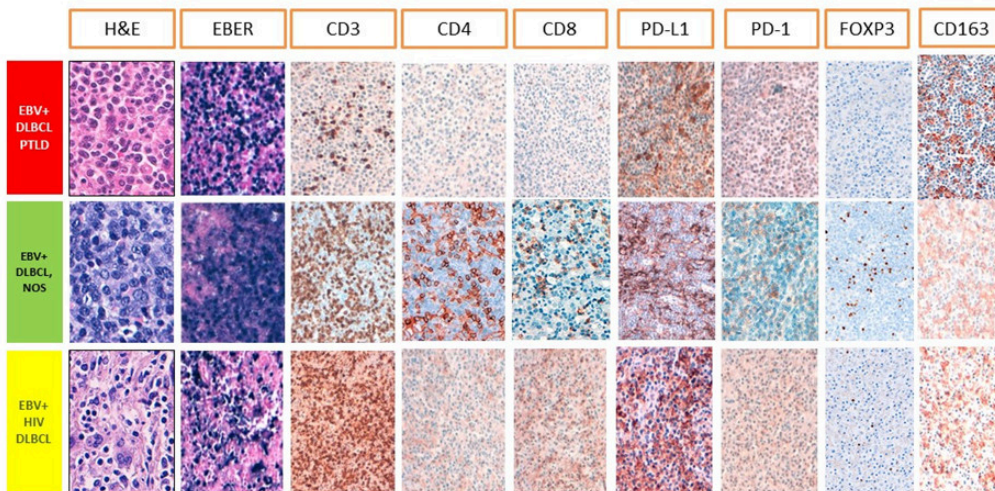


Figure 2 - 695

IHC: EBV+ LPD



Conclusions: Our results indicate that the nature of the underlying immunodeficiency impacts the TME in EBV+ DLBCL. However, the distinctive EBV+ immunodeficiency associated LPD share common deregulated immune pathways related to the presence of EBV and its latent proteins. Additionally, we identified potential biomarkers, which may help implement personalized therapies.

696 Chronic Lymphocytic Leukemia/Small Lymphocytic Lymphoma (CLL/SLL) with Reed-Sternberg-Like Cells and Classic Hodgkin Lymphoma Transformation of CLL/SLL: Does This Distinction Matter?

Alia Gupta¹, Paul Kurtin¹, Sameer Parikh¹, Rebecca King¹
¹Mayo Clinic, Rochester, MN

Disclosures: Alia Gupta: None; Paul Kurtin: None; Rebecca King: None

Background: Clinicopathologic distinction between chronic lymphocytic leukemia/small lymphocytic lymphoma (CLL/SLL) with isolated RS cells (CLL-RS) and overt transformation to classic Hodgkin lymphoma (CLL-HL) is incompletely understood.

Design: We identified CLL/SLL patients with a tissue biopsy showing RS cells from 1990-2020. On pathology re-review, patients were classified as CLL-RS (isolated RS cells in a background of CLL) or CLL-HL (RS cells in an inflammatory milieu). Clinical characteristics, therapy, and outcomes were abstracted.

Results: 44 patients were identified: 29(66%) were classified as CLL-HL and 15(34%) as CLL-RS. Two CLL-HL cases had discrete, separate areas of CLL-RS. Background milieu in CLL-HL comprised of lymphocytes, histiocytes, and fibrosis without eosinophils in majority of cases (52%). CLL-RS had a background composed predominantly of small B-cells (CLL/SLL). By CD3 IHC, 8/12(67%) cases showed rosetting of T-cells around RS cells suggesting the beginning of a Hodgkin-like milieu. EBER was positive in RS cells in 8/9(89%) CLL-RS and 15/23(65%) CLL-HL. Phenotypic data is shown in Table 1. Median age of all patients was 64 years with a male predominance (75%). Median time from CLL diagnosis to either CLL-RS or CLL-HL was 6.3 years (CLL-RS: 4.9 years, CLL-HL: 6.7 years). One patient with CLL-RS transformed to CLL-HL in 19 months. One with CLL-HL had a subsequent biopsy showing CLL-RS in 32 months. 7/15 (47%) patients with CLL-RS had received prior CLL therapy compared to 19/29 (65%) patients with CLL-HL. Of 15 patients with CLL-RS, 7 received CLL directed therapy, 6 received HL directed therapy, and 2 had no therapy. Of 29 patients with CLL-HL, 16 received ABVD-based therapy, 7 received non-ABVD-based HL-directed therapy, and 4 received other therapy (2 with CLL directed treatment, 1 radiotherapy and 1 unknown). Median overall survival (OS) from time of CLL-RS or CLL-HL diagnosis was 30.9 months (Figure 1a) Although the OS was shorter in patients with CLL-RS compared to CLL-HL (17.7 vs. 31.5 months), this was not statistically significant (p= 0.32). Notably, patients with CLL-RS who received CHL-directed therapy had better OS than those who received CLL directed therapy (Figure 1b).

Table 1: Phenotypic findings in patients with CLL-RS and CLL-HL.

Stain	CLL-RS	CLL-HL	P- value
	Positive/total (%)	Positive/total (%)	Fisher exact test
EBER	8/9(89%)	15/23(65%)	P=0.383
CD30	11/11(100%)	24/24(100%)	P=1.0
CD15	6/11(55%)	18/24(75%)	P=0.263
CD20	3/11(27%)	1/24(4%)	P=0.0819
CD45	0/11(0%)	0/24(0%)	P=1.0
PAX5	10/11(91%)	21/23(91%)	P=1.0

Figure 1 - 696

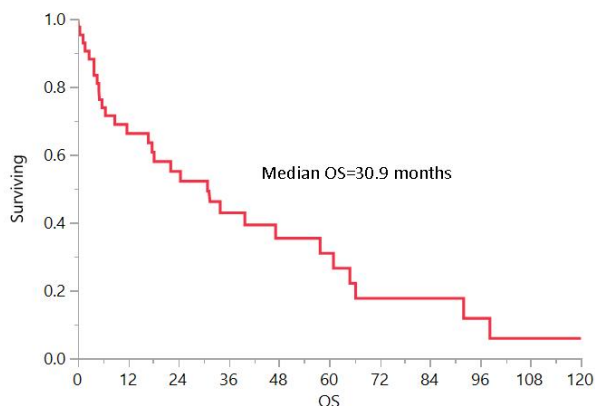


Figure 1a: Overall survival (in months) of all patients (n=44) with CLL/SLL who have RS cells in tissue biopsy

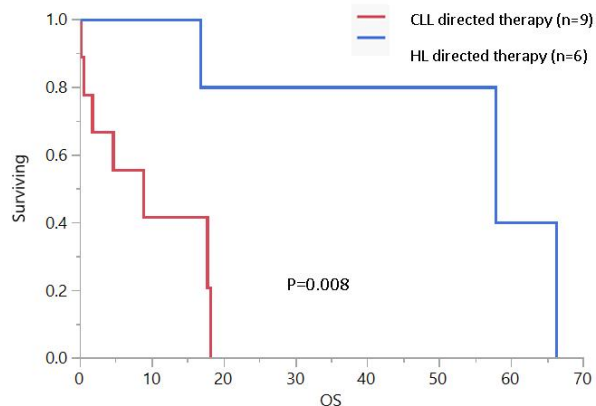


Figure 1b: Overall survival (in months) of patients with CLL-RS, according to the type of treatment received; CLL-directed (n=9) and HL directed therapy (n=6)

Conclusions: Distinction between CLL-RS and CLL-HL lies predominantly in the background cellular milieu. Our clinical and pathologic findings suggest a biologic continuum between CLL-RS and CLL-HL, and suggest CLL-RS patients may benefit from CHL-directed therapy.

697 Quantitative Analysis of Megakaryocytes in Autopsy Lungs and Bone Marrow of Patients with COVID-19

Jack Harbert¹, Fernanda Da Silva Lameira², Sharon Fox³, Gordon Love¹, Rachna Jetly Shridhar²
¹Louisiana State University Health Sciences Center, New Orleans, LA, ²LSUHSC School of Medicine New Orleans, New Orleans, LA, ³SLVHCS/ Louisiana State University, New Orleans, LA

Disclosures: Jack Harbert: None; Fernanda Da Silva Lameira: None; Sharon Fox: *Consultant*, Boehringer Ingelheim; Gordon Love: None; Rachna Jetly Shridhar: None

Background: Autopsy studies report increased lung megakaryocyte counts (MKC) in respiratory and cardiovascular disease states. COVID-19 caused by SARS-CoV-2 can have severe complications including coagulopathies, hyperinflammatory response and respiratory failure. There is evidence of increased lung MKC in severely ill patients likely caused by cytokines released as part of an inflammatory response. We analyzed the effect of COVID-19 on lung and bone marrow (BM) MKC in autopsy patients and impact of disease severity based on duration of ventilator support was assessed.

Design: Case (N=11) and non-COVID-19 control (N=5) patients were randomly selected. On each patient, one BM and four lung sections, one from each major lobe, were stained with CD61. The slides were digitized and de-identified using a Leica Aperio AT2 whole slide image scanner. Five 1x1 mm areas of interest were selected on each slide for image analysis by two residents to exclude potential artifact. Image analysis software modified for selection of megakaryocytes was utilized within selected areas to determine the CD61+ MKC /5 mm² quantitatively (figure). An n-way analysis of variance (ANOVA-n) was employed to examine the effects of group (COVID-19 cases versus controls), and ventilator use on MKC, as well as the interaction between these two factors.

Results: The effect of group (COVID-19 versus control) was found to be significant, with the MKC elevated in the lungs of COVID-19 group (F=4.51, p=0.041), while this effect of group was not seen in BM (F=0.18, p=0.6812). Ventilator time had only a marginally significant effect, with COVID-19 patients on ventilators having higher lung MKC as compared to control patients not on ventilators. Additional analyses of the region of lung sampling and clinical characteristics were performed.

Figure 1 - 697

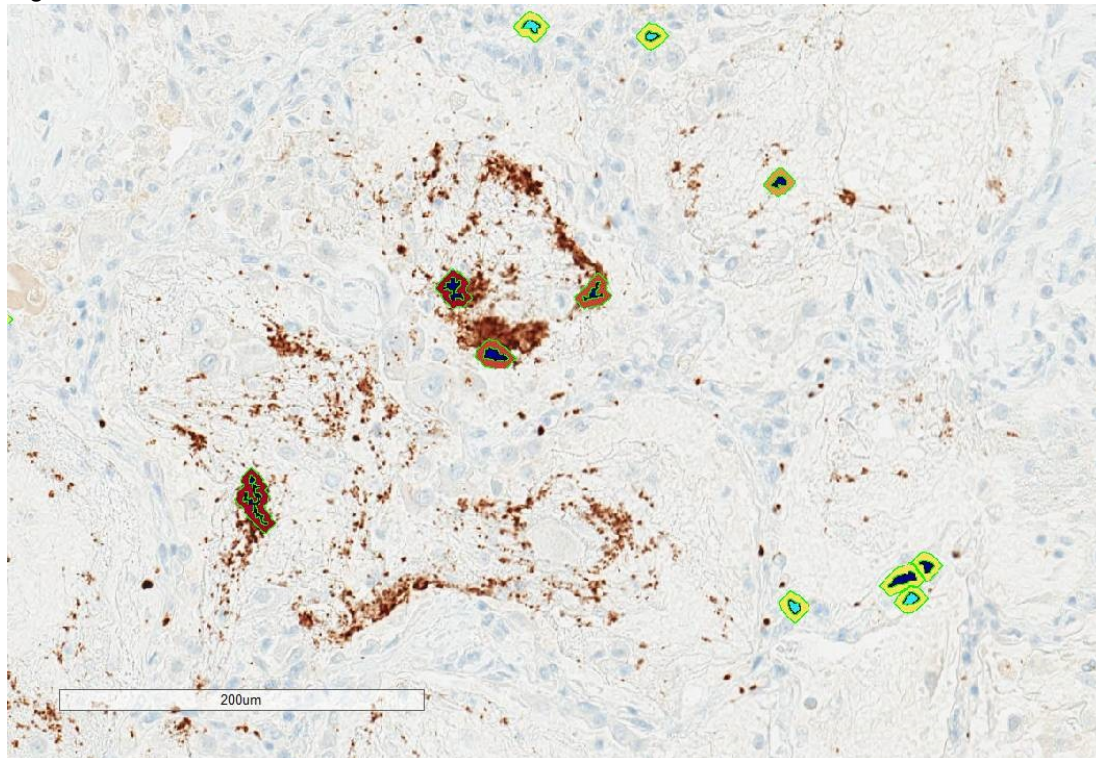


Image analysis of CD61 IHC-stained slide - Cells with dark nuclei and brown cytoplasm are counted as a megakaryocyte whereas cells with lighter nuclei and yellow cytoplasm are not counted

Conclusions: While findings may not be specific to COVID-19, increase in lung MKC in COVID-19 patients suggests a response to inflammatory stimuli which also directly relates to disease severity. Lack of increase in BM MK count is interesting and supports recent literature that lung may be home to distinct MK populations. These likely include circulating MKs originating from the BM thrombopoietic pool and a separate resident MK population of uncertain origin localized within the lung interstitium that may play a role in lung immunity. Additionally, increased lung MKs potentially release activated platelets contributing to coagulopathies in severely ill patient.

698 Global Tissue Metabolomics of Follicular Lymphoma Shows Overt Reprogramming of the Normal Lymph Node Metabolome, Including Signatures Suggestive of Increased Fatty Acid β Oxidation

Pedro Horna¹, Linda Dao¹, Paul Kurtin¹, Andrew Feldman¹, Surendra Dasari¹, Ellen McPhail¹
¹Mayo Clinic, Rochester, MN

Disclosures: Pedro Horna: None; Linda Dao: None; Paul Kurtin: None; Andrew Feldman: None; Surendra Dasari: None; Ellen McPhail: None

Background: Follicular lymphoma (FL) is the second most common B-cell neoplasm, characterized by close morphologic and immunophenotypic resemblance to benign germinal center hyperplasia (GCH), and a highly variable clinical course. Several lines of evidence have shown an overt metabolic reprogramming in cancer, driven by genetic, epigenetic and environmental changes; and of potential importance for novel targeted therapies. However, the metabolic changes in the specific case of FL remain largely unexplored.

Design: Fresh frozen aliquots of lymph node biopsies with low-grade FL (16), GCH (10) and normal-appearing morphology (NAL, 10), were homogenized and diluted to an equivalent tissue weight per volume. The samples were precipitated with methanol, and analyzed by 4 different ultra-performance liquid chromatography/tandem mass spectrometry platforms (Metabolon, Morrisville, NC). Metabolites and other biochemicals were identified by

comparison to a library of purified standards, quantified using log-transformed areas-under-the-curve, normalized to the median, and imputed with the minimum. A $p < 0.05$ and $q < 0.1$ was considered statistically significant.

Results: Of 924 detected biochemicals, 193 (21%) were over (163) or underrepresented (30) in FL compared to NALs; including increased lactate, nucleotide metabolites, amino-acid metabolites, acylcarnitines, phospholipids, UDP-nucleotides and polyamines; and decreased glucose, folate, histidine and di-/monoacylglycerols (Figure 1). Of these, 19 biochemicals were also over (16) or underrepresented (3) in FL compared to GCH, including 11 increased acylcarnitines. Random forest, principal component and hierarchical cluster analyses showed distinct clustering of FL with a prediction accuracy of 87%, but poor discrimination between GCH and NAL (Figure 2). Notably, 11 of the 30 (37%) most discriminative metabolites in FL were acylcarnitines.

Figure 1 - 698

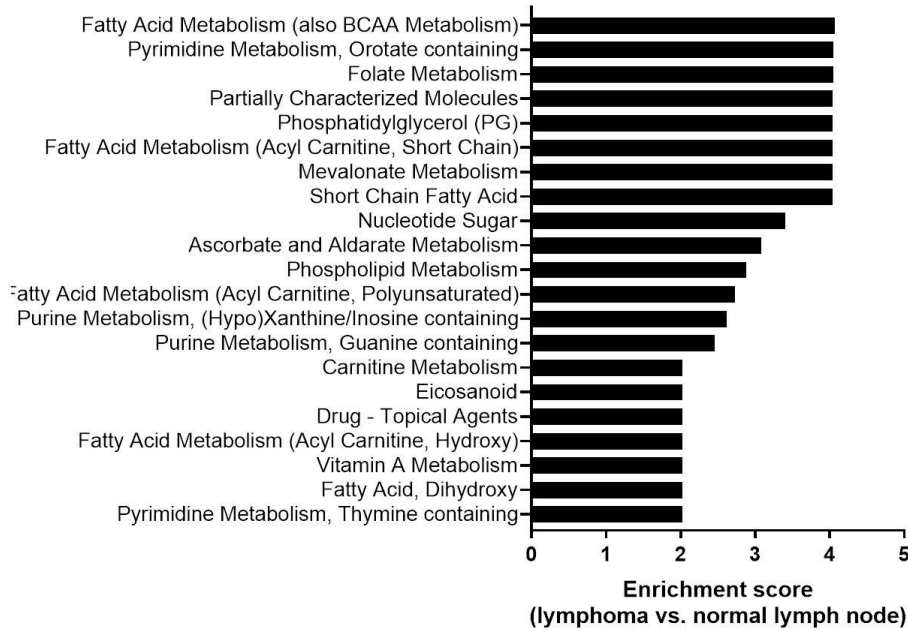
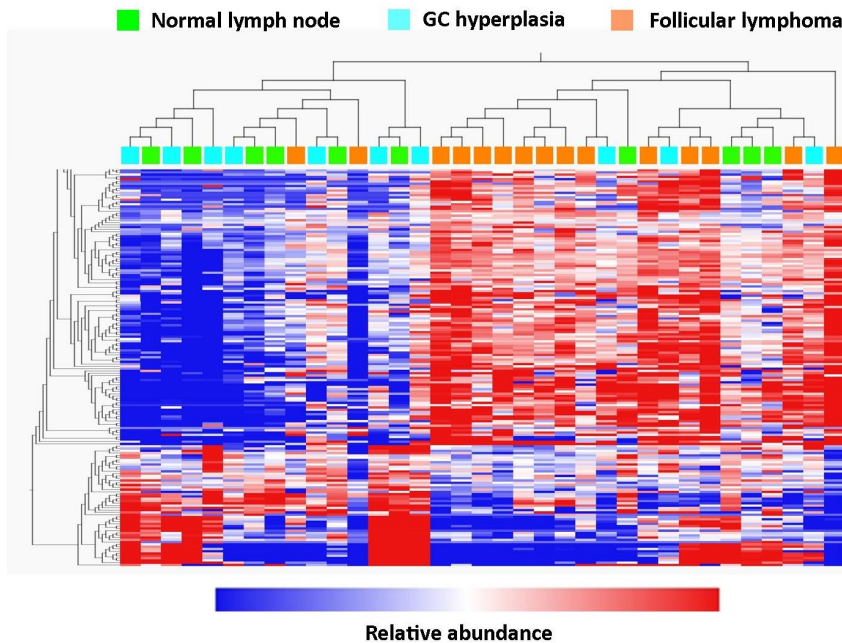


Figure 2 - 698



Conclusions: The metabolome of FL is highly suggestive of increased mitochondrial fatty acid β oxidation, as evidenced by several overrepresented acylcarnitines necessarily produced by the shuttling of fatty acids into the mitochondria. Increased phospholipids and decreased di-/monoacylglycerols point towards broader disruptions in lipid metabolism. Alterations in glucose, nucleotide, amino-acid and polyamine metabolites provide further insights into the metabolome of FL. These findings warrant consideration of available inhibitors of fatty acid β oxidation as potential therapeutic strategies in FL.

699 Whole Transcriptome Sequencing of Castleman Disease Shows Deregulation of the Complement and Coagulation Cascades; Overexpression of Selected Cytokines, Chemokines and Growth Factors; and Possible Role of RAP1 Signaling and Extracellular Matrix Remodeling

Pedro Horna¹, Dragan Jevremovic¹, Rebecca King¹, Angela Dispenzieri¹
¹Mayo Clinic, Rochester, MN

Disclosures: Pedro Horna: None; Dragan Jevremovic: None; Rebecca King: None; Angela Dispenzieri: None

Background: Castleman disease (CD) is a rare lymphoproliferation of unknown etiology characterized by lymphadenopathy with a unique histomorphology, in addition to variably associated inflammatory symptoms. Besides the suspected role of IL-6 and VEGF, the cellular and molecular mechanisms of CD are poorly understood, and targeted therapeutic options are limited.

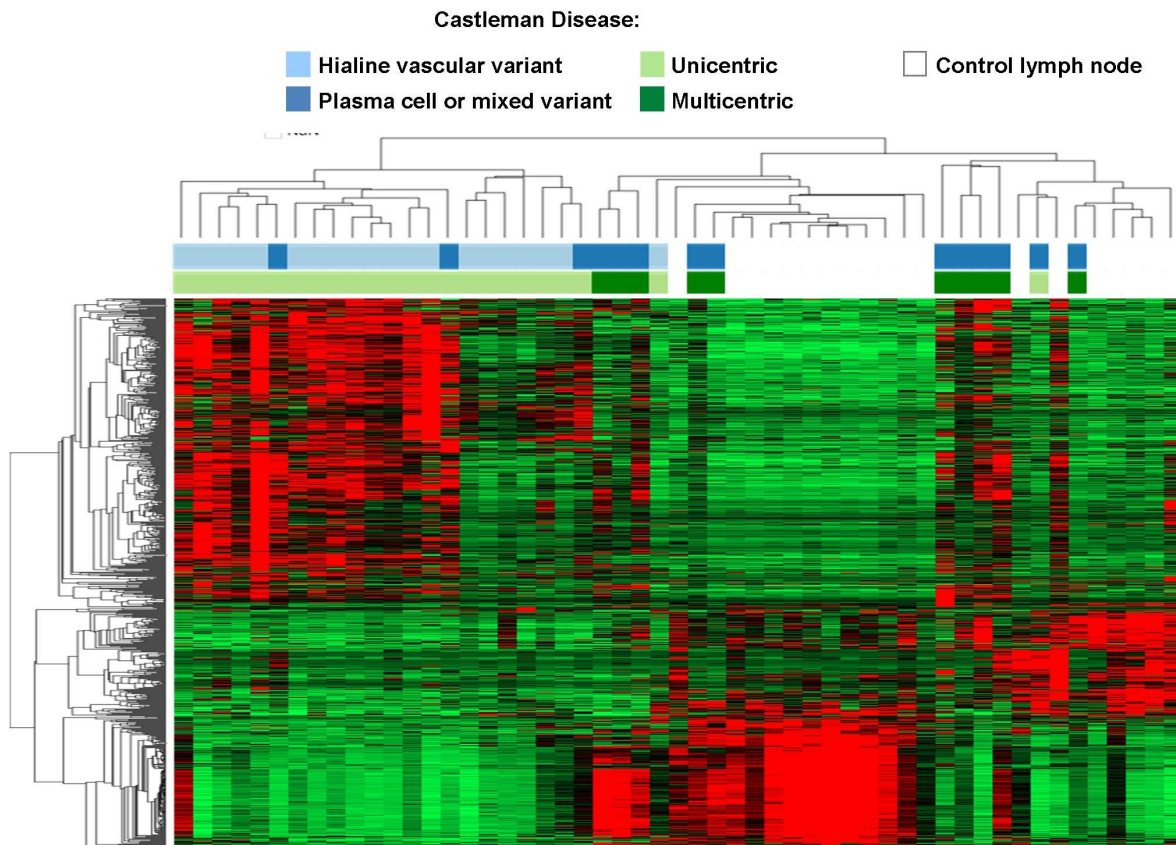
Design: We performed whole transcriptome sequencing on fresh-frozen aliquots from lymph node biopsies with confirmed CD (34); including cases of unicentric (24) or multicentric (10) disease; and cases with hyaline vascular (20), plasma cell (7) or mixed (7) histomorphology. Control lymph nodes with normal-appearing morphology (16) were also similarly studied. Differentially expressed genes on CD compared to control samples were identified using normalized log-transformed transcript counts, and considering a $p < 0.01$ and a greater than two-fold difference. Gene set enrichment was studied based on curated gene ontology and KEGG pathway annotations.

Results: A total of 887 differentially expressed genes in Castleman disease were identified, of which 764 were protein-coding genes (418 upregulated and 346 downregulated)(Figure 1). Enrichment analysis showed increased transcription of genes involved in the complement and coagulation cascades (C1R, C1S, C3, C4b-binding protein, complement factors I and H, plasminogen activator inhibitor 1, α 2 antiplasmin and factor XII)(Table 1). While IL-6 and VEGF were not found to be upregulated in this study, transcripts of several chemokines (CCL2, CCL19, CCL21, CCL24, CXCL13), growth factors (PGF, FGF1, FGF7, amphiregulin), and angiogenic mediators (angiopoietin 2, FLT1) were overrepresented in CD. Increased transcription of activators (adenosine receptor A2B and FLT1) and modulators (RAP1GAP, RAPGEF4) of RAP1 suggest a role of this signaling pathway in CD. Finally, transcription of several components and modulators of the extracellular matrix were upregulated in CD.

Selected Upregulated Genes in Castleman disease, Curated by Known Biological Process			
Category	Gene ID	Gene Name	Ontology/Pathway (enrichment P)
Complement/ Coagulation	BDKRB2	bradykinin receptor B2	KEGG map4610 (p<0.0001) GO:0051917 (p=0.01) GO:0030194 (p=0.02) GO:0010755 (p=0.03)
	C1R	complement C1r	
	C1S	complement C1s	
	C3	complement C3	
	C4BPA	complement component 4 binding protein alpha	
	CFH	complement factor H	
	CFHR1	complement factor H related 1	
	CFI	complement factor I	
	CLU	clusterin	
	F12	coagulation factor XII	
	SELP	selectin P	
	SERPINE1	Plasminogen activator inhibitor 1	
	SERPINF2	Alpha2 plasmin inhibitor	
	THBS1	thrombospondin 1	
Cytokines, Chemokines and receptors	APLN	apelin	GO:0005125 (NS)
	CCL19	C-C motif chemokine ligand 19	
	CCL2	C-C motif chemokine ligand 2	
	CCL21	C-C motif chemokine ligand 21	
	CCL24	C-C motif chemokine ligand 24	

	CXCL13	C-X-C motif chemokine ligand 13	GO:0008009
	IL1R2	interleukin 1 receptor type 2	
	OSMR	oncostatin M receptor	(NS)
	SCG2	secretogranin II	
	SPP1	secreted phosphoprotein 1	
	TNFRSF11B	TNF receptor superfamily member 11b	
Growth factors and receptors	ANGPT2	angiopoietin 2	GO:0008083
	AREG	amphiregulin	
	CTGF	connective tissue growth factor	(NS)
	CYR61	cysteine rich angiogenic inducer 61	
	DKK1	dickkopf WNT signaling pathway inhibitor 1	
	ERBB4	erb-b2 receptor tyrosine kinase 4	GO:0019838
	FGF1	fibroblast growth factor 1	
	FGF7	fibroblast growth factor 7	(NS)
	FLT1	fms related tyrosine kinase 1	
	GDF5	growth differentiation factor 5	
	INHBB	inhibin beta B subunit	GO:0070851
	PGF	placental growth factor	
	TGFB3	transforming growth factor beta 3	(NS)
RAP-1 Signaling	ADCY2	adenylate cyclase 2	KEGG Ko04015
	ADORA2B	adenosine A2b receptor	
	CNR1	cannabinoid receptor 1	(p=0.005)
	EFNA5	ephrin A5	
	GRIN2A	glutamate ionotropic receptor NMDA type subunit 2A	
	ITGB3	integrin subunit beta 3	
	LPAR1	lysophosphatidic acid receptor 1	
	PLCE1	phospholipase C epsilon 1	
	RAP1GAP	RAP1 GTPase activating protein	
	RAPGEF4	Rap guanine nucleotide exchange factor 4	
Extracellular Matrix	ADAMTS1	ADAM metalloproteinase with thrombospondin type 1 motif 1	GO:0030198
	ADAMTS4	ADAM metalloproteinase with thrombospondin type 1 motif 4	
	ADAMTS8	ADAM metalloproteinase with thrombospondin type 1 motif 8	(p<0.0001)
	BGN	biglycan	
	COL10A1	collagen type X alpha 1 chain	
	COL11A1	collagen type XI alpha 1 chain	GO:0022617
	COL13A1	collagen type XIII alpha 1 chain	
	COL15A1	collagen type XV alpha 1 chain	(p=0.03)
	COL4A1	collagen type IV alpha 1 chain	
	COL5A2	collagen type V alpha 2 chain	
	CTSK	cathepsin K	GO:0004222
	FAP	fibroblast activation protein alpha	
	HAS2	hyaluronan synthase 2	(NS)
	HTRA1	HtrA serine peptidase 1	
	LUM	lumican	GO:0005201
	MATN3	matrilin 3	
	MMP1	matrix metalloproteinase 1	
	MMP10	matrix metalloproteinase 10	(NS)
	MMP16	matrix metalloproteinase 16	
	MMP19	matrix metalloproteinase 19	GO:0005518
	POSTN	periostin	
	SULF1	sulfatase 1	(NS)
	TIMP1	TIMP metalloproteinase inhibitor 1	
	VCAN	versican	
	VTN	vitronectin	GO:0008237
			(NS)
			GO:0050840
		(NS)	

Figure 1 - 699



Conclusions: We describe for the first time the transcriptome of Castleman disease, including overexpression of elements of the complement and coagulation cascades, several cytokines and chemokines, several growth factors, and signatures suggestive of a role of RAP1 signaling and extracellular matrix remodeling.

700 Flow Cytometric Evaluation of Surface and Cytoplasmic TRBC1 Expression in the Differential Diagnosis of Immature T-Cell Proliferations

Pedro Horna¹, Min Shi¹, Dragan Jevremovic¹, Horatiu Olteanu¹
¹Mayo Clinic, Rochester, MN

Disclosures: Pedro Horna: None; Min Shi: None; Dragan Jevremovic: None; Horatiu Olteanu: None

Background: Flow cytometric detection of T-cell clonality is challenging, particularly in the differential diagnosis of immature T-cell proliferations. This scenario often occurs when immunophenotyping mediastinal tissue biopsies that may be involved by T-lymphoblastic leukemia/lymphoma (T-ALL) or by expansions of normal thymocytes (thymoma or thymic hyperplasia). The rearrangement of the *TCRB* gene involves the random and mutually exclusive utilization of one of two constant β chain genes (*TRBC1* and *TRBC2*), analogous to the kappa and lambda gene utilization by B cells. Several studies have shown the utility of a single TRBC1 antibody, in conjunction with other T-cell associated markers, as a reliable, simple and rapid assay to identify T-cell clonality by flow cytometry, including in tissue biopsies. However, one of the limitations of surface TRBC1 expression is that it cannot be detected in surface CD3-negative T cells, such as normal or abnormal immature T-cell precursors. Here, we assess the surface and cytoplasmic TRBC1 expression patterns in the differential diagnosis of T-ALL vs. normal thymocyte expansions.

Design: 40 tissue, bone marrow or peripheral blood specimens from patients with a known diagnosis of a T-ALL or thymoma/thymic hyperplasia were analyzed. Available medical record data including morphologic pathology

reports; molecular, cytogenetic and other laboratory results; clinical notes and imaging studies were reviewed to identify these patients. Flow cytometry was performed with an antibody panel, including CD2, CD3, CD4, CD5, CD7, CD8, CD45, TRBC1, with both surface and cytoplasmic staining for CD3 and TRBC1. TRBC1 expression was assessed on both normal and aberrant T-cell subsets. Restricted (monotypic) TRBC1 expression was defined when present on > 85% or <15% of a distinct T-cell cluster.

Results: Specimens comprised mediastinal masses (n=27), lymph nodes (n=3), bone marrow (n=5), and peripheral blood (n=5), and were obtained from 20 M and 20 F (median age=51 years; range, 4-86). Patients had a diagnosis of thymoma/thymic hyperplasia (n=23) and T-ALL (n=17). We examined TRBC1 expression in surface CD3-negative, T-lymphoblast populations identified based on their immunophenotypic aberrancies, and all were surface TRBC1-negative, as expected. We then evaluated cytoplasmic TRBC1 expression in 8 patients with T-ALL, and all showed monotypic TRBC1 expression (3 positive and 5 negative, respectively). We applied a similar gating strategy to the 20 cases of thymoma/thymic hyperplasia, and found that all cases revealed a characteristic and reproducible surface CD3/TRBC1 expression pattern, that allows distinction from cases of T-ALL.

Conclusions: Evaluation of surface and cytoplasmic TRBC1 expression by flow cytometry is a simple and robust assay that can aid in the detection of T-cell clonality and in the differential diagnosis of immature T-cell proliferations.

701 T-Cell Prolymphocytic Leukemia (T-PLL) with t(X;14)(q28; q11.2): A Report of 17 Cases

Zhihong Hu¹, Mina Xu², Ji Yuan³, Deniz Peker⁴, Lina Shao⁵, Adan Rios⁶, L. Jeffrey Medeiros⁷, Shimin Hu⁷
¹The University of Texas Health Science Center at Houston, Houston, TX, ²Yale University, New Haven, CT, ³Mayo Clinic, Rochester, MN, ⁴Emory University, Atlanta, GA, ⁵University of Michigan, Ann Arbor, MI, ⁶McGovern Medical School at UTHealth, The University of Texas Health Science Center at Houston, Houston, TX, ⁷The University of Texas MD Anderson Cancer Center, Houston, TX

Disclosures: Zhihong Hu: None; Mina Xu: None; Ji Yuan: None; Deniz Peker: *Advisory Board Member*, Seattle Genetics; *Consultant*, Gerogia Composite Medical Boards; Lina Shao: None; L. Jeffrey Medeiros: None; Shimin Hu: None

Background: T-PLL is a rare mature T-cell leukemia characterized by inv(14)(q11.2q32)/t(14;14)(q11.2;q32), and rarely t(X;14)(q28;q11.2). We aimed to investigate the clinical and pathologic features of T-PLL with t(X;14)(q28;q11.2).

Design: Cases of T-PLL with t(X;14)(q28; q11.2) diagnosed in six institutions from January 1, 2010 through October 20, 2020 were reviewed.

Results: The study group included 17 patients diagnosed with T-PLL with t(X;14) (q28;q11.2): 11 women and 6 men, with a median age of 64 years (range, 44-82). All 17 patients had leukocytosis with lymphocytosis, 6 lymphadenopathy, 5 splenomegaly, 3 hepatomegaly, 2 effusions, 2 central nervous system involvement, and 1 bilateral parotid lymphoepithelial cyst. The disease was detected incidentally in 11 patients. Morphologically, the leukemic cells were of prolymphocyte type in 11 cases, small cell variant 5, and cerebriform variant 1. Bone marrow was hypercellular in all 17 cases, and in 13/17 cases leukemic cells distributed in an interstitial pattern. The leukemic cells were positive for CD3, CD5, CD7, CD26, CD52, TCR-AB and CD2 (16/17), CD4 (15/17), and CD8+ (11/17). All cases were positive for T-cell receptor gene rearrangement by PCR. An NGS panel showed mutations of JAK3 in 4/5, STAT5B in 2/5, and JAK1, BCORL1, IL2RG, TET2, and TP53 each in 1/5 cases. One patient had concurrent JAK3 and JAK1 mutations, one patient had concurrent JAK3 and STAT5B mutations, and one patient had concurrent JAK3 and IL2RG mutations. Complex karyotype was detected in 16 cases, and TRA-TRD/MTCP1 rearrangement was detected by FISH in 3 cases. Fifteen of 17 patients received therapy after diagnosis, including 10 with alemtuzumab, 5 pentostatin, and 5 stem cell transplant. After a median follow-up of 15 months (range 1.6-41.0), 7 of 16 patients expired. The median overall survival was 18.4 months.

Conclusions: T-PLL with t(X;14) (q28; q11.2) is rare and frequently shows a complex karyotype and mutations of the JAK/STAT pathway. Despite being diagnosed incidentally in most of patients, T-PLL with t(X;14)(q28;q11.2) is an aggressive disease and patients with the disease have a dismal outcome.

702 Challenges with Communicating Minimal Residual Disease Findings for Acute Myeloid Leukemia in Pathology Reports

Huiya Huang¹, Steven Kroft¹, Tavinder Ark¹, Maria Hintzke¹, Alexandra Harrington¹

¹Medical College of Wisconsin, Milwaukee, WI

Disclosures: Huiya Huang: None; Steven Kroft: None; Tavinder Ark: None; Maria Hintzke: None; Alexandra Harrington: None

Background: The assessment and reporting of acute myeloid leukemia (AML) with minimal residual disease (MRD) can be challenging due to the variabilities of normal, regenerating, and neoplastic myeloblast immunophenotypes (IPs) and confusion around the definition of MRD. We sought to review our bone marrow reports for diagnostic wording in AML follow-ups and to survey our oncologists and pathologists for their interpretation of these reports.

Design: A retrospective review was performed to summarize AML follow-up bone marrow diagnoses between 2017 and 2019 at our institution. A survey was created with representative diagnoses (scenarios) and questions to assess the understanding of the diagnostic language, European Leukemia Net (ELN) guidelines, and preferred wording for each scenario. The survey was distributed to both clinicians and hematopathologists involved in the care of AML patients at our institution.

Results: Low-level residual AML (<5% blasts) accounted for 128 of 875 (14.6%) reports in the 3-year period. In 59 cases (6.7%), residual disease was only detected by flow cytometry, with no morphologic evidence of AML. The language used in these reports was variable and organized into 10 representative scenarios based on blast IP and blast percentage. We received 14 responses (54% of those surveyed), including 8 oncologists, 5 hematopathologists and 1 physician assistant. When MRD was stated in the diagnostic line, 92% interpreted it confidently as MRD. When the diagnosis stated only "(mildly) aberrant blasts," there was increased uncertainty of whether MRD was present or not. Most (82%) preferred the pathology report to follow the ELN guidelines; however, in questions asking whether a certain diagnosis met the ELN guidelines for MRD positivity, up to 75% responded "maybe", with 42-92% correctly identifying ELN positivity in the various scenarios. Across scenarios with <2% blasts, and when asked about preferred diagnostic language, respondents favored reporting "minimal residual AML" in the diagnostic line. Verbal communication was preferred in 36-100% of scenarios and was least requested when MRD was directly stated. When there was low level but more overt disease than MRD, i.e., >2% aberrant blasts, the preferred diagnostic language was "low level residual AML". When the blast IP was aberrant but different from the diagnostic IP, the preferred diagnosis was "suspicious for AML" with an explanation of the IP, and 100% preferred a verbal communication in this scenario.

Conclusions: A wide range of verbiage is used in our bone marrow pathology reports for low level AML diagnoses and MRD assessment. Most respondents preferred the pathology report to follow the ELN guidelines in reporting MRD positivity, and if positive, to clearly state "minimal residual disease" in the diagnostic line. Verbal communication between pathology and oncology was preferred in most scenarios.

703 Use of the Lymphgen Tool in a Cohort of Patients with Diffuse Large B-cell Lymphoma Treated with R-CHOP

Ryan Jackson¹, Anamarija Perry², Alex Herrera¹, Victoria Bedell¹, Joyce Murata-Collins¹, Nina Rahimi³, Raju Pillai¹, Wing Chan¹, Dennis Weisenburger¹, Joo Song¹

¹City of Hope National Medical Center, Duarte, CA, ²University of Michigan, Ann Arbor, MI, ³City of Hope Cancer Center, Duarte, CA

Disclosures: Ryan Jackson: None; Anamarija Perry: None; Alex Herrera: None; Victoria Bedell: None; Joyce Murata-Collins: None; Nina Rahimi: None; Raju Pillai: None; Wing Chan: None; Dennis Weisenburger: None; Joo Song: None

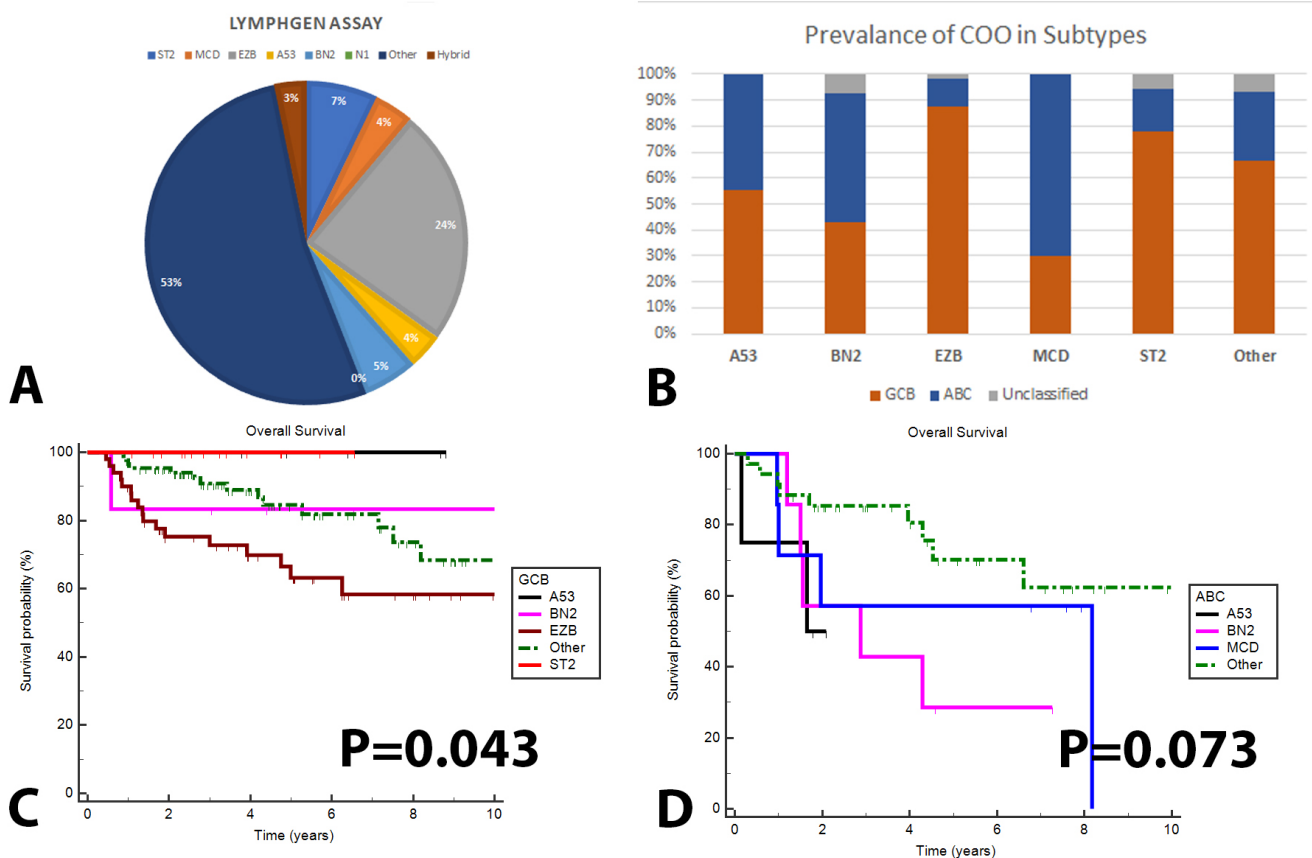
Background: Diffuse large B-cell lymphoma (DLBCL) is a heterogeneous disease that has been further classified into germinal center B-cell (GCB) and activated B-cell (ABC) types. Recently, extensive mutation profiling was performed and Wright et al (Cancer Cell, 2020) have devised a tool (Lymphgen) which highlights targetable genetic

abnormalities for therapeutics. In this study, we describe our experience with the Lymphgen tool in an independent cohort of *de novo* DLBCL treated with R-CHOP.

Design: We identified 252 cases of *de novo* DLBCL that had ample tissue for histologic review and clinical follow-up at two cancer centers. Immunostaining (Hans algorithm, MYC, BCL2) and the Lymph2Cx assay (Nanostring) were performed to determine the cell of origin (COO). We used a 334 gene targeted sequencing panel, copy number analysis (CNA) using Oncoscan, and FISH analysis for *MYC*, *BCL2*, and *BCL6* and the genomic information was uploaded to the Lymphgen tool data portal and the output genetic subtypes were incorporated into our dataset. Kaplan Meier survival analysis was used to determine overall survival (OS) and the Mann-Whitney test was used to compare groups.

Results: There were 172 cases (68%) of GCB DLBCL, 63 cases (25%) of ABC DLBCL, 12 cases of unclassified DLBCL (5%), and 5 cases (2%) for which we did not have sufficient tissue to determine the COO. Using the Lymphgen tool, more than half of the cases (53%) could not be classified (Other), which is more than in the Wright et al study (38%). The remaining categories (core) were as follows: EZB (60 cases, 24%), ST2 (18 cases, 7%), BN2 (14 cases, 6%), MCD (10 cases, 4%), and A53 (9 cases, 4%) (Figures A and B). There were 8 cases that were intermediate between different subtypes (hybrid). The OS for GCB DLBCL showed that the EZB group had the worst OS (Figure C). The OS for ABC DLBCL showed a trend for better OS in “Other” group (Figure D). In both COO types the “Other” group had an intermediate OS. Further review of the “Other” group showed they had frequent mutations in *KMT2D* (21%), *B2M* (14%), *TNFAIP3* (14%), and *TP53* (14%) but had fewer mutations compared to the core group (median: 9 mutations/case vs 13 mutations/case, $P < 0.0001$).

Figure 1 - 703



Conclusions: We find that the Lymphgen tool can be used to generate genetic subtypes of DLBCL after extensive analysis is performed (mutation profile, CNA, and FISH analysis). The Lymphgen tool identified a high proportion of “Other” category cases which may be related to the lack of certain mutations in a proportion of our cases. We find that the GCB DLBCL genetic categories have a similar prognosis to those in the Wright et al study, and the “Other” group has an intermediate prognosis in both COO types.

704 The Clinicopathological Features of DNMT3A R882 Mutant Myeloid Neoplasms

Majd Jawad¹, Gang Zheng¹
¹Mayo Clinic, Rochester, MN

Disclosures: Majd Jawad: None

Background: R882 is a well known hotspot and account for about 40% of DNMT3A mutations in myeloid neoplasms (MNs), raising the hypothesis that DNMT3A R882 mutations confer unique biological and clinical features in MNs. The objective of this study is to compare the clinicopathological characteristics of DNMT3A R882 mutant MNs to those with non-R882 mutations.

Design: Myeloid genomics data in cBioPortal was used for mining the coexisting mutations in DNMT3A R882 and non-R882 mutant MNs. We also retrospectively reviewed the bone marrow pathology reports and myeloid NGS (next generation sequencing) data of patients with MNs evaluated at our institution from 01/2017 to 12/2019 that harbored pathogenic DNMT3A mutations. Statistical significance in different groups was determined using Chi-Square Test with a contingency table, or Fisher exact test. A P value less than 0.05 was considered statistically significant.

Results: Based on the genomic data from 6472 patients with MNs in cBioPortal, NPM1 and PTPN11 mutations are enriched in DNMT3A R882 mutant myeloid neoplasms, while U2AF1 and TP53 mutations were enriched in DNMT3A non-R882 mutant myeloid neoplasms. In our institution 84 MN patients were identified to harbor DNMT3A mutations, among which 38 with DNMT3A R882 mutation and 46 with DNMT3A non-R882 mutation. 28 (74%) with R882 mutations had AML diagnosis at presentation, compared to 15 (33%) with DNMT3A non-R882 mutations (P <0.05), in contrast MDS, MDS/MPN or MPN were more prevalent in the DNMT3A non-R882 group (P value <0.05). More importantly, 50% (5/10) of MDS cases with DNMT3A R882 mutations, compared to 17% (4/24) with non-R882 mutations, show excess blasts (P <0.05).

Conclusions: DNMT3A R882 mutant MNs show unique clinicopathological characteristics. They are more associated with AML and high-grade MDS at presentation in comparison to DNMT3A non-R882 mutant MNs. A clinical study with a larger cohort is needed to further address the diagnostic and prognostic utilities of DNMT3A R882 mutations.

705 Clinicopathologic Features of Therapy-Related Myeloid Neoplasms in Myeloma Patients in The Era of Novel Therapies: A Study of 60 Patients

Fatima Zahra Jelloul¹, Richard Yang¹, Shaoying Li¹, Guilin Tang¹, Keyur Patel¹, L. Jeffrey Medeiros¹, Pei Lin¹

¹The University of Texas MD Anderson Cancer Center, Houston, TX

Disclosures: Fatima Zahra Jelloul: None; Richard Yang: None; Shaoying Li: None; Guilin Tang: None; Keyur Patel: None; L. Jeffrey Medeiros: None; Pei Lin: None

Background: A subset of myeloma patients develops therapy-related myeloid neoplasms (t-MN) despite having been treated primarily with proteasome inhibitors (PI) and immunomodulating (IMiD) agents. The single high dose of melphalan for autologous stem cell transplant (SCT) conditioning and preexistent clonal hematopoiesis of undetermined potential (CHIP) are considered the major risk factors for developing t-MN. The clinicopathological features including molecular profiles of these t-MN cases have not been studied extensively. We summarize the clinicopathologic features of 60 such patients.

Design: A search was conducted of our database for patients with history of plasma cell myeloma who subsequently developed t-MN from 1/2010 through 9/2020. We identified 60 patients. The morphologic, cytogenetic and next generation sequencing were reviewed.

Results: The study group included 43 men and 17 women, with a median age of 72 years (range, 51-88 years). All 60 patients were treated with PI, in combination with IMiD or steroids, and 58 (96.7%) underwent auto-SCT. 17 patients also received cyclophosphamide. The time interval from SCT to t-MN diagnosis ranged from 7-215

months, with a median of 50 months; 14 patients developed t-MN within 2 years of SCT. MDS with multilineage dysplasia (MDS-MLD) was the most common type (n=45), followed by MDS with excess blasts (n=10), t-AML (n=3) and MDS/MPN (n=2). The most common cytogenetic aberrations included del7q/-7 and/or del5q/-5 (23, 38.3%) followed by complex aberrations (21, 35%). The most frequent molecular aberration was *TP53* mutation, detected in 34 (56.7%) patients, which represented the sole mutation detected in 12 (20%) patients. The other mutations detected involved *DNMT3A* (17, 28.3%), *TET2* (6, 10%), *RUNX1* (6, 10%), *ASXL1* (5, 8.3%), *U2AF1* (4, 6.7%), *SRSF2* (3, 5%), *EZH2* (2, 3.3%), *STAG2* (2, 3.3%), *NRAS* (2, 3.3%), *SETBP1* (1, 1.7%), *SF3B1* (1, 1.7%) and *SF3A1* (1, 1.7%). *RUNX1* mutations were more common in patients who developed t-MN within 2 years, compared to the other patients (21% vs 6.5%, $p=0.11$). 36 patients died. The median overall survival was 13 months (range, <1 months-65 months). The cyclophosphamide treated group had a similar mortality rate, latency interval and survival duration ($p=0.77$, 0.39 and 0.32, respectively) compared to patients without exposure to the drug.

Conclusions: t-MN develops in a very small subset of myeloma patients treated with novel therapies and auto-SCT. *TP53* mutation is the molecular hallmark and del7q/-7 and/or del5q/-5 are common in these patients. *RUNX1* mutations are more common in a subset of patients who developed t-MN within 2 years. While the overall features are comparable to those seen in patients treated with other alkylating agents, the short interval from SCT to t-MN (<2 years) in these patients suggests the possibility of pre-existing underlying predisposition to t-MN. The overall survival and prognosis are poor.

706 Impact of WHO-2017 Guidelines and Sociodemographic Factors on Pathology Evaluation of Diffuse Large B-Cell Lymphomas in Louisiana

Rachna Jetly Shridhar¹, Tingting Li², Mei-Chin Hsieh², Brent Mumphy², Xiaocheng Wu²
¹LSUHSC School of Medicine New Orleans, New Orleans, LA, ²LSUHSC School of Public Health, New Orleans, New Orleans, LA

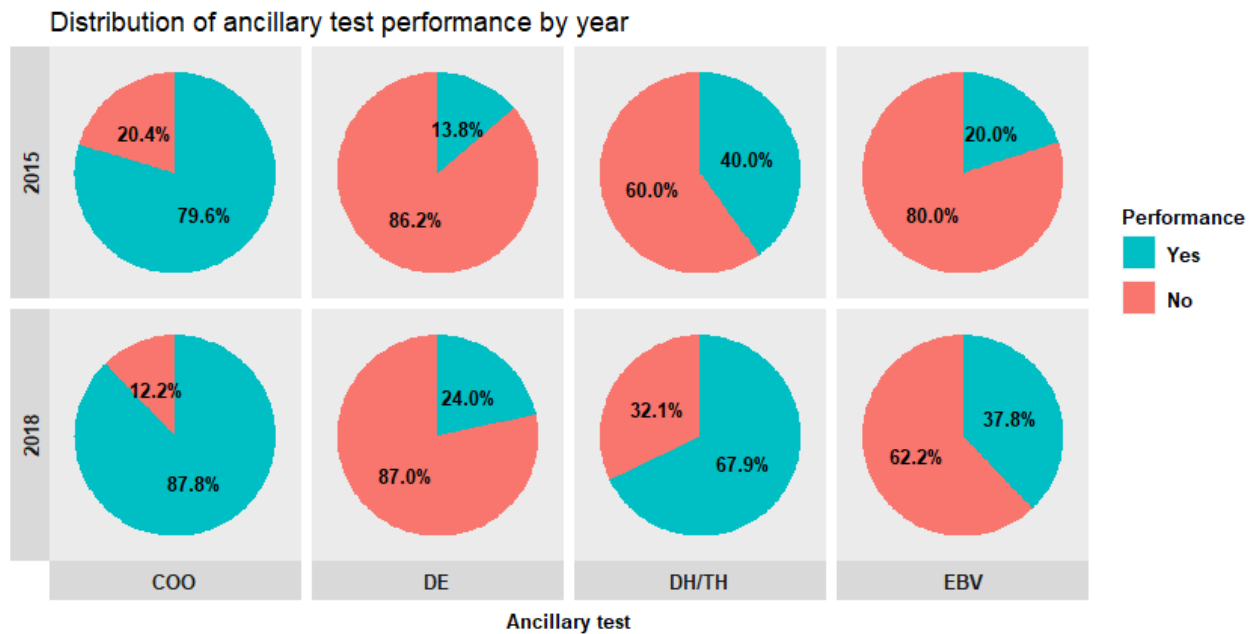
Disclosures: Rachna Jetly Shridhar: None; Tingting Li: None; Mei-Chin Hsieh: None; Brent Mumphy: None; Xiaocheng Wu: None

Background: Diffuse large B-cell lymphoma not otherwise specified (DLBCL-NOS) is clinically heterogeneous needing prognostic subcategorization for clinical management. Ancillary tests evaluate for cell of origin (COO), double expressors (DE), high-grade B-cell lymphomas with MYC and BCL2 and/or BCL6 rearrangements (HGBL-DH/TH) and EBV+ LBCL. COO testing is required on all cases post publication of updated WHO-2017 classification, however no consensus referral testing guidelines for other categories are currently provided.

Design: Pathology reports from the Louisiana Tumor Registry were reviewed on de novo DLBCL cases diagnosed in 2015 (N=275) and 2018 (N=246) to compare ancillary testing pre- and post-WHO-2017 respectively and by sociodemographic factors (age, race, gender, public/private insurance, free-standing/hospital-based and urban/rural labs). Chi-square tests were used to compare trends in ancillary testing. Multivariate logistic models were employed to assess for changes in testing from 2015 to 2018 after adjusting for sociodemographic confounders.

Results: Testing increased ($p<0.05$) from 2015 to 2018 (Figure). Significantly increased testing was observed for COO in patients aged <60, females, whites, rural and public insurance; for DE in patients aged <60, males, whites, hospital-based, urban and public insurance; for HGBL-DH/TH across all sociodemographic categories except blacks; and for EBV in all age groups, males/females, whites, hospital-based, urban and public insurance. Within each subgroup, in 2018, testing was significantly higher for DE in patients aged <60, hospital-based and public insurance patients and for EBV in patients aged <60, hospital-based, urban and public insurance patients. After adjusting for sociodemographic confounders, the odds of the ancillary testing were still significantly higher in 2018 than in 2015 with OR (95% CI) as- COO: 1.86 (1.14-3.02); DE: 2.09 (1.32-3.33); DH/TH: 3.21 (2.24-4.61) and EBV: 2.48 (1.66-3.71).

Figure 1 - 706



Conclusions: Significant increase in DLBCL ancillary testing was observed post WHO-2017 and trends differed across all types of facilities and demographic groups. Mandated testing was effective in alleviating disparities in COO testing across many sociodemographic groups. Although tests with no consensus referral guidelines increased post-WHO-2017, these were performed on fewer patients compared to COO. Our study indicates the positive impact of defined specific guidelines as an effective measure towards standardization of pathology reports.

707 T-Cell Receptor (TCR) Signature of EBV-Positive Diffuse Large B-Cell Lymphoma (EBV+ DLBCL) Reveals Two Microenvironmental Subgroups

Xiang Nan Jiang¹, Si-Geng Huang¹, Wanhui Yan¹, Xiaoqiu Li²

¹Fudan University Shanghai Cancer Center, Shanghai, China, ²Shanghai Cancer Center, Shanghai, China

Disclosures: Xiang Nan Jiang: None; Si-Geng Huang: None; Wanhui Yan: None; Xiaoqiu Li: None

Background: EBV+ DLBCL is an aggressive B-cell neoplasm, featuring frequently an over-expression of the T-cell inhibitory ligand, PD-L1, thus the biological behavior of the tumor might be effected by the tumor microenvironment (TME). It has been suggested the diversity of intra-tumoral T-cells, reflected by the TCR repertoire, may correlate with the clinical outcome in various subtypes of lymphomas, however, little is known about the impact of TME, or TCR signature, on the survival of patients with EBV+ DLBCL.

Design: Fourteen cases with EBV+ DLBCL were studied using FFPE tumor tissues. The lineage and microenvironment-associated markers (CD20, CD3, CD4, CD8, PD-1 and PD-L1) were immunohistochemically detected. And the TCR gene rearrangement was analyzed via a PCR system using BIOMED-2 primers and capillary electrophoresis. The monoclonally rearranged peaks of TCR γ /TCR β /TCR δ within the effective range were evaluated and counted. Based on their number of rearranged TCR peaks, all cases were subdivided into a narrow-TCR-repertoire (NTR) (≤ 65) and a broad-TCR-repertoire (BTR) (> 65) group. The primary endpoints of the research included 3-year overall survival (OS) and progression-free survival (PFS).

Results: Seven cases each belonged to the NTR and BTR group. The NTR group was associated with an inferior 3-year OS rate of 71.4% [95% CI, 43.2%–81.4%], compared with the 85.7% (95% CI, 69.7%–90.5%) of the BTR

group ($P = 0.0178$). And the NTR also predicted an inferior 5-year PFS rate of 57.1% (95% CI, 21.6%–68.9%) compared with the 71.4% (95% CI, 53.2%–86.7%) of the BTR ($P = 0.0129$). Pathologically, most NTR cases displayed a DLBCL-like morphology, featuring lower-level PD-1/PD-L1 expression and comparable intra-tumoral CD4+/CD8+ T-cells, whereas the BTR cases manifested more often with a classical Hodgkin lymphoma (CHL)-like morphology and relatively higher PD-1/PD-L1 expression level and CD4+ T-cell predominant reaction. Interestingly, while 42.8% NTR cases demonstrated a monoclonal *TCRγ* rearrangement, none of the BTR ones showed *TCRγ* rearrangement ($P = 0.0039$). Furthermore, cases with monoclonal *TCRγ* rearrangement also showed a worse OS ($P = 0.0093$) and PFS ($P = 0.0045$) and down-regulated expression of PD-1/PD-L1.

	Narrow-TCR-repertoire, n (%)	Broad-TCR-repertoire, n (%)	P value
	7 cases	7 cases	
Clinical parameters	60.5 (23-76)	53 (33-72)	0.496
Median age (range)	5 (71)	4 (57)	0.780
Male	2 (29)	3 (43)	
Female	4 (57)	5 (71)	
IPI 0-2	3 (43)	2 (29)	
IPI 3-5			
Immunophenotype	3 (43)	6 (85.5)	0.266
CD4>CD8	0 (0)	0 (0)	0.041
CD4<cd8< span=""></cd8<>	4 (57)	1 (14.5)	0.032
CD4≈CD8	15	25	0.597
PD1 (TILs, %)	29	40	
PD-L1 (TPS, %)	1 (14)	2 (29)	
GCB	6 (86)	5 (71)	
Non-GCB			
TCR gene rearrangement	70 (33)	142 (67)	0.046
TCRγ	131 (30.9)	292 (69.1)	0.022
TCRβ	88 (44)	112 (56)	0.086
TCRδ			
Therapy data	7 (100)	7 (100)	>0.999
R-CHOP	4 (57)	5 (71)	
CR	1 (14)	1 (14.5)	
PR	2 (29)	1 (14.5)	
PD			

Figure 1 - 707

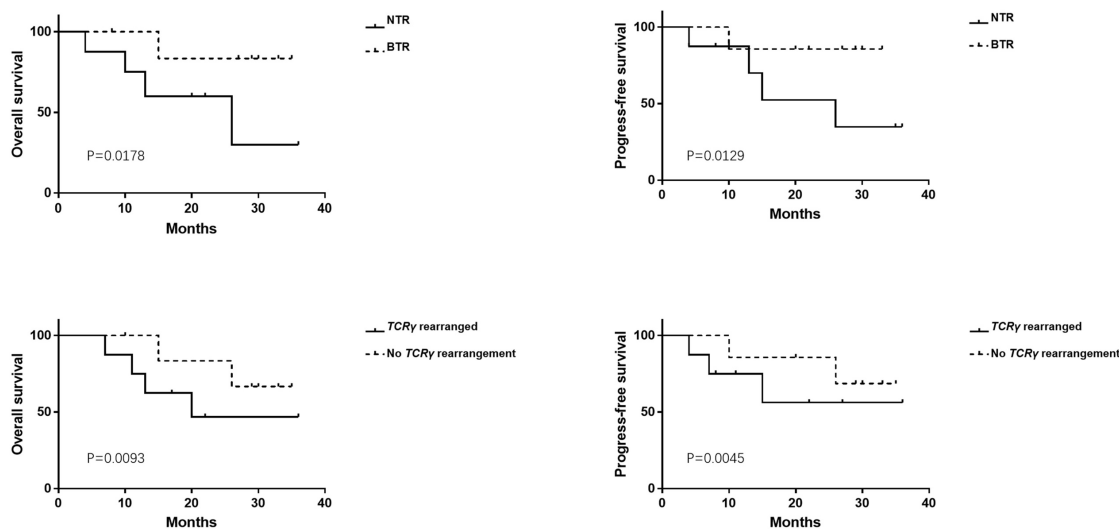
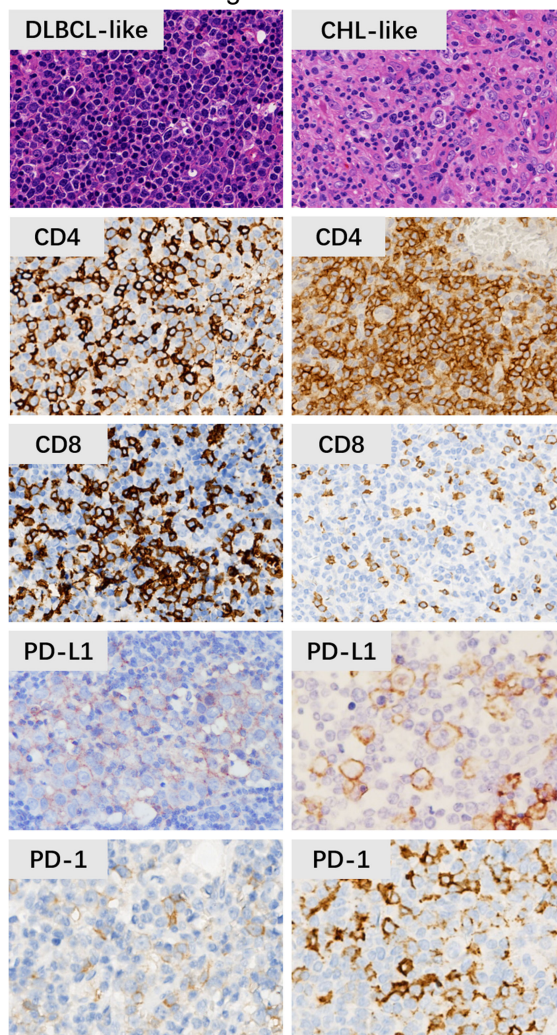


Figure 2 - 707



Conclusions: The TCR signature can thus be viewed as a useful surrogate to reflect the TME of EBV+ DLBCL. The more aggressive tumors feature more frequent decreased T-cell diversity, *TCR γ* clonal expansions, and inhibition of immune checkpoint molecules.

708 Discordances in Measurable Residual Disease Detection Between Molecular Analysis and Multiparametric Flow Cytometry in Acute Myeloid Leukemia with Mutated NPM1

Steven Johnson¹, Ashley Crosby², Will Pulley², Daniel Richardson², Hendrik Van Deventer², Catherine Coombs², Matthew Foster², Joshua Zeidner², Jonathan Galeotti², Nathan Montgomery²

¹University of North Carolina Hospitals, Chapel Hill, NC, ²The University of North Carolina at Chapel Hill, Chapel Hill, NC

Disclosures: Steven Johnson: None; Will Pulley: None; Daniel Richardson: None; Hendrik Van Deventer: None; Nathan Montgomery: None

Background: Measurable residual disease (MRD) burden after therapy has important prognostic impact in acute myeloid leukemia (AML). Both multiparametric flow cytometry (MFC) and quantitative reverse transcription polymerase chain reaction testing (qRT-PCR) may be used for MRD assessment in patients with AML with mutated *Nucleophosmin-1* (AML-*NPM1*). However, serial monitoring using these methods concurrently can produce discordant results, the significance of which is unclear.

Design: All adult AML-*NPM1* patients with at least 1 bone marrow (BM) sample with concurrent MFC and qRT-PCR testing between February 2018 and June 2020 at our institution were retrospectively identified. MFC was performed at a major MRD testing reference laboratory, and qRT-PCR was performed at our institution. Clinicopathologic and genetic features at diagnosis, and risk of relapse for patients with discordances were analyzed.

Results: Forty-two patients (male:female 0.8:1) were included, with a median age at diagnosis of 58.5 years. All patients had *de novo* AML with intermediate-risk cytogenetics. In total, 152 post-treatment BM samples were concurrently analyzed (median 3 per patient). Fifty-nine samples had discordant MFC/qRT-PCR results (i.e. either +/- or -/+). Only 1 discordant sample was MFC-positive/qRT-PCR-negative, with MFC being positive at the assay's 0.1% limit of detection in this case. The remaining 58 samples were MFC-negative/qRT-PCR-positive, with a median qRT-PCR value of 0.12% mutant *NPM1* transcripts (range 0.01%-57.12%). In total, 36 patients had ≥ 1 MFC-negative sample (Figure), all but 1 of whom achieved clinical remission prior to a discordant result. After excluding samples collected within 3 months of initial therapy, patients with ≥ 1 MFC-negative result with a high qRT-PCR value ($\geq 1.0\%$ mutant *NPM1* transcripts) were more likely to relapse during the study period (6/7: 86%) than patients with ≥ 1 MFC-negative result whose highest qRT-PCR value was $<1.0\%$ mutant *NPM1* transcripts (7/26: 27%; $p = 0.006$).

Figure 1 - 708

Figure 1. MFC-negative samples (n = 114) stratified by percent mutant *NPM1* transcript value in 36 patients.

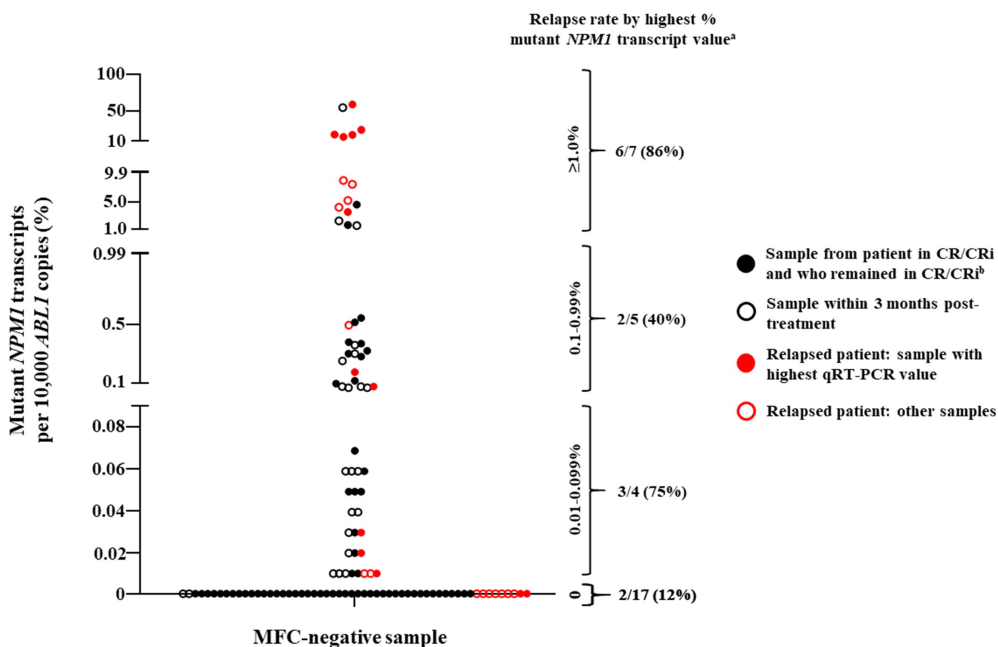


Figure 1. MFC-negative samples (n = 114) stratified by percent mutant *NPM1* transcripts in 36 patients.

MFC: multiparametric flow cytometric analysis for measurable residual disease; CR: clinical remission; CRi: clinical remission with incomplete hematologic recovery; qRT-PCR: quantitative reverse transcription polymerase chain reaction testing

^a Relapse analysis includes 33 patients; 3 other patients whose only sample was an MFC-negative/qRT-PCR discordance within the first 3 months of therapy were excluded.

^b Median follow-up 11.6 months.

Conclusions: Post-treatment discordance between MRD measured by MFC and qRT-PCR occurs in a substantial minority of AML-*NPM1* patients, and qRT-PCR appears informative in predicting relapse even in MFC-negative cases. Our results suggest that concurrent MFC may not provide additional clinical value for most AML-*NPM1* patients when monitoring by qRT-PCR is available.

709 Concordance of Peripheral Blood and Bone Marrow Next Generation Sequencing in Hematolymphoid Neoplasm

Chayanit Jumniensuk¹, Alexander Nobori¹, Dinesh Rao¹, Thomas Lee², T. Niroshi Senaratne¹, Sheeja Pullarkat¹

¹David Geffen School of Medicine at UCLA, Los Angeles, CA, ²UCLA Medical Center, Los Angeles, CA

Disclosures: Chayanit Jumniensuk: None; Alexander Nobori: None; Dinesh Rao: None; Thomas Lee: None; T. Niroshi Senaratne: None; Sheeja Pullarkat: None

Background: Mutational analysis by next-generation sequencing (NGS) is increasingly used in clinical practice when evaluating hematologic diseases. Mutational analysis obtained by peripheral blood NGS has been of clinical interest to use as a minimally invasive screening tool. Our study aims to evaluate the correlation between NGS performed on peripheral blood and bone ma

Design: We evaluated patients who had NGS for hematologic malignancy performed on both peripheral blood and bone marrow within 1-year interval of each other. We excluded cases in which chemotherapy or bone marrow transplant occurred in the interval between the two tests. The NGS results from peripheral blood and bone marrow were recorded. Cases were then classified as complete concordance, partial concordance, and discordance. A chi square test for independence was performed to evaluate the relationship between positivity for pathogenic genes by NGS on peripheral blood versus NGS on bone marrow. NGS testing was performed using Illumina sequencing covering the most clinically significant mutations reported in hematologic malignancy, including *ABL1*, *ASXL1*, *BCOR*, *BCORL1*, *BRAF*, *CALR*, *CBL*, *CBLB*, *CSF3R*, *CUX1*, *DNMT3A*, *ETV6*, *EZH2*, *FLT3*, *IDH1*, *IDH2*, *JAK2*, *KIT*, *KRAS*, *MPL*, *NPM1*, *NRAS*, *RAD21*, *RUNX1*, *SETBP1*, *SF3B1*, *SRSF2*, *STAG2*, *TET2*, *TP53*, *U2AF1*, and *ZRSR2*.<<

Results: A total of 109 patients were studied. Concordance of peripheral blood and bone marrow NGS found in 98 patients (89%, chi-squared test *P*-value <.001). A higher rate of concordance was seen when the interval between peripheral blood and bone marrow testing was less than 30 days (95%, *P*-value <.001). Myeloid neoplasms showed concordant results in 43/44 cases (98%). Lymphoid neoplasm showed concordant results in 20/24 cases (83%). Acute leukemia showed concordant results in 12/14 cases (85%). Non-neoplastic abnormal blood count cases showed concordant results in 34/40 cases (86%).

NGS on peripheral blood demonstrated 83% sensitivity and 53% specificity in the detection of any hematolymphoid malignancy. NGS on bone marrow demonstrated 87% sensitivity and 43% specificity in the detection of any hematolymphoid malignancy.<

Table 1: Correlation of NGS result between peripheral blood and bone marrow NGS

grouped by diagnoses

Diagnoses	Cases with interval		Cases with interval	
	within 30 days		within 1 year	
	Number	%	Number	%
Non-neoplastic abnormal blood count				
Concordance	14	94%	34	86%
Complete concordance	13	87%	31	78%
Partial concordance	1	7%	3	8%
Discordance	1	7%	6	15%
MDS				
Concordance	3	100%	11	100%
Complete concordance	2	67%	8	73%
Partial concordance	1	33%	3	27%
Discordance	0	0%	0	0%
MPN				
Concordance	6	100%	11	100%
Complete concordance	5	83%	9	82%
Partial concordance	1	17%	2	18%
Discordance	0	0%	0	0%
MDS/MPN				

Concordance	6	100%	10	100%
Complete concordance	4	67%	8	80%
Partial concordance	2	33%	2	20%
Discordance	0	0%	0	0%
AML				
Concordance	9	90%	10	91%
Complete concordance	7	70%	7	64%
Partial concordance	2	20%	3	27%
Discordance	1	10%	1	9%

Table 2 (Cont): Correlation of NGS result between peripheral blood and bone marrow NGS

grouped by diagnoses

Diagnoses	Cases with interval		Cases with interval	
	within 30 days		within 1 year	
	Number	%	Number	%
B-ALL				
Concordance	1	50%	1	50%
Complete concordance	0	0%	0	0%
Partial concordance	1	50%	1	50%
Discordance	1	50%	1	50%
MPAL				
Concordance	1	100%	1	100%
Complete concordance	0	0%	0	0%
Partial concordance	1	100%	1	100%
Discordance	0	0%	0	0%
CLL				
Concordance	1	100%	4	100%
Complete concordance	0	0%	3	75%
Partial concordance	1	100%	1	25%
Discordance	0	0%	0	0%
Hairy cell leukemia				
Concordance	1	100%	2	100%
Complete concordance	1	100%	2	100%
Partial concordance	0	0%	0	0%
Discordance	0	0%	0	0%
Myeloma				
Concordance	1	100%	2	100%
Complete concordance	1	100%	1	50%
Partial concordance	0	0%	1	50%
Discordance	0	0%	0	0%
Other lymphoid neoplasm				
Concordance	5	100%	11	78%
Complete concordance	4	80%	10	71%
Partial concordance	1	20%	1	7%
Discordance	0	0%	3	21%
Mastocytosis				
Concordance	0	0%	1	100%
Complete concordance	0	0%	0	0%
Partial concordance	0	0%	1	100%
Discordance	0	0%	0	0%
Total	51	100%	109	100%

Figure 1 - 709

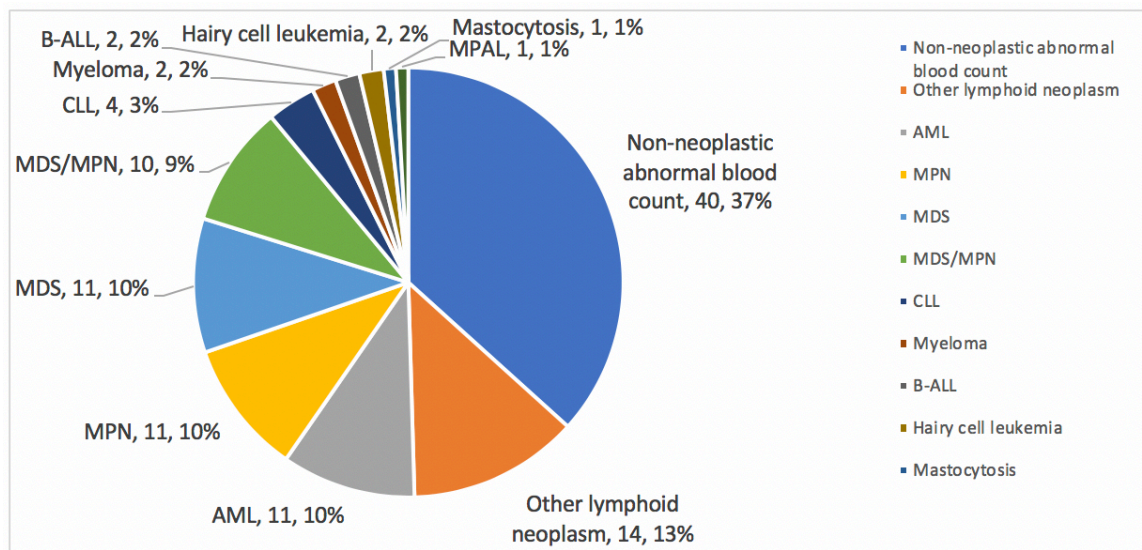


Figure1 Distribution of diagnoses in study population

Conclusions: Mutational analysis by peripheral blood NGS showed significant concordance with bone marrow NGS. This degree of concordance was even higher in the subset of patients in which the interval between peripheral blood and bone marrow specimen procurement was less than 30 days. Myeloid neoplasms showed a very high concordance (98%), while slightly lower levels of concordance were seen in lymphoid neoplasms (83%) and non-neoplastic abnormal blood counts (86%). Peripheral blood NGS showed a similar sensitivity with bone marrow NGS to detect any hematolymphoid malignancy (83% and 87% respectively). In conclusion, our findings demonstrate that peripheral blood NGS is a reliable and less invasive tool for mutational analysis for screening and monitoring disease status in hematolymphoid neoplasms specific

710 Plasmablastic Lymphoma (PBL): Cross-Talk Between Overexpressed Transforming Growth Factor Beta (TGFB) Pathway Molecules With The Wnt/ Beta-Catenin Pathway May Identify Potential Therapeutic Targets

Hamza Kamran¹, Ghaleb Elyamany², Ariz Akhter¹, Hassan Rizwan¹, Meer-Taher Shabani-Rad³, Adnan Mansoor¹

¹University of Calgary, Calgary, Canada, ²Prince Sultan Military Medical City, Riyadh, Saudi Arabia, ³Cumming School of Medicine, University of Calgary, Calgary, Canada

Disclosures: Hamza Kamran: None; Ghaleb Elyamany: None; Ariz Akhter: None; Hassan Rizwan: None; Meer-Taher Shabani-Rad: None; Adnan Mansoor: None

Background: Plasmablastic lymphoma (PBL) is rare with a dismal clinical outcome, hence new treatment strategies are needed. Advanced understanding of deranged signal transduction in cancer is providing effective targeted therapies. The *TGFβ* signaling plays a critical role to the pathogenesis / progression of diffuse large B-cell lymphoma (DLBCL); while its role in PBL remains unknown. We reported that upregulation of *Wnt/β-catenin* pathway ligands, receptors, and downstream targets are linked with disease progression in PBL. It has been shown recently that *Wnt/β-catenin* and *TGFβ* pathways are deeply intertwined through the cytoplasmic interaction of several pathway members (Smad/β-catenin/LEF1 protein complex). In solid cancers, these molecules are implicated in cancer progression, and inhibition/ knock-out resulted in restraining cancer growth and invasion. Our current study investigated the expression pattern of key molecules in the *TGFβ* pathway and its impact on other pathways, especially *Wnt/β-catenin* pathway in a subset of PBL patients as it compared to DLBCL.

Design: Diagnostic FFPE RNA (PBL=33 & ABC-DLBCLs =18) were analyzed for the expression of key *Wnt/β-catenin* & *TGFβ* pathway molecules (nCounter -NanoString Technologies). Statistical analysis was performed on

Qluore Omics Explorer (v3.6) and SPSS(v21.3) using standard criteria (fold change >2.0; p<0.01 and q <0.05). GSEA identified the cluster of genes linked with the *TGFβ* and *Wnt/β-catenin* pathway.

Results: A total of 27 *TGFβ* pathway genes were upregulated along with 20 *Wnt/β-catenin* genes in PBL compared to ABC-DLBCL (Fig 1A & 1C). *ID1*, *SHC1*, *SMAD4*, and *ACVR1C* were identified as key overexpressed *TGFβ* pathway genes (Figure 1B). *ID1* is a downstream target of the *TGFβ* pathway through the transcription factor Smad4 and is key in the progression/metastasis of solid cancers, while *SHC1* has been linked to breast carcinogenesis. *ACVR1C* encodes a type 1 receptor of the *TGFβ* pathway and its aberrant expression is known in retinoblastoma invasion and growth. The consistent presence of these *TGFβ* pathway members in facilitating other forms of cancers lends support to this pathway playing a distinct role in PBL. Expression of *ID1*, *SHC1*, *ACVR1C*, and *SMAD4* significantly related to each other in the *TGFβ* pathway. The clustered heat map analysis signify overexpressed key *Wnt* pathway members (*WNT10B*, *WNT5B*, and *FZD3*) in PBL. The simultaneous up-regulation of the *Wnt/β-catenin* and *TGFβ* pathway signify their combined involvement in PBL.

Figure 1 - 710

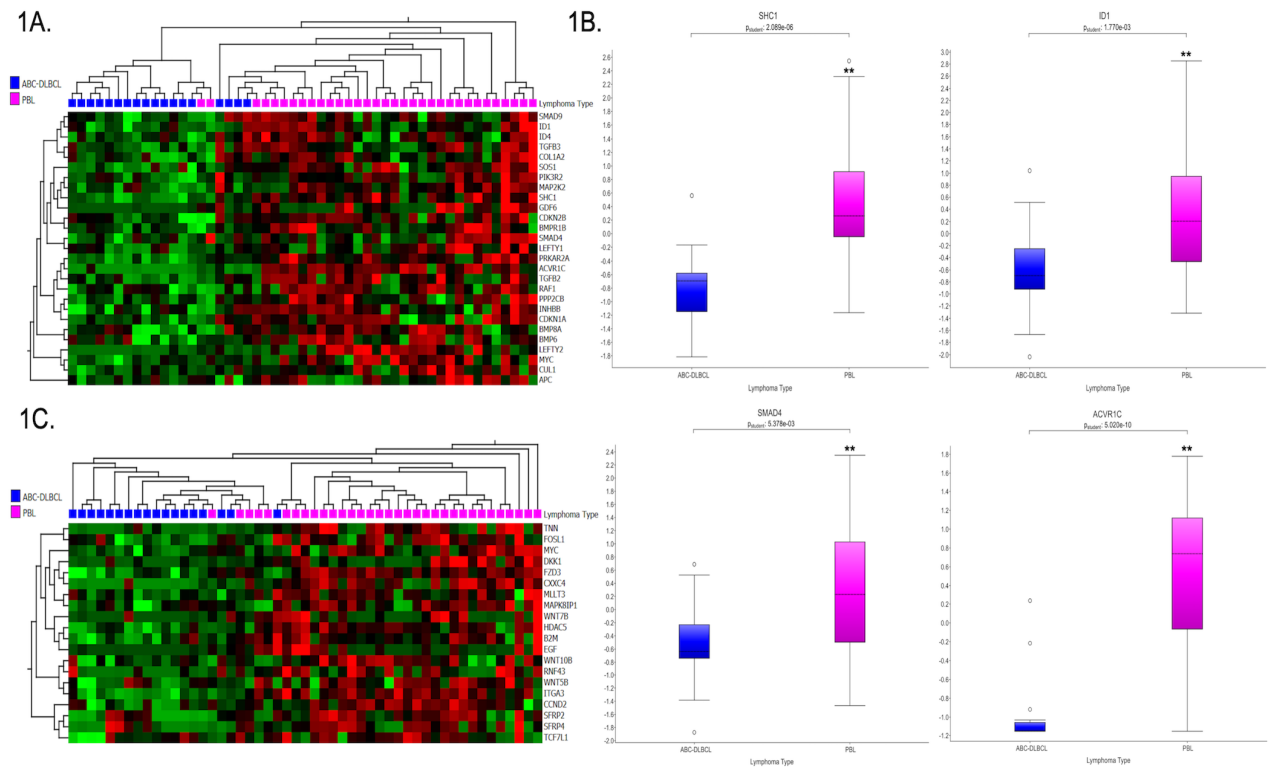


Figure 1A. Hierarchical clustered heat map illustrating the expression of functionally enriched *TGFβ* signalling pathway genes in PBL patients compared to ABC-DLBCL patients. 1B. Box and whisker plots illustrating comparisons of log expression of key *TGFβ* pathway genes between the two groups. (** = p < 0.01, q < 0.05). 1C. Hierarchical clustered heat map illustrating the expression of functionally enriched *Wnt/β-catenin* pathway genes in PBL patients compared to ABC-DLBCL patients.

Conclusions: In conclusion, we report a combined high expression of key *Wnt/β-catenin* and *TGFβ* pathway molecules in PBL compared to ABC-DLBCL. The presence of “crosstalk” between *Wnt/β-catenin* and *TGFβ* pathways identify the potential for novel therapeutic strategies targeting key pathway members such as SMAD4 and ID1; as is being evaluated with effective results in some solid cancers.

711 Comprehensive Genomic Assessment using both NGS and CGH-SNP Analysis is Essential to Identify Clonal Abnormalities in Idiopathic Cytopenia(s) of Undetermined Significance

Rashmi Kanagal-Shamanna¹, Andrew Evans², Carlos Bueso-Ramos¹, Guillermo Garcia-Manero¹, L. Jeffrey Medeiros¹, M. Anwar Iqbal²

¹The University of Texas MD Anderson Cancer Center, Houston, TX, ²University of Rochester Medical Center, Rochester, NY

Disclosures: Rashmi Kanagal-Shamanna: None; Andrew Evans: None; Carlos Bueso-Ramos: None; Guillermo Garcia-Manero: None; L. Jeffrey Medeiros: None; M. Anwar Iqbal: None

Background: Clonal hematopoiesis with unexplained cytopenia(s) includes idiopathic cytopenia of undetermined significance (ICUS) and clonal cytopenia of undetermined significance (CCUS, in the presence of a clonal abnormality), in the absence of sufficient morphologic dysplasia for myelodysplastic syndrome (MDS). It is important to differentiate them since CCUS has a higher risk of MDS progression. Standard modalities for clone detection includes conventional cytogenetics (CC) and NGS sequencing. Evidence suggests that high-resolution chromosomal microarray (CMA) can detect sub-microscopic copy number abnormalities (CNA) and uniparental disomy (UPD) that are important in MDS. But, few studies have explored its utility in ICUS. Here, we performed a comprehensive genomic assessment using NGS + CMA on 77 ICUS patients.

Design: We selected consecutive patients who underwent bone marrow examination for unexplained cytopenia(s), but did not meet WHO criteria for MDS (<10% of cells showing dysplasia in all 3 lineages; no MDS-defining cytogenetic abnormalities) and showed normal karyotype (NK) by conventional cytogenetics (CC). We performed genomic evaluation: (a) 81-gene NGS at research core facility, 500x coverage; minimum 5% VAF (b) CMA analysis [4x180K aCGH+SNP, Agilent Technologies]; cut-off criteria: 250 kb for CNAs and 5-10 Mb for UPD.

Results: There were 77 ICUS patients [38 men, 39 women; median age, 66 yrs (range, 22-95)]. By NGS, a total of 13 (17%) patients met the criteria for CCUS; nine patients showed 1 mutation, and 4 showed 2 mutations. The mutated genes included *U2AF1*, *ASXL1* (x2), *SRSF2* (x3), *TET2* (x2), *ASXL1*, *KIT*, *SF3B1* (x2), *GATA1*, *DNMT3A* (x3), *IDH1*, *IDH2* and *BCOR*. The median VAF was 42% (range, 6-94). Based on CMA previously done, a total of 37 (48%) patients showed a clonal abnormality with >20% clonal burden [either CNA or UPD, in MDS related genes such as *TET2*, *ETV6*, *EZH2*), thereby meeting CCUS criteria. The gene mutation frequencies in 4 groups based on the presence of CNA/UPD by CMA were: CNA+/UPD- (8%); CNA-/UPD+ (35%), CNA+/UPD+ (25%) and CNA-/UPD- (7%), the highest frequency of gene mutations were noted in UPD+ groups. Clonal abnormalities by CMA were far more frequent than NGS alone. CMA upgraded the classification to CCUS in 28 (44%) patients without somatic mutations, while NGS upgraded the classification in 4 (10%) patients without CMA abnormalities, emphasizing the complementarity of these two approaches. In total, 41 (53%) were classified as CCUS using the combined approaches. Follow-up BM data collection is underway.

Conclusions: We identified 53% CCUS among patients with idiopathic cytopenia with normal karyotype and not meeting criteria for MDS. Comprehensive genomic assessment using CC, NGS, and CMA analysis is critical to identify those with clonal cytopenia (CCUS) and a higher risk of MDS progression.

712 Peripheral Blood Morphologic and Laboratory Predictors of Death in Hospitalized COVID-19 Patients

Afreen Karimkhan¹, Zarrin Hossein-Zadeh², Prabhjot Sekhon¹, Nibash Budhathoki², Bebu Ram³, Amy Rapkiewicz⁴, Virginia Donovan⁵, Christopher Park⁶, Marc Braunstein²

¹NYU Grossman School of Medicine, New York, NY, ²NYU Winthrop Hospital, New York, NY, ³NYU Langone Health/NYU Winthrop Hospital, Mineola, NY, ⁴NYU Langone Health, New York, NY, ⁵NYU Langone Health/NYU Winthrop Hospital, New York, NY, ⁶NYU School of Medicine, New York, NY

Disclosures: Afreen Karimkhan: None; Zarrin Hossein-Zadeh: None; Prabhjot Sekhon: None; Nibash Budhathoki: None; Bebu Ram: None; Amy Rapkiewicz: None; Virginia Donovan: None; Christopher Park: None; Marc Braunstein: *Advisory Board Member*, Celgene; *Advisory Board Member*, Janssen; *Advisory Board Member*, Karyopharm; *Advisory Board Member*, AstraZeneca; *Advisory Board Member*, Takeda, Epizyme, TG Therapeutics, Morphosys

Background: Numerous predictors of poor outcome in COVID-19 patients have been identified, including alterations in the composition of leukocytes in the peripheral blood. There nonetheless remains a need to improve predictions of patient outcomes following hospitalization in order to appropriately triage patients. We addressed this question by evaluating hematologic parameters and peripheral blood smear morphology in patients who either died or recovered following hospitalization.

Design: The study groups included 48 patients who died following admission (“cases”) and 48 age-matched controls who recovered (“controls”). Laboratory values were collected for PCR-positive COVID-19 hospitalized patients at two time points: T1- the time of admission, and T2 - the time of discharge/death. Peripheral blood smears from two-time points for patients who died were analyzed independently by 4 pathologists.

Results: Study patient demographic details are shown in Table 1. Anemia and thrombocytopenia were present at the time of admission in both groups, and there was a significant decline in hemoglobin and RBC count between T1 and T2; PLT counts decreased, but not in a statistically significant manner (Table 2). WBC and absolute neutrophils increased following admission specifically in patients who died of disease (Table 2). No statistically significant differences were observed in all other hematologic parameters evaluated. Blood from patients who died showed pseudo Pelger-Huet changes 60.41% (n=29), toxic granulations 8.3% (n=4), atypical lymphocytes 91% (n=44), and giant platelets 94% (n=45) with immature myeloid forms increasing at T2. In contrast to patients who recovered, patients who died showed increased D-dimer values at admission; D-dimer values did not correlate with the presence of thrombocytopenia.

Figure 1 - 712

Demography	Cases (n=48)	Controls (n=48)
Mean Age	70.8 years	71.4 years
Range	43–120 years	24-96 years
Sex	2:1	1.2:1
Coronary Artery Disease (% of pts)	14	27
Hypertension (% of pts)	47	40
Diabetes mellitus (% of pts)	27	30
Malignancy (% of pts)	14	25
Mean hospitalization (days)	9	6

Table 1: Demographic and clinical features of hospitalized COVID-19 positive patients

Figure 2 - 712

Hematological Parameters (mean)	Cases			Controls			Case vs Controls (p value)	
	T1	T2	p value	T1	T2	p value	T1	T2
WBC (cells/uL)	10,054	17,471	<0.0001	8,871	9,933	0.3032	0.2470	0.0002
Absolute lymphocytes (cells/uL)	1,023	1,227	0.1397	1,070	986	0.173	0.9408	0.7114
Hemoglobin (g/dl)	11.7	9.783	<0.0001	11.31	10.21	<0.0001	0.5548	0.3228
Platelets (10 ³ /uL)	201.8	176.3	0.1037	206.8	172.6	0.14	0.8088	0.8197
D-dimer levels (ng/mL)	5,651	7,732	0.2795	1,921	1,921	-	0.2468	0.1408

Table 2. Hematological parameters in cases and controls

Conclusions: Hospitalized COVID-19 patients who died showed: 1) elevated D-dimer levels at admission; and 2) increasing WBC and neutrophil counts during their hospitalization. While several morphologic changes were observed in the blood in those who subsequently died, the changes observed were not specific to COVID-19; however, the presence of immature myeloid precursors in hospitalized patients was associated with subsequent neutrophilia and death. This finding suggests that in addition to closely monitoring the two laboratory parameters describe above, special care should be taken to assess blood films for the presence of immature myeloid precursors. Additional studies will be required to validate these findings in a larger group of hospitalized patients

713 Ultrasensitive RNA in situ hybridization for Kappa and Lambda Light Chains Assists in the Differential Diagnosis of Nodular Lymphocyte Predominant Hodgkin lymphoma

Hatem Kaseb¹, Zhen Wang¹, James Cook¹
¹Cleveland Clinic, Cleveland, OH

Disclosures: Hatem Kaseb: None; Zhen Wang: None; James Cook: None

Background: Nodular lymphocyte predominant Hodgkin lymphoma (nLPHL) is relatively uncommon, comprising approximately 10% of Hodgkin lymphoma. Establishing a diagnosis of nLPHL is often challenging as the differential diagnosis is broad, including classic Hodgkin lymphoma (cHL) and progressive transformation of germinal centers (PTGC) among other considerations. Our group has recently described an ultrasensitive RNA in situ hybridization (ISH) assay for kappa and lambda light chains that can detect B-cell clonality with a sensitivity comparable to flow cytometry. In this study we investigate the utility of this ISH assay in distinguishing nLPHL from cHL and PTGC.

Design: 73 cases were examined, including cHL (n=32), nLPHL (n=22) and PTGC (n=19). ISH was performed on a Ventana Discovery (Roche Diagnostics) using two-color probes for kappa and lambda with brown and red chromogens, respectively (Advanced Cell Diagnostics). ISH stains were assessed by two pathologists for light chain restriction in large neoplastic cells, background B-cells and plasma cells.

Results: In nLPHL, large neoplastic cells were light chain restricted in 21/22 (95%) cases (16 kappa, 5 lambda) (Figure 1). In contrast, Reed-Sternberg cells of cHL were negative for kappa and lambda in all cases (0/32, 0%; $p < 0.001$, Fisher exact test)(Figure 2). Monotypic small B-cells were identified by ISH in 3 cases: One nLPHL with nodules of kappa restricted small B-cells undetected by FC; one cHL with concurrent kappa restricted CLL/SLL, and one cHL with admixed lambda restricted small CD5 positive B-cells. The remaining cases of Hodgkin lymphoma (n=51) showed variable numbers of background polytypic B-cells. In PTGC, polytypic B-cells were noted in mantle zones and germinal centers in all cases. Once case showed very focal collections of larger

kappa predominant cells of uncertain significance. Polytypic plasma cells were present in each of the 73 cases examined.

Figure 1 - 713

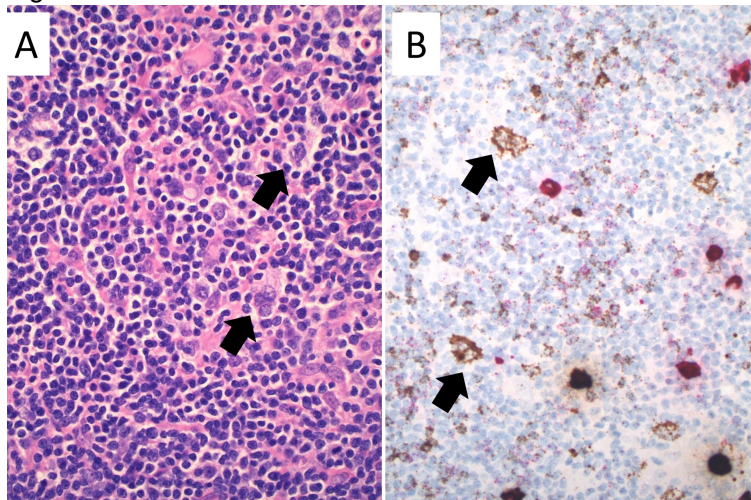
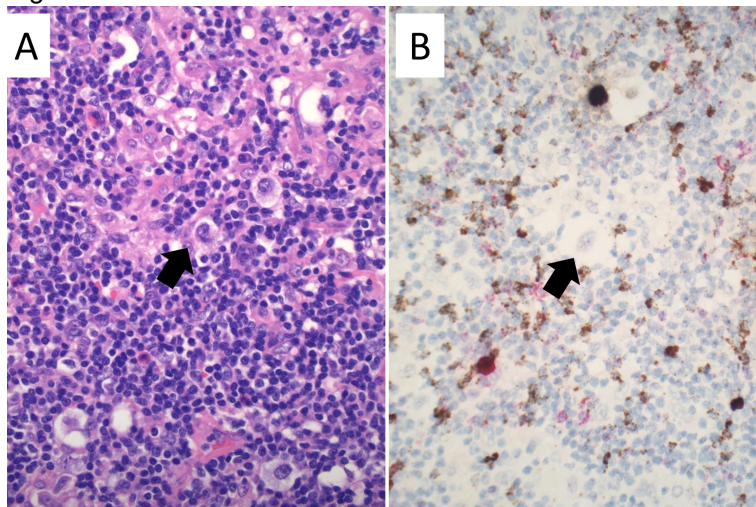


Figure 2 - 713



Conclusions: Ultrasensitive ISH for kappa and lambda light chains demonstrate light chain restriction in the vast majority of cases of nLPHL, facilitating the differential diagnosis from cHL and PTGC. This technique allows for evaluation of light chain restriction in the context of preserved cellular morphology and can identify background coexisting small B-cell proliferations that may otherwise go unrecognized. Ultrasensitive ISH for kappa and lambda is a useful addition to a standard immunophenotyping panel for the evaluation of suspected nLPHL.

714 The Clinicopathologic Significance of NPM1 Mutation and Ability to Detect NPM1 by Immunohistochemistry in Non-AML Myeloid Neoplasms

Hatem Kaseb¹, Valeria Visconte¹, Daniel Socha¹, Genevieve Crane¹, Lisa Durkin¹, James Cook¹, Jarslow Maciejewski¹, Eric Hsi², Heesun Rogers¹

¹Cleveland Clinic, Cleveland, OH, ²Wake Forest Baptist Health, Winston-Salem, NC

Disclosures: Hatem Kaseb: None; Valeria Visconte: None; Daniel Socha: None; Genevieve Crane: None; Lisa Durkin: None; James Cook: None; Jarslow Maciejewski: None; Eric Hsi: None; Heesun Rogers: None

Background: NPM1 mutated (NPM1+) AML shows clonal multilineage involvement and favorable prognosis. Rare NPM1+ non-AML myeloid neoplasms (MN; <20% blasts) are associated with aggressive clinical course in few studies. NPM1 immunohistochemistry (IHC) has shown conflicting results in AML and has not been studied in non-AML MN to predict NPM1 mutation.

Design: This retrospective study evaluates clinicopathologic features of non-AML MN patients with NPM1 mutation by Sanger or targeted next generation sequencing (NGS). Cytoplasmic NPM1 expression (NPM1c) was assessed by IHC to evaluate its ability to predict NPM1 mutation.

Results: We evaluated 34 NPM1+ MN patients (median age 65.5 years; 22 males, 12 female) comprising MDS (22), MPN (3) and MDS/MPN (9 including 4 CMML). They commonly presented with anemia (88%), thrombocytopenia (58%) and leukopenia (50%) (median Hb 9.2 g/dL, platelet 98.5 k/uL, WBC 3.85 k/uL). Median BM blasts were 3.5% (range 0-18%). Dysplasia was common (79%; megakaryocyte 60%, erythroid 50%, granulocyte 35%); 44% multilineage dysplasia. Karyotype was often normal (61%). Del(20q) was common (15%) among abnormal karyotype cases. NGS for MN-associated mutations (n=6) showed median 3 mutations; commonly DNMT3A, TET2 and KRAS. NPM1 mutations were missense (65%) or frameshift insertion/duplication (ins/dup; 35%). Variant allele fraction (VAF) was higher in ins/dup than missense (mean 26% vs 8%, p=.0002). NPM1c by IHC was positive in 48% and associated with higher VAF than negative patients (mean 21% vs 9%, p=.001; positive predictive value of 80% with VAF cutoff of 10%). All patients with ins/dup (VAF range 11-44%) were positive NPM1c. 47% expired during follow-up (range 1-128 months (mo)). The median overall survival (OS) was 70 mo. Most patients received therapy; 55% hypomethylating agent, 7% chemotherapy, 24% BM transplant. 9 patients (6 MDS-EB, 1 CMML2, 1 MDS-MLD, 1 MDS/MPN) progressed to AML. Blast% and OS are different between patients with and without progression to AML (median blasts 9% vs 2% p=.02, OS 20 vs 128 mo logrank p=.05).

Conclusions: NPM1+ non-AML MN patients commonly had cytopenia, dysplasia, normal karyotype, mutations in multiple genes and an unfavorable clinical outcome, including a high rate of progression to AML (27%). Our data identify NPM1c by IHC as a useful tool to predict NPM1 mutation in non-AML MN, particularly in VAF higher than 10% and with ins/dup. The ability to rapidly detect NPM1 mutation may facilitate its use as a prognostic marker in these patients.

715 **GLUT1 Immunohistochemistry is a Reliable Marker of Erythroid Differentiation**

Benjamin Kaumeyer¹, Shiraz Fidai², Beenu Thakral³, Sa Wang³, Sandeep Gurbuxani², Girish Venkataraman⁴

¹University of Chicago Medicine, Chicago, IL, ²University of Chicago, Chicago, IL, ³The University of Texas MD Anderson Cancer Center, Houston, TX, ⁴University of Chicago Medical Center, Chicago, IL

Disclosures: Benjamin Kaumeyer: None; Shiraz Fidai: None; Beenu Thakral: None; Sa Wang: None; Sandeep Gurbuxani: None; Girish Venkataraman: *Speaker*, EUSA Pharma

Background: Within the hematopoietic compartment, GLUT1, a glucose transporter, is a highly expressed protein on the membranes of erythrocytes with upregulation of transcripts beginning at the basophilic erythroblast stage. In light of these findings, we evaluated its immunohistochemical expression profile in bone marrow and assessed the sensitivity and specificity of GLUT1 for erythroid lineage in reactive and malignant hematopoietic conditions.

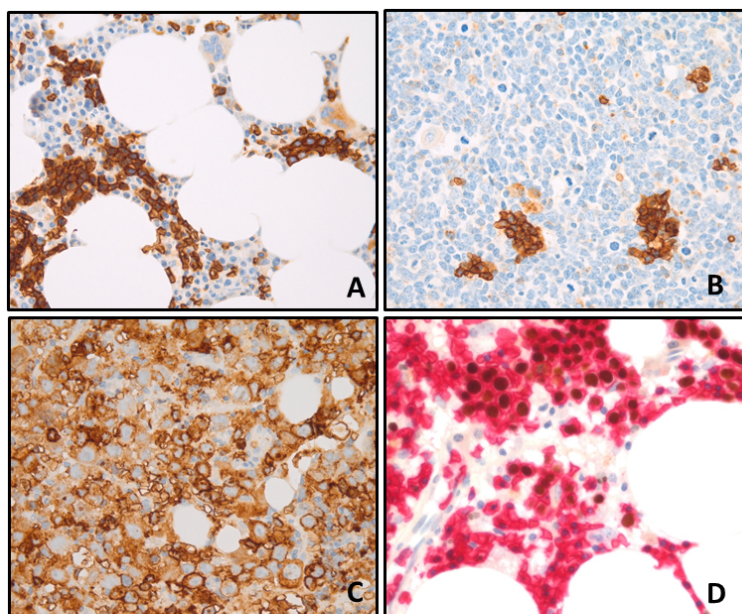
Design: A wide spectrum of cases including acute myeloid leukemia (AML), myelodysplastic syndrome (MDS), therapy related myeloid neoplasms (t-AML and t-MDS), B-acute lymphoblastic leukemia (B-ALL), reactive erythroid hyperplasia and normal bone marrows (see table 1) were examined. GLUT1 immunostain (Millipore, Polyclonal 1:600) was performed on the B5-fixed marrow core biopsies using the H1/30 protocol retrieval on Leica Bond III. Each case was evaluated for (1) early, intermediate, and late erythroid precursor staining (2) staining of blasts and (3) staining of other hematopoietic cells. Erythroid differentiation was confirmed in the majority of cases using Glycophorin-C or E-cadherin IHC. A GATA1/GLUT1 double stain was performed on one case to confirm coexpression of GLUT1 on GATA1+ erythroid precursors.

Results: GLUT1 demonstrated strong membranous and cytoplasmic staining of early, intermediate, and late erythroid precursors as well as erythrocytes in all cases with full spectrum erythropoiesis. GLUT1 staining was

specific to cells of the erythroid lineage with the exception of weak non-specific cytoplasmic staining of megakaryocytes seen in a subset of cases. B-ALL lymphoblasts also showed weak staining in 2/4 cases. In cases of AML and t-AML, which included a wide range of genetic subtypes and phenotypic differentiation, GLUT1 showed strong to intermediate membranous staining of malignant cells in only the cases of erythroid leukemia and t-AML with erythroid differentiation, while it was negative on these cells in all other non-erythroid cases. GATA1/GLUT1 double stain showed co-expression of cytoplasmic GLUT1 staining and nuclear GATA1 staining in all erythroid precursors including a significant subset of early erythroid precursors (See figure).

Diagnosis	Number of cases	GLUT1 positive malignant blasts
AML with recurrent genetic abnormalities		
AML with inv(16) (<i>CBFB/MYH11</i>)	1	0/1
AML with myelodysplastic changes	1	0/1
AML with biallelic mutations of <i>CEBPA</i>	1	0/1
AML, not otherwise specified (NOS)		
AML-NOS with minimal differentiation	1	0/1
AML-NOS with maturation	1	0/1
Acute erythroid leukemia	5	5/5 (strong to intermediate)
MDS		
MDS-EB-2 with expansion of erythroid precursors	2	0/2
MDS, NOS with marked erythroid preponderance	1	0/1
t-AML		
t-AML with erythroid differentiation	2	2/2 (strong)
t-AML with myelomonocytic differentiation	1	0/1
t-MDS	1	0/1
B-ALL	4	2/4 (weak)
Reactive erythroid proliferation	4	NA
Benign/post treatment with minimal disease	6	NA

Figure 1 - 715



A. GLUT1 strongly stains erythroid precursors along with weak cytoplasmic staining of megakaryocytes B. GLUT1 is negative in blasts in a case of AML. C. GLUT1 is strongly positive in pure erythroid leukemia. D. GLUT1 (red)/GATA1 (brown) double stain highlights co-expression of cytoplasmic GLUT1 in nuclear positive GATA1 erythroid precursors

Conclusions: GLUT1 IHC shows strong membranous and cytoplasmic staining of erythroid precursors of all developmental stages and erythrocytes while being largely negative in other hematopoietic cell lineages. GLUT1 can serve as a reliable alternative marker for erythroid differentiation in addition to Glycophorin, GATA1 and E-cadherin.

716 Frequent Presentation with Advanced Phase Disease in Chronic Myeloid Leukemia in Children and Young Adults – a Single Institution Experience

Benjamin Kaumeyer¹, Angela Lager², Sandeep Gurbuxani²

¹University of Chicago Medicine, Chicago, IL, ²University of Chicago, Chicago, IL

Disclosures: Benjamin Kaumeyer: None; Angela Lager: None; Sandeep Gurbuxani: None

Background: Chronic myeloid leukemia (CML) is primarily a disease of older adults with a median age of diagnosis of 64 years. Although rare, CML can also present in the pediatric population and in young adults. Interestingly, compared to adults, CML in this younger population tends to present with more aggressive clinical features such as higher white blood cell count and a higher proportion of cases presenting with advanced disease. Due to the rare nature of pediatric and young adult CML, there are only a limited number of studies on the topic. More data on the clinical and pathological characteristics of CML in this cohort would be beneficial for understanding the disease from presentation and diagnosis to treatment response.

Design: After IRB approval, retrospective chart review was performed to identify patients less than or equal to 30 years of age presenting to our institution with a morphologically and genetically confirmed diagnosis of CML. When available, the following data were collected from the time of initial diagnosis: age, sex, presence of organomegaly (splenomegaly or hepatomegaly), peripheral blood white blood cell count (WBC), blast percentage, basophil percentage, hemoglobin, platelet count, bone marrow cellularity, bone marrow fibrosis, dwarf megakaryocytes, dysplasia, and genetic findings.

Results: A total of 23 patients were identified which met inclusion criteria. The median age was 22 and age ranged from 10-27 years. Specific hematologic and pathologic parameters can be found in table 1. At initial diagnosis of CML, 21.7% (5/23) presented in advanced phase of the disease (1 in accelerated phase (AP), and 4 in blast phase (BP)). Interestingly, for 2/4 (50%) of the patients presenting in BP, the blast lineage was B-lymphoid.

Clinical and pathologic characteristics at diagnosis		
Demographics n = 23		
	Median age (range)	22 years (10 -27)
	Males	12
	Females	11
Diagnosis n = 23		
	CML-CP	18 cases
	CML- AP	1 case
	CML-BP (myeloid)	2 cases
	CML-BP (lymphoid)	2 cases
Organomegaly present		13/16 cases
Peripheral blood		
	Median WBC (range) n = 19	187 K/uL (13 - 552)
	Median %blast (range) n = 18	2% (0 - 15)
	Median %basophils (range) n = 17	4% (1 - 51)
	Median Hgb (range) n = 18	11.5 g/dL (6.3 - 13.5)
	Median platelet count (range) n = 18	383 K/uL (36 - 1174)
Bone Marrow		
	Median %cellularity (range) n = 19	100% (80 - 100)
	Increased bone marrow fibrosis	3/13 cases
	Dwarf megakaryocytes present	20/20 cases
	Dysplasia	0/21 cases
Note: Data was not available for every patient therefore n may be less than 23		

Conclusions: This younger cohort presented with evidence of high disease burden including a high proportion of organomegaly (13/16 cases) and a median white blood cell count (187 K/uL) higher than described in older adults. The proportion of patients presenting with advanced disease (AP Or BP) was also high when compared to older adults. Interestingly, half (2/4) of the patients who presented in blast phase had morphologic and immunophenotypic findings of lymphoblasts. While lymphoid blasts lineage in CML-BP is well documented, it is

significantly less common than a myeloid blast lineage. Although this is only a small, single institution study, it helps to create a more complete picture of this common disease in a rare population of patients.

717 Association of Kikuchi Fujimoto-Like Lymphadenitis and Malignancy: A Retrospective Clinicopathologic Analysis

Neslihan Kayraklioglu¹, Robert Ohgami¹, Ronald Balassanian¹, Roberto Ruiz-Cordero¹
¹University of California, San Francisco, San Francisco, CA

Disclosures: Neslihan Kayraklioglu: None; Robert Ohgami: None; Ronald Balassanian: None; Roberto Ruiz-Cordero: None

Background: Kikuchi-Fujimoto disease (KFD) is a rare disorder of unknown etiology, presenting as histiocytic necrotizing lymphadenitis. The pathogenesis of KFD is believed to be an aberrant immune response to unknown antigenic stimuli mediated by T cells and histiocytes. KFD can clinically, radiographically and histologically overlap with autoimmune or infectious lymphadenitis, as well as primary and metastatic cancers. The distinction of KFD versus metastasis is particularly crucial in cancer patients, given the dramatic difference in the outcomes. To determine if there is an association between KFD-like lymphadenitis and malignancy, we investigated patients with various concurrent cancers and KFD-like lymphadenitis.

Design: An institutional database search was conducted for KFD using the words “Kikuchi”, “Kikuchi Fujimoto”, “Kikuchi lymphadenitis” and “Necrotizing lymphadenitis” across 1980-2020. 135 patients were identified. 19 cases were excluded due to proven infectious etiology. 15 patients with KFD-like lymphadenitis and concurrent cancer diagnosis were identified. Cases were reviewed and clinicopathologic data were obtained from the electronic medical records.

Results: When compared to our cases of KFD, KFD-like lymphadenitis in patients with a concurrent cancer diagnosis (n=15) were older (KFD vs KFD-like; 30.5 vs 42, p<0.01) but showed a similar female predisposition (female:male ratio of 69:32 vs 10:5 respectively). Two groups were identified among the 15 patients with concurrent cancer. KFD-like lymphadenitis that was immediately coincident with the cancer (n=12), and KFD-like lymphadenitis that preceded a diagnosis of cancer in a separate biopsy (n=3). First group had hematolymphoid (3/12) and non-hematolymphoid cancers (9/12); including carcinoma (7/12), cutaneous melanoma (1/12) and hemangioendothelioma of liver (1/12). Interestingly, all patients with non-hematolymphoid cancers also showed metastatic cancer in another lymph node. Of the 3 patients in the second group, a future biopsy (range 1-3 years later) revealed cancer, including carcinoma (1/3) and hematolymphoid neoplasms (2/3).

Group 1: KFD-like lymphadenitis with immediately coincident cancer				
Age	Gender	Cancer	LN involvement	Treatment prior to LN biopsy
11	F	Mucoepidermoid carcinoma	Present	None
29	F	Ductal breast carcinoma	Present	Docetaxel, Paclitaxel, Carboplatin, Trastuzumab, Pertuzumab
49	F	Papillary Thyroid Carcinoma	Present	Thyroid lobectomy, I-131 treatment.
33	F	Hemangioendothelioma of liver	Present	Liver transplant, Tacrolimus, Mycophenolic acid, Prednizone
64	M	Squamous cell carcinoma of pharynx	Present	None
39	M	Cutaneous melanoma	Present	Local wide excision
51	M	Nasopharyngeal carcinoma	Present	Radiation
90	F	Ampullary-ductal carcinoma	Present	None
33	F	Papillary Thyroid Carcinoma	Present	None
16	F	B-ALL	N/A	Chemotherapy, haplocompatible PBSCT
33	F	Peripheral T-cell lymphoma	N/A	None
38	M	Hodgkin Lymphoma	N/A	Unknown
Group 2: KFD-like lymphadenitis preceding cancer				
Age	Gender	Cancer	Time from LN biopsy to cancer	
61	F	Ductal breast carcinoma	3 years	

30	F	Anaplastic large cell lymphoma	3 years
53	M	Peripheral T-cell lymphoma	1 year

Conclusions: KFD-like lymphadenitis can be associated with various types of cancer. These patients are likely to be older and present with lymph node metastasis. Careful examination of lymph nodes from patients with a KFD-like lymphadenitis is recommended to specifically evaluate for a concurrent cancer, though a subset of patients may be diagnosed with cancer only on later biopsy. Our observation of concurrent malignancy in these patients also raises the possibility of tumor-specific antigens in disease pathogenesis and warrants further investigation.

718 Blastoid B-cell Lymphoma Initially Presenting in Bone Marrow: A Diagnostic Challenge

Mahsa Khanlari¹, Pei Lin¹, Jie Xu¹, M. James You¹, Guilin Tang¹, C. Cameron Yin¹, Lianqun Qiu¹, Carlos Bueso-Ramos¹, L. Jeffrey Medeiros¹, Shaoying Li¹

¹The University of Texas MD Anderson Cancer Center, Houston, TX

Disclosures: Mahsa Khanlari: None; Pei Lin: None; Jie Xu: None; M. James You: None; Guilin Tang: None; C. Cameron Yin: None; Lianqun Qiu: None; Carlos Bueso-Ramos: None; L. Jeffrey Medeiros: None; Shaoying Li: None

Background: The 2017 WHO classification introduced the category of high-grade B cell lymphoma (HGBL), which included blastoid B cell lymphoma (BCL). Establishing this diagnosis in bone marrow (BM) and distinguishing it from B-lymphoblastic leukemia (B-ALL) can be challenging, and related data is limited.

Design: We studied 31 cases of blastoid BCL initially diagnosed in BM, and compared them to 22 cases of B-ALL. Immunophenotyping was performed mainly by flow cytometry and supplemented by immunohistochemical analysis. *MYC*, *BCL2*, *BCL6*, and *CCND1* status were assessed by fluorescence in situ hybridization analysis and/or conventional karyotyping. Mutation status was evaluated in a subset of cases by targeted next generation sequencing study.

Results: Following the WHO classification, the 31 blastoid cases were classified as: 14 HGBL with *MYC* and *BCL2* and/or *BCL6* rearrangements (double/triple hit lymphomas, or D/THL), 11 HGBL, not otherwise specified (NOS), and 6 cases that were difficult to classify. These 6 cases included 4 with TdT expression and 2 which were CD5+, cyclin D1-, and SOX11+ (diffuse), likely representing *CCND1*-negative blastoid mantle cell lymphoma. Compared with B-ALL, blastoid BCL more often showed increased expression/intensity of CD20, CD38, CD45 and BCL6, and less frequent bright CD10 and TdT ($p < 0.01$ for all). All but one B-ALL cases expressed CD34. Blastoid BCL more frequently had *MYC* rearrangement and complex karyotype (both $p = 0.0001$) and *TP53* mutation ($p = 0.005$) than B-ALL. Except CD34 expression, no other single factor, including TdT, is sensitive or specific enough to define a blastoid BM tumor as lymphoma vs B-ALL. Therefore, we developed a scoring system using 6 distinctive features (Table 1), with a score of ≥ 3 define blastoid lymphoma, which has a sensitivity of 100%, specificity 95%, positive predictive value 97%, and negative predictive value 100%. By using this scoring system, the 4 cases with TdT expression have been classified as HGBL (3 D/THL, 1 HGBL-NOS).

Table 1. A scoring system to aid distinguish blastoid BCL from B-ALL

Parameter	Presence	Absence
CD45 intensity > Granulocytes	1	0
CD38 bright	1	0
CD10 Not bright	1	0
CD20>dim	1	0
TdT Negative	1	0
MYC Rearrangement	1	0

Conclusions: Blastoid BCL showed distinct immunophenotypic, cytogenetic, and molecular features compared to B-ALL. Except CD34, no other single factor, including TdT, is sensitive and specific enough to define a blastoid BM tumor as lymphoma vs B-ALL. Using multiple immunophenotypic markers combined with molecular cytogenetic

features, such as our scoring system, is very helpful for the classification of diagnostically challenging blastoid BM lymphoid tumors.

719 Clinicopathologic and Comprehensive Molecular Analysis of Mast Cell Leukemia with Associated Hematologic Neoplasm

Philippa Li¹, Giulia Biancon², Timil Patel², Zenggang Pan¹, Shalin Kothari², Stephanie Halene¹, Thomas Prebet², Mina Xu³

¹Yale School of Medicine, New Haven, CT, ²Yale New Haven Hospital, Yale School of Medicine, New Haven, CT, ³Yale University, New Haven, CT

Disclosures: Philippa Li: None; Giulia Biancon: None; Timil Patel: None; Zenggang Pan: None; Shalin Kothari: None; Stephanie Halene: None; Thomas Prebet: None; Mina Xu: None

Background: Mast cell leukemia (MCL) is an exceedingly rare form of aggressive systemic mastocytosis (SM) with a diagnostic criteria requiring >20% mast cell involvement in the bone marrow aspirate. MCL can be diagnosed alongside an associated hematologic neoplasm (MCL-AHN). As our understanding of aggressive mast cell diseases expands, molecular studies continue to reveal the complex nature of MCL-AHN, which likely plays a role in treatment refractoriness of the disease.

Design: All institutional cases of MCL-AHN were retrieved and the diagnoses were confirmed. Five patients (Table 1) aged 45-74 were identified. Whole exome sequencing was performed on tissues from 3 patients with adequate archival samples. DNA was extracted using QIAGEN DNeasy Blood & Tissue kit, and sequenced (Illumina NovaSeq, paired-end 100 bp). Variants were annotated using ANNOVAR (2019Oct24) and COSMIC v90 and v91, and filtered in the selection of deleterious variants. PD-L1 expression (E1L3N antibody, Cell Signaling Technologies) was evaluated on formalin-fixed paraffin-embedded tissue and intensity was graded as follows: 0 no staining, 1+ weak/equivocal, 2+ moderate, and 3+ strong. Tumor staining for PD-L1 was considered positive if ≥5% of the tumor cell population showed 2+ or 3+ membrane staining.

Results: Except for patient 1, all other patients received their diagnosis of MCL after their initial hematologic diagnosis. The average survival time was 32 months after the diagnosis of MCL. WES results revealed pathogenic variants in *KIT*, *RUNX1*, *PHF6*, *ATM*, and *PLXNB2* in patient 1; *DNMT3A*, *JAK2*, *PTPN11*, *DHRS4L2*, *EXOC7*, and *NR2F6* in patient 2. Patient 5's peripheral blood with primarily AML showed *KIT*, *JAK2*, *DNM2*, *CACNA1C*, *ANO4*, *WFIKKN2*, and *NR2F6* while her subsequent bone marrow with primarily MCL contained pathogenic variants in *GNB1*, *CACNA1C*, *ANO4*, *WFIKKN2*, and *NR2F6*. PD-L1 staining demonstrated patient 1 with 0 (negative) staining, patient 2 with 3+ in 100% of tumor cells, and patient 5 with 2+ in 40% of tumor cells.

	Patient 1	Patient 2	Patient 3	Patient 4	Patient 5
Age (at first diagnosis), gender, race	45yoM Caucasian	71yoM Caucasian	74yoM Caucasian	60yoM Caucasian	69yoF Caucasian
MCL type	Aleukemic <i>de novo</i> MCL	Aleukemic <i>de novo</i> MCL, subsequent diagnosis	Aleukemic secondary MCL, subsequent diagnosis	Aleukemic secondary MCL, subsequent diagnosis	Aleukemia <i>de novo</i> MCL, subsequent diagnosis
AHN type	AML	ETP-ALL	MDS with ringed sideroblasts	AML	AML
Aspirate findings at diagnosis	48% mast cells, 23% blasts	31% lymphoblasts, 63% mast cells on subsequent aspirate	3% myeloblasts, 20% mast cells on subsequent aspirate	78% myeloblasts, 37% mast cells on subsequent aspirate	72% myeloblasts, 34% mast cells on subsequent aspirate
WES (source)	<i>KIT</i> , <i>RUNX1</i> , <i>PHF6</i> , <i>ATM</i> , <i>PLXNB2</i> (BM)	<i>DNMT3A</i> , <i>JAK2</i> , <i>PTPN11</i> , <i>DHRS4L2</i> , <i>EXOC7</i> , <i>NR2F6</i> (PB)	N/A	N/A	<i>KIT</i> , <i>JAK2</i> , <i>DNM2</i> , <i>CACNA1C</i> , <i>ANO4</i> , <i>WFIKKN2</i> , <i>NR2F6</i> (PB, primarily AML) <i>GNB1</i> , <i>CACNA1C</i> , <i>ANO4</i> , <i>WFIKKN2</i> , <i>NR2F6</i> (BM, primarily MCL)

PD-L1 expression	0	3+, 100% of tumor cells	N/A	N/A	2+, 40% of tumor cells
Outcome	Alive	Deceased	Deceased	Deceased	Deceased
Interval time between MCL and AHN diagnosis	Concurrent diagnosis	3 months	9 years 10 months	10 months	2 months
Survival time from first diagnosed malinancy	10 months	21 months	14 years 3 months	21 months	47 months

Acronyms: MCL mast cell leukemia, AML acute myeloid leukemia, ETP-ALL early T-cell precursor acute lymphoblastic leukemia, MDS myelodysplastic syndrome, WES whole-exome sequencing, BM bone marrow, PB peripheral blood

Figure 1 – 719

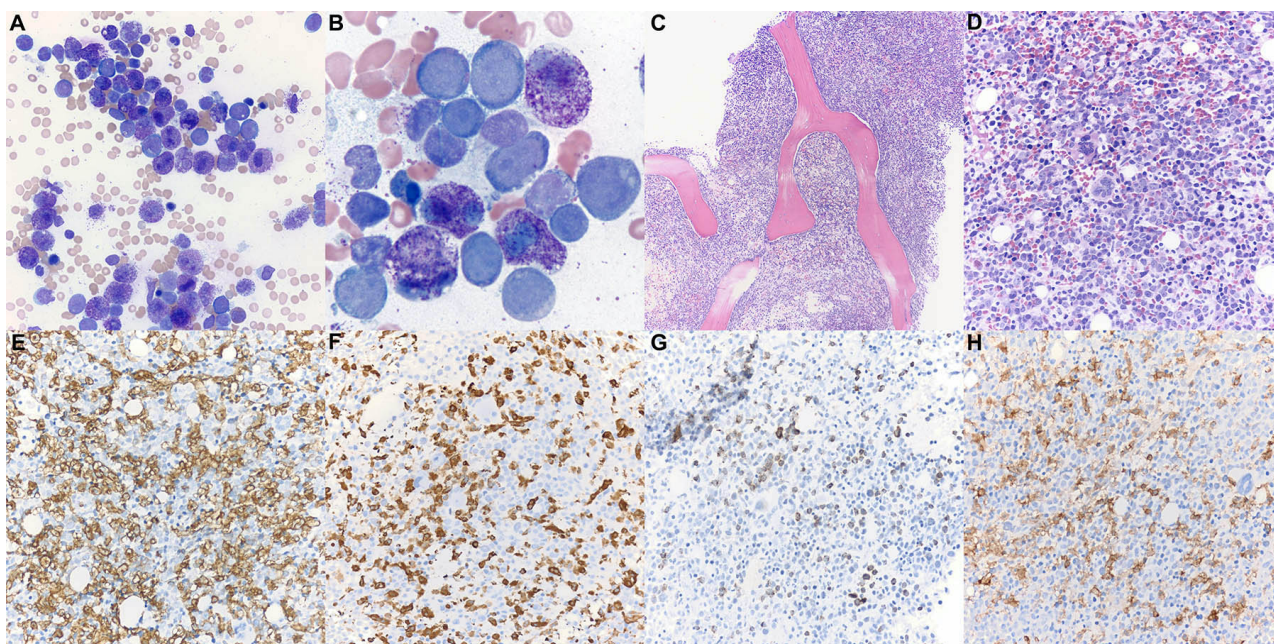


Figure 1: Bone marrow aspirate and trephine biopsy. A-B. Patient 1 MCL-AML bone marrow aspirate smear (Wright-Giemsa, 400X, 1000X) is notable for numerous mast cells intermixed with myeloblasts. C-D. The hypercellular bone marrow biopsy (H&E, 100X, 400X). E. CD117 immunostain (400X). F. Mast cell tryptase immunostain (400X). G. CD34 immunostain (400X) highlights blast elements. H. CD25 immunostain (400X) is positive in the neoplastic mast cells.

Figure 2 – 719

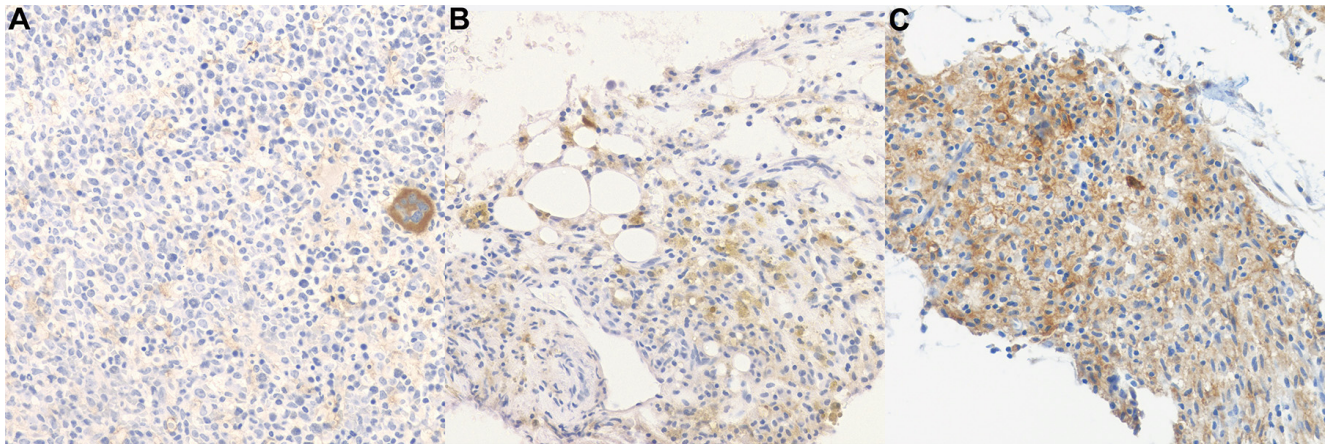


Figure 2: PD-L1 expression. A. No staining (0) in patient 1. B. 2+ staining in 40% tumor cells in patient 5. C. 3+ staining in 100% tumor cells in patient 2.

Conclusions: The depth of molecular analysis in these MCL-AHN cases aids in fully characterizing rare tumors that are extremely difficult to treat. *NR2F6* appears to play a role in immune checkpoint regulation (Klepsch, V. et al. 2018). We show that the cases with mutant *NR2F6* also exhibit overexpression of PD-L1 on abnormal mast cells, potentially offering additional opportunities for targeted immune therapies.

720 Clinicopathologic Features of Precursor Lymphoid Neoplasms Arising After Solid Organ or Allogeneic Stem Cell Transplantation

Wen-Hsuan Wendy Lin¹, Rebecca Leeman-Neill², David Park³, Govind Bhagat³, Bachir Alobeid¹
¹Columbia University Irving Medical Center, New York-Presbyterian Hospital, New York, NY, ²Columbia Medical Center, New York, NY, ³Columbia University Irving Medical Center, New York, NY

Disclosures: Wen-Hsuan Wendy Lin: None; Rebecca Leeman-Neill: None; David Park: None; Govind Bhagat: None; Bachir Alobeid: None

Background: Post-transplant lymphoproliferative disorders (PTLD) represent a heterogeneous group of hematolymphoid proliferations arising after solid organ (SOT) or allogeneic stem cell transplantation. The majority of PTLDs are of B-cell lineage, whereas PTLDs of T-cell lineage represent only a minority. PTLDs of precursor B- or T-cell origin are rarely reported. Here we evaluated a series of lymphoblastic neoplasms (B-ALL/LBL and T-ALL/LBL) occurring after SOT or allogeneic stem cell transplantation diagnosed at our institution to review their clinicopathologic characteristics.

Design: We searched our departmental database for cases of precursor lymphoid neoplasms diagnosed after SOT or allogeneic stem cell transplants over a 20-year period (2001-2020). Morphologic and immunophenotypic features were evaluated, and flow cytometry findings, as well as results of cytogenetic and molecular studies, were reviewed. Clinical and laboratory data, including EBV serostatus, types of organs transplanted, therapies, and clinical outcomes, were obtained from the electronic medical records.

Results: Five cases of post-transplant precursor lymphoid neoplasms were identified, including 3 T-ALL, 1 T-LBL, and 1 B-ALL occurring after kidney, heart, liver, lung, and allogeneic stem cell transplantation (n=1 each). All patients were male. The median time from transplant to diagnosis was 90 months (52-192 months) and the median age at diagnosis was 38 years (18-60 years). Precursor lymphoid PTLD occurred more frequently in patients receiving Tacrolimus immunosuppressive therapy (3/4, 75%). All patients were seropositive for EBV and had low or undetectable EBV viral load at PTLD diagnosis. Cytogenetic abnormalities were detected in the majority of cases (4/5, 80%) and clonal TCR rearrangements in half the T-ALL/LBLs. The incidence of precursor lymphoid PTLD after SOT was 0.037% (B-ALL= 0.009% and T-ALL/LBL=0.028%).

	Age	Sex	Tx	Dx	Time from Tx (mos)	Status/Time from Dx (yrs)	EBER	Cytogenetics	TCR beta rearrangement
1	59	M	Kidney	B-ALL	90	Alive/<1.0	negative	High hypodiploid karyotype. monosomy 13 and 17, deletion of TP53, ETV6, and loss of IKZF1.	Not performed
2	38	M	Single lung	T-ALL	63	Alive/<1.0	negative	t(7;14)(p15;q32) and del(9q).	Clonal
3	18	M	Allo SCT	ETP T-ALL	120	Dead/2.5	Not performed	Normal karyotype, positive for MLL rearrangement.	Polyclonal
4	18	M	Liver (x3)	T-ALL	192	Alive/9.0	negative	Normal karyotype. Negative for (TCR) alpha/delta rearrangement	Clonal
5	60	M	Heart	T-LBL	52	Dead/2.9	negative	del(5)(q15q31)	Polyclonal

Conclusions: Precursor lymphoid neoplasms represent rare forms of late onset PTLDs that are not associated with EBV infection. They may occur after SOT or allogeneic stem cell transplantation. A striking male predominance was observed and T-ALL/LBL was the most common type. The cytogenetic profile was similar to that seen in similar neoplasms in immune-competent patients. Although a coincidental occurrence cannot be ruled out; the incidence of T-ALL/LBL in our cohort was 75-200 fold higher than in the general US population (0.13 to 0.36 per 100000). Future studies are warranted to determine risk and contributing factors.

721 Blinatumomab Induces Bone Marrow Lymphoid Infiltrates That Correlate with Response in B-ALL

Andrew Lytle¹, Colleen Croy², Gerald Wertheim³, Michele Paessler⁴, Susan Rheingold⁵, Vinodh Pillai⁵
¹The Hospital of the University of Pennsylvania, Philadelphia, PA, ²The Children's Hospital of Philadelphia, Philadelphia, PA, ³Children's Hospital of Philadelphia, University of Pennsylvania, Philadelphia, PA, ⁴The Children's Hospital of Philadelphia, Perelman School of Medicine at the University of Pennsylvania, Philadelphia, PA, ⁵Children's Hospital of Philadelphia, Philadelphia, PA

Disclosures: Andrew Lytle: None; Colleen Croy: None; Gerald Wertheim: None; Michele Paessler: None; Susan Rheingold: Grant or Research Support, Pfizer; Employee, Optinose; Vinodh Pillai: None

Background: Blinatumomab is a CD3 T-cell engager targeting CD19 which shows superior response rates compared to standard of care chemotherapy for treatment of relapsed/refractory (R/R) as well as minimal residual disease (MRD)-positive B-ALL. Blinatumomab induces activation of multiple T cell subsets *in vitro*, and clinical trials have demonstrated an expansion of activated peripheral blood T cells during blinatumomab infusion. However, the dynamics of bone marrow T cell populations during blinatumomab therapy in B-ALL have not been investigated.

Design: We searched pathology databases at our institution for bone marrow core biopsies from patients treated with blinatumomab for R/R B-ALL from 2011-2020. Marrow core biopsies were collected from timepoints immediately prior to blinatumomab administration (pre-treatment) and during or immediately following one or more cycles of treatment (post-treatment). Core biopsies were analyzed histologically, and CD3, CD4 and CD8 immunostains were performed to characterize T cell populations. T cell infiltration (percentage of CD3+ cells) and lymphoid aggregate formation (>15 CD3+ T cells) were correlated to response to blinatumomab of <0.1 % MRD level assessed by flow cytometry.

Results: We identified 16 patients with R/R B-ALL who were treated with blinatumomab (median age 12 years, range 1-23). Thirteen pre-treatment and 23 post-treatment marrow core biopsies were examined. Pre-treatment marrow involvement by B-ALL ranged from <0.01% to >95% (median: 5.5%). CD3+ T cells were increased in post-treatment biopsies compared to pre-treatment biopsies (13.4% vs 6.7%, p=0.025). T cell aggregates increased in response to multiple cycles of blinatumomab (46% of pre-treatment biopsies, 57% following 1st cycle, 88% following 2nd, 100% following 3rd and 4th). Lymphohistiocytic aggregates (n=4 biopsies) were seen exclusively post-treatment in <0.1% MRD responders with a high burden of pre-treatment disease (>30%

involvement) and contained nearly even proportions of CD4+ and CD8+ T cells (0.8:1). Lymphoid aggregates (n=18 biopsies) were CD8-predominant (0.36:1). For 8 patients with matched pre- and post-treatment biopsies, post-treatment biopsies with MRD <0.1% response to blinatumomab (n=14) showed increased CD3+ T cells compared to matched pre-treatment biopsies (16.9% vs 8.9%, p=0.039). Matched biopsies with residual disease >0.1% post-treatment (n=3) showed no significant increase in marrow CD3+ T cells. Pre-treatment biopsy T cell percentages were not associated with response.

Conclusions: Increased bone marrow CD3+ T cell infiltration following blinatumomab infusion correlated with treatment response, and may serve as a biomarker of blinatumomab response in R/R B-ALL.

722 BCR-ABL1 Kinase Domain Mutations in Front-Line Drug Intolerant or Resistant Chronic Myeloid Leukemia Patients in India: A Single Laboratory Experience

Atreye Majumdar¹, Aastha Gupta¹, Rahul Katara¹, Avshesh Mishra¹, Aayushi Singh¹, Deepak Sharma¹, Aman Shrivastava¹, Shivani Sharma², Sambit Mohanty³

¹Core Diagnostics, Gurugram, India, ²Core Diagnostics, Gurgaon, India, ³AMRI Hospital, Chandigarh, India

Disclosures: Atreye Majumdar: None; Aastha Gupta: None; Rahul Katara: None; Avshesh Mishra: None; Aayushi Singh: None; Deepak Sharma: None; Aman Shrivastava: None; Shivani Sharma: None; Sambit Mohanty: None

Background: Chronic myeloid leukemia (CML) in therapy often encounters resistance to first- or second-generation tyrosine kinase inhibitors (TKIs). Among the BCR-ABL1 dependent mechanisms of resistance, acquisition of mutations in the kinase domain (KD) of the gene is the best studied with over 100 KD mutations already characterized. KD analysis aids in appropriate TKI selection using the prognostic value of detected mutations. The objective of this study was to identify and evaluate frequency of mutations in the BCR-ABL1 KD of CML patients who showed suboptimal response to their current tyrosine kinase Inhibitor (TKI) regime and to assess their clinical value in further treatment decisions.

Design: Peripheral and/or bone marrow were collected from 791 CML patients. RNA was extracted, reverse transcribed and Sanger sequencing method was utilized to detect single nucleotide variants (SNVs) in BCR-ABL1 KD.

Results: Thirty eight different single nucleotide variants (SNVs) were identified in 29.8% (n=236/791) patients. T315I, E255K and M244V were among the most frequent single mutations detected (Table). A subset of patients from the above mentioned harbored compound mutations (13.3%,n= 33/236)(Fig 2) and T315I was the most frequent co-mutation in these patients. One patient harbored a novel L298P mutation with T315I as a co-mutant. Follow up data was available in of 28 patients that demonstrated the efficacy of TKIs in correlation with mutation analysis and BCR-ABL1 quantitation. Molecular response was attained in 50% patients following an appropriate TKI shift. A dismal survival rate of 40% was observed in T315I harboring patients on follow up (Fig 1)

Fig.1 Distribution and frequency of mutations based on their structural positions in the kinase domain with most frequent (in bold) and novel mutation (in bold italics)

Structure	Hotspot mutation	No. of cases* (N=236)	Frequency
P-loop	M244V	30	12.7118644
	L248V	5	2.11864407
	G250E	19	8.05084746
	Q252H	6	2.54237288
	Y253F	1	0.42372881
	Y253H	15	6.3559322
	E255K	32	13.559322
	E255V	6	2.54237288
C -helix	E275K	2	0.84745763
	D276G	4	1.69491525
	E279K	6	2.54237288
	I293V	1	0.42372881

	L298P	1	0.42372881
	V299L	2	0.84745763
ATP-binding site	F311L	3	1.27118644
	F311I	11	4.66101695
	T315I	48	20.3389831
	F317L	17	7.20338983
SH2	M351T	10	4.23728814
	E355G	4	1.69491525
Substrate binding site	F359V	22	9.3220339
	F359I	3	1.27118644
A loop	E373K	1	0.42372881
	L387M	3	1.27118644
	M388L	2	0.84745763
	H396P	3	1.27118644
	H396R	9	3.81355932
	H396Y	1	0.42372881
	A397P	1	0.42372881

*Total number of cases (with frequency) in which mutation was detected either single or with a co-mutation

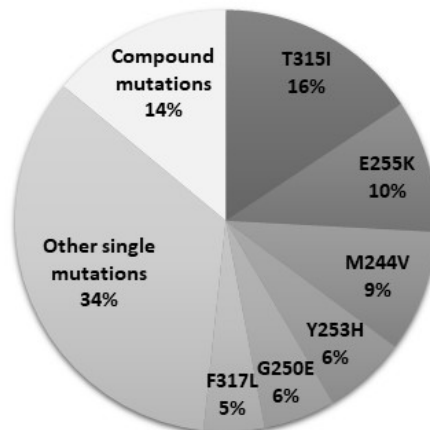
Figure 1 - 722

Tyrosine kinase inhibitor shifts and associated response in 28 patients on follow up															
Age	Gender	Disease phase	1st line TKI	Time of first mutation analysis since diagnosis (months)	Mutation detected	2nd line TKI	Time of follow up since TKI shift (months)	BCR-ABL1 transcript level % (other symptom)	TKD analysis repeated (months since diagnosis)	Mutation detected	3rd line TKI	Time of follow up since TKI shift (months)	BCR-ABL1 transcript level % (other symptom)	Other	Status (March 2020)
51	M	CML-CP	Imatinib	16	No mutation	Dasatinib	14	0.3 MR	Yes (36)	E255 K	Nilotinib	5	0.1 MMR		Alive
59	M	CML-CP	Imatinib	24	E255 K	Dasatinib	3	19.1 (cytopenia)	Not tested	Not tested	Nilotinib	5	Not tested		Alive
36	M	CML-CP	Imatinib	24	F359 V, G250 E	Dasatinib	24	33.4	Yes (48)	E255 K	Bosutinib	1	No response		Dead
28	M	CML-CP	Imatinib	96	E255 K	Imatinib	13	Not tested							Alive
80	M	CML-CP	Imatinib	64	E255 V	Dasatinib	12	Not tested							Alive
33	M	CML-CP	Imatinib	24	E255 V	Nilotinib	2	No response							Dead
16	M	CML-CP	Imatinib	19	E279 K	Nilotinib	7	0.1 MR							Alive
46	M	CML-CP	Imatinib	132	E355 G	Dasatinib	7	0.003 MR4.5							Alive
40	M	CML-CP	Nilotinib	58	F3111	Nilotinib resumed	12	0.12 MR							Alive
45	M	CML-CP	Imatinib	204	F311 L	Imatinib	4	No response							Dead
37	M	CML-CP	Imatinib	36	F317 L	Nilotinib	4	0.6 -CCyR							Alive
48	F	CML-CP	Imatinib	60	F317 L	Nilotinib	4	Not tested							Alive
42	M	CML-CP	Imatinib	27	F317 L	Dasatinib	7	23.9	No	No	Nilotinib	6	5.21 -PCyR		Alive
25	F	CML-CP	Imatinib	144	F359 V	Nilotinib	48	Not tested (leukocytosis)			Dasatinib	12	Not tested		Alive
47	F	CML-CP	Dasatinib	168	F359 V	Nilotinib	3	1.98 -PCyR							Alive
39	M	CML-CP	Nilotinib	15	F359 V	Dasatinib	3	0 DMR							Alive
29	M	CML-CP	Imatinib	48	G250 E	Nilotinib	8	0 DMR							Alive
45	M	CML-CP	Imatinib	Not tested	-	Nilotinib	Not tested	Not tested (intolerance)	Yes (9)	G250 E	Dasatinib	15	2.9 -CCyR		Alive
51	M	CML-CP	Imatinib	144	H396 P	Dasatinib	12	0.29 -MR							Alive
39	F	CML-CP	Imatinib	72	H396 R	Nilotinib	6	No response							Dead
30	F	CML-CP	Imatinib	Not tested	-	Dasatinib	60	28.82	Yes (192)	M244V	Nilotinib	7	1.91 -CCyR		Alive
29	M	CML-CP	Imatinib	24	Y235 H	Imatinib	6	Not tested (Leukocytosis)	Not tested	Not tested	Dasatinib	3	No data		Alive
36	M	CML-CP	Imatinib	24	M380 I	Imatinib continued	6	0.07 MMR	Yes (6)	No mutation detected					Alive
26	M	CML-CP	Imatinib	24	No mutation detected	Nilotinib	7	No response	Yes (72)	T315 I	Ponatinib	7	No response		Dead
37	M	CML-CP	Imatinib	Not tested	-	Nilotinib	3	Not tested (T-lymphoid blast crisis)	Yes (84)	T315 I	Ponatinib	12	No response	ASCT	Dead
53	F	CML-CP	Imatinib	No data	T315I	Dasatinib	3	15.24	No	No	Ponatinib	8	0.04 MMR		Dead
32	M	CML-CP	Imatinib	Not tested	-	Nilotinib	60	Not tested	Yes (84)	T315 I	Ponatinib	15	0.01 MMR4		Alive
52	M	CML-CP	Imatinib	6	T315I	Imatinib	5	4.18 -PCyR							Alive

Abbreviations- CML- chronic myeloid leukemia, CP- chronic phase , MR-molecular response, MMR- major molecular response, CyR- Cytogenetic response, PCyR – partial cytogenetic response , ASCT- allogenic stem cell transplant

Figure 2 - 722

Distribution of mutations detected (n=236)



Pie chart representation of the type of KD mutations with T315I, M244V and E255K as the most commonly detected single mutation followed by decreasing incidence of other mutations (grey to light grey). Compound mutations harbouring patients form a separate section (white).

Conclusions: This study shows the incidence and pattern of mutations in one of the largest sets of Indian CML patients. It has been demonstrated that T315I is the most common mutation observed in the Indian population. However the access to the only eligible TKI- Ponatinib by the economically challenged must be addressed. It is advisable to perform BCR-ABL1 kinase domain (KD) mutation analysis before administering a new TKI at any time point to attain desirable results. Novel mutations such as L298P as identified in this study can have distinct response to TKIs and thus, are recommended to be monitored for their clinical significance. Our findings strengthen the prognostic value of KD mutation analysis among strategies to overcome TKI resistance.

723 Morphological Patterns of High-Grade B-Cell Lymphoma with MYC and BCL2 and/or BCL6 Rearrangements

Victoria Malone¹, Walker Jan¹, Castriciano Giuseppa¹, Mark Wright¹, Cliona Grant¹, Larry Bacon¹, Elisabeth Vandenberghe¹, Barbara Dunne¹, Michael Jeffers², Richard Flavin¹

¹St. James's Hospital, Dublin, Ireland, ²Tallaght University Hospital, Dublin, Ireland

Disclosures: Victoria Malone: None; Castriciano Giuseppa: None; Mark Wright: None; Michael Jeffers: None; Richard Flavin: None

Background: High-grade B-cell lymphoma, with rearrangements of MYC and BCL2 and/or BCL6 has recently been defined as a distinct entity within the WHO classification (1). Timlin et al (2) recently described that 10% of lymphomas in our institution with diffuse large B cell lymphoma (DLBCL) morphology had a double hit (DH) or triple hit (TH) rearrangement involving MYC and BCL2 and/or BCL6, aligning with International levels. In this study we evaluated the morphology of double hit lymphoma (DHL) or triple hit lymphoma (THL) cases in our institution.

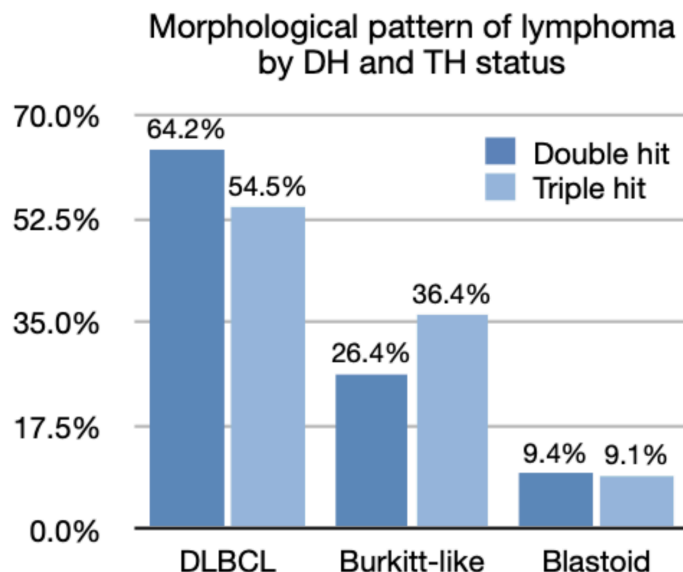
Design: All cases of DHL or THL from 2013 to 2019 in our institution were identified within our database. Slides from each of these cases were examined by the authors and morphologically categorised as "DLBCL", "Blastoid" or "Burkitt-like". Stastical tests were performed using the SciPy package for Python v3.7.

Results: In total 68 DH or TH lymphoma cases were identified. Of these, 4 cases were excluded from the study. Of the remaining 64 cases, 63% (n=40) were morphologically classed as DLBCL, 28% (n=18) as Burkitt-like and 9% (n=6) as Blastoid. Overall 83% (n=53) of the cases had a double hit while 17% (n=11) had a triple hit. Of the 53 DH lymphomas, 90.6% (n=48) had rearrangements of MYC/BCL2, while 9.4% (n=5) had rearrangements of

MYC/BCL6. Of the DH cases 64% (n=34) had DLBCL morphology, 26% (n=14) Burkitt-like and 9% (n=5) blastoid. Of the 11 TH lymphomas 55% (n=6) had DLBCL morphology, 36% (n=4) Burkitt-like and 9% (n=1) blastoid. Of the 40 cases with DLBCL morphology, 35% (n=14) had immunoblastic morphology, accounting for 38.2% (n=13 of 34) of the DH cases, and 16.7% (n=1 of 6) of the TH cases. Using Fischer's exact test, the difference in DLBCL versus non-DLBCL morphology did not reach significance between DH and TH lymphomas (OR = 1.491, p = 0.734), between MYC/BCL2 and MYC/BCL6 rearrangements across all cases (OR = 1.308, 0.774), nor between MYC/BCL2 and MYC/BCL6 rearrangements within the DH subgroup (OR = 1.216, p = 1.0).

Morphological classification of lymphoma cases by double and triple hit status.					
Morphology	Double Hit			Triple Hit	Total
	All DH	MYC/BCL2	MYC/BCL6		
DLBCL	34	31	3	6	40
Burkitt-like	14	12	2	4	18
Blastoid	5	5	0	1	6
Total	53	48	5	11	64

Figure 1 - 723



Conclusions: The majority (63%) of DHL/THL in our institution show DLBCL morphology. Burkitt-like (28%) and blastoid (9%) patterns are seen in just over a third of cases (37%). A not insignificant percentage of DLBCL cases had immunoblastic morphology (35%) in this cohort of patients, and this pattern could alert pathologists to the possibility of a DH or TH lymphoma on H&E slide examination.

References:

1. Swerdlow SH, Campo E, Harris NL, Jaffe ES, Pileri SA, Stein H, Thiele J. WHO Classification of Tumours of Haematopoietic and Lymphoid Tissues. WHO Classification of Tumours, Revised 4th Edition, Volume 2, 2017
2. Timlin, D. M., et al. (2018). "FISH studies in DLBCL: correlations with cell of origin: the Irish experience." J Clin Pathol 71: 947-948.

724 Low Total T-cell Content and Low PD1-Positive T-cells Identified by Multiplex Immunofluorescence is Associated with Poor Survival in Diffuse Large B-cell Lymphoma

Hany Meawad¹, Alex Herrera¹, Mary Nwangwu¹, Ting-Fang He¹, Victoria Bedell¹, Joyce Murata-Collins¹, Raju Pillai¹, Anamarija Perry², Dennis Weisenburger¹, Joo Song¹

¹City of Hope National Medical Center, Duarte, CA, ²University of Michigan, Ann Arbor, MI

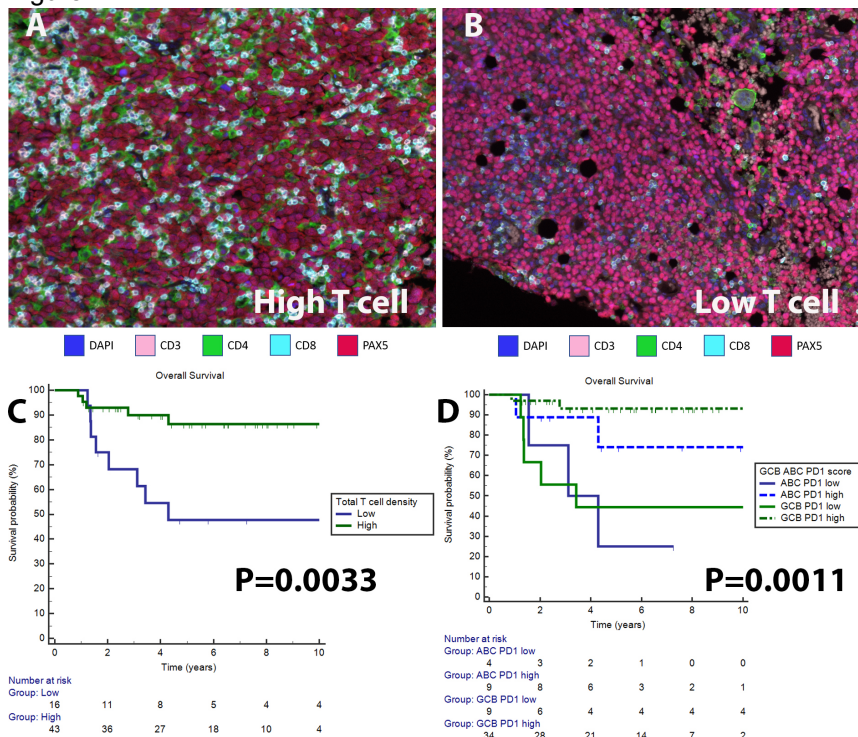
Disclosures: Hany Meawad: None; Alex Herrera: None; Mary Nwangwu: None; Ting-Fang He: None; Victoria Bedell: None; Joyce Murata-Collins: None; Raju Pillai: None; Anamarija Perry: None; Dennis Weisenburger: None; Joo Song: None

Background: Diffuse large B-cell lymphoma (DLBCL) is a heterogeneous disease with distinct biological and survival differences between the germinal center B-cell type (GCB) and activated B-cell phenotype (ABC) DLBCL. For DLBCL, the majority of the cell content is usually tumor cells and the microenvironment (TME) has not been well characterized in regards to prognosis. We sought out to determine whether the cell densities of the different populations correlated with survival.

Design: We identified 59 cases of de novo DLBCL that had ample material for TMA construction at two major cancer centers and who were treated with R-CHOP. Immunostaining (Hans algorithm, MYC, BCL2), and the Lymph2Cx assay (Nanostring) were performed to determine the cell of origin (COO). For multispectral immunofluorescence (mIF), staining was performed using the Opal 7 kit and two panels were used (1: CD3, CD8, CD4, PD1, PAX5, DAPI; 2: PAX5, CD163, CD79a, PD-L1, CD56, DAPI) and scanned on the Vectra spectral imaging system and analyzed using the InForm software. Logistic regression and survival analysis was performed using multiple parameters (nearest neighbor analysis, T cell subset densities, etc). Cutoffs were determined using ROC curves and groups were categorized as high or low. Mann-Whitney independent test and Kaplan Meier survival analysis was used to determine overall survival (OS).

Results: There were 43 cases (73%) that were GCB, 13 cases (22%) that were ABC, and 3 cases (5%) that were unclassified DLBCL. There were 5 cases that were double- and triple-hit lymphoma. The median for cell densities in all cases of DLBCL was: 17% for T cells, 51% for tumor B cells, 2% for histiocytes, 3% for CD8+ T cells, and 7% for PD1+ T-cells. Using logistic regression analysis, three immune cell subtypes in the TME were associated with poorer OS, which were 1) low total T-cell density by CD3 (Figure A and B), 2) low PD1-positive T-cell density (CD3+PD1+/total cells), and 3) low CD8+ PD1- T-cell density (CD3+CD8+PD1-/total cells) (cutoffs: 8%, 2.55%, and 7%, respectively). We did not see correlation with nearest neighbor analysis or histiocyte densities. The 5-year OS between low (16/59 cases) and high (43/59 cases) total T-cell density was 48% vs 86% (P=0.0033, Figure C), low (13/59 cases) vs high (46/59 cases) PD1-positive T-cell density was 39% vs 87% (P=0.0002), and low (44/59 cases) vs high (15/59 cases) CD8+ PD1- T-cell density was 67% vs 100% (P=0.03). Interestingly, we see these same survival differences with low and high densities based on COO (Figure D).

Figure 1 - 724



Conclusions: Performing mIF, we saw associations between the density of immune cells subsets and survival in DLBCL, particularly in regards to the total T-cells and T-cell subsets such as PD1 and CD8. We find that cases of DLBCL with low T-cell content, low PD1 T-cell density, and low CD8+ T-cells have a poor prognosis, irrespective of COO. Our findings suggest the TME may play an important prognostic role that merits further investigation.

725 Flow Cytometry Findings in Clonal Cytopenia and Undetermined Significance

Howard Meyerson¹, Khaled Alayed²

¹University Hospital Case Medical Center, Cleveland, OH, ²King Saud University, Case Western Reserve University, University Hospitals/Case Medical Center, Aurora, IL

Disclosures: Howard Meyerson: None; Khaled Alayed: None

Background: Clonal cytopenia of undetermined significance (CCUS) is a group of myeloid disorders in which somatic genetic aberrations are identified in patients with cytopenias lacking features diagnostic for myelodysplastic syndrome (MDS). We and others have published flow cytometric (FC) findings that correlate with MDS with high specificity and sensitivity. Here we examined FC abnormalities in CCUS.

Design: 83 CCUS cases were identified from 2017-2020 at UH Cleveland Medical Center. Ten flow cytometry parameters were assessed including granulocyte SSC, myeloblast percentage (Myb%), myeloblast CD45 expression (MybCD45), B cell progenitor percent (B%), CD177% expression, CD56 expression on granulocytes and monocytes, CD5 and CD56 expression on myeloid blasts and red cell CD71 expression. Our MDS diagnostic scheme (Meyerson Alayed scoring scheme or MASS) incorporating SSC, Myb%, MybCD45, B%, and CD177% was also determined (Alayed et. al. *AJCP* 2020). The results were compared to cytopenic controls (n=100) and MDS samples (n=100).

Results: Two or more FC abnormalities were noted in 37/83 (45%) CCUS cases, significantly more often than controls (16%), p<0.001. The most common abnormalities were a decrease in B% (51%), low CD177% (25%), abnormal MybCD45 (20%) and monocyte expression of CD56 (19%). A positive MASS score (> 1) was identified in 30% of cases. This frequency was less than that observed in low-grade MDS (85%) p<0.001, but more often than controls (9%) p<0.001. CCUS with variant allele fraction (VAF) > or =20% (CCUS>20%) showed >1 FC

abnormalities more frequently than CCUS with VAF<20% (CCUS<20%), 64% vs 24%, p<0.001 but less than low grade MDS (86%) p=0.007. Similarly a positive MASS score was observed more commonly in CCUS>20% than in CCUS<20%, 41% vs 17%, p=0.03 but less than low grade MDS (85%) p <0.001. The frequency of >1 FC abnormality or a positive MASS score in CCUS<20% was not statistically different from controls (MASS 17% vs ctrl 9%, p=0.14; >1 FC abnl 24% vs ctrl 16%, p= 0.24).

Conclusions: The data support the concept of CCUS with >20% VAF as a lesion with features intermediate between MDS and cytopenic controls.

726 SNP Microarray Characterization of Pure Erythroid Leukemia – A Study of Five Cases

Andres Mindiola Romero¹, Michael Johnston¹, Justin Giffin¹, Wahab Khan¹, Joel Lefferts¹, Eric Loo¹
¹Dartmouth-Hitchcock Medical Center, Lebanon, NH

Disclosures: Andres Mindiola Romero: None; Michael Johnston: None; Justin Giffin: None; Wahab Khan: None; Joel Lefferts: None; Eric Loo: None

Background: The revised 4th edition World Health Organization classification significantly altered the acute erythroid leukemia (AEL) category; integrating erythroleukemia into myelodysplastic syndromes, and leaving pure erythroid leukemia (PEL) as the sole type of AEL. PEL is a rare and highly aggressive form of acute leukemia, and the underlying genetic drivers of disease remain poorly characterized. Presently, no specific genetic drivers have been identified for PEL, though cases will frequently have *TP53* mutations and complex karyotypes. We assessed the utility of single nucleotide polymorphism (SNP) microarray in the evaluation of a series PEL cases at our institution.

Design: Institutional records from 2016-2020 were searched for cases meeting WHO criteria for PEL. Frozen nucleic acid samples from these bone marrow biopsies were analyzed using a Cytoscan™ HD Array (Affymetrix/Thermo Fisher, Santa Clara, CA), clinically validated for constitutional testing. CMA findings were correlated against previously acquired karyotype, FISH, and molecular sequencing results.

Results: Five cases of PEL were identified (2 male, 3 female, age range: 46-93 yrs). Overall survival ranged from 0.3 to 4.8 months (avg 1.9). Multiple and some otherwise undetected aberrancies were demonstrated by SNP array in all cases, including two cases with normal karyotype and one with a cell culture failure. SNP array demonstrated additional aberrancies in two cases with highly complex karyotypes. Four of the five cases appeared to show chromothripsis/instability of chromosome 19. Three of five cases showed recurrent losses in chromosome 12q. Only one of the five cases did not carry a *TP53* sequence alteration, and this case was found to have copy-neutral loss of heterozygosity (cnLOH) affecting one third of the distal end of chromosome 1p and nearly all of chromosome 11q. cnLOH of 11q was seen in one other case. Losses in chromosomes 4, 5q (proximal), 7p (*CDKN2A* locus), 7q, 11p, 12p, 16p, 17, and X, were also noted to occur twice in our case subset.

CASE #	AGE/S EX	CYTOGENETICS	CYTOSCAN	GENE VARIANTS
1	46, F	<ul style="list-style-type: none"> Karyotype failure No AML FISH 	arr[hg19] 3q25.33q29(160,098,157-197,737,818)x1,(4,12,16,17,18,X),5p15.33q35.1(355,018-171,525,805)x1,7p14.1q36.3(43,063,246-159,119,707)x1,9q21.11q34.3(70,984,704-140,716,973)x1,11p15.5q13.1(234,172-65,713,004)x1,11q13.1q25(65,823,243-134,938,470)x2 hmz,15q21.2q21.3(51,252,609-56,527,828)x1,15q22.2q22.31(61,947,693-64,147,050)x1,19p13.3(2,389,731-4,426,119)x1,19p13.3p13.11(6,107,003-17,816,422)x3,19p13.11q13.12(19,740,273-36,739,067)x1,20q11.22q13.12(32,781,558-43,480,170)x1,20q13.13q13.33(48,535,065-62,881,533)x1	<ul style="list-style-type: none"> TP53 p.L19 4H
2	74, M	<ul style="list-style-type: none"> 39-49,XY,+X,-Y,-2,-3,add(3)(p21),-4,-4,del(5)(q13q33),+7,add(7)(q22),-9,-10,add(10)(p11.2),add(11)(q11),+12,add(12)(q13)x2,-13,-15,add(15)(q24),-19,-21,+2-7r,+3-8mar[cp9]/46,XY[2] No AML FISH 	arr[hg19](1-22,XY)cx Complex array findings: multiple abnormalities involving chr4,5,7,9,12,19,21,Y	<ul style="list-style-type: none"> TP53 p.K13 2R TP53 c.376-1G>A
3	68, M	<ul style="list-style-type: none"> 46,XY[20] Normal AML FISH 	arr[GRCh37] 1p36.33p34.3(882803_36559621)x2 hmz,11q13.1q25(65140209_134942626)x2 hmz	<ul style="list-style-type: none"> NPM1 p.W28 8Cfs STAG 2

CASE #	AGE/S EX	CYTOGENETICS	CYTOSCAN	GENE VARIANTS
4	93, F	<ul style="list-style-type: none"> 46,XX[20] AML FISH: Three copies of ABL1 locus, Loss of PML locus. 	<p>arr[GRCh37] (7p)x1,(9)ct,(12q)x1,13q12.11(21514150_23135814)x1,16p13.3(85881_5542382)x1,(19)ct</p>	<p>p.Y89 3fs*2</p> <ul style="list-style-type: none"> TP53 p.R19 6* TP53 p.F27 0L
5	62, F	<ul style="list-style-type: none"> 43,X,del(X)(p22.2),der(3)t(3;15)(p11;q11.1)-11,-13,-15,add(19)(p13.3),+add(19)(p13.3),-22[14]/4 6,XX[1],nuc ish(RPN1x3,MECOMx3)[25/200],(RPN1x2,MECOMx3)[7/200],(DEK,NUP214)x2[200],(RUNX1T1x2,RUNX1x3)[10/200],(RUNX1T1x3,RUNX1x2)[5/200],(RUNX1T1x4,RUNX1x2)[9/200],(ABL1,BCR)x2[200],(KMT2Ax2)[200],(PM Lx3,RARAx2)[11/200],(CBFBx2)[200],(RARAx2)[200] AML FISH: Extra copies of loci involving RPN1/GATA2, MECOM, RUNX1, RUNX1T1, and PML. 	<p>arr[GRCh37] (Xp,3p,11p)x1,13q11q21.31(19436287_65002606)x1,(17p)x2 hmz,(19)ct</p>	<ul style="list-style-type: none"> TP53 p.V21 6M

Conclusions: DNA microarray can complement traditional cytogenetic testing in PEL, and may be particularly useful in cases with culture failure or for resolution of unusual or cryptic findings by karyotype or FISH. In future studies, microarray data may additionally provide more insight into disease pathogenesis.

727 Clinical, Immunophenotypic, and Genomic Analysis of Gamma Delta T-lymphoblastic Leukemia/Lymphoma

Michael Moravek¹, Juehua Gao¹, Yanming Zhang², Madina Sukhanova³, Qing Chen³, Yi-Hua Chen¹
¹Northwestern Memorial Hospital, Chicago, IL, ²Memorial Sloan Kettering Cancer Center, New York, NY, ³Northwestern University Feinberg School of Medicine, Chicago, IL

Disclosures: Michael Moravek: None; Juehua Gao: None; Yanming Zhang: None; Madina Sukhanova: None; Qing Chen: None; Yi-Hua Chen: None

Background: T-lymphoblastic leukemia/lymphoma (T-ALL) expressing TCR gd is rare, particularly in adults. These cases can pose diagnostic challenge in differentiating from other mature gd T-cell neoplasms. The molecular genetic features of gd T-ALL are not well understood.

Design: Database search of T-ALL cases diagnosed at our institution from 2008 to 2019 identified three cases of gamma delta T-ALL. The clinical features, morphologic findings, immunohistochemistry, flow cytometric analysis and cytogenetic studies were reviewed. Additional studies were performed including SNP microarray and next generation sequencing (NGS).

Results: As summarized in Table 1, our patients included 2 males and 1 female with ages at diagnosis of 32, 64 and 24 years. Two patients presented with blood and extensive bone marrow involvement while one patient presented as an anterior mediastinal mass with no blood and bone marrow involvement. Flow cytometric and immunohistochemical analysis demonstrated immature T-cell phenotype including diffusely CD99+ (3/3), TdT+ (2/3), partial CD1a+ (1/3), strong CD34+ (1/3), partial CD117+ (2/3). All three cases showed strong TCR gamma delta staining. In contrast to conventional T-ALL, all three gamma delta T-ALL expressed mature T-cell markers including surface CD3, CD2, CD5 and CD7 but were negative for both CD4 and CD8. One case showed aberrant expression of myeloid associated antigen CD13. Cytogenetic analysis revealed complex karyotype in 2 of 3 cases, and microarray analysis confirmed the complex genomic imbalanced profiles in these two cases including loss of chromosomes and deletion of regions with known tumor suppression genes, 9p/CDKN2A/B and 13q/RB, as well as T cell-related genes, CN-LOH of IRF4/DUSP22. In both cases, deletion of 5q, 9p, 16p were observed. NGS identified mutations in NOTCH1 or FBXW7, a negative regulator of NOTCH1, in two cases. The other case had a STAT3 mutation, another common oncogene commonly seen in T-cell neoplasms. Mutations involving other lymphoid and myeloid neoplasms were also identified including IKZF1, NRAS, BRAF (Table 1). The clinical outcome appeared variable. Two patients died within 18 months, one from T-ALL and another from mast cell sarcoma as a rare form of trans-differentiation of the T-ALL based on comparative genomic analysis. The other patient remained disease free 9 years after chemotherapy and stem cell transplant.

	Case 1	Case 2	Case 3
Age/Sex	32/M	24/F	64/M
CBC	Anemia, Thrombocytopenia, Leukocytosis, 81% Blasts	Normal HGB, Normal PLT, Normal WBC, No Blasts	Anemia, Thrombocytopenia, Leukocytosis, 80% Blasts
Biopsy	Bone marrow, 90% involvement	Mediastinal mass with sheets of blasts, bone marrow negative	Bone marrow, >95% involvement
Flow Cytometry	CD34-, dim CD117+, dim TdT+, partial dim CD1a bright surface CD3+, CD2+, CD5+, CD7+, CD10- CD4-, CD8-, alpha/beta-, gamma/delta+	CD34+, CD117-, TdT-, CD1a- surface CD3+, CD2+, CD5+, CD7+, CD10- CD4-, CD8-, alpha/beta-, gamma/delta+ CD13-, CD33-, HLA-DR-	CD34-, moderate CD117+, TdT- surface CD3+, CD2+, dim CD5+, dim CD7+, CD10- CD4-, CD8-, alpha/beta-, gamma/delta+ dim CD13+, CD33-, HLA-DR-
Immunohistochemistry	CD34 negative, CD117 negative, TdT positive, CD1a partial positive, CD99 positive, TCR gamma/delta positive	CD34 positive, CD117 partial positive, TdT partial positive, CD1a negative, CD99 positive, TCR gamma/delta positive	CD34 negative, CD117 partial positive, TdT negative, CD1a negative, CD99 positive, TCR gamma/delta positive
Cytogenetics	46,XY[20]	44,XX,del(1)(p32p36.3),t(2;4)(q37;q21),del(3)(q21q29),del(5)(q22q35),-7,del(9)(p13p24),add(15)(p11.2),inc[cp6]/ 46,XX[14]	46,XY,add(5)(q13),del(12)(p11.2p13)[11]/90,idemx2,-15,-16[8]/46,XY[1]
NGS	<i>BRAF</i> p.G464Val (53%) <i>ASXL1</i> p.Gln768* (44%) <i>RUNX1</i> p.Val164Argfs*12 (44%) <i>PHF6</i> p.Cys283Alafs*12 (87%) <i>BCOR</i> p.Leu279Pro (13%) <i>FBXW7</i> p.Arg505Cys (37%) <i>FBXW7</i> p.Val544Asp (51%) <i>CEBPA</i> p.Pro187_Pro189del (12%)	<i>STAT3</i> p.Pro695Leu (48%) <i>DNMT3A</i> p.Glu865Gly (51%) <i>DNMT3A</i> p.? (45%) <i>U2AF1</i> p.Ser34Tyr (39%) <i>IKZF1</i> p.Asp98Thrfs*20 (42%)	<i>NRAS</i> p.Gly12Ser (31%) <i>WT1</i> p.Arg385*69 (35%) <i>WT1</i> p.Val376Cysfs*14 (43%) <i>MAP2K1</i> p.Phe129Leu (21%) <i>NOTCH1</i> p.Ser2486_Ala2553del (41%) <i>NOTCH1</i> p.Tyr1532Cys (38%)
SNP-microarray	Focal deletion at 17q (NF1)	Losses: chromosomes 4, 11, 13 and 16, 5q (56Mb, <i>APC</i>), 9p (2.9Mb, <i>CDKN2A/B</i> , <i>IRF4/DUSP22</i>), 12p (18.4Mb, including <i>KRAS</i> , <i>CNKN1B</i> , and <i>ETV6</i> , focal deletion of <i>RB1</i> locus resulting in homozygous deletion of <i>RB1</i>) CN-LOH: terminal 6p (26Mb)	Losses: 1p (33.6Mb), 2p (22.2Mb, <i>REL</i>), 3q (whole arm), terminal 5q (88.1Mb, <i>APC</i>), proximal 7p (19Mb) and proximal 7q (63Mb), 9p (23.4Mb, homozygous deletion of <i>CNKN2A/B</i>), focal 9q (<i>GNAQ</i>), 16p (28Mb, <i>CREBBP</i>)
Follow-up	The patient subsequently developed mast cell sarcoma and died 18 months after their initial diagnosis of T-ALL.	The patient was treated with chemotherapy and bone marrow transplant and currently remains under observation 9 years after their initial diagnosis.	The patient was treated with treated with induction chemotherapy followed by re-induction and stem cell transplant. The patient died 7 months after their initial diagnosis.

Conclusions: Our study demonstrated that gamma delta T-ALL is a rare type of T-ALL with unique immunophenotypic features and complex genomic imbalanced profiles. Our cases showed mutations involving *NOTCH1* pathway, which is commonly altered in conventional T-ALL. However, the complex genomic imbalanced profiles involving T-cell related genes and deletion of tumor suppressor genes may provide alternative mechanisms contributing to the development of gamma delta T-ALL.

728 Overlapping Features of Primary Cutaneous Marginal Zone Lymphoma and Primary Cutaneous CD4+ Small/Medium T cell Lymphoproliferative Disorder: A Diagnostic Challenge

Ifeyinwa Obiorah¹, Laura Brown², Hao-Wei Wang³, Trinh Hoc-Tran Pham¹, Liqiang Xi¹, Mark Raffeld⁴, Stefania Pittaluga⁵, Elaine Jaffe¹

¹National Cancer Institute, National Institutes of Health, Bethesda, MD, ²University of California, San Francisco, San Francisco, CA, ³National Institutes of Health, Bethesda, MD, ⁴National Cancer Institute, Bethesda, MD, ⁵National Institutes of Health, Washington, DC

Disclosures: Ifeyinwa Obiorah: None; Laura Brown: None; Hao-Wei Wang: None; Trinh Hoc-Tran Pham: None; Liqiang Xi: None; Mark Raffeld: None; Stefania Pittaluga: None; Elaine Jaffe: None

Background: Primary cutaneous marginal zone lymphoma (PCMZL) and primary cutaneous CD4+ small/medium T cell lymphoproliferative disorder (CD4+ TLPD) are indolent lymphoproliferative disorders that occur predominantly in the dermis. The two entities can be differentiated based on the location, number of lesions and the immunophenotype of the tumor cells. In CD4+ TLPD, the lesions are usually solitary and occur primarily in the head and neck region with the neoplastic T cells positive for TFH markers. In contrast, multiple lesions are more frequent in PCMZL, usually presenting in the upper extremities and characterized by monotypic plasma cells. However,

there are cases that show overlapping features. We performed a comprehensive clinical, pathologic and molecular review to examine areas of potential diagnostic overlap.

Design: We identified 50 CD4+ TLPD and 34 PCMZL cases from our pathology archives. Comprehensive clinical and morphologic features were reviewed. Immunohistochemistry was performed for PD1, kappa, lambda, CD20, CD3, CD4, CD8 and MUM1. PCR for immunoglobulin (Ig) and T-cell receptor gamma (TRG) gene rearrangements was analyzed.

Results: CD4+ TLPD presented mostly (90%) as solitary lesions, located in the head and neck area (64%), mainly in adults (median age: 55.5 y [range, 4 to 85]). Cases of PCMZL presented in the upper extremity (53%), primarily in adults (median age: 49.5 y [range, 16 to 89]). Lesions were sometimes multiple (40%) and recurrences (26%) were more common. Cases of PCMZL had an increase in reactive CD3+ T cells, with frequent PD1 expression, whereas cases of CD4+ TLPD often contained abundant reactive B cells. Twenty three cases (Table 1) were identified as having overlapping features between PCMZL and CD4+ TLPD: 4 cases of PCMZL showed both B cell and T-cell gene rearrangement; 2 cases of PCMZL had TRG gene rearrangement and lambda light chain restricted plasma cells; 10 cases of CD4+ TLPD had both clonal B cell and clonal/oligoclonal T cell rearrangement; and 7 cases of CD4+ TLPD had either kappa or lambda light chain restricted plasma cells. Next generation sequencing studies are in progress.

Table 1. Patients with overlapping features of CD4+ TLPD and PCMZL

Case	Age (yr)	Sex	SITE	# of lesions	PD1 (%)	Light chain restriction	TCRG	IG	Diagnosis
1	78	M	UE	1	40	lambda	Clonal	IGH, IGK	PCMZL
2	69	F	Head	1	40	lambda	clonal	IGH, IGK	PCMZL
3	77	F	trunk	2	10	kappa	clonal	IGH, IGK	PCMZL
4	64	F	UE/buttock	2	10	kappa	Clonal	IGH	PCMZL
5	69	F	Trunk/UE	3	50	lambda	clonal	Polyclonal	PCMZL
6	55	F	leg	1	5	lambda	clonal	Polyclonal	PCMZL
7	79	M	Head	1	30	polytypic	clonal	IGH, IGK	CD4+ TLPD
8	79	M	UE	1	20	polytypic	clonal	IGH	CD4+ TLPD
9	71	M	UE/trunk	2	60	polytypic	clonal	IGH	CD4+ TLPD
10	85	M	Head	1	50	lambda	clonal	IGH, IGK	CD4+ TLPD
11	4	F	trunk	1	50	Kappa	clonal	IGH, IGK	CD4+ TLPD
12	52	M	Head	1	30	polytypic	clonal	IGH, IGK	CD4+ TLPD
13	40	M	Head	2	40	polytypic	clonal	IGH, IGK	CD4+ TLPD
14	34	M	trunk	1	50	kappa	clonal	IGH	CD4+ TLPD
15	64	M	Head	1	30	polytypic	clonal	IGH, IGK	CD4+ TLPD
16	55	M	Head	1	10	polytypic	oligoclonal	IGH	CD4+ TLPD
17	32	M	Head	1	70	lambda	clonal	indeterminate	CD4+ TLPD
18	65	M	Head	1	30	lambda	clonal	Polyclonal	CD4+ TLPD
19	61	M	Head	1	80	lambda	clonal	Polyclonal	CD4+ TLPD
20	63	M	UE	1	40	lambda	clonal	Polyclonal	CD4+ TLPD
21	62	M	Head	1	40	lambda	clonal	Polyclonal	CD4+ TLPD
22	19	F	UE	1	40	lambda	clonal	Polyclonal	CD4+ TLPD
23	72	M	Head	1	20	kappa	clonal	Polyclonal	CD4+ TLPD

Age, Age at diagnosis; Yr, year; M, male; F, female; #, number; UE, upper extremity; TRCG, T cell receptor gamma; IG, immunoglobulin; PCMZL, primary cutaneous marginal zone lymphoma; CD4+ TLPD, primary cutaneous CD4 positive small/medium T cell lymphoproliferative disorder

Conclusions: CD4+ TLPD and PCMZL frequently show overlapping histologic and immunophenotypic features. While differences in clinical presentation exist, both lesions are indolent. The concept of antigen driven atypical immune responses should be entertained, with conservative clinical management. Ongoing NGS studies may provide further insight.

729 Blood and Bone Marrow Abnormalities Frequent and Unexpected in GATA2 Mutation Positive “Asymptomatic” Relatives of Patients with GATA2 Deficiency

Ifeyinwa Obiorah¹, Weixin Wang², Amy Hsu³, Janine Daub², Joie Davis³, Cindy Palmer², Dennis Hickstein¹, Steven Holland⁴, Katherine Calvo⁴

¹National Cancer Institute, National Institutes of Health, Bethesda, MD, ²Clinical Center, National Institutes of Health, Bethesda, MD, ³National Institute of Allergy and Infectious Diseases, National Institutes of Health, Bethesda, MD, ⁴National Institutes of Health, Bethesda, MD

Disclosures: Ifeyinwa Obiorah: None; Weixin Wang: None; Amy Hsu: None; Janine Daub: None; Joie Davis: None; Cindy Palmer: None; Dennis Hickstein: None; Steven Holland: None; Katherine Calvo: None

Background: Germline mutations in *GATA2* can predispose to a constellation of clinical disease manifestations including immunodeficiency with susceptibility to nontuberculous mycobacterial infections, HPV, CMV, EBV, lymphedema, and myeloid neoplasms including myelodysplastic syndrome (MDS), acute myeloid leukemia (AML), and chronic myelomonocytic leukemia (CMML). Previous studies have reported asymptomatic *GATA2* mutation positive relatives of probands that demonstrate no (or minimal) disease

Design: We performed hematologic and bone marrow (BM) assessment of 26 *GATA2* mutation positive relatives of probands with *GATA2* deficiency, who were deemed “healthy” or had minimal disease.

Results: The median age was 53 years (range 7-81) with 14 males and 12 females. Eleven had abnormal CBC blood counts comprising leukopenia (3), anemia (3), monocytosis (3), monocytopenia (3), leukocytosis (2), neutropenia (2), thrombocytopenia (1), and lymphopenia (1). 3 patients had abnormal BM cytogenetics (monosomy 7 or trisomy 8). Eleven showed abnormalities in BM flow cytometry including absent precursor B-cells (6), monocytopenia (4), absent dendritic cells (3), monocytosis (1). Significant BM disease was identified in 12 (46%) patients including 5/26 (19%) hypocellular marrow (<30% cellularity), 2/26 with hypercellular marrow, 2/26 with monoclonal B cell lymphocytosis, 2/26 (8%) with CMML (one with monosomy 7), 1/26 (4%) with hypoplastic marrow with monosomy 7 normal peripheral blood counts, and 1/26 with increased blasts (10%) and trisomy 8 with normal blood counts with the exception of mild monocytopenia. 7 had clonal/abnormal T cell gene rearrangements and 2 had clonal B cell gene rearrangements. Four patients identified as high risk (ages 15, 17, 17, and 36) were treated with hematopoietic stem cell transplant.

Conclusions: Asymptomatic relatives of probands with germline *GATA2* mutations may harbor unrecognized myeloid neoplasms and be at imminent risk of transformation to high grade MDS, AML or CMML. Several patients in our study had normal or near normal peripheral blood counts and unexpected evolving myeloid neoplasms with monosomy 7, trisomy 8, or increased blasts in the marrow that were not easily classified based on current WHO criteria. These findings suggest that relatives of probands with *GATA2* deficiency should be tested for germline *GATA2* mutations and if positive should undergo regular monitoring with baseline bone marrow evaluation.

730 Upregulation of Germinal Center Markers by Extranodal Marginal Zone Lymphoma in Colonized Follicles, a Diagnostic Pitfall with Follicular Lymphoma

Julio Poveda¹, Daniel Cassidy², Yi Zhou³, Juan Alderuccio⁴, Izidore Lossos⁵, Francisco Vega⁶, Jennifer Chapman¹

¹University of Miami, Miller School of Medicine, Miami, FL, ²Jackson Memorial Hospital, Miami, FL, ³University of Miami, Miami, FL, ⁴University of Miami/Jackson Memorial Hospital, Miami, FL, ⁵University of Miami/Sylvester Cancer Center, FL, ⁶The University of Texas MD Anderson Cancer Center, Houston, TX

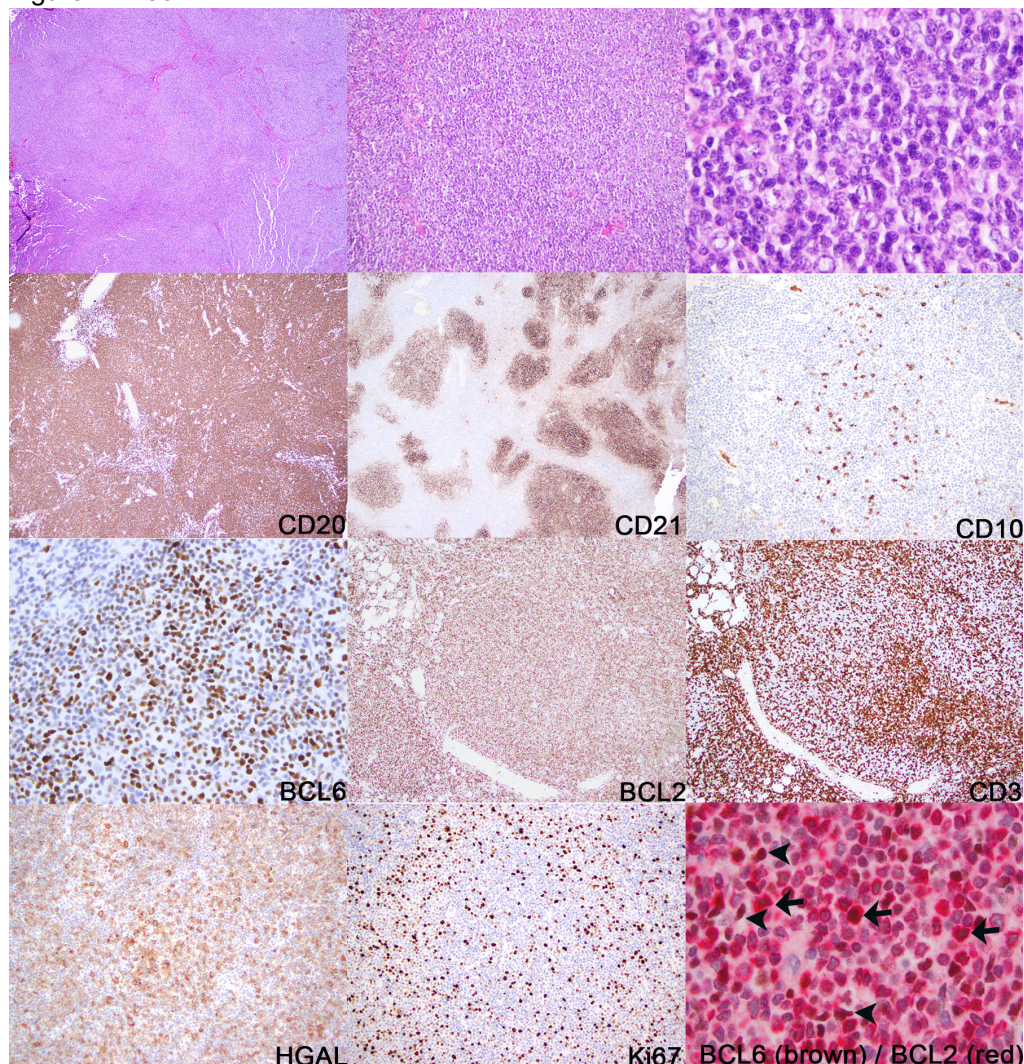
Disclosures: Julio Poveda: None; Juan Alderuccio: None; Izidore Lossos: None; Francisco Vega: *Speaker*, Society of Hematology Oncology; *Grant or Research Support*, CRISP Therapeutics; *Speaker*, i3Health; Jennifer Chapman: None

Background: Expression of BCL6, and other germinal center (GC) markers, is rarely reported in marginal zone lymphoma (MZL). When MZL cells express BCL6, particularly in GC foci, the histopathologic overlap with follicular lymphoma (FL) can be striking and lead to diagnostic errors.

Design: We reviewed 341 cases of MZL (47) or FL (294) to identify cases that were difficult to classify due to perceived focal coexpression of BCL6 and BCL2 by tumor cells in follicular foci. We developed dual BCL6/BCL2 immunohistochemistry (IHC) to assess coexpression in individual cells. Usual IHC and t(14;18) evaluation was performed in all cases.

Results: Seven of 341 cases (2%) were difficult to classify between MZL and FL due to suspected focal coexpression of BCL2 and BCL6 in follicular foci. Dual staining confirmed coexpression by tumor cells in 6 of 7 cases, all extranodal MZL (ENMZL) based on overall histopathologic features, and representing 13% of MZL in our series (Figure 1). All involved MALT sites, showed extensive follicular colonization, and were CD10 negative without *IgH-BCL2* rearrangement. MZL cells expressing BCL6 were restricted to follicular foci. HGAL (50%) and LMO2 (57%) expression was also seen, also restricted to follicular foci. In all MZL expressing BCL6, non-neoplastic GC B cells (GCBCs) in colonized follicles showed low/absent CD10 expression but preserved BCL6 and high ki67 proliferative rate.

Figure 1 - 730



Conclusions: We confirm that MZL cells have plasticity with regard to protein expression within the GC microenvironment, a diagnostic pitfall. In all MZL expressing BCL6, non-neoplastic GCBCs in colonized follicles showed downregulated CD10 expression, suggesting that GCBCs can alter CD10 expression when colonized by MZL, possibly due to NF- κ B pathway dysregulation. Features useful in differentiating these MZL from FL include: expression of GC markers was restricted to follicular foci, variable in intensity and not seen in all colonized follicles; in follicles colonized by BCL6/BCL2 positive MZL, BCL6 positive/BCL2 negative residual GCBCs are identifiable;

and all cases in our series were CD10 negative, warranting caution when considering a diagnosis of CD10 negative FL, particularly in MALT sites.

731 Leukemic ALK-negative ALCL is Characterized by Thrombocytopenia, Bone Marrow Involvement, CD7 Positivity, Complex Karyotype, and a Poor Prognosis

Lianqun Qiu¹, Mahsa Khanlari¹, Shaoying Li¹, Guilin Tang¹, C. Cameron Yin¹, Sa Wang¹, Swami Iyer¹, M. James You¹, Sergej Konoplev¹, Roberto Miranda¹, L. Jeffrey Medeiros¹, Jie Xu¹

¹The University of Texas MD Anderson Cancer Center, Houston, TX

Disclosures: Lianqun Qiu: None; Mahsa Khanlari: None; Shaoying Li: None; Guilin Tang: None; C. Cameron Yin: None; Sa Wang: None; Swami Iyer: None; M. James You: None; Sergej Konoplev: None; Roberto Miranda: None; L. Jeffrey Medeiros: None; Jie Xu: None

Background: Patients with anaplastic large cell lymphoma (ALCL) rarely develop leukemic disease. Leukemic ALCL cases reported in the literature are almost exclusively patients with ALK+ ALCL, most often associated with small cell variant, t(2;5)(p23;q35), and a poorer prognosis. Reports of leukemic ALK-negative ALCL cases are rare. In this study, we investigated the clinicopathologic and prognostic features of patients with leukemic ALK-negative ALCL. We also compared this cohort with their non-leukemic counterpart.

Design: Among 149 patients with systemic ALK-negative ALCL seen at our institution from 2007 through 2018, 42 patients had peripheral blood assessed by morphology and/or flow cytometric immunophenotypic analysis. Nine cases were found to have circulating lymphoma cells (leukemic disease). The clinical, pathologic, and outcome data were compared between patients with leukemic versus non-leukemic disease. Differences were evaluated using Fisher's exact test. Overall survival (OS) was analyzed using the Kaplan-Meier method and compared using the log-rank test.

Results: Comparing patients with leukemic versus non-leukemic ALK-negative ALCL, the former group more often had thrombocytopenia (60% vs 14%, $p = 0.048$) and bone marrow involvement (50% vs 15%, $p = 0.066$). There were no significant differences in other clinical features between the leukemic versus non-leukemic groups (all $p > 0.05$). Leukemic cases were more often positive for CD7 than non-leukemic cases (71% vs. 19%, $p = 0.02$). There were no significant differences between leukemic versus non-leukemic groups in the expression of other T cell antigens, cytotoxic markers, or Ki-67 proliferation index (all $p > 0.05$). Four of 6 (67%) leukemic patients had an abnormal karyotype, including 3 (50%) with complex karyotype. The treatment and response rate in patients with leukemic disease were similar to those with non-leukemic disease (all $p > 0.05$). After a median follow-up of 23 months (range, 0.3-140 months), 7 of 9 (78%) patients with leukemic disease died, and their OS was significantly shorter than patients with non-leukemic disease (median 15 months vs. 60 months, $p = 0.036$).

Conclusions: These data show that patients with leukemic ALK-negative ALCL have a greater frequency of thrombocytopenia, bone marrow involvement, CD7 positivity, a complex karyotype and poorer survival, suggesting that ALK-negative ALCL patients with a leukemic disease are candidates for more aggressive therapy.

732 Clinical and Genomic Findings of Myeloid Sarcoma with an Emphasis on NPM1 Mutations: A study from the Bone Marrow Pathology Group

Maximiliano Ramia de Cap¹, Leo Wu¹, German Pihan², Sanjay Patel³, Wayne Tam⁴, Carlos Bueso-Ramos⁵, Rashmi Kanagal-Shamanna⁵, Phil Raess⁶, Alexa Siddon⁷, Damodaran Narayanan⁸, Elizabeth Morgan⁸, Geraldine Pinkus⁸, Emily Mason⁹, Eric Hsi¹⁰, Heesun Rogers¹¹, Laura Toth¹², Kathryn Foucar¹², Stephanie Hurwitz¹³, Adam Bagg¹⁴, Anton Rets¹⁵, Tracy George¹⁶, Attilio Orazi¹⁷, Daniel Arber¹⁸, Robert Hasserjian¹⁹, Olga Weinberg²⁰

¹Beth Israel Deaconess Medical Center, Harvard Medical School, Boston, MA, ²Beth Israel Deaconess Medical Center, Boston, MA, ³Weill Cornell Medical College, New York, NY, ⁴Weill Cornell Medicine, New York, NY, ⁵The University of Texas MD Anderson Cancer Center, Houston, TX, ⁶Oregon Health & Science University, Portland, OR, ⁷Yale School of Medicine, New Haven, CT, ⁸Brigham and Women's Hospital, Boston, MA, ⁹Vanderbilt University Medical Center, Nashville, TN, ¹⁰Wake Forest Baptist Health, Winston-Salem, NC, ¹¹Cleveland Clinic, Cleveland, OH, ¹²University of New Mexico, Albuquerque, NM, ¹³Hospital of the University of Pennsylvania, Philadelphia, PA, ¹⁴University of Pennsylvania, Philadelphia, PA, ¹⁵ARUP Laboratories, University of Utah, Salt Lake City, UT, ¹⁶The University of Utah, Salt Lake City, UT, ¹⁷Texas Tech University Health Science Center, El Paso, TX, ¹⁸University of Chicago, Chicago, IL, ¹⁹Massachusetts General Hospital, Harvard Medical School, Boston, MA, ²⁰UTSouthwestern Medical Center, Dallas, TX

Disclosures: Maximiliano Ramia de Cap: None; Leo Wu: None; German Pihan: None; Sanjay Patel: None; Wayne Tam: None; Carlos Bueso-Ramos: None; Rashmi Kanagal-Shamanna: None; Phil Raess: None; Alexa Siddon: None; Damodaran Narayanan: None; Elizabeth Morgan: None; Geraldine Pinkus: None; Emily Mason: None; Eric Hsi: None; Heesun Rogers: None; Laura Toth: None; Kathryn Foucar: None; Stephanie Hurwitz: None; Adam Bagg: None; Anton Rets: None; Tracy George: None; Attilio Orazi: None; Daniel Arber: None; Robert Hasserjian: None; Olga Weinberg: None

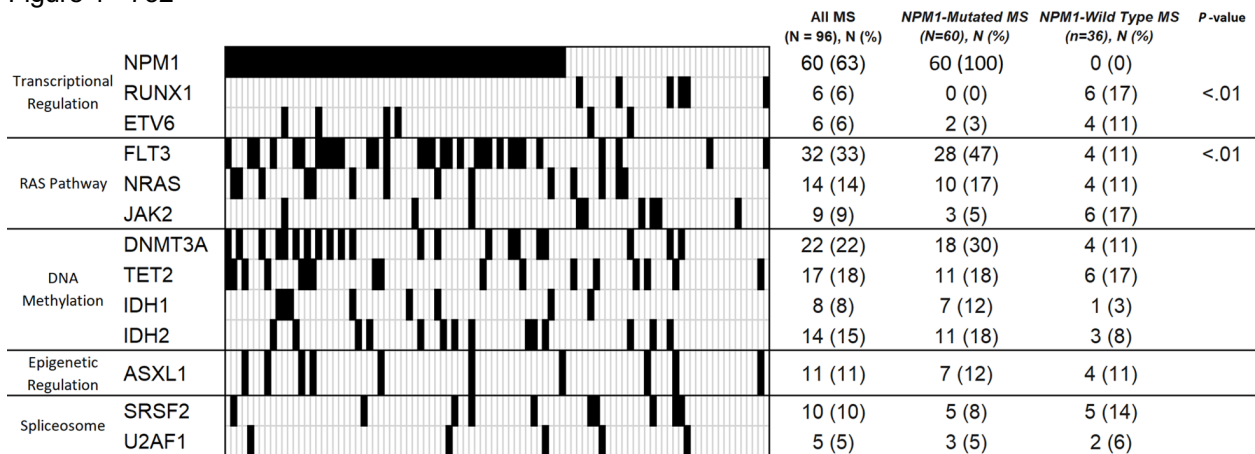
Background: The genetics and outcome of myeloid sarcoma (MS) are controversial when compared to de novo acute myeloid leukemia (AML) and chronic myeloid neoplasms of bone marrow (CMN). In a small series, *NPM1* mutations have been suggested to occur more frequently in MS and to correlate with worse outcome. This study aimed to determine the prognostic significance of genetic mutations in MS and to establish the prognostic significance of *NPM1*-mutated MS versus *NPM1*-mutated myeloid neoplasms involving the bone marrow.

Design: Ninety-six MS cases from nine medical centers were identified. Data pertaining to each patient's MS diagnosis, initial diagnostic bone marrow specimen and demographic information were extracted by medical record review. *NPM1*-mutated AML/CMN datasets were used for comparative analysis. Overall survival (OS) and event-free survival (EFS) were evaluated by multivariate Cox regression analysis.

Results: Patient demographics are listed in Table 1 and genetic mutations in Figure 1. MS without *NPM1* mutation occurred more frequently in men ($P=.01$). Compared to *NPM1*-wild type MS, *NPM1*-mutated MS had more frequent *RAS*-pathway (specifically *FLT3*, both $P<.01$) and less frequent *RUNX1* mutations ($P<.01$). Within the *NPM1*-mutated MS subgroup, worse OS correlated with presence of abnormal cytogenetics ($P<.01$) and concurrent AML in bone marrow ($P=.05$) but not presence of *FLT3* or *DNMT3A* mutations ($P>.05$). As compared to de novo *NPM1*-mutated AML, cases of *NPM1*-mutated MS were enriched in *ETV6* ($P<.01$), *ASXL1* ($P<.01$), *U2AF1* ($P=.02$) and *JAK2* ($P=.02$) mutations and had decreased number of *PTPN11* and *DNMT3A* (both $P<.01$) mutations. Additionally, *NPM1*-mutated MS predicted shorter OS in both normal and abnormal karyotype groups ($P=.05$ and $P<.01$, respectively) when compared to de novo *NPM1*-mutated AML. When compared to a group of *NPM1*-mutated CMN patients, cases of *NPM1*-mutated MS had more frequent *IDH2* ($P=.03$) and *FLT3* ($P<.01$) mutations and also correlated with worse OS ($P<.01$). Site specific *NPM1*-mutated MS in lymph node ($P=.01$) and skin ($P<.01$) correlated with worse OS when MS presented with concurrent AML. In the multivariable analysis of the entire MS group, both OS and EFS were adversely affected by older age (HR 1.03, $P=.03$; HR 1.02, $P=.02$), presence of cytogenetic abnormalities (HR 2.01, $P=.02$; HR 1.89, $P=.02$), *NRAS* mutation (HR 2.22, $P=.02$; HR 2.54, $P<.01$), underlying myeloid neoplasm of the bone marrow (OS; HR 3.42, $P=.05$) and *CBL* mutation (OS; HR 2.80, $P=.05$).

	All MS patients (N = 96)	<i>NPM1</i> -Mutated MS (N=60)	<i>NPM1</i> -Wild Type MS (n=36)	P-value
Patient characteristics				
Median age at MS diagnosis (range), y	63 (20-86)	62 (20-82)	62 (23-86)	
Male/female ratio	1.66	1.00	3.5	<.01
Clinical parameters				
Median WBC (range), ×10 ⁹ /L	7.15 (0.3-201)	7.0 (0.4-201)	7.9 (0.3-182)	
Median Platelet count (range), ×10 ⁹ /L	113 (5-1007)	107 (5-441)	110 (7-1007)	
Median Hgb concentration (range), g/dL	9.65 (5.6-15.3)	10.6 (5.8-15.3)	9.4 (5.6-15.2)	
Median BM blasts (range), %	20 (0-96)	40 (1-95)	8 (0-96)	.02
Abnormal cytogenetics, N (%)	51 (53)	24 (40)	28 (78)	<.01
Initial Bone Marrow Disease				
AML, N (%)	64 (66)	44 (73)	20 (56)	
NAMN, N (%)	17 (18)	8 (13)	9 (25)	
None (confirmed by biopsy), N (%)	15 (16)	8 (13)	7 (19)	
Site of MS				
Skin & Oropharyngeal Mucosa	45 (47)	34 (57)	11 (31)	
Lymph Node	17 (17)	8 (13)	9 (25)	
Bone & Soft Tissue	30 (31)	18 (30)	12 (40)	
Other	29 (30)	14 (23)	15 (42)	
Outcome, N (%)				
Alive at last follow-up	55 (57)	25 (42)	16 (44)	

Figure 1 - 732



Conclusions: We find that *NRAS* and *CBL* mutations were associated with adverse outcome in myeloid sarcoma patients. *NPM1*-mutated myeloid sarcoma occurs more frequently in the setting of concurrent marrow AML/CMN, but rarely in the absence of medullary disease. Our study suggests that presence of extramedullary disease in *NPM1*-mutated AML is associated with poorer outcome in a site-specific manner.

733 LEF1 Expression in Classic Hodgkin Lymphoma and Nodular Lymphocyte Predominant Hodgkin Lymphoma

Aishwarya Ravindran¹, Paul Kurtin¹, Andrew Feldman¹, Karen Rech¹, Ellen McPhail¹, Min Shi¹
¹Mayo Clinic, Rochester, MN

Disclosures: Aishwarya Ravindran: None; Paul Kurtin: None; Andrew Feldman: None; Karen Rech: None; Ellen McPhail: None; Min Shi: None

Background: Lymphoid enhancer binding factor (LEF1) is a crucial nuclear mediator of the wingless-type mouse mammary tumor virus integration site (WNT)/ β -catenin pathway. LEF1 is involved in early lymphocyte development and normally expressed in T-cells and pro-B cells, but absent in mature B-cells. Previous studies have shown LEF1 as a useful marker in diagnosis of non-Hodgkin lymphomas, particularly in low-grade B-cell lymphomas. Large scale studies for LEF1 expression in Hodgkin lymphomas are lacking. We aimed to study the LEF1 expression in Classic Hodgkin Lymphoma (CHL) and Nodular Lymphocyte Predominant Hodgkin Lymphoma (NLPHL).

Design: Using our institutional database, we screened pathology reports over the past 25 years. We selected cases with a diagnosis of CHL or NLPHL where adequate formalin-fixed paraffin-embedded tissue was available for ancillary studies. LEF1 expression was evaluated by an immunohistochemical study. LEF1 nuclear expression was graded as negative (0), weak (1+), intermediate (2+) or strong (3+), with percentage of LEF1-positive neoplastic cells recorded. β -catenin expression was also assessed by immunohistochemistry in all cases. LEF1 and β -catenin expression was considered as positive if at least 20% tumor cells showed staining.

Results: A total of 72 cases were included in the study. Of these 72 cases, 47 were CHL and 25 NLPHL. Overall, 96% (n=45) of CHL showed LEF1 expression compared to 64% (n=16) of NLPHL in at least >20% of tumor cells (P value <0.001). The sensitivity and specificity of LEF1 expression in CHL were 96% and 36%, respectively. Further, more than two-thirds of positive CHL cases (68%, n=32) showed LEF1 expression in >75% Hodgkin cells, compared to 12% (n=3) of NLPHL cases, regardless of the expression intensity. All LEF1-positive cases in our series were negative for nuclear β -catenin expression.

Conclusions: Our study showed a vast majority of CHL cases expressed LEF1. LEF1 immunostain could be used as an additional marker in immunophenotyping of CHL versus NLPHL. Although LEF1 is a coactivator of Wnt/ β -catenin pathway, the absence of β -catenin expression in all cases further suggests that LEF1 overexpression is independent of the Wnt/ β -catenin signaling pathway.

734 CD164 as an Adjunct Marker for Circulating Abnormal T Cells in Mycosis Fungoides and Sézary Syndrome

Beth Rawson¹, Danielle Maracaja², Shashi Mehta³
¹Yale New Haven Hospital, New Haven, CT, ²Wake Forest School of Medicine, Winston-Salem, NC, ³Rutgers University, Newark, NJ

Disclosures: Beth Rawson: None; Danielle Maracaja: None; Shashi Mehta: None

Background: Mycosis fungoides (MF) and Sézary syndrome (SS) are together the most common forms of cutaneous T-cell lymphomas (CTCL). Flow cytometry (FC) is a useful tool in diagnosing and staging these conditions that usually share a common mature CD4+ immunophenotype. There is no specific marker for the diagnosis of MF/SS, and the criteria include the identification of abnormal populations of T-cells with loss of CD7 and/or CD26.

Design: We prospectively collected data for 100 consecutive samples received between May and July 2019 for routine FC testing due to clinical suspicion or confirmed diagnosis of T-cell lymphoproliferative disease (T-LPD). A normal control group (NC) consisted of 135 specimens selected from samples submitted for routine CBC analysis within the same time frame. Forty-eight patients were classified within the MF/SS group (32 patients with MF and 16 patients with SS), with diagnosis established based on information collected through review of the pathology results and electronic medical record. Thirty-five patients were classified with other T-LPD, and 12 patients were classified as inflammatory skin conditions (ISC). Five patients were excluded due to the diagnosis of B-cell lymphoma or issues affecting sample viability. The BD Multitest 6-color TBNK assay was utilized to evaluate and

enumerate T cells using CD45, CD3, CD4, CD8, CD16/56 and CD19. The samples were then evaluated in a 6-color two-tube assay for CD3, CD4, CD7, CD26, CD45, and CD164. The FC was interpreted by two pathologists with consideration of the patient's history and ancillary testing.

Results: In our cohort of 48 cases classified as MF/SS, 14 patients showed circulating abnormal CD3+CD4+ T-cell populations, mainly characterized by loss of CD26 (n= 13), followed by loss of CD7 (n=10), and gain of CD164 (n=7). One patient in the MF/SS group showed CD3+ CD4+ CD164+ T cells with normal expression of CD7 and CD26. In the T-LPD group, only one patient showed CD164+ T cells. No abnormal circulating T cells were detected in the ISC group. CD164 was not positive on T cells from patients in the ISC or NC groups. The presence of CD164 showed a specificity of 97.5% for the diagnosis of circulating Sézary cells.

Conclusions: The abnormal expression of CD164 on CD4+ T cells showed high specificity in the diagnosis of CTCLs when compared to other T-LPD and ISC. CD164 can be used as an adjunct marker in detecting the presence of circulating abnormal T cells in MF/SS.

735 Overexpression of Histone Deacetylase 6 (HDAC6) Impedes the Survival of Acute Myeloid Leukemia (AML) in Older Patients in Association with K-Ras Effector Molecules

Hassan Rizwan¹, Ariz Akhter¹, Hamza Kamran¹, Meer-Taher Shabani-Rad², Adnan Mansoor¹

¹University of Calgary, Calgary, Canada, ²Cumming School of Medicine, University of Calgary, Calgary, Canada

Disclosures: Hassan Rizwan: None; Ariz Akhter: None; Hamza Kamran: None; Meer-Taher Shabani-Rad: None; Adnan Mansoor: None

Background: Acute myeloid leukemia in older patients (>=60 years) (AML) is a distinct entity with a dismal prognosis due to genomic heterogeneity / epigenetic derangements and treatment toxicities. Indolent novel targeted therapies, specifically epigenetic modulators are providing positive promises for these patients. As targeting a single layer of epigenetic deregulation is insufficient, additional studies are required to expand this repertoire. Histone deacetylase 6 (HDAC6) plays a role in oncogenesis by regulating gene expression through chromatin remodeling. HDAC6 has been implicated in AML pathogenesis by conferring resistance to apoptosis in cell lines. HDAC6 is also considered a viable candidate for targeted therapy in solid tumors as well as in leukemia. Furthermore, HDAC6 hyperactivity is associated with the upregulation of K-Ras effector molecules including SOX9 and BMP2. Inhibition of HDAC6 impede KRAS⁺ colorectal cancer growth but not in hematogenous leukemias/AML, indicating a synergistic interaction between K-RAS signaling and histone regulation. The aim of our study was to investigate the correlative expression of HDAC6 in AML with other oncogenic pathway molecules. This data will help future research in developing targeted therapies for treating AML in older patients.

Design: Diagnostic FFPE RNA in a series of AML patients (n=100) were screened for major oncogenic pathway molecules (n=760) utilizing nCounter (NanoString Technologies) platform. Patients were categorized as older (> 60 yrs. n=34), adult (between 18-60 yrs. n=32) and pediatric (< 18- yrs. n=34). Gene Set Enrichment Analysis (GSEA) was performed for further correlation utilizing public data sets. Standard statistical criteria (fold-change > 2.0, p < 0.05, q < 0.1) were applied engaging Qlucore Omics Explorer (v3.6) and SPSS (v-26.0) software.

Results: Receiver operating characteristic (ROC) curve analysis identified HDAC6 as a gene of interest in older AML cohort with optimal cutoff (AUC: 0.79, sensitivity: 0.72, specificity: 0.78, p-value: 0.012) (Figure 1A). The study cohort was dichotomized as overexpression (20/34; 59%) and underexpression (14/34, 41%). High HDAC6 expression exerted poor OS compared to low expression (Log-rank = 0.004) (Figure 1B). No survival associations were noted for HDAC6 with other age cohorts. The gene expression profile analysis detected the overexpression of K-Ras signaling genes (SOX9 & BMP2) alongside HDAC6 in the older AML cohort (Figures 1C – 1E).

Figure 1 - 735

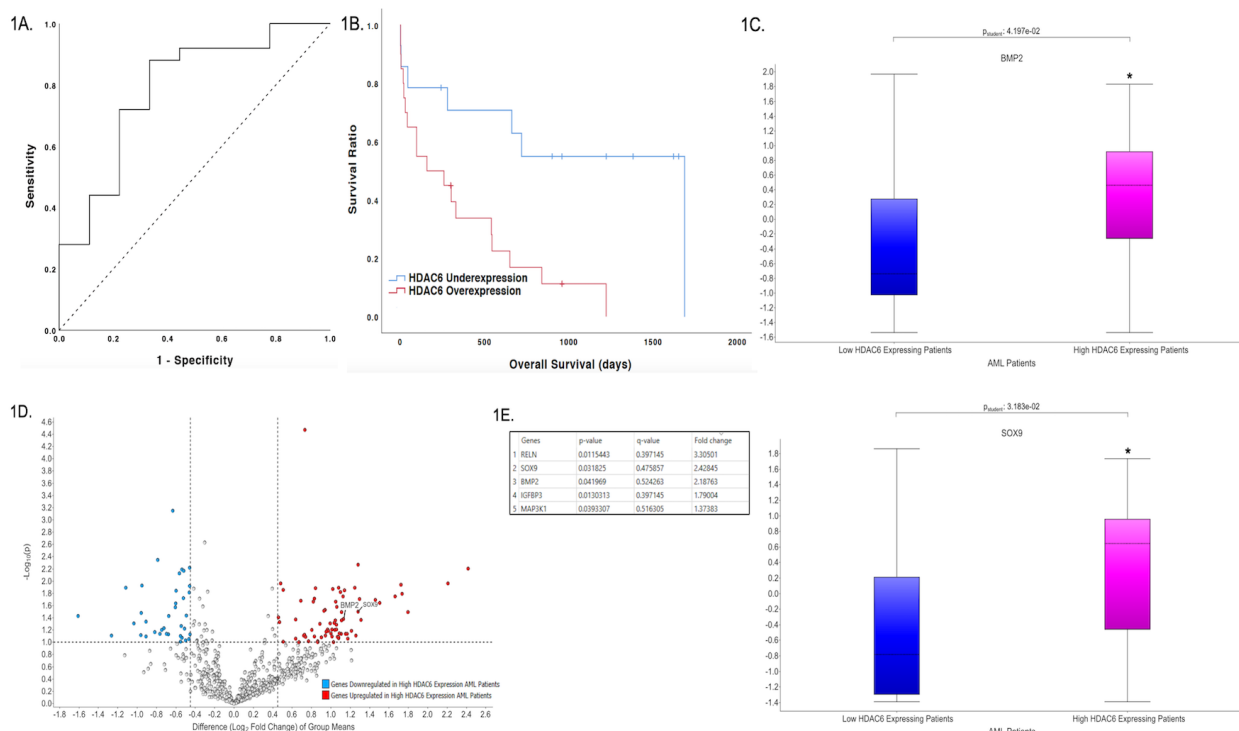


Figure 1A. Receiver Operating Curve (ROC) for predicting the impact of HDAC6 overexpression on elderly AML patient survival outcomes (optimal cut-off HDAC6 expression = 172.625, p = 0.012). 1B. Kaplan-Meier curve depicting the disparities of elderly AML patient survival likelihoods through differential HDAC6 expression (Log rank p = 0.004). 1C. Box and whisker plots illustrating comparisons of log expression of key KRAS pathway genes between the two groups. (* = p < 0.05, q < 0.05, fold change > 2). 1D. A volcano plot illustrating the genes that are upregulated or downregulated in AML patients above the age of 60 with high HDAC6 expression compared to AML patients over 60 years of age with low HDAC6 expression. 1E. Table detailing the statistical data for KRAS pathway genes revealing the most significant variation.

Conclusions: Our pilot study has identified that HDAC6 is differentially expressed in older AML patients impacting disease prognosis and OS. HDAC6 activity is also associated with hyperactivity of K-RAS effector proteins (SOX9 and BMP2). These results reinforce the development and utilization of targeted therapies for managing AML in older patients.

736 Algorithmic Approach for the Diagnosis of T- Lymphoblastic Leukemia/Lymphoma by Flow Cytometry

Krasimira Rozenova¹, Dragan Jevremovic¹, Kaaren Reichard¹, Phuong Nguyen¹, Pedro Horna¹, Horatiu Olteanu¹, Min Shi¹

¹Mayo Clinic, Rochester, MN

Disclosures: Krasimira Rozenova: None; Dragan Jevremovic: None; Kaaren Reichard: None; Phuong Nguyen: None; Pedro Horna: None; Horatiu Olteanu: None; Min Shi: None

Background: Multiparametric flow cytometry plays an essential role in diagnosing T-lymphoblastic leukemia/lymphoma (T-ALL). Given the lack of surface CD3 by the majority of T-ALLs, expression of cytoplasmic CD3 (cCD3) must be established. However, cCD3 detection by flow cytometry requires additional processing and may be technically and interpretationally challenging, rendering it impractical for T-ALL screening. Since CD2 and CD7 are expressed on the surface of T cells throughout maturation, we aim to investigate whether CD2/CD7 can be used as screening markers to identify the subset of acute leukemias for which a diagnosis of T-ALL is likely and warrants subsequent testing for cCD3.

Design: We retrospectively reviewed flow cytometry immunophenotyping of 234 acute leukemias, and analyzed the relationship between CD2 and CD7 expression with cCD3 expression in each case. To avoid selection bias, we prospectively studied 233 consecutive acute leukemias for which cCD3, CD2 and CD7 were simultaneously incorporated into antibody panels.

Results: The 234 retrospective acute leukemias are displayed in Fig.1A. We found that all 38 T-ALLs had uniformly strong cCD3, while 7 T/myeloid cases showed partial cCD3 expression. Interestingly, all acute leukemias expressing cCD3 had uniform expression ($\geq 75\%$) of CD2 and/or CD7. The remaining 189 cases did not have cCD3, while a subset (11%, 20/189) showed uniform expression of CD2 or CD7 (Fig.2A). These findings indicate that uniform expression ($\geq 75\%$) of CD2 and/or CD7 has 100% sensitivity and 89% specificity for the diagnosis of acute leukemia with T-lineage differentiation.

We then incorporated cCD3, CD2 and CD7 simultaneously into the routine flow cytometric assessment of 233 consecutive acute leukemias (Fig.1B). Similar to the retrospective cohort, all T-ALL and T/myeloid cases had cCD3 and uniform expression of CD2 and/or CD7. 12% of cCD3 negative cases showed uniform expression of CD2 or CD7 (Fig.2B). The sensitivity and specificity of uniform expression of CD2 and/or CD7 for the diagnosis of T-lineage acute leukemia was 100% and 88%, respectively.

Figure 1 - 736

Fig.1. Acute leukemia cases in retrospective (A) and prospective (B) studies

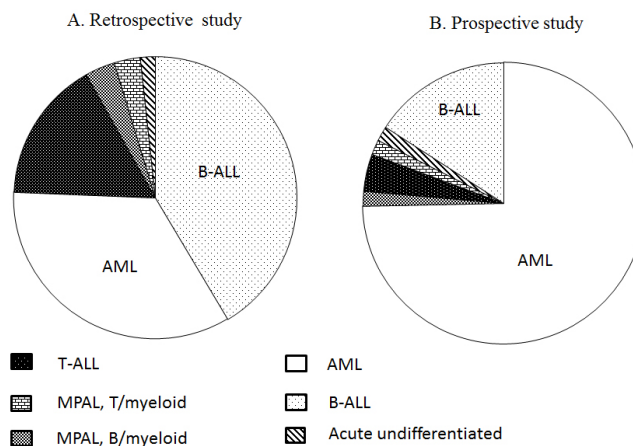
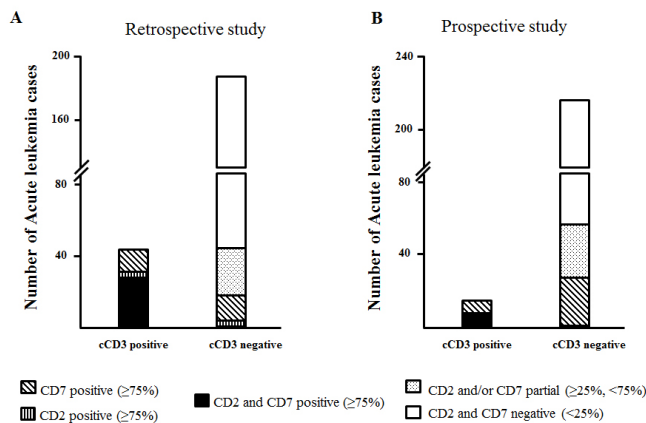


Figure 2 - 736

Fig.2. Expression of cell surface markers CD2 and CD7 on cCD3-positive and cCD3-negative acute leukemia cases in retrospective (A) and prospective (B) studies



Conclusions: Our retrospective and prospective studies both demonstrated that uniform expression of CD2 and/or CD7 was 100% sensitive for the diagnosis of T-ALL. Hereby, we propose a sensitive and cost-effective flow

cytometry algorithmic approach in which CD2 and CD7 serve as screening markers for subsequent cCD3 testing to establish the diagnosis of T-ALL.

737 Usefulness of the MYC Tricolor Break Apart Probe for the Detection of MYC Rearrangement in Aggressive B-Cell Lymphomas

Marta Salido¹, Maria Rodriguez-Rivera², Anna Puiggros³, Melero Carme¹, Xavier Calvo³, Leonor Arenillas³, Ana Ferrer¹, Ivonne Vazquez¹, Blanca Espinet³, Luis Colomo¹

¹Hospital del Mar, Barcelona, Spain, ²Hospital del Mar-Parc de Salut Mar-IMIM, ³IMIM-Hospital del Mar, Barcelona, Spain

Disclosures: Marta Salido: None; Maria Rodriguez-Rivera: None; Anna Puiggros: None; Melero Carme: None; Xavier Calvo: None; Blanca Espinet: None; Luis Colomo: None

Background: Background. *MYC* gene rearrangements (rMYC) are present in 6-15% of diffuse large B-cell lymphomas (DLBCL), high-grade B lymphomas and in 80-100% of Burkitt's lymphomas. FISH using break-apart probes (BAP) has been widely used to characterize rearrangement as a routine method. However, it has been reported recently that FISH BAP assays lack the ability to detect a proportion of *MYC* locus rearrangements (5-10%) due to the variability in breakpoint location and/or limitation of BAPs design, some of them with narrow gap sizes.

Design: Design. The aim of our study is to evaluate the usefulness of a new tricolor *MYC* BAP (Metasystems), and to characterize the *MYC* breakpoint (proximal or distal) in a series of patients with known rMYC. A series of 26 previously identified rMYC high-grade B lymphomas diagnosed between 2018 and 2020 are selected. In addition, a patient with a dendritic follicular cell sarcoma and *MYC* amplification is included (Table 1). All cases have been previously studied with the *MYC* BAP and *MYC/IGH/CEP8* double fusion probes (Abbott Molecular). The BAP probe used for diagnosis flanks the *MYC* gene and marks the proximal region with a Spectrum Orange and the distal region with Spectrum Green fluorochromes. The tri-color probe design (Metasystems) adds a third probe labeled in Spectrum Aqua that includes *MYC* gene (Figure 1). This design allows the identification of rMYC and to differentiate location of breakpoint: proximal (5') or distal to the *MYC* gene (3'). In cases with distal *MYC* rearrangement, *IGK* and *IGL* BAP (Metasystems) have also been studied. The immunohistochemical study included the usual panel of B and T markers, including LMO2 (clone 1A9-1) and *myc* (clone Y6) (Ventana-Roche). The cut-off values for both markers are 30 and 40%, respectively.

Results: Clinicopathological characteristics of the series are shown in table1. In all rearranged cases (n=26) the tricolor probe confirmed the presence of rMYC. In 20 cases (77%), breakage of the Spectrum Aqua probe (containing *MYC*) is observed and 12 (60%) of them presented a *MYC-IGH* rearrangement. In 3 cases, proximal rearrangements are identified (5' *MYC* break); all 3 had *MYC-IGH* rearrangement. Three cases have a distal rearrangement (3' *MYC* break) with different partners: *IGH*, *IGK* and non-*IG*. No association between different location of breakpoints and the partners *IG* vs. no-*IG* has been observed (p> 0.05); 7 out of 13 double or triple hit lymphomas had a non-*IG* partner, while all (n=7) DLBCL presented *MYC-IGH* rearrangement (p = 0.02). No statistical association has been observed between the location of *MYC* breakpoint and the diagnostic categories. The tricolor probe allows the identification of *MYC* amplification in follicular dendritic cell sarcoma sample.

Age at diagnosis	67 (35-92)
Male gender	18 (66.6%)
Extranodal location*	17 (63%)
Histological diagnosis	
DLBCL	7
High grade lymphoma, NOS	2
High grade lymphoma <i>MYC</i> + <i>BCL2/BCL6</i> +	13
<i>Burkitt</i> lymphoma	3
Mantle cell lymphoma	1
Follicular dendritic cell sarcoma	1
<i>MYC</i> rearrangement (FISH)	
<i>MYC-IGH</i>	16/26 (62%)
<i>MYC</i> tricolor probe patterns	

5' MYC proximal	3 (11.5%)
3' MYC distal	3 (11.5%)
MYC included	20 (77%)
MYC amplification	1
Immunohistochemistry (IHC)	
MYC positive	24/27 (89%)
LMO2 negative	21/24 (88%)
Other FISH markers	
BCL2 rearranged	13/24 (54%)
BCL6 rearranged	5/24 (21%)
TP53 deleted	6/14 (42%)

Figure 1 - 737

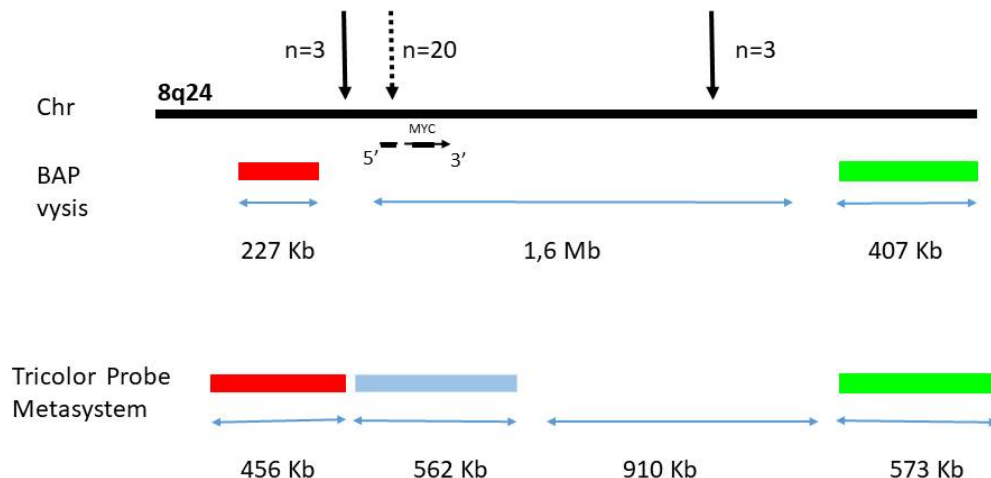


Figure 1. Scheme of the probes used in the study

Conclusions: The tri-color BAP is useful for detecting rMYCs. In our series, most of the rMYC cases presented breakpoints that include or are close to MYC. The tricolor FISH probe design does not allow inferring the partner of translocation (IG vs. no-IG).

738 Ultra-Rapid Reporting of TP53 Mutation in Myeloid Neoplasms by Using Next Generation Sequencing

Wen Shuai¹, Wei Chen¹, Kristen Floyd¹, Mark Routbort¹, Francis San Lucas¹, Rashmi Kanagal-Shamanna¹, Zhuang Zuo¹, Sanam Loghavi¹, Chi Young Ok¹, C. Cameron Yin¹, Rajyalakshmi Luthra¹, L. Jeffrey Medeiros¹, Keyur Patel¹

¹The University of Texas MD Anderson Cancer Center, Houston, TX

Disclosures: Wen Shuai: None; Wei Chen: None; Kristen Floyd: None; Mark Routbort: None; Francis San Lucas: None; Rashmi Kanagal-Shamanna: None; Zhuang Zuo: None; Sanam Loghavi: None; Chi Young Ok: None; C. Cameron Yin: None; Rajyalakshmi Luthra: None; L. Jeffrey Medeiros: None; Keyur Patel: None

Background: TP53 mutation status and burden are extremely important in the diagnosis, prognosis, and treatment selection of myeloid neoplasms. In myelodysplastic syndromes (MDS), TP53 mutations are associated with aggressive disease, predict shorter survival, confer increased risk of leukemic transformation and predict an inferior response to lenalidomide. TP53 mutations are more frequent in acute myeloid leukemia (AML) with myelodysplasia-related changes and therapy-related myeloid neoplasms than in de novo AML or MDS. Based on

these data, *TP53* mutation analysis has been incorporated into clinical practice guidelines for patients with myeloid neoplasms. However, timely availability of results for clinical decision-making remains a challenge. We describe an innovative next generation sequencing (NGS)-based approach to report *TP53* mutations in a clinical setting within 48 hours from sample collection facilitating timely diagnosis, prognostication and predictive utility.

Design: To facilitate fast reporting of NGS results, we developed an Ultra-rapid Reporting of GENomic Targets (URGENTseq) method as previously described (J Mol Diagn 21:89, 2019), which allows us to report actionable mutations as early as 48 hours from sample collection. To validate URGENTseq for *TP53*, we compared URGENTseq NGS versus conventional NGS results for 3,261 samples across 395 NGS analysis runs on a MiSeq instrument. The concordance between these methods was determined by comparing the calls and variant allelic frequency (VAF) at the variant call format (vcf) file level. VAF cut-off for comparison was set at 5%. Minimum coverage was 250x for conventional NGS and 125x for the URGENTseq NGS platform.

Results: A total of 457 *TP53* mutations were detected in 3,261 samples (vcf files) using conventional NGS analysis. URGENTseq NGS analysis of the same cohort showed 452 *TP53* mutations (vcf files) and 456 mutations by a combined vcf+manual review resulting in 98.9% and 99.8% concordance, respectively with the conventional NGS platform. Five (5/457, 1.1%) false-negative *TP53* mutation results were primarily due to a combination of differences in the coverage, low VAF and position of the mutation towards the end of the target region. There was a 100% concordance for all negative *TP53* calls between two NGS platforms.

Conclusions: These data indicate that *TP53* mutation status can be reported within 48 hours of sample collection in a clinical setting with a high degree of accuracy using the URGENTseq NGS platform. Timely availability of *TP53* mutation status supports the diagnostic workup as well as clinical decision making for patients with a range of myeloid neoplasms.

739 Therapeutic Monoclonal Antibody (t-mAb) Effect on the Interpretation of Serum Protein Electrophoresis (SPE) and Immunofixation (IF) in Patients with Plasma Cell Myeloma (PCM)

Amrit Singh¹, Daisy Alapat¹, Hoda Hagrass²

¹University of Arkansas for Medical Sciences, Little Rock, AR, ²University of Arkansas for Medical Science, Little Rock, AR

Disclosures: Amrit Singh: None; Daisy Alapat: None; Hoda Hagrass: None

Background: According to the International Myeloma Working Group consensus criteria for diagnosing and monitoring patients with myeloma related diseases, SPE and IF are critical tests. False-positive results induced by t-mAbs in PCM patients can be problematic as the contemporary guidelines define the complete remission (CR) criteria as non-detectable M-protein by SPE or IF.

The purpose of this study is to investigate the effect of four t-mAb: daratumumab, denosumab, elotuzumab and obinutuzumab on the interpretation of SPE and IF in PCM patients receiving t-mAb.

Design: Our pharmacy informatics group provided us with the list of patients with PCM, at the University of Arkansas for Medical Sciences Myeloma center, taking t-mAb from 10/1/2018 – 11/1/2019. Out of the 260 patients on t-mAb (183 patients on daratumumab, 69 patients on denosumab, 4 patients elotuzumab and 4 patients on obinutuzumab) 57 patients on daratumumab and denosumab were randomly selected, along with all eight patients who were on elotuzumab and obinutuzumab. Detection of t-mAbs and their migration patterns were assessed in these 65 patients by retrospective review of SPE/IF gels ordered during the course of therapy over the 13-month period. SPE and IF were performed using the Helena laboratories V8 Nexus capillary analyzer and Helena laboratories immunofixation system (Beaumont, TX, USA), respectively.

Of the 65 patients analyzed (Table-1), IF could distinguish between t-mAb and original M-protein in 46 patients (70.8%). SPE could distinguish between t-mAb and M-protein in 16 patients only (24.6%). The ability to distinguish t-mAb one SPE or IF was highest for daratumumab (77.8%) followed by denosumab (66.7%), elotuzumab (75.0%) and obinutuzumab (25.0%). Therapeutic mAb was undetected by either method in six patients (9.2%).

Results: We detected characteristic migration patterns by standard SPE/IF: daratumumab has a cathodal migration (far gamma region, **black arrows**) (**Fig. 1**), while elotuzumab and denosumab are more anodal in the γ -globulin region (mid gamma region, **blue arrows**) (**Fig. 2**).

Monoclonal Antibody (t-mAb)	Number of patients receiving therapy	Number of patients with t-mAb distinguished on IF or SPE	Number of patients with t-mAb distinguished on IF	Number of patients with t-mAb distinguished on SPE	Number of patients with t-mAb not distinguished on IF or SPE	Number of patients with undetected t-mAb
Daratumumab	36 (55.4%)	28 (77.8%)	28 (77.8%)	14 (38.9%)	8 (22.2%)	0 (0%)
Denosumab	21 (32.3%)	14 (66.7%)	14 (66.7%)	2 (9.5%)	5 (23.8%)	2 (9.5%)
Elotuzumab	4 (6.2%)	3 (75.0%)	3 (75.0%)	0 (0%)	0 (0%)	1 (25.0%)
Obinutuzumab	4 (6.2%)	1 (25.0%)	1 (25.0%)	0 (0%)	0 (0%)	3 (75.0%)
Total	65 (100%)	46 (70.8%)	46 (70.8%)	16 (24.6%)	13 (20.0%)	6 (9.2%)

Figure 1 - 739

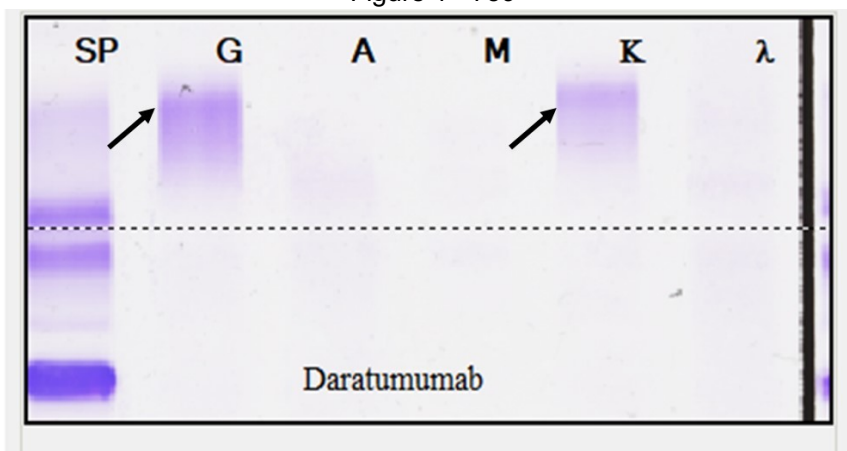
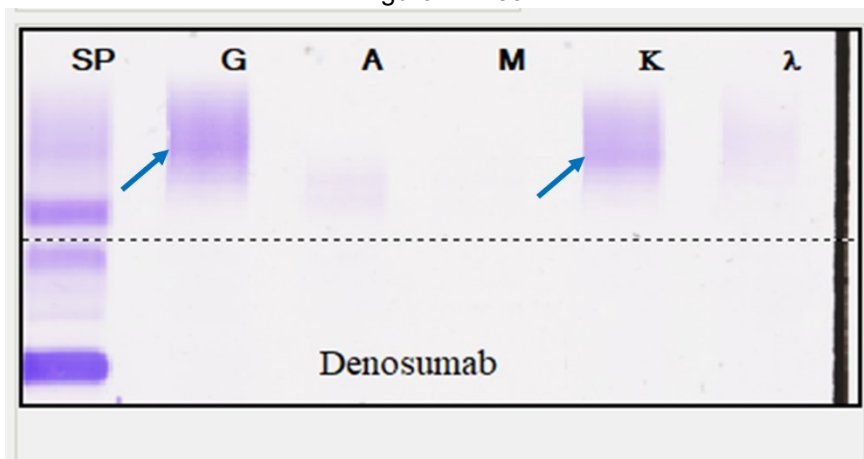


Figure 2 - 739



Conclusions: The growing list and increasing use of t-mAb poses a problem for clinical pathologists and oncologists with interpreting SPE and IF results for patients with PCM. The t-mAb artifact is detected in nearly all patients undergoing treatment which affects the interpretation of SPE/IF results and subsequently can impact monitoring of the patients with PCM. Therefore, clinical pathologists should be familiar with the position of commonly prescribed t-mAb at their institutions. Also, the oncologists should be aware of the potential false-positive

results. IF is more sensitive than SPE to distinguish t-mAb from M-protein. Care must be exercised to follow the patients on monoclonal antibody therapy with IF and SPE, and not SPE alone.

740 Utility of LEF1 and CD200 in a Single Tube Flow Cytometric Analysis in the Diagnosis of Chronic Lymphocytic Leukemia (CLL) with Atypical Immunophenotype

Kevin Song¹, Aaron Victor¹, Washington Lim¹, Serhan Alkan², Sumire Kitahara¹

¹Cedars-Sinai Medical Center, Los Angeles, CA, ²Cedars-Sinai Medical Center, Beverly Hills, CA

Disclosures: Kevin Song: None; Aaron Victor: None; Washington Lim: None; Serhan Alkan: None; Sumire Kitahara: None

Background: Studies have demonstrated the utility of CD200 and LEF1 separately in differentiating CLL from other B-cell lymphoproliferative disorders (B-LPD). In this study, we utilize flow cytometry immunophenotyping (FCI) to combine both markers in a single tube panel to evaluate cases of typical CLL (tCLL), CLL with atypical immunophenotype (aCLL) and mantle cell lymphoma (MCL). We describe its performance characteristics and an approach to support a diagnosis of CLL in cases showing atypical features.

Design: A single tube analysis with CD45 KO/CD19 ECD/CD5 PC7/CD200 A750/LEF1 PE (intranuclear permeabilization) was performed on cases of CD5+ clonal B-LPD that were identified on routine FCI of blood, bone marrow or tissue. tCLL cases were defined by expression of CD23, dim CD20, dim or negative CD22 and dim or negative surface light chain by FCI, with or without supporting evidence for the absence of BCL1 translocation by FISH or BCL1 immunostain negativity. Cases of aCLL lacked one or more of the aforementioned FCI features. MCL diagnoses were confirmed by FISH analysis for BCL1 translocation. The median fluorescent intensity (MFI) of CD200 and LEF1 in the CD19+/CD5+ and internal negative control populations were evaluated. For CD200 and LEF1, CD5+ T-cells and CD19-/CD5- NK cells served as the negative controls, respectively. Statistics were calculated as a simple percentage, average ± SEM, or by student's T-test, as appropriate.

Results: 65 cases, including 27 tCLL, 32 aCLL (of which 21 are CD23-/dim) and 6 MCL were analyzed. CD200 and LEF1 were more frequently expressed in tCLL (89% and 74%) than in aCLL (84% and 47%) and MCL (0% and 0%). All aCLL cases with LEF1 expression also expressed CD200 (15/32, 47%). Among these, 10/21 CD23-/dim aCLL cases expressed both LEF1 and CD200 (48%). Co-expression was observed more frequently in tCLL cases (18/27, 67%). aCLL had higher CD200 expression than MCL (16.2±2.0 vs 4.8±0.9, p=0.02). Similarly, expression of LEF1 was higher in aCLL than MCL (25.6±3.2 vs 9.5±2.3, p=0.04). By normalizing MFI to internal controls, p values decreased for CD200 (0.01) and LEF1 (0.03) comparisons between aCLL and MCL.

Figure 1 - 740

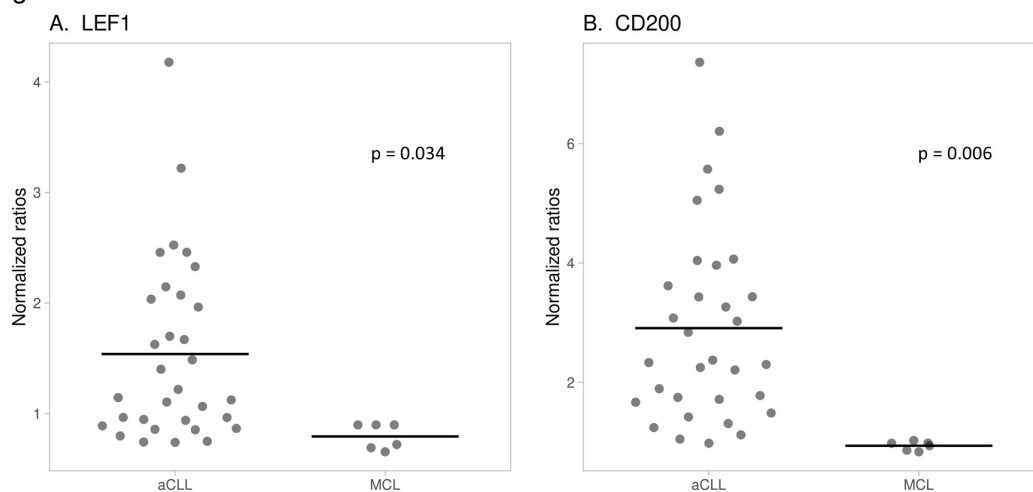


Figure 1. Normalized ratios of LEF1 and CD200 expression in aCLL and MCL. MFI corresponding to either LEF1 or CD200 was determined and normalized to internal negative controls, CD5-/CD19- NK cells for LEF1 and CD5+ T-cells for CD200, for each case. (A) Comparison of normalized LEF1 expression in aCLL and MCL cases. (B) Comparison of normalized CD200 expression aCLL and MCL cases.

Conclusions: FCI assessment of both LEF1 and CD200 in a single tube is feasible to perform. These markers may support a diagnosis of CLL in cases with an atypical immunophenotype, particularly in cases lacking CD23, when MCL is the major differential diagnosis.

741 Diagnostic Utility of FISH in CSF for Leukemia and Lymphoma

Jasmine Steele¹, Robert Willim², Phillip Michaels²

¹Beth Israel Deaconess Medical Center, Boston, MA, ²Beth Israel Deaconess Medical Center, Harvard Medical School, Boston, MA

Disclosures: Jasmine Steele: None; Robert Willim: None; Phillip Michaels: None

Background: Cerebrospinal fluid (CSF) involvement is found in 5-50% of hematologic malignancies and its presence may alter therapy, thus reliable identification of malignant cells is important. While cytomorphology (CM) is the “gold standard” for detection of hematologic malignancies within CSF, flow cytometric analysis (FCA) is widely used and may show greater sensitivity than CM review. However, there are no guidelines for the use of FCA in CSF. In this study, we aim to show that fluorescence in situ hybridization (FISH) may be used as another reliable modality for testing in CSF in comparison to FCA.

Design: A retrospective review was conducted on CSF samples sent for FCA at Beth Israel Deaconess Medical Center, Boston, MA between 1/1/2015 and 8/7/2020. FCA results were classified as diagnostic or non-diagnostic. If FCA was diagnostic, then further stratification was performed in which it was positive or negative for leukemia/lymphoma. CM interpretation was resulted as negative, suspicious or positive. FISH results were classified as negative or positive. Statistical analyses were performed with SPSS 27.0 (IBM, Armonk, NY).

Results: A total of 1038 CSF samples were submitted for FCA and 311 CSF samples had concurrent FISH studies. FCA was cancelled on 125 samples and FISH was undetermined in 12. When FCA results were compared to FISH in the remaining 174 specimens, the 134 non-diagnostic specimens were often negative by FISH (OR = 4.55, p-value <0.001). When restricted to the 40 diagnostic FCA samples, 16 were positive by FCA and FISH, however, and interestingly, 4 were negative by FCA but positive by FISH. Of the remaining 20 diagnostic FCA samples, 4 were positive by FCA and negative by FISH while 16 were negative by both modalities. Importantly, of the 43 samples that were positive by FISH and had concurrent FCA, 23 were non-diagnostic by FCA.

Figure 1 – 741

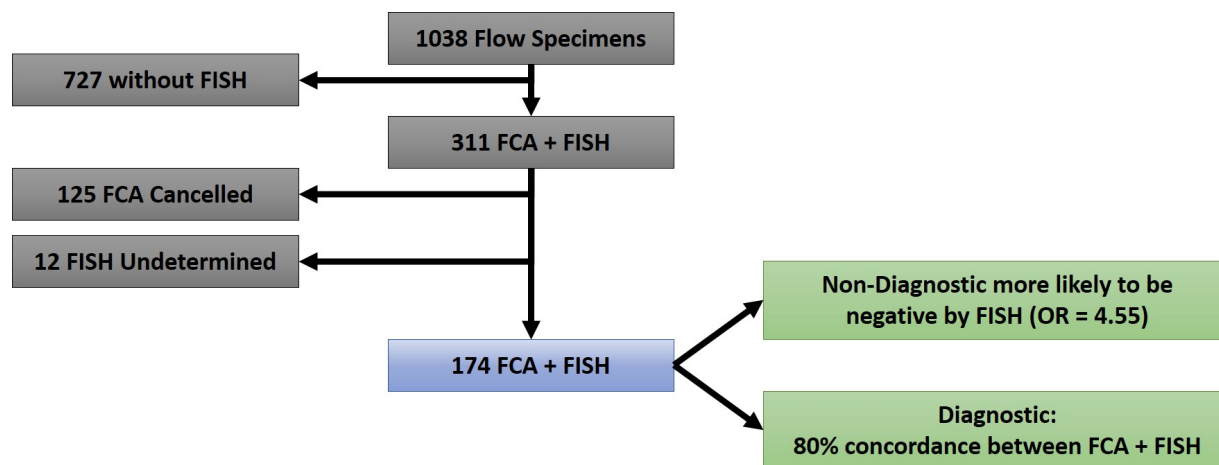
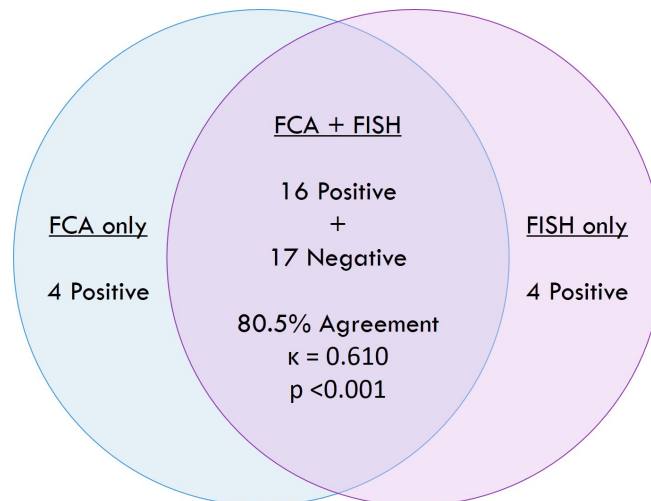


Figure 2 – 741



Conclusions: In this study, we demonstrated that FISH is a reliable and sensitive test for detection of leukemia/lymphoma in CSF in comparison to FCA. Our results demonstrated a high level of concordance among FCA and FISH when FCA was considered diagnostic. When FCA was considered non-diagnostic, FISH was able to detect a neoplastic population in 23 cases, thus underscoring the diagnostic utility of FISH in those circumstances. This analysis highlights that FISH is a sensitive ancillary technique for detecting leukemia/lymphoma in CSF where FCA may be limited in detecting clonal neoplastic populations.

742 Clinical and Immunophenotypic Characterization of Reactive $\gamma\delta$ T-cell Expansions

Hamza Tariq¹, Zubair Ilyas¹, Kristy Wolniak², Yi-Hua Chen³

¹Feinberg School of Medicine/Northwestern University, Chicago, IL, ²Northwestern University, Evanston, IL, ³Northwestern Memorial Hospital, Chicago, IL

Disclosures: Hamza Tariq: None; Zubair Ilyas: None; Kristy Wolniak: None; Yi-Hua Chen: None

Background: The $\gamma\delta$ T-cells comprise a minor population (0.5-5%) of T cells in the peripheral blood in normal subjects and play important roles in tumor and microbial surveillance, epithelial maintenance, and modulation of immune response. Malignancies arising from $\gamma\delta$ T-cells are relatively well-characterized and often aggressive. However, reactive expansions of $\gamma\delta$ T-cells are less well understood and may cause diagnostic confusion

Design: A total of 97 patients with a discrete $\gamma\delta$ T-cell population >15% of total T-cells identified by flow cytometry in the peripheral blood or bone marrow from 2001-2015 were identified in our database. Of those, 19 patients fulfilled the WHO criteria for $\gamma\delta$ -T-cell leukemia/lymphoma and were excluded from the study. The remaining 78 patients (25 blood and 53 bone marrow samples) were evaluated including the associated underlying clinical conditions, CBC/differential and the results of flow cytometric immunophenotyping including expressions of T-cell antigens, NK-cell antigens, cytotoxic markers and KIRs. The clinical follow-up was also reviewed.

Results: The age of the patients ranged from 20-83 years (median: 60 years). Absolute lymphocytosis (> 4.0 k/uL) at the time of flow cytometric analysis was present in 9/78 (11.5%) patients. The percentage and absolute count of $\gamma\delta$ T-cells ranged from 10 to 63% (mean 27.2%) and 8.6 to 2954/uL (mean 301/uL), respectively. The associated underlying medical conditions included various B- and T- cell lymphomas, myeloid neoplasms, autoimmune/inflammatory disorders, infections, post-transplant states and others (Table 1). As shown in Figures 1 and 2, $\gamma\delta$ T-cells were CD4-CD8- in most cases (63/78; 80.7%) and CD4-/partial CD8+ in a subset of cases (15/78; 19.3%). Brighter CD3 staining was seen in 63/78 (80.7%) cases, and lack of CD5 expression in 21/78 (26.9%) cases. Cytotoxic proteins were variably expressed, and no KIR restriction was seen. Review of clinical follow-up (6 months to 13 years; average 6 years) showed that no significant further expansion of $\gamma\delta$ T-cell population in 7 of 7 patients who had repeat analysis, and none of the 78 patients developed $\gamma\delta$ T-cell neoplasms.

Table 1: The underlying medical conditions associated with reactive $\gamma\delta$ -T-cell expansion

Underlying hematologic neoplasm (n=56)	Autoimmune/inflammatory disease (n=18)	Infections (n=6)	Transplant (n=18)	Miscellaneous conditions (n=8)
B-cell lymphoma-37 (CLL-13, FL-10, DLBCL-5, LPL-4, MZL-2, PTLD-DLBCL-3)	Idiopathic thrombocytopenia purpura – 4	HIV with CMV – 2	Hematopoietic stem cell transplant - 12	Sickle cell disease – 1
Plasma cell neoplasm-4 (MM-3, MGUS-1)	Systemic lupus erythematosus – 3	Invasive aspergillosis in the setting of chemotherapy for AML – 1	Solid organ transplant - 6	Cyclic neutropenia – 1
T-cell lymphomas-3 (CTCL-2, CLPD-NK-1)	Sarcoidosis – 2	Disseminated VZV in the setting of iatrogenic immunosuppression post-transplant – 1		Possible iatrogenic neutropenia – 3
Acute Leukemia-9 (AML-5, B-ALL-4)	Rheumatoid arthritis – 1	Active hepatitis C – 1		Gout – 1
Myeloproliferative neoplasm-3 (PMF-1, PV-1, CML- 1)	Autoimmune neutropenia – 1	Infectious mononucleosis - 1		Iron deficiency anemia – 1
	Focal segmental glomerulosclerosis – 2			Allergic rhinitis – 1
	Hashimoto thyroiditis – 1			
	Scleroderma – 1			
	Relapsing polychondritis – 1			
	Pernicious anemia – 1			
	Type 1 Diabetes - 1			

Figure 1 - 742

T/NK-cell markers	Expression in $\gamma\delta$ T-cells	Percentage of positive $\gamma\delta$ T-cells
CD3	Brighter than $\alpha\beta$ T-cells	63/78 (80.7%)
	Same intensity as $\alpha\beta$ T-cells	15/78 (19.3%)
CD2	Positive	78/78 (100%)
CD5	Positive	57/78 (73.1%)
	Negative	21/78 (26.9%)
CD7	Positive	68/78 (87.2%)
	Dim/partial positive	10/78 (12.8%)
CD4/CD8	CD4-/CD8-	63/78 (80.7%)
	CD4-/partial CD8+	15/78 (19.3%)
CD56	Partial positive	48/74(64.8%)
	Negative	26/74 (35.2%)
CD16	Partial positive	8/38 (21.0%)
	Negative	30/38 (79.0%)
CD57	Partial positive	15/58 (25.8%)
	Negative	43/58 (74.2%)
TIA-1	Partial positive	11/11 (100%),
Granzyme B	Partial positive	7/11 (64%)
Perforin	Partial positive	6/11 (55%)
CD158 (a, b, e)	No restricted expression	12/12 (100%)

Figure 2 - 742

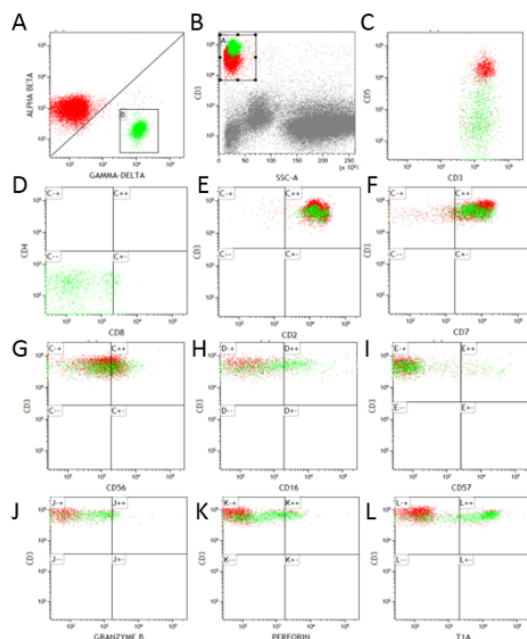


Figure 2. A representative patient with reactive expansion of $\gamma\delta$ T-cell population without development of $\gamma\delta$ T-cell neoplasm after long-term follow-up. Flow cytometric analysis showed a discrete $\gamma\delta$ T-cell population (A). These $\gamma\delta$ T-cells (green) were brighter CD3+ than $\alpha\beta$ T cells (red, B), CD5- (C), CD4- and partial dim CD8+ (D), CD2+ (E), CD7+ (F), dim CD56+ (G), dim CD16+ (H), predominantly CD57- (I), and positive for cytotoxic proteins, granzyme B, perforin and TIA-1 (J, K, L)

Conclusions: Our study demonstrated that reactive expansion of $\gamma\delta$ T-cells in the peripheral blood and bone marrow can be seen in a variety of clinical conditions with no progression to $\gamma\delta$ T-cell neoplasms based on the long-term follow-up. The $\gamma\delta$ T cells exhibit a unique immunophenotype. Lack of CD5 expression is relatively common in $\gamma\delta$ T cells and does not necessarily indicate immunophenotypic aberrancy as studies have shown a subset of normal $\gamma\delta$ T cells do not express CD5. Recognition of the wide spectrum of clinical conditions associated with reactive expansion of $\gamma\delta$ T-cells and their unique phenotype is important in interpretation of flow cytometric analysis.

743 De Novo and Therapy-Related Pure Erythroid Leukemia Harbor Distinct TP53 Genetic Alterations

Mehrnoosh Tashakori¹, Wei Wang¹, Sa Wang¹, Rashmi Kanagal-Shamanna¹, Sanam Loghavi¹, L. Jeffrey Medeiros¹, Kadia Tapan¹, Naval Daver¹, Farhad Ravandi-Kashani¹, Joseph Khoury¹
¹The University of Texas MD Anderson Cancer Center, Houston, TX

Disclosures: Mehrnoosh Tashakori: None; Wei Wang: None; Sa Wang: None; Rashmi Kanagal-Shamanna: None; Sanam Loghavi: None; L. Jeffrey Medeiros: None; Joseph Khoury: None

Background: Pure erythroid leukemia (PEL) is a rare leukemia with a dismal prognosis. *TP53* mutations are known to be integral to the pathogenesis of PEL, but the differential characteristics of *TP53* genetic alterations in *de novo* PEL versus therapy-related PEL (t-PEL) are not known.

Design: We identified all cases of PEL with *TP53* mutations seen at our institution. Clinical and laboratory data were obtained from the electronic medical records. Mutation analysis was performed using next-generation sequencing (Illumina Inc., San Diego, California). Loss of heterozygosity (LOH) was determined by fluorescence *in situ* hybridization (FISH) using a probe set specific for the *TP53* gene locus.

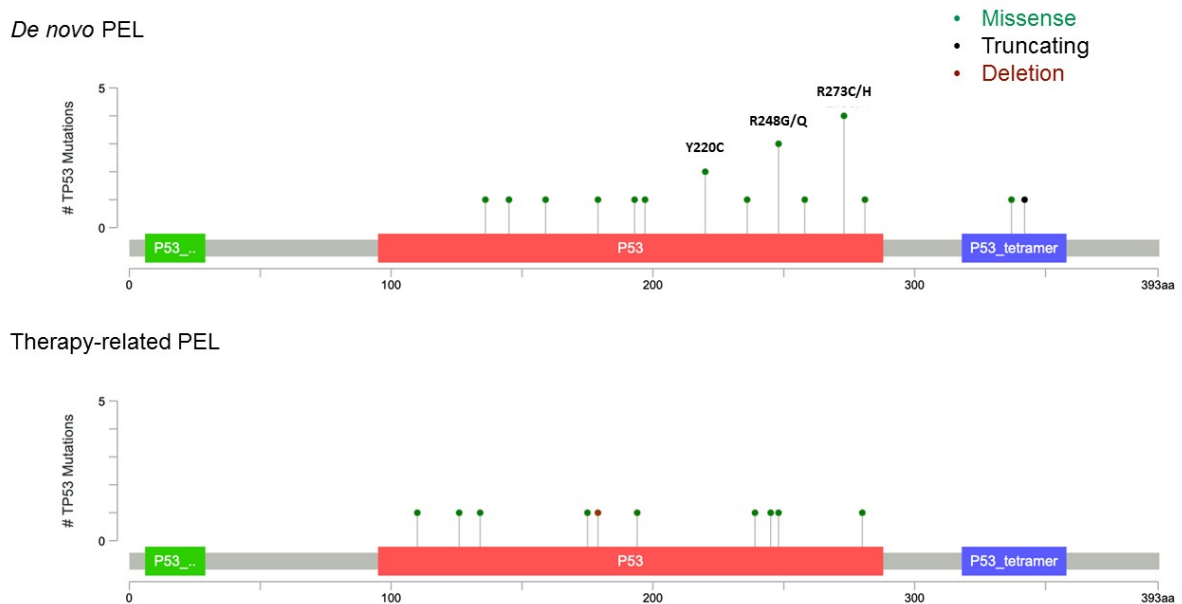
Results: The study group included 16 (66.7%) patients with *de novo* PEL and 8 (33.3%) with t-PEL. Both groups had comparable clinical findings and overall survival (Table 1). All cases had a complex karyotype and myelodysplasia-related cytogenetic abnormalities, most frequently involving chromosomes 5 and 7. Monosomy 17 or del(17p) were more common in t-PEL compared to *de novo* PEL (66.7% vs 26.6%). *TP53* mutation was present in the dominant clone in all cases. In *de novo* PEL, 10 (62.5%) cases had 1 *TP53* mutation and 6 (37.5%) had 2 *TP53* mutations. In t-PEL, 7 (87.5%) cases had 1 *TP53* mutation and 1 (12.5%) had 3 mutations. Most (~90%) mutations were missense in both groups. In the *de novo* PEL group, 2 cases had splice site mutations, and both also had a missense mutation. In the t-PEL group, 1 case had deletion mutation. In the *de novo* PEL group, 56.2% had hotspot mutations, whereas in the t-PEL group only 2 cases had hotspot mutations. Notably, the latter 2 patients had a clinical predisposition to *TP53* mutations: one had a germline *BRCA1* mutation and R175H mutation in exon 5; the other was HIV+ and had a R248W mutation in exon 7, a commonly involved exon in HIV+ patients. None of the t-PEL cases had hotspot *TP53* mutations (Figure 1). Of note, LOH was common in t-PEL, possibly due to selection pressure, and was less frequent in *de novo* PEL, perhaps due to the dominant negative effect of hotspot mutations.

Variable	<i>de novo</i> PEL (n=16) n (%) [range]	t-PEL (n=8) n (%) [range]
Age (years)	68 [37-87]	65 [51-70]
Male	10 (62.5%)	4 (50%)
Hb	8.7 [6.5-12.1]	8 [7.4-8.5]
WBC (x10 ⁹ /L)	3.7 [0.3-7.6]	2.4 [0.2-6.1]
Plt (x10 ⁹ /L)	34 [2-92]	15.6 [6-26]
LDH	1377 [391-4872]	1745 [335-9039]
Complex karyotype	15 (100%)*	6 (100%)**
MDS CG	15 (100%)*	6 (100%)**
del 5/del 5q	14 (93.3%)*	5 (83.3%)**
del 7/del 7q	8 (57%)*	3 (50%)**
del 17/del 17p	4 (26.6%)*	4 (66.7%)**
survival (mo)	4.5 [0.7-14.3]	4.6 [1.7-7.3]
Co-mutations (VAF)	3 cases: <i>DNMT3A</i> L798P (n/a) <i>DNMT3A</i> R882H (10.3) <i>ASXL1</i> G646fs* (30.5)	3 cases: <i>TET2</i> C1289Y (1.4) <i>NOTCH1</i> R1107G; T518R (6.1) <i>NRAS</i> G13D (5.3)
# <i>TP53</i> mut per case		
1 mut	10 (62.5)	7 (87.5)
2 mut	6 (37.5)	0
3 mut	0	1 (12.5)
Type of <i>TP53</i> mut		
ms	20 (91)	9 ms (90)
sp	2 (9)	0
del	0	1 (10)
Maximum VAF	34.7 [8.2-94.4]	27.5 [12-79]

* not available for 1 case; ** not available for 2 cases

MDS CG: myelodysplasia related cytogenetic abnormalities; mut: mutation; ms: missense mutation; sp: splice site mutation; del: deletion mutation; VAF: Variant of allele frequency

Figure 1 - 743



Conclusions: The *de novo* PEL group had >1 *TP53* mutation, hotspot *TP53* mutations, and less common *TP53* LOH compared to t-PEL. *TP53* hotspot mutation in t-PEL were only observed in the presence of a strong predisposing condition. Overall, these findings show distinct *TP53* genetic alterations in *de novo* PEL and t-PEL, possibly reflecting different selective fitness advantages associated with *TP53* dysregulation.

744 Reversibility of Red Blood Cell Swelling in Aged Whole Blood Specimens Stored in Room Temperature

Patricia Tsang¹, A Mika¹

¹Geisinger Health, Wilkes Barre, PA

Disclosures: Patricia Tsang: None; A Mika: None

Background: It is known that room temperature storage of whole blood specimens collected in EDTA can lead to RBC swelling and artificial increase in the MCV and RDW in automated CBC counts. Storage or transportation of blood specimens in non-refrigerated conditions may be either unintentional or intentional based on convenience and/or cost avoidance. It is unknown if the phenomenon of falsely elevated MCVs can be remedied or reversed. In this prospective study, we conducted experiments to assess the factors and reversibility of falsely elevated MCV values in the setting of normocytic-appearing red blood cells on corresponding peripheral blood smear microscopy.

Design: We collected 18 cases with elevated MCV associated with normocytic RBCs on peripheral blood smear, and analyzed their preanalytical storage conditions, including temperature and lag times. Prospective experiments using split or parallel samples were designed and conducted to analyze the following variables on cell swelling: a) BD versus Greiner blood tube manufacturer, b) full versus half-filled blood tube using split samples, c) room temperature versus refrigerated specimen storage, and d) room temperature storage followed by refrigeration to test for reversibility of cell swelling.

Results: In room temperature, the MCV (but not hemoglobin) increased on average of 2.8% after 12 hours, 6.6% after 24 hours, and 8.6% after 36 hours compared to baseline values. The RDW also increased with room temperature storage (average of 6.8% after 36hours). Refrigeration of preanalytical samples led to negligible cell swelling with essentially stable MCV and RDW values. There was a slight tendency for blood collected in BD tubes to swell more than that in Greiner tubes but it did not reach statistical significance. No difference was

observed in the CBC counts between full and half-filled blood tubes. Interestingly, RBC swelling after being in room temperature for 24 hours (MCV increase = 6.2%) could be partly reversed by refrigeration for 12 hours (MCV increase = 3.2%) compared to baseline MCV values.

Mean MCV	Baseline	12 hr	24 hr	36 hr	% difference at 36 hrs
Greiner (Samples 1-5)	89.6	92.0	95.3	96.9	8.1%
BD (Samples 1-5)	89.4	92.0	95.6	97.6	9.2%
Refrigeration (Samples 6-10)	90.2	90.3	90.5	90.4	0.2%
Room Temp followed by Refrigeration	91.5	n.d.	97.2	94.4	3.2%

Conclusions: Falsely elevated MCV values can potentially mislead clinicians to diagnose macrocytic anemia and pursue excessive laboratory evaluation of folate and vitamin B12. Our study has demonstrated that refrigerated specimen storage can prevent RBC swelling and stabilize the MCV and RDW for at least 36 hours. The blood tube vendor and full/half-filled specimen appeared to have no influence on cell swelling. The phenomenon of falsely elevated MCV could be partly reversed or remediated by specimen refrigeration for 12 hours before analysis.

745 Optimization of Laboratory Diagnosis of Heparin-Induced Thrombocytopenia Using AcuStar Assay

Catherine Tucker¹, Ziver Sahin¹, Ruben Rhoades¹, Jerald Gong²

¹Thomas Jefferson University Hospital, Philadelphia, PA, ²Thomas Jefferson University, Philadelphia, PA

Disclosures: Catherine Tucker: None; Ruben Rhoades: None

Background: Diagnostic assays with high sensitivity and prompt turnaround times are critical in the diagnosis and management of patients with suspected heparin-induced thrombocytopenia (HIT). PF4 enzyme-linked immunoabsorbant assay (ELISA) is the most commonly used screening assay for HIT in the US. HemosIL-AcuStar-HIT-IgG assay (AcuStar) is a newly available screening assay that offers the advantages of rapid turnaround and shorter hands-on time. However, previous studies indicate that there are a high number of false-negative results associated with the manufacturer-recommended cutoff value of 1.0 U/mL. We compared the performance of these two assays in a large cohort of suspected HIT cases and determined the optimal cutoff value for AcuStar.

Design: We performed a retrospective cohort study on 96 random samples from patients evaluated for possible or suspected HIT at our institution from 2018 to present. We assessed the performance of AcuStar in comparison to ELISA using the Serotonin-release assay (SRA) as our gold standard. We analyzed a series of cutoff values, and produced a diagnostic algorithm in the context of 4T score using an AcuStar cutoff value with optimal sensitivity and negative predictive value (NPV).

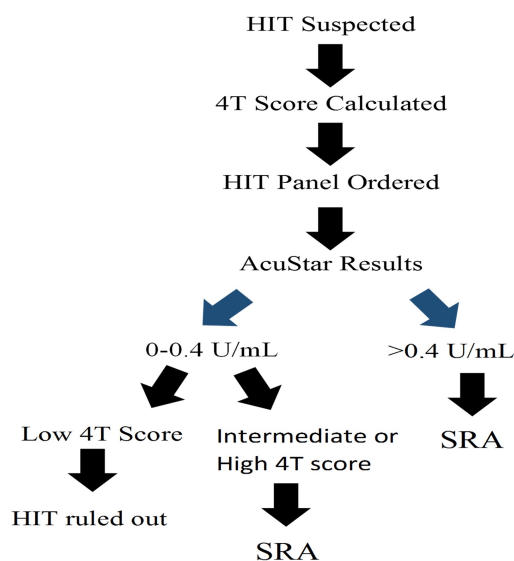
Results: First, using ROC analysis, we found that AcuStar has slightly higher discriminatory power than ELISA, with AUC values of 0.871 and 0.866, respectively (p=0.7362). The ‘optimal’ cutoff value for AcuStar using ROC analysis, in the absence of additional diagnostic tests, is 0.5842 (calculated using Youden’s index). We then analyzed sensitivity, specificity, positive predictive value (PPV) and NPV using various cutoff values of 0.2, 0.4, 0.6, 0.8, and 1.0 U/mL. These values are increments of 0.2 from the point at which NPV is 100% (0.2 U/mL), and include Youden’s index (0.6 U/mL) and the manufacturer-recommended cutoff (1.0 U/mL) for the AcuStar assay. Using 0.4 as cutoff in combination with 4T score, the NPV reached 100%. The same analysis was conducted for the ELISA assay with the established cutoff value of 0.4 OD (Table 1). Using a cutoff of 0.4 U/mL for both assays, the number of reflexed confirmatory SRA’s is 91% and 95.5% for Acustar and ELISA, respectively. The results of our analyses produced a new diagnostic algorithm to be implemented in our laboratory (Figure 1).

Table 1.

Cutoff value	Sensitivity (95% CI)	Specificity (95% CI)	PPV (95% CI)	NPV (95% CI)
AcuStar				
0.2 U/mL	100% (87.23-100)	50% (37.02-62.98)	46.55% (33.34-60.13)	100% (88.78-100)
0.4 U/mL	88.89% (70.84-97.65)	59.68% (46.45-71.95)	48.98% (34.42-63.66)	92.50% (79.61-98.43)
0.6 U/mL*	85.19% (66.27-95.81)	67.74% (54.66-79.06)	53.49% (37.65-68.82)	91.3% (79.21-97.58)
0.8 U/mL	77.78% (57.74-91.38)	67.74% (54.66-79.06)	51.22% (35.13-67.12)	87.50% (74.75-95.27)
1.0 U/mL	77.78% (57.74-91.38)	69.35% (56.35-80.44)	52.50% (36.13-68.49)	87.76% (75.23-95.37)
ELISA				
OD 0.2	100% (87.23-100)	45.16% (32.48-58.32)	44.26% (31.55-57.55)	100% (87.66-100)
OD 0.4	100% (87.23-100)	48.39% (35.50-61.44)	45.76% (32.72-59.25)	100% (88.43-100)
OD 0.6	92.59% (75.71-99.09)	64.52% (51.34-76.26)	53.19% (38.08-67.89)	95.24% (83.84-99.42)
OD 0.8	81.48% (61.92-93.70)	72.58% (59.77-83.15)	56.41% (39.62-72.19)	90.00% (78.19-96.67)
OD 1.0	74.07% (53.72-88.89)	82.26% (70.47-90.80)	64.52% (45.37-80.77)	87.93% (76.70-95.01)

*Approximation of Youden’s index, representative of optimal cutoff value

Figure 1 - 745



Conclusions: Our study suggests that using a combined approach of 4T score (4 and above) and AcuStar (>0.4 U/ml), we are able to reach an NPV of 100%. AcuStar has the considerable advantage of short turnaround and less hands-on time, with the added advantage of requiring fewer reflex SRA tests in order to confirm HIT. By implementing this newly available screening assay, we will be able to provide better patient management and care while simultaneously conserving laboratory resources.

746 Analysis of the T-cell Receptor Beta Repertoire in Post-Transplant Lymphoproliferative Disorders by Next Generation Sequencing

Karine Turcotte¹, Weiwei Zhang², Courtney Schweikart², Roberto Silva Aguiar², Timothy Greiner²

¹CHU de Québec/Université Laval, Québec, Canada, ²University of Nebraska Medical Center, Omaha, NE

Disclosures: Karine Turcotte: None; Weiwei Zhang: None; Courtney Schweikart: None; Roberto Silva Aguiar: None; Timothy Greiner: None

Background: We have previously studied the diversity of the T-cell Receptor Gamma (TRG) gene rearrangements in post-transplant lymphoproliferative disorders (PTLD). The aim of this current study was to analyze the diversity of the T-cell Receptor Beta (TRB) gene rearrangements in PTLD. Our goal was to compare the T-cell repertoire between EBV-positive monomorphic (Mono) and EBV-positive polymorphic (Poly) PTLD; and between PTLD and infectious mononucleosis (IM). To our knowledge, there has been no publication on the diversity of the TRB repertoire in PTLD.

Design: The PTLD cases that were analyzed in the previous IRB-approved TRG study that had remaining frozen tissue or DNA available were used in this study. 12 cases of EBV-positive Mono-PTLD, 23 cases of EBV-positive Poly-PTLD, 5 cases of EBV-negative Mono-PTLD, and 3 cases of IM from 1989 to 2015 were used in the study. We collected clinicopathologic data, reviewed the slides to confirm the diagnosis and confirmed the EBV status by either Southern blot, LMP1 stain and/or EBERs in situ hybridization. DNA was PCR amplified using the Oncomine™ TCR Beta-SR (DNA) kit (Thermo Fisher Scientific). Samples were sequenced using the Ion Torrent Personal Genome Machine (Thermo Fisher Scientific). TRB sequence data were analyzed with Torrent Suite™ software 5.10 and Ion Reporter™ software 5.10 (Thermo Fisher). The mean number of total raw TRB reads, aligned T-cell TRB reads and unique TRB clones was determined for each group. A one-tailed T-test was used to assess the diversity of the TRB repertoire measured by the Shannon index.

Results: The mean total number of raw *TRB* reads was 881,496 for EBVpos Mono-PTLD, 993,294 for EBVpos Poly-PTLD, 889,808 for EBVneg Mono-PTLD, and 735,633 for IM. The mean number of aligned T-cell *TRB* reads was 449,041 for EBVpos Mono-PTLD, 571,329 for EBVpos Poly-PTLD, 437,228 for EBVneg Mono-PTLD, and 469,169 for IM. The mean number of unique *TRB* clones was 1,227 for EBVpos Mono-PTLD, 3,761 for EBVpos Poly-PTLD, 4,122 for EBVneg Mono-PTLD, and 9,493 for IM. The Shannon index of the TCR repertoire shows less diversity in EBVpos Mono-PTLD (mean=7.59) than in EBVpos Poly-PTLDs (mean=9.03; One tailed T-test P = 0.048), less diversity in EBVpos Mono-PTLD than in IM (mean=12.04; P=0.001) and less diversity in Poly-PTLD than in IM (P=0.012). No difference was seen between EBVpos and EBVneg Mono-PTLD. We identified three *TRB* rearrangement sequences that are seen in the EBV positive PTLD groups, but not seen in EBV-negative PTLD and three sequences in the EBV positive PTLD groups, but not seen in the IM group.

Conclusions: Our findings show that there is a more limited diversity of the TRB T-cell repertoire in monomorphic PTLD compared to polymorphic PTLD or infectious mononucleosis. This is concordant with our previous results in the diversity of the TRG repertoire. *We have also identified putative EBV specific TRB sequences that warrant further study and confirmation.*

747 Acute Myeloid Leukemia and Myelodysplastic Syndrome with MYC Rearrangement

Xiaoqiong Wang¹, Guilin Tang¹, Zhihong Hu², Wei Wang¹, Gokce Toruner¹, Zhenya Tang¹, Carlos Bueso-Ramos¹, L. Jeffrey Medeiros¹, Shimin Hu¹

¹The University of Texas MD Anderson Cancer Center, Houston, TX, ²The University of Texas Health Science Center at Houston, Houston, TX

Disclosures: Xiaoqiong Wang: None; Guilin Tang: None; Zhihong Hu: None; Wei Wang: None; Gokce Toruner: None; Zhenya Tang: None; Carlos Bueso-Ramos: None; L. Jeffrey Medeiros: None; Shimin Hu: None

Background: 8q24/*MYC* rearrangement has been studied in various types of B-cell lymphoma and plasma cell neoplasms, and was reported recently in blastic plasmacytoid dendritic cell neoplasm. However, *MYC* rearrangement has not been reported in myeloid neoplasms. We aimed to investigate clinicopathologic features and outcome of the patients diagnosed with myeloid neoplasms harboring 8q24/*MYC* rearrangement.

Design: Myeloid neoplasms harboring 8q24/*MYC* rearrangement diagnosed in our institution from 2014 through 2019 were reviewed retrospectively.

Results: The study group included 12 patients, 8 men and 4 women, with a median age of 63 years (range, 38-82). Eight patients were diagnosed with acute myeloid leukemia (AML) and 4 had myelodysplastic syndromes with excess blasts (MDS-EB1, MDS-EB2). No patients with myeloproliferative neoplasms harboring 8q24/*MYC* rearrangement were identified. 8q24/*MYC* rearrangement was present at time of initial diagnosis of AML or MDS in 8 patients and emerged during therapy in 2 patients. In the remaining 2 patients, the exact time that 8q24/*MYC* rearrangement emerged is unknown because the initial diagnosis was rendered at other institutions. Multilineage dysplasia was observed in all 12 cases. FISH analysis was positive for *MYC* rearrangement in all 10 tested cases, and karyotype was complex in 7/12 cases. A next generation sequencing panel was performed in 11 cases and limited targeting sequencing was performed in the remaining case. The mutated genes included: *TP53* (4/10), *SRSF2* (2/7), *RUNX1* (2/10), *TET2* (2/10), *NRAS* (2/11), *BCOR* (1/7), *BCORL1* (1/7), *BRINP3* (1/7), *JAK3* (1/7), *ASXL1* (1/10), *CEBPA* (1/10), *GATA2* (1/10), *IDH2* (1/10), *PTPN11* (1/10) and *KRAS* (1/11). Eleven patients received chemotherapy including 4 patients who also received stem cell transplant. One patient lost in follow-up. At time of last follow-up, 7 patients had refractory or progressive disease, 3 achieved complete remission after stem cell transplant, and 2 had unknown disease status. Seven of 11 patients died with a median survival of 17 months after initial diagnosis.

Conclusions: 8q24/*MYC* rearrangement is uncommonly observed in patients with AML and MDS with excess blasts, but not in patients with myeloproliferative neoplasms. *MYC* rearrangement is associated with multilineage dysplasia and a complex karyotype. Patients with AML or MDS harboring 8q24/*MYC* rearrangement often have refractory disease and a dismal survival.

748 Morphological and Immunophenotypic Characterization of CAR T Cells

Jane Wei¹, Sophia Faude², Xiaoming Xu¹, Gerald Wertheim³, Michele Paessler⁴, Vijay Bhoj¹, Vinodh Pillai²
¹Perelman School of Medicine at the University of Pennsylvania, Philadelphia, PA, ²Children's Hospital of Philadelphia, Philadelphia, PA, ³Children's Hospital of Philadelphia, University of Pennsylvania, Philadelphia, PA, ⁴The Children's Hospital of Philadelphia, Perelman School of Medicine at the University of Pennsylvania, Philadelphia, PA

Disclosures: Jane Wei: None; Sophia Faude: None; Xiaoming Xu: None; Gerald Wertheim: None; Michele Paessler: None; Vijay Bhoj: None; Vinodh Pillai: None

Background: CAR T cell products are now approved by the Food and Drug Administration for the treatment of relapsed/refractory B-ALL, diffuse large B cell lymphoma and multiple myeloma. CAR T cells are under active investigation for the treatment of other hematological malignancies, solid tumors, and non-malignant etiologies. The morphological and immunophenotypic features of CAR T cells have not been analyzed in detail.

Design: One hundred and sixty six consecutive cases of B-lymphoblastic leukemia/lymphoma who received CD19-directed CAR T cell therapy between April 2012 and December 2017 were identified. Pre and post CAR complete blood counts (CBC), cerebrospinal fluid (CSF) cell counts and peripheral blood (PB) flow cytometric data were analyzed. Wright Giemsa stained peripheral blood smears that were imaged and archived on CellaVision were identified in 118 patients. All images from the first month after infusion were reviewed. Lymphocytes, large granular lymphocytes (LGL), atypical lymphocytes and blast images were analyzed. CSF morphology and differential was evaluated on H&E stained cytopsin preparations. *In vitro* CAR T cell activation experiments were performed to simulate *in vivo* conditions. Cell culture smears were made and analyzed similar to clinical peripheral blood smears.

Results: Peripheral blood smears showed small mature lymphocytes before CAR T cell infusion. Atypical large lymphoid cells with mature chromatin with deeply basophilic cytoplasm were prominent at end of first week. Marked expansion of lymphocytes was noted in the second week after infusion. A high proportion of the lymphocytes were classified as variant or atypical cells on automated and manual review. These atypical lymphocytes were large with variably basophilic cytoplasm or prominently granulated cytoplasm. Nuclear and cytoplasmic aberrancies were noted that distinguished them from activated cells of viral infections. Peak levels of such cells were noted at a median of 8 days (mean 8.42 days) post infusion. The highest proportion of atypical cells was 24.7% (median

17.6%, range 0.9% to 100%). Expanding lymphocytes were composed of both CD4+ and CD8+ T cells though they predominate in CD8+ T cells at peak expansion. Loss or variable CD7 was frequently noted but other immunophenotypic abnormalities were not seen. Eventually atypical LGLs were replaced by more typical LGLs in the 3rd to 4th week. Similar sequence of changes were noted under in vitro activation conditions in both CD4+ and CD8+ sorted CAR T cells. Marked pleomorphic lymphocytosis was noted in the CSF that persisted even at 12 month post infusion time point.

Conclusions: CAR T cells show characteristic sequence of morphological changes after infusion in peripheral blood and CSF that is distinct from morphological features of activated cells in viral infections. CAR T cells are composed of both CD4 and CD8 T cells but predominate in CD8.

749 Specific Expression of PLK-1 in Nodular Lymphocyte Predominant Hodgkin Lymphoma Correlates with Disease Stage, and Selective PLK-1 Inhibition with Volasertib May Constitute a Viable Therapeutic Alternative

Jonathan Weiss¹, Bindu Niravel², Noah Brown¹, Ryan Wilcox³, Kedar Inamdar⁴, Carlos Murga-Zamalloa²
¹University of Michigan, Ann Arbor, MI, ²University of Illinois at Chicago, Chicago, IL, ³Michigan Medicine, University of Michigan, Ann Arbor, MI, ⁴Henry Ford Health System, Detroit, MI

Disclosures: Jonathan Weiss: None; Noah Brown: None; Carlos Murga-Zamalloa: None

Background: Nodular lymphocyte predominant Hodgkin Lymphoma (NLPHL) represents approximately 15% of Hodgkin lymphoma cases and it is characterized by overall good survival rates with durable responses to initial therapies. In contrast to classic Hodgkin lymphoma, the tumor cells in NLPHL are negative for CD30 and CD15, and display strong CD20 expression. Importantly, the diagnosis of NLPHL may pose a challenge since no specific markers are available for the identification of the neoplastic cells. In addition, approximately 15% of patients diagnosed with NLPHL will show recurrences that are characterized by higher disease stage, and poor-responses to current chemotherapy or radiation therapies. Previous studies demonstrated that polo-like kinase 1 (PLK-1) expression correlates with advanced stage in diffuse large B-cell lymphomas. PLK-1 expression within lymphoma cells promotes proliferation, likely by stabilizing c-MYC expression. Importantly, therapeutic agents that target PLK-1 activation has demonstrated to be a successful alternative for the treatment of aggressive lymphomas that feature c-MYC dependent tumor progression.

Design: PLK-1 expression was evaluated by immunohistochemistry using a monoclonal antibody (208G4, Cell Signaling Technology). PLK-1 H-score was calculated by multiplying the percentage of PLK-1 positive tumor cells by staining intensity (scale 1-3). Multiplexing immunofluorescence panel was performed using the OPAL system and Vectra 3 reader (Perkin Elmer).

Results: We evaluated 34 samples of NLPHL cases for expression of PLK-1 by immunohistochemical analysis. We identified specific expression of PLK-1 staining in 97% of NLPHL cases analyzed. Importantly, analysis of classic Hodgkin lymphoma cases (n = 80) demonstrated that Reed-Sternberg/Hodgkin cells were negative for PLK-1 expression. Additionally, the H-score of PLK-1 expression was correlated with lymphoma tumor stage (advanced stage mean H-score 181.81, limited stage mean H-score 103.33, p=0.0095). Lastly, inhibition of PLK-1 with the selective inhibitor volasertib demonstrated decreased proliferation of NLPHL cell lines, with concomitant abrogation of c-MYC expression.

Conclusions: The findings demonstrate that PLK-1 may be a useful diagnostic tool in NLPHD. Moreover, the findings indicate that PLK-1 nuclear expression levels are associated with advanced tumor stage, and selective inhibition of PLK-1 with volasertib may constitute a relevant therapeutic approach for patients at advanced stage or relapse.

750 Development of a Novel Flow Cytometric Technique for Quantitative Measurements of Transcriptional Addiction and Drug Resistance in Leukemia Cells

Amber Willbanks¹, Shaun Wood¹, Jason Cheng¹

¹University of Chicago, Chicago, IL

Disclosures: Amber Willbanks: None; Shaun Wood: None; Jason Cheng: None

Background: Gene dysregulation and transcriptional addiction are the characteristic features of cancer/leukemia cells and the major determinants for drug response and resistance in cancer/leukemia (Braden et al. Cell 2017; Pagliarini, et al. EMBO Rep. 2015). Our recent study demonstrated that RNA polymerase II (RNAPII) interacts with RNA cytosine methyltransferases, namely NSUN1 and NSUN2, to form drug-resistant active transcription complexes at newly synthesized (nascent) RNA, which renders leukemia cells refractory to the epigenetic modifying drug azacitidine and correlates with resistance to the BCL2 selective inhibitor venetoclax (Cheng et al. Nature Communications 2018; Wood et al. Unpublished data). However, it has been a challenge to quantitatively measure nascent RNA and transcriptional rates in an overwhelming background of previously synthesized RNA, including ribosomal RNA (rRNA), transfer RNA (tRNAs) and messenger RNA (mRNA), in normal and cancer/leukemia cells in clinical settings.

Design: The experimental design includes three steps: 1. Development of a flow cytometry protocol based on 5-ethynyl uridine (5-EU) click chemistry and conducting the proof-of-principle in leukemia cell lines; 2. Characterization of lineage- and drug-associated transcription addiction in various drug-resistant vs. -sensitive leukemia cell lines; and 3. Clinical application using the novel 5-EU click chemistry-based flow cytometry on clinical specimens to predict drug response and resistance.

Results: In this study, we developed a novel flow cytometric technique based on 5-EU click chemistry, which allows quantitative measurement of transcription rates and characterization of transcriptional addiction in drug-sensitive and drug-resistant leukemia cells. Drug-resistant SC cells and drug-sensitive M2 leukemia cells were treated with 5-EU for 0, 30 and 60 min. Alexa-Fluor 647 (AF-647)-conjugated azide was then used as the clicking reagent to label 5-EU incorporation into nascent RNA in 0, 30, and 60 min EU-treated samples. Samples were then run on the Attune NxT 4-14 flow cytometer and data was gated for positive AF-647 signal. AF-647 signal quantification revealed an increased transcription rate in SC cells as compared with M2 cells due to the increased 5-EU incorporation into nascent RNA. The drug-resistant SC cell line had a much higher transcriptional activity compared to the drug-sensitive M2 cell line, even though these two cell lines had a similar cell doubling time.

Figure 1 - 750

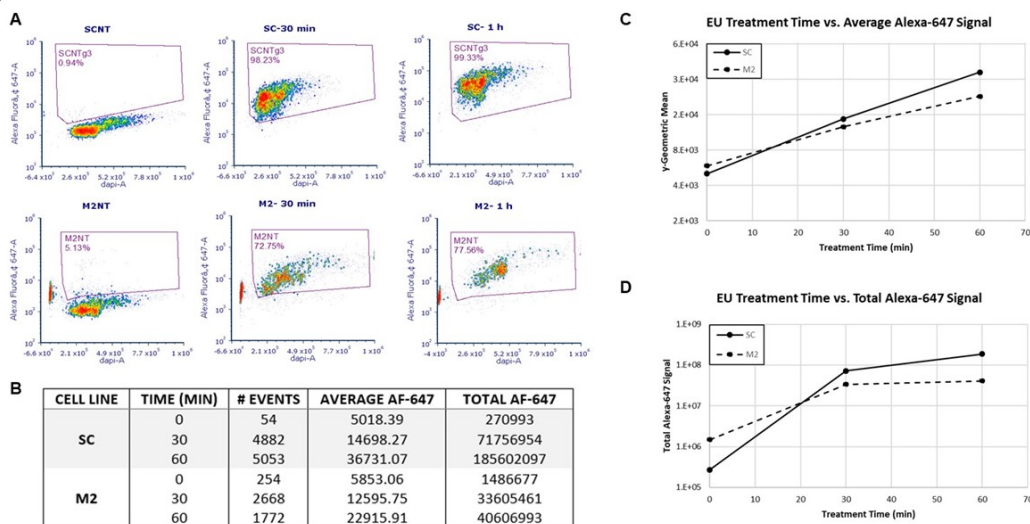


Figure 1. Transcriptional activities of SC and M2 leukemia cell lines as measured by EU-clicking chemistry flow cytometry at 0, 30 and 60 minutes. A. Flow data and gating parameters used to calculate transcriptional activity. NT- no treatment (0 min) population was used to exclude background signal. B. Average AF-647 and Total AF-647 signal were calculated in the gated cell population from Panel A. C-D. Average AF-647 and Total AF-647 signal is plotted for both cell lines at 0 min, 30 min, and 60 min. SC leukemia line is resistant to venetoclax and moderately sensitive to azacitidine. In contrast, M2 cell line is highly sensitive to both venetoclax and azacitidine. Alexa-Fluor 647 (AF-647)-conjugated azide was used as the clicking agent to label 5-EU incorporation into nascent RNA. The increase in AF-647 signal indicates incorporation of 5-EU into newly synthesized RNAs and reflects the transcription rates in those cells.

Conclusions: We have established the protocol of a novel 5-EU click chemistry-based flow cytometry for quantitative measurements of newly synthesized (nascent) RNAs and transcriptional rates in leukemia cell lines, which has paved the way for characterizing transcriptional addiction and drug resistance in leukemia/cancer cells in clinical settings.

751 TCF-4 and CD56 Co-Expression is Highly Effective for Distinguishing Neoplastic and Non-Neoplastic Plasmacytoid Dendritic Cells

Sarah Wu¹, Sam Sadigh², Geraldine Pinkus¹

¹Brigham and Women's Hospital, Boston, MA, ²Brigham and Women's Hospital, Harvard Medical School, Boston, MA

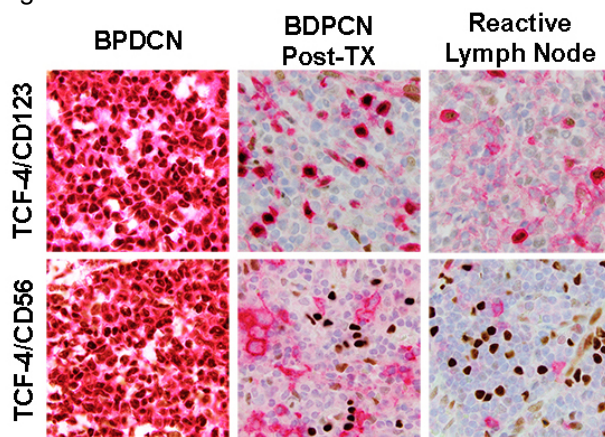
Disclosures: Sarah Wu: None; Sam Sadigh: None; Geraldine Pinkus: None

Background: Blastic Plasmacytoid Dendritic Cell Neoplasm (BPDCN) is a rare hematologic malignancy of skin, bone marrow, and lymph nodes with poor prognosis and survival. A recent study (Suskwai et al. 2019) demonstrated that TCF-4 and CD123 immunohistochemical dual expression is highly sensitive for diagnosing BPDCN and permits its distinction from other malignancies. However, TCF-4/CD123 co-expression is also observed in non-neoplastic plasmacytoid dendritic cells (pDCs). With the development of BPDCN targeted therapies, in the post-treatment setting, the distinction between residual disease and background pDCs may be challenging, particularly in cases of skin involvement where concurrent flow cytometry is unavailable. Therefore, markers such as CD56 that have been shown to be positive in BPDCN and negative in pDCs may aid in detection of residual disease. We hypothesized that dual expression of TCF-4 and CD56 by immunohistochemistry may differentiate between BPDCN and pDCs.

Design: 98 cases of BPDCN were identified at our institution, including skin, bone marrow, and lymph node samples. 62.2% (61/98) were post treatment samples. Slides were stained using a double staining protocol for the following marker combinations (TCF-4/CD123, TCF-4/CD56), using a brown chromogen for TCF-4 and a red chromogen for CD123 and CD56. BPDCN samples included bone marrow (6) and skin (8). As a control group, other hematologic malignancies were evaluated, including AML (5), CLL/SLL (5), CMML (4), B-ALL (1), CML (1), hairy cell leukemia (1), CLL (1), and CHL (1). Non-neoplastic controls included reactive lymph nodes (3), skin (2), tonsil (4), bone marrow (9), and Kikuchi-Fujimoto lymphadenitis (1).

Results: TCF-4/CD123 double staining was observed in BPDCN as well as in scattered cells in BPDCN post-treatment specimens and pDCs in reactive lymph nodes. The TCF-4/CD56 studies showed double staining in BPDCN but stained separate populations of cells in the post-treatment specimens and in reactive lymph nodes. Concordant co-expression of TCF-4/CD123 and TCF-4/CD56 were observed in BPDCN only (skin 8/8, bone marrow 5/6). Lesional cells of other malignancies lacked co-expression of TCF-4/CD123 and TCF-4/CD56. Scattered pDCs in non-neoplastic control tissues and in neoplastic disorders other than BPDCN were TCF-4+/CD123+ and TCF4+/CD56-.

Figure 1 - 751



Conclusions: Our initial results suggest that TCF-4/CD56 co-expression may be effective for distinguishing BPDCN from pDCs and extremely valuable to identify residual BPDCN in the post-treatment setting.

752 An 8-Gene Expression Signature to Improve Prognosis Prediction of Diffuse Large B-Cell Lymphoma Beyond International Prognostic Index

Wanhui Yan¹, Xiangnan Jiang¹, Yifeng Sun², Qinghua Xu², Xiaoqiu Li¹

¹Fudan University Shanghai Cancer Center, Shanghai, China, ²Canhelp Genomics, Hangzhou, China

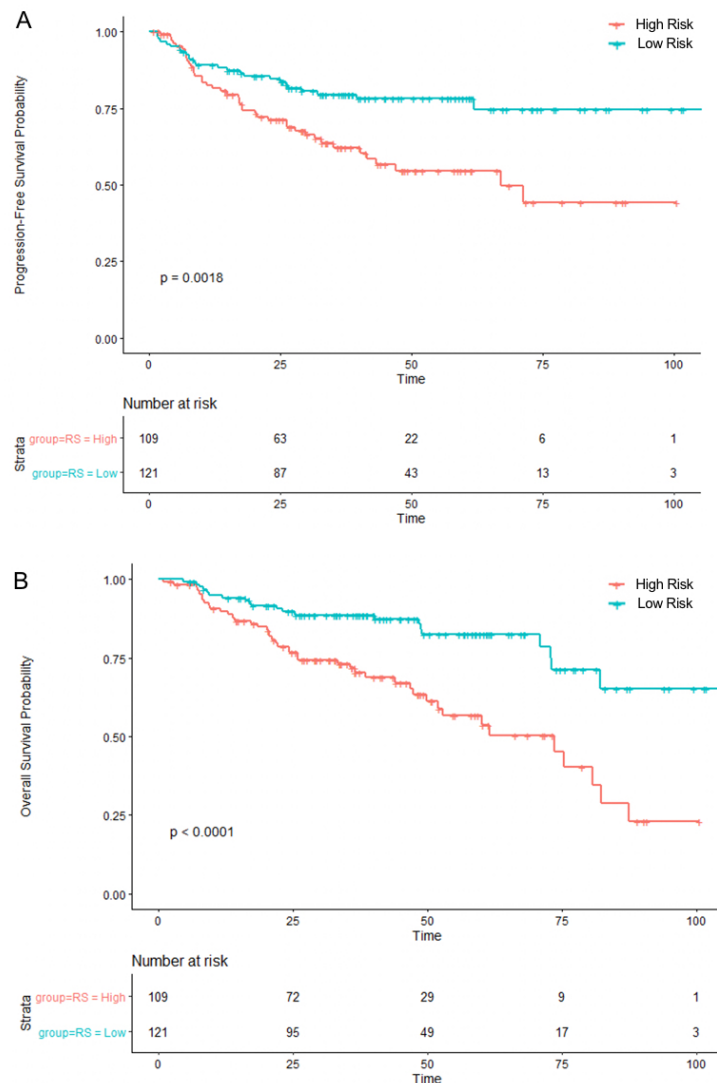
Disclosures: Wanhui Yan: None; Xiangnan Jiang: None; Yifeng Sun: None; Qinghua Xu: None; Xiaoqiu Li: None

Background: International prognostic index (IPI) is the most widely used and robust stratification system for diffuse large B-cell lymphoma (DLBCL). However, a precise therapeutic strategy requires further stratifying DLBCL patients with IPI-intermediate risk.

Design: A genomic prognosis score (GPS) signature was established based on transcriptomic profiling of eight prognostic genes in DLBCL. A total of 470 DLBCL patients receiving the R-CHOP frontline therapy were stratified with both revised-IPI (R-IPI) and GPS signature. DLBCL patients with intermediate-risk were stratified with GPS signature in further regarding the progression free survival (PFS) and overall survival (OS).

Results: R-IPI identified 44 low-risk, 230 intermediate-risk and 150 high-risk patients, respectively, out of 424 patients with sufficient clinical information. Multivariate survival analysis using Cox's regression model demonstrated an independent prognostic value of GPS signature beside the R-IPI by identifying 242 low-risk patients and 228 high-risk patients. Among 230 intermediate-risk patients identified by R-IPI, GPS signature further stratified them into the low-risk group (121 patients) and high-risk group (109 patients) with 5-year PFS rate of 80% vs. 53% ($P < 0.001$) and 5-year OS rate of 83% vs. 52% ($P = 0.0018$), respectively (Figure 1).

Figure 1 - 752



Conclusions: The GPS signature provides additional prognostic information besides R-IPI in DBCL patients receiving frontline therapy. The GPS signature can be used to re-map R-IPI intermediate-risk patients into low-risk and high-risk, who may receive reduced therapy with lower toxicity, or receive enhanced therapy or clinical study, respectively.

753 Intravascular Natural Killer/T Cell Lymphoma: Comprehensive Analysis of its Clinicopathological, Molecular Features and Prognostic Factors

Bao-Hua Yu¹, Wei-Qi Sheng², Xiao-Yan Zhou², Xiao-Qiu Li²

¹Fudan University Shanghai Cancer Center, Shanghai, China, ²Fudan University Shanghai Cancer Center, Shanghai Medical College, Fudan University, Shanghai, China

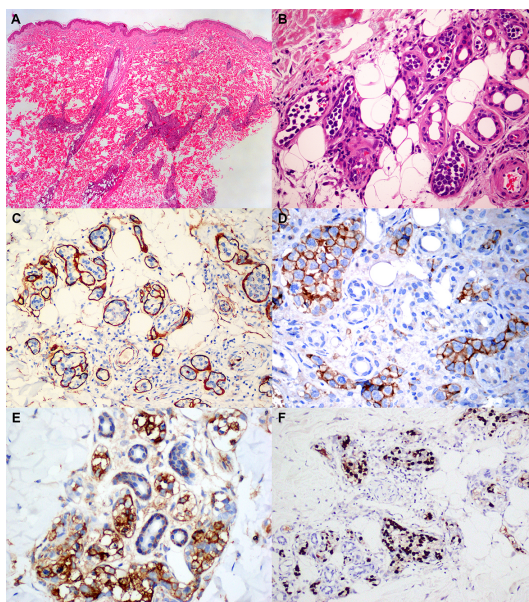
Disclosures: Bao-Hua Yu: None; Wei-Qi Sheng: None; Xiao-Yan Zhou: None; Xiao-Qiu Li: None

Background: Intravascular Natural Killer/T Cell Lymphoma (IVNKTL) is an extremely rare variant of lymphoma. Its clinicopathological characteristics, molecular features as well as the prognostic factors were poorly understood. This study was aimed to comprehensively investigate the features of this peculiar disease.

Design: Seven patients with IVNKTL were retrieved and the clinicopathologic characteristics were analyzed. Comprehensive genomic profiling of 3 patients was conducted using a 481-gene panel assay. A comprehensive analysis of all reported cases in the English literature to date was performed to investigate the prognostic factors.

Results: The median age of our 7 patients were 57 years (range, 33-68 years). Six patients presented with skin lesions, one of which had concomitant involvement of central nervous system (CNS), and the other patient exhibited unique testis involvement. Histologically, atypical lymphoid cells almost exclusively proliferated within the blood vessels, with subtle extravascular infiltration in one case. Neoplastic cells were positive for CD3, CD56, TIA1, and EBER in all cases, with high Ki-67 index (80% to nearly 100%). PD-L1 expression was observed in some tumor cells in all 3 detected cases. There were 18 clinically relevant gene mutations among 3 detected cases, including TP53, APC, ABCB1, PIK3CD, NOTCH1, PML, B2M, FAS, BCOR, ECT2L, FANCC, FGFR4, LAMP1, RET, STAT5A, STXBP2, TEK and UGT1A1. Among these, high frequency of three pathways was observed, including microRNAs in cancer, human papillomavirus infection and herpes simplex virus 1 infection-related pathways. Our analysis of the total 32 IVNKTLs (including the previously published cases and ours) revealed that dermatological lesions (26/32, 81.3%) was the most common manifestation, followed by CNS involvement. Median survival was 8 months and one-year overall survival rate was 36%. Multivariate analysis showed that both sex ($p=0.038$) and initial CNS involvement ($p=0.011$) were independent prognostic indicators.

Figure 1 – 753



Conclusions: In conclusion, IVNKTL is a highly aggressive lymphoma, with dermatological lesions as the most common manifestation, followed by CNS involvement. Male patients and initial CNS involvement might have worse prognosis. Better awareness of this lethal disease might be of importance for accurate diagnosis and timely intervention and comprehensive genomic profiling of more cases might shed light on potential therapeutic opportunities so as to improve the patients' survival.

754 Yin Yang 1 Overexpression Predicts a Favorable Survival in Diffuse Large B Cell Lymphoma

Bao-Hua Yu¹, Tian Xue², Xiao-Yan Zhou², Xiao-Qiu Li²

¹Fudan University Shanghai Cancer Center, Shanghai, China, ²Fudan University Shanghai Cancer Center, Shanghai Medical College, Fudan University, Shanghai, China

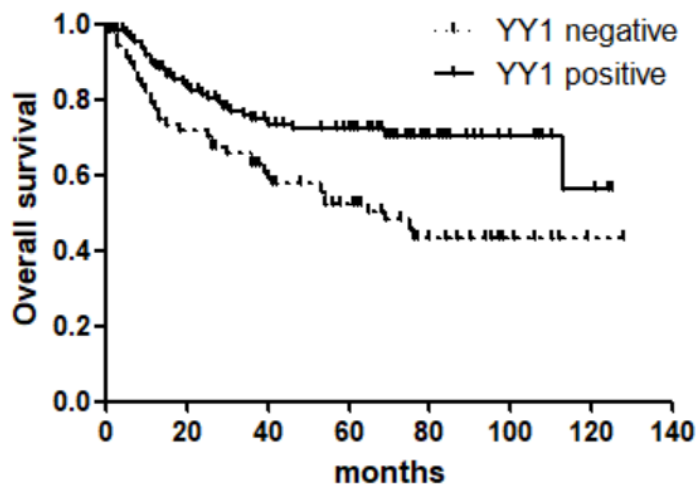
Disclosures: Bao-Hua Yu: None; Tian Xue: None; Xiao-Yan Zhou: None; Xiao-Qiu Li: None

Background: Diffuse large B cell lymphoma (DLBCL) accounts for the majority of non-Hodgkin lymphoma, studies on exploring practical immunohistochemical indicators for the prognostic prediction of DLBCL were limited. Yin Yang 1 (YY1) is a multifunctional transcription factor, which involves in tumor development and progression. However, its role in DLBCL has not been fully investigated. This study aimed to reveal the clinicopathological relevance of YY1 as well as its prognostic value in DLBCL.

Design: One hundred and ninety-eight cases of DLBCL were retrospectively analyzed. Immunohistochemical staining of YY1, MYC, CD10, BCL2, BCL6, MUM1, pAKT and CXCR4 were employed. Correlation analysis and survival analysis were performed.

Results: Among 198 cases of DLBCL, YY1 was expressed in 61.1% (121/198) cases. YY1 expression was significantly more frequent in cases of GCB subgroup (69/98) than that in non-GCB group (48/95, $p=0.005$). YY1 was positively correlated with the expression of MUM1 (53/61, $p<0.001$), BCL6 (93/120, $p<0.001$), pAKT (96/140, $p=0.001$) and MYC/BCL2 double-expression (66/72, $p<0.001$). However, YY1 was negatively associated with the expression of CXCR4 (58/113, $p=0.001$). We failed to find any remarkable relationships with clinical characteristics, including age, gender, Ann Arbor stage, localization, and B symptoms ($p>0.05$). The follow-up information was available in 185 patients with a median follow-up time of 44 months (range, 0.5-128 months). The 5-year overall survival rate of YY1-positive group (85/115, 73.9%) was significantly higher than that of YY1-negative group (35/70, 50.0%, $p<0.001$). Multivariate analysis indicated that YY1 negative was an independent risk factors for inferior overall survival regardless of age, gender, Ann Arbor Stage, B symptoms and cell of origin type ($p<0.05$). Furthermore, YY1 was helpful for stratifying DLBCL patients into different risk groups when combined with double expression status ($p<0.001$).

Figure 1 - 754



Conclusions: YY1 was highly expressed in DLBCL, especially in those with GCB phenotype and with MYC/BCL2 double-expresser. As an independent prognostic factor, YY1 expression could predict a better outcome. It was assumed that the interactions between YY1 and pAKT or CXCR4 might be intricate, which is warranted to be investigated further.

755 Flow Cytometric Detection of Lambda-restricted Plasmablasts in Body Cavity Effusion of HHV-8-associated Multicentric Castleman Disease: A Potential Diagnostic

Ting Zhou¹, Maryalice Stetler-Stevenson², Hao-Wei Wang³, Mark Raffeld⁴, Constance Yuan²
¹Bethesda, MD, ²National Cancer Institute, National Institutes of Health, Bethesda, MD, ³National Institutes of Health, Bethesda, MD, ⁴National Cancer Institute, Bethesda, MD

Disclosures: Ting Zhou: None; Maryalice Stetler-Stevenson: None; Hao-Wei Wang: None; Mark Raffeld: None; Constance Yuan: None

Background: Patients with HHV-8-associated multicentric Castleman disease (MCD) carry a poor prognosis if untreated. The diagnosis currently relies on histologic examination of lymph nodes, which is often challenging. These patients may also concurrently present with other HHV-8-associated diseases, including Kaposi sarcoma and primary effusion lymphoma (PEL). Since both MCD and PEL may manifest with body cavity effusions, examination of fluid is critical to establishing a correct diagnosis. A monotypic but polyclonal lambda-restricted plasmablastic (LRP) population is a typical finding in lymph nodes involved by MCD. However, it remains unknown whether this population also resides in extranodal locations such as body fluids, and whether this finding has diagnostic utility.

Design: This study reports the clinicopathological features of ten cases with body cavity effusion developing in the context of MCD. The fluid samples were assessed by multiparametric flow cytometry, and immunoglobulin gene (IG) configuration using polymerase chain reaction (PCR)-based techniques.

Results: Of the nine males and one female, the median age was 37 years (range: 28-68). All patients had typical clinical manifestation of MCD, and the diagnosis was pathologically confirmed in eight. They all had synchronous or metachronous Kaposi sarcoma and nine were positive for HIV infection. Flow cytometry detected the LRP population in fluid specimens of six patients, ranging from 0.01% to 8.7% of the total mononuclear cells. These cells express relatively bright CD45, bright CD38, variable CD19, IRF4, and are negative for CD138. They show surface and intracytoplasmic lambda restriction. Among them, one had concurrent PEL showing a different immunophenotype with lack of CD19 and light chain expression, and CD30 positivity. One had subsequent PEL involving pleural fluid and cerebrospinal fluid, and interestingly, LRP was no longer detectable after the emergence of PEL. Among the four patients without detectable LRP, three had PEL. Furthermore, clonal IG rearrangements were detected only in PEL, whereas MCD-only specimens were all polyclonal.

Table 1. Clinicopathological features of patients with multicentric Castleman disease

Patient	Age (yrs)	Sex	HIV	Biopsy-proven MCD	Fluid type	PEL	Lambda-restricted Plasmablasts %†	Status	F/U post MCD (yrs)	IG clonality
1	37	M	Yes	Yes	Ascites	Yes	Not identified	Dead	0.9	Clonal
					CSF					Clonal
2	30	M	Yes	Yes	Pleural	Yes	Not identified	Dead	NA	Polyclonal
3	37	M	Yes	Yes	Pleural	Yes	Not identified	Alive	0.8	Polyclonal
4	28	M	Yes	Yes	Pleural	No	Not identified	Alive	6.7	Polyclonal
5	27	M	Yes	No, clinically	Pleural #1	No	0.50	Dead	NA	Polyclonal
						Yes				Clonal
					Pleural #2	Yes	Not identified			Not identified
6	66	M	Yes	Yes	CSF			Alive	8.0	Clonal
					Pleural	Yes	0.30			
					Ascites	Yes	2.30			NA
7	55	M	Yes	Yes	Pleural	No	0.08	Alive	1.5	Polyclonal
8	31	M	Yes	Yes	Pleural	No	0.03	Dead	0.7	Polyclonal
9	68	F	Yes	No, clinically	Pleural	No	8.70	Alive	0.4	Polyclonal
10	53	M	No	Yes	Pleural	No	0.01	Alive	0.7	Polyclonal

†Frequency of plasmablasts out of total mononuclear cells by flow cytometric analysis

Abbreviations: CSF; cerebrospinal fluid; F/U, follow up; IG, immunoglobulin; MCD, multicentric Castleman disease; mos, months; NA, not available/applicable; PEL, primary effusion lymphoma; yrs, years

Figure 1 - 755

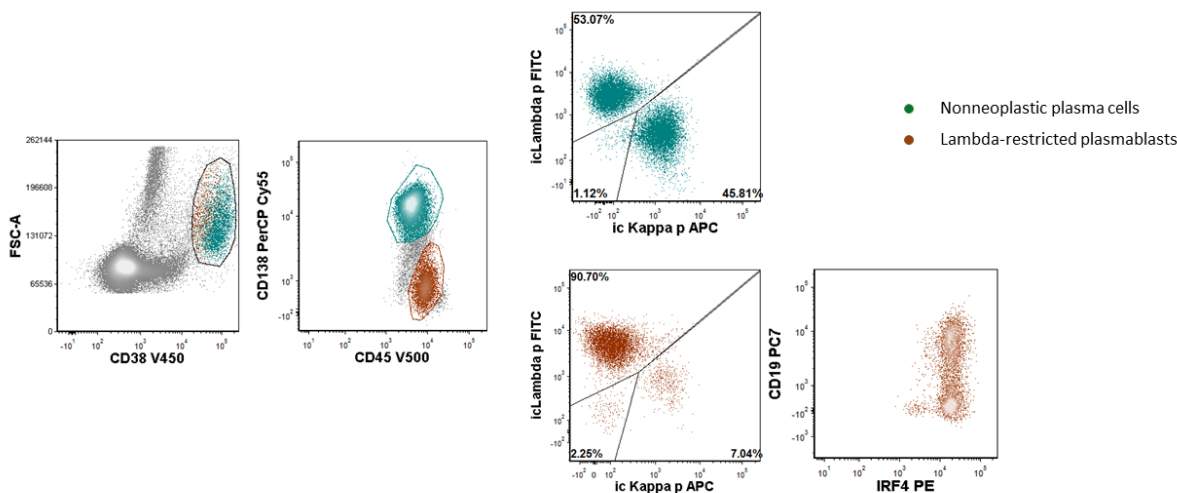


Figure 1. Immunophenotypic profile of lambda-restricted plasmablasts.

Conclusions: LRP is present in body cavity effusions in 60% of MCD patients studied. In the clinical context of HIV, Kaposi sarcoma, and HHV-8 positivity, this finding is useful to corroborate the diagnosis of MCD. In conjunction with other immunophenotypic profiling for PEL and ancillary clonality studies, assessment for the presence of LRP is useful to establish the etiology of body cavity effusions in these patients.

756 Circulating CD19-Negative CD22-Positive Progenitor Population: A Diagnostic Pitfall for Minimal Residual Disease Detection in B-Lymphoblastic Leukemia Post CD19-Targeted Immunotherapy

Ting Zhou¹, Constance Yuan², Maryalice Stetler-Stevenson², Hao-Wei Wang³

¹Bethesda, MD, ²National Cancer Institute, National Institutes of Health, Bethesda, MD, ³National Institutes of Health, Bethesda, MD

Disclosures: Ting Zhou: None; Constance Yuan: None; Maryalice Stetler-Stevenson: None; Hao-Wei Wang: None

Background: Minimal residual disease (MRD) is one of the most important factors for predicting relapse and guiding treatment of B-lymphoblastic leukemia (B-ALL). Detection of peripheral blood MRD has been shown to predict disease relapse in the bone marrow. Multiparametric flow cytometry (MFC) is of great utility for the detection of MRD, and conventional flow cytometric strategies utilize CD19 to identify the B-cell lineage. However, recent advances in CD19-targeted immunotherapy, including antibody-based and chimeric antigen receptor modified T-cell (CAR-T) therapies, have posed challenges for MRD detection due to downregulation or loss of CD19 after therapy. We recently encountered a CD19-negative, CD22-positive progenitor population in the peripheral blood of B-ALL patients, which may phenotypically overlap with leukemic blasts and result in false-positive MRD outcomes, especially in the setting of CD19-targeted therapy.

Design: We investigated this progenitor population by MFC-based MRD assays in 169 blood samples from 34 patients with refractory B-ALL, pre- and post-therapy with CD19 and/or CD22 CAR-T therapies. We further explored its immunophenotype to establish distinction from MRD.

Results: Of the 23 males and 11 females, the median age was 19 years (range: 7-62). Prior to enrollment, 12 patients had received CD19 CAR-T. Flow cytometry revealed this progenitor population at low levels (range, 0.00016%-0.43%) in 105 samples. It was detected in all patients at least once during the course of the study. These cells showed a consistent immunophenotype, expressing CD22, bright CD34, moderate/dim CD38, variable CD10, and dim CD45, in the absence of all other tested B-cell markers including CD19, CD20, CD24, and

intracytoplasmic CD79a. The immunophenotype is distinct from the circulating myeloblasts or lymphoblasts. Despite variability in immunophenotype of B-ALL, none of the patients exhibited an immunophenotypic profile identical to that of this progenitor population. The consistent and distinct immunophenotype, especially the combination of bright CD34, moderate/dim CD38, narrow range of dim CD45, spectrum of CD10, and lack of other B-cell lineage markers (except CD22) aid in their distinction from B-ALL MRD.

Table 1. Clinical and immunophenotypic features of B-lymphoblastic leukemia patients before CAR-T therapy.

Patient	Age/Sex	CAR-T	CD19	CD20	iCD79a	CD22	CD24	CD10	CD34	CD38	CD58	CD45	CD13	CD33
1	8/F	CD19/22	+	par	+	+	+	+	(-)	br	br	mod to dim	(-)	(-)
2	15/F	N/A*	+	NA	NA	NA	NA	NA	NA	NA	NA	NA	NA	NA
3	13/M	N/A*	(-)	+	+	+	+	br	(-)	+	br	dim to (-)	(-)	(-)
4	23/M	CD19/22	+	mod	+	+	+	br	par	dim	+	dim	(-)	(-)
5	10/M	CD22	(-)†	+	+	+	+	dim	(-)	+	br	dim	par	dim
6	9/F	N/A*	(-)†	NA	NA	+	br	par	(-)	+	NA	NA	(-)	(-)
7	15/M	CD22	(-)†	(-)	dim	dim	+	br	+	dim	+	dim	(-)	(-)
8	20/F	CD19/22	+	mod to (-)	+	+	+	br to mod	par	dim	br	mod	(-)	NA
9	21/M	N/A*	+	par	+	+	+	br	par	dim	+	mod to dim	(-)	(-)
10	18/M	CD22	+†	mod to (-)	+	+	par	br	br to mod	+	br	dim	(-)	(-)
11	19/F	CD22	(-)†	mod to (-)	dim	+	+	br	par	dim	NA	dim	NA	NA
12	12/M	CD22	+†	+	NA	+	+	br	dim to (-)	+	NA	dim	(-)	(-)
13	7/M	N/A*	+	(-)	+	+	(-)	par	(-)	+	+	par, dim	(-)	NA
14	21/M	CD19/22	+	+	dim	+	+	br	br	dim	+	mod	(-)	NA
15	62/M	CD19	+	(-)	NA	+	+	br	br	dim	+	+	(-)	(-)
16	26/M	N/A*	+	par	+	+	NA	+	+	NA	NA	NA	NA	NA
17	29/F	CD19/22	+	+	NA	+	NA	NA	NA	NA	NA	NA	NA	NA
18	5/M	CD22	+†	(-)	+	+	+	+	par	dim	br	dim	(-)	(-)
19	10/F	CD19/22	+†	(-)	NA	+	+	br to (-)	par	dim	br	dim	dim to (-)	(-)
20	19/M	CD19/22	+	(-)	+	+	+	mod to (-)	(-)	dim	+	dim	+	NA
21	24/F	N/A*	+†	NA	NA	+	+	br	br to (-)	+	NA	dim to (-)	(-)	(-)
22	20/M	CD19/22	+†	dim to (-)	+	+	(-)	br	(-)	dim	+	dim	NA	NA
23	32/F	CD19	+	(-)	+	+	+	br	+	dim	NA	dim to (-)	(-)	(-)
24	29/M	CD19/22	+	+	+	+	br	br	par	br to (-)	br	dim	(-)	dim
25	28/F	N/A*	+	NA	NA	par	+	mod to (-)	+	dim	NA	dim	NA	NA
26	44/M	N/A*	+	(-)	NA	+	+	br	+	dim to (-)	br	dim	dim	dim
27	28/M	CD19/22	+	NA	+	+	dim	mod	+	dim	br	dim	dim	NA
28	11/M	CD22	(-)†	(-)	+	+	+	(-)	br	+	NA	dim	(-)	NA
29	7/F	CD22	(-)†	NA	NA	dim	br	mod to (-)	par	dim	NA	(-)	(-)	NA
30	8/M	CD22†	(-)	(-)	+	+	+	+	+	dim	NA	dim to (-)	(-)	(-)
31	23/M	N/A*	+	NA	+	+	NA	+	+	NA	NA	NA	NA	NA
32	39/M	CD19	+	dim	+	+	br	br	br to (-)	dim	br	dim to (-)	(-)	(-)
33	28/M	CD19/22	+	(-)	+	+	+	br	+	dim	br	par, dim	NA	NA
34	18/M	CD22	+	par	NA	+	(-)	br	+	dim	+	dim	(-)	(-)

*These patients were not eligible for CAR-T therapy, or they did not receive CAR-T over the course of the study.

†The patient previously received CD19 CAR-T therapy prior to study enrollment.

Abbreviations: br, bright; mod, moderate; iCD79a, intracytoplasmic CD79a; NA, not available; par, partial positivity.

Figure 1 - 756

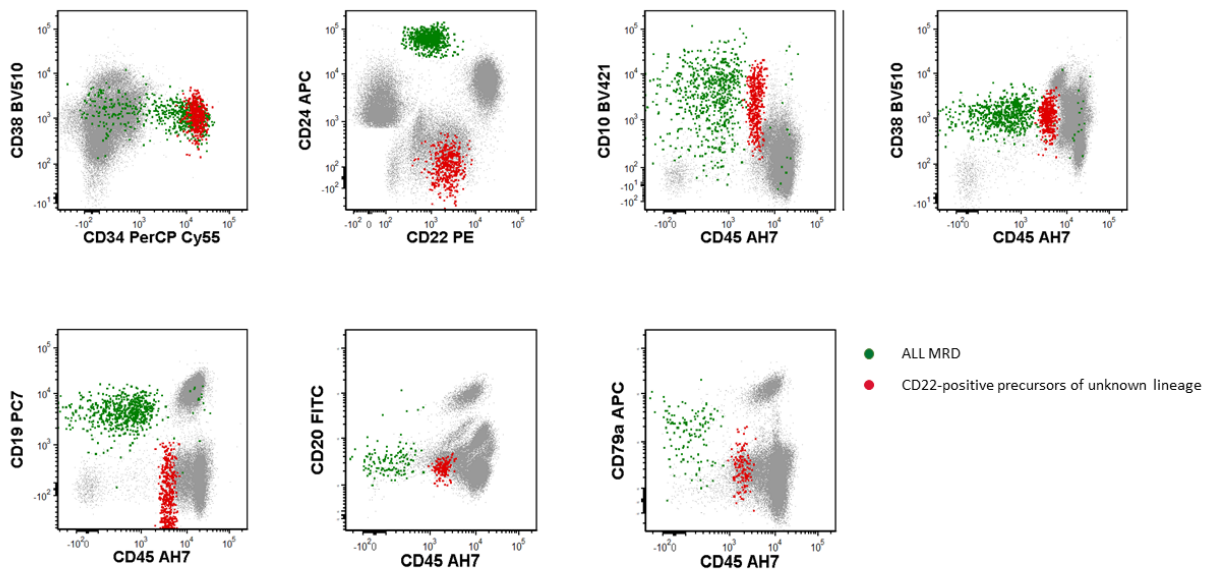


Figure 1. Immunophenotypic profile of the circulating CD19⁻ CD22⁺ precursors (red) in a representative case with B-ALL MRD (green).

Figure 2 - 756

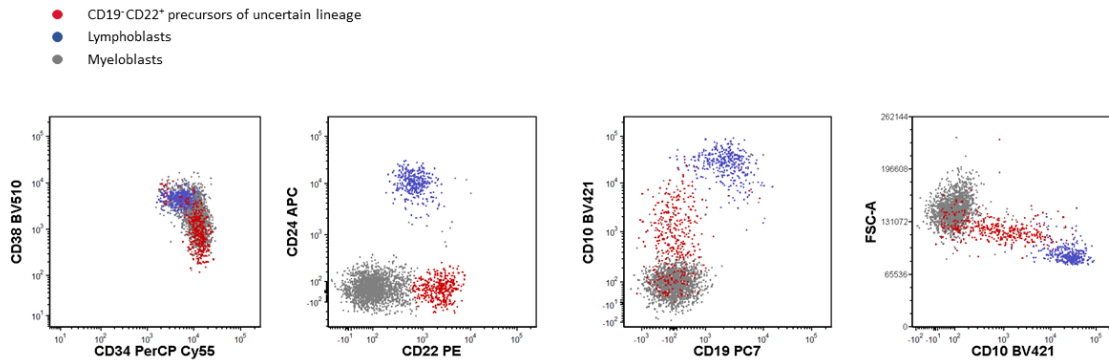


Figure 2. Immunophenotypic profile of the circulating CD19⁻ CD22⁺ precursors (red), in comparison to that of circulating myeloblasts (gray) and lymphoblasts (blue) in a MRD-negative case.

Conclusions: Circulating CD19-negative CD22-positive precursors are commonly detected at low levels in peripheral blood samples, they should be distinguished from B-ALL MRD especially in the setting of CD19-targeted therapy.